

The
U

M

A
Journal
P

Publisher
COMAP, Inc.

Executive Publisher
Solomon A. Garfunkel

ILAP Editor
Chris Arney
Associate Director,
Mathematics Division
Program Manager,
Cooperative Systems
Army Research Office
P.O. Box 12211
Research Triangle Park,
NC 27709-2211
David.Arney1@ar1.army.mil

On Jargon Editor
Yves Nievergelt
Department of Mathematics
Eastern Washington University
Cheney, WA 99004
ynievergelt@ewu.edu

Reviews Editor
James M. Cargal
Mathematics Dept.
Troy University—
Montgomery Campus
231 Montgomery St.
Montgomery, AL 36104
jmcargal@sprintmail.com

Chief Operating Officer
Laurie W. Aragón

Production Manager
George W. Ward

Director of Educ. Technology
Roland Cheyney

Production Editor
Pauline Wright

Copy Editor
Timothy McLean

Distribution
Kevin Darcy
John Tomicek

Graphic Designer
Daiva Kiliulis

Vol. 26, No. 3

Editor

Paul J. Campbell
Campus Box 194
Beloit College
700 College St.
Beloit, WI 53511-5595
campbell@beloit.edu

Associate Editors

Don Adolphson
Chris Arney
Aaron Archer
Ron Barnes
Arthur Benjamin
Robert Bosch
James M. Cargal
Murray K. Clayton
Lisette De Pillis
James P. Fink
Solomon A. Garfunkel
William B. Gearhart
William C. Giauque
Richard Haberman
Jon Jacobsen
Walter Meyer
Yves Nievergelt
Michael O'Leary
Catherine A. Roberts
John S. Robertson
Philip D. Straffin
J.T. Sutcliffe

Brigham Young University
Army Research Office
AT&T Shannon Research Laboratory
University of Houston—Downtown
Harvey Mudd College
Oberlin College
Troy University—Montgomery Campus
University of Wisconsin—Madison
Harvey Mudd College
Gettysburg College
COMAP, Inc.
California State University, Fullerton
Brigham Young University
Southern Methodist University
Harvey Mudd College
Adelphi University
Eastern Washington University
Towson University
College of the Holy Cross
Georgia Military College
Beloit College
St. Mark's School, Dallas

Subscription Rates for 2005 Calendar Year: Volume 26

Membership Plus

Individuals subscribe to *The UMAP Journal* through COMAP's Membership Plus. This subscription also includes a CD-ROM of our annual collection *UMAP Modules: Tools for Teaching*, our organizational newsletter *Consortium*, on-line membership that allows members to download and reproduce COMAP materials, and a 10% discount on all COMAP purchases.

(Domestic)	#2520	\$ 99
(Outside U.S.)	#2521	\$111

Institutional Plus Membership

Institutions can subscribe to the *Journal* through either Institutional Plus Membership, Regular Institutional Membership, or a Library Subscription. Institutional Plus Members receive two print copies of each of the quarterly issues of *The UMAP Journal*, our annual collection *UMAP Modules: Tools for Teaching*, our organizational newsletter *Consortium*, on-line membership that allows members to download and reproduce COMAP materials, and a 10% discount on all COMAP purchases.

(Domestic)	#2570	\$456
(Outside U.S.)	#2571	\$479

Institutional Membership

Regular Institutional members receive print copies of *The UMAP Journal*, our annual collection *UMAP Modules: Tools for Teaching*, our organizational newsletter *Consortium*, and a 10% discount on all COMAP purchases.

(Domestic)	#2540	\$198
(Outside U.S.)	#2541	\$220

Web Membership

Web membership does not provide print materials. Web members can download and reproduce COMAP materials, and receive a 10% discount on all COMAP purchases.

(Domestic)	#2510	\$41
(Outside U.S.)	#2510	\$41

To order, send a check or money order to COMAP, or call toll-free
1-800-77-COMAP (1-800-772-6627).

The UMAP Journal is published quarterly by the Consortium for Mathematics and Its Applications (COMAP), Inc., Suite 210, 57 Bedford Street, Lexington, MA, 02420, in cooperation with the American Mathematical Association of Two-Year Colleges (AMATYC), the Mathematical Association of America (MAA), the National Council of Teachers of Mathematics (NCTM), the American Statistical Association (ASA), the Society for Industrial and Applied Mathematics (SIAM), and The Institute for Operations Research and the Management Sciences (INFORMS). The Journal acquaints readers with a wide variety of professional applications of the mathematical sciences and provides a forum for the discussion of new directions in mathematical education (ISSN 0197-3622).

Periodical rate postage paid at Boston, MA and at additional mailing offices.

Send address changes to: info@comap.com

COMAP, Inc. 57 Bedford Street, Suite 210, Lexington, MA 02420
© Copyright 2005 by COMAP, Inc. All rights reserved.

Table of Contents

Editorial

Back to the Future

Solomon A. Garfunkel.....185

About This Issue (and Others to Come).....187

Special Section on the MCM

Results of the 2005 Mathematical Contest in Modeling

Frank Giordano189

Abstracts of the Outstanding Papers and the Fusaro Papers217

From Lake Murray to a Dam Slurry

Clay Hambrick, Katie Lewis, and Lori Thomas229

Through the Breach: Modeling Flooding from a Dam Failure in South Carolina

Jennifer Kohlenberg, Michael Barnett, and Scott Wood245

Analysis of Dam Failure in the Saluda River Valley

Ryan Bressler, Christina Polwarth, and Braxton Osting263

Judge's Commentary: The Outstanding Flood Planning Papers

Daniel Zwillinger279

The Booth Tolls for Thee

Adam Chandler, Matthew Mian, and Pradeep Baliga283

A Single-Car Interaction Model of Traffic for a Highway Toll Plaza

Ivan Corwin, Sheel Ganatra, Nikita Rozenblyum299

Lane Changes and Close Following: Troublesome Tollbooth Traffic

Andrew Spann, Daniel Kane, and Dan Gulotta317

A Quasi-Sequential Cellular-Automaton Approach to Traffic Modeling

John Evans and Meral Reyhan331

The Multiple Single Server Queueing System

Azra Panjwani, Yang Liu, and HuanHuan Qi.....345

Two Tools for Tollbooth Optimization

Ephrat Bitton, Anand Kulkarni, and Mark Shlimovich355

For Whom the Booth Tolls

Brian Camley, Bradley Klingenberg, and Pascal Getreuer373

Judge's Commentary: The Outstanding Tollbooths Papers

Kelly Black.....391

COMAR

Publisher's Editorial

Back to the Future

Solomon A. Garfunkel
 Executive Director
 COMAP, Inc.
 57 Bedford St., Suite 210
 Lexington, MA 02420
 s.garfunkel@mail.comap.com

First, a mea culpa. I recently attended a showing of the movie “Good Night and Good Luck” and was taken by the courage of Edward R. Murrow, Fred Friendly, et al. at CBS during the McCarthy era. And I felt embarrassed. For a number of years, I have watched several of my colleagues in mathematics and mathematics education work hard to destroy much of the progress that we have made—and I have been silent. The pressure to stay quiet is strong. COMAP lives in part on our ability to secure grants from the National Science Foundation. NSF doesn't enjoy controversy. Moreover, any number of the people that I see as destructive sit on proposal review panels from time to time. And they are very political. Single-issue politics is always quite ugly. I suspect that most if not all of this group would consider themselves to be liberals; but they have no trouble working with this most conservative of administrations as long as their views of mathematics education prevail—even if that means the end of science education at NSF.

In the early 1970s, when I first became seriously involved in mathematics education and the world of proposals, grants, etc., there was a constant complaint from program officers at NSF: Mathematicians simply did not write proposals, and when called upon to review proposals, they invariably savaged their mathematical colleagues. Hence mathematics education grants were well below the numbers that the importance of the subject justified. NSF program officers came to mathematics conferences and all but begged us to ask them for money. They also pleaded with us to speak with one voice, that is, to iron out our differences, figure out for ourselves what the priorities should be, and get to work together on attacking the important problems rather than each other.

And believe it or not, by the end of the 1980s, mostly because of the courage of the NCTM leadership and the good offices of MSEB, we got our collective act together. We all quoted the *Standards* and *A Nation at Risk*, and *Everybody Counts*,

The UMAP Journal 26 (3) (2005) 185–186. ©Copyright 2005 by COMAP, Inc. All rights reserved. Permission to make digital or hard copies of part or all of this work for personal or classroom use is granted without fee provided that copies are not made or distributed for profit or commercial advantage and that copies bear this notice. Abstracting with credit is permitted, but copyrights for components of this work owned by others than COMAP must be honored. To copy otherwise, to republish, to post on servers, or to redistribute to lists requires prior permission from COMAP.

and we wrote proposals to make the vision of those documents come to pass. We began to receive funding at a level that made real change possible—and we are reaping the benefits today with increased NAEP and SAT scores.

So what did we decide to do? Shoot ourselves in whatever foot we could find! We began the math wars; we went back to savaging our colleagues; we made NSF look bad in the eyes of Congress; we gave succor and ammunition to our enemies; and we lost our intellectual honesty in the name of winning political favor. The result is an NSF science education budget that is greatly reduced and skewed against mathematics. Funding has moved dramatically from curriculum- and staff-development to “research” in mathematics education. People and organizations directly responsible for the demonstrated successes of the past two decades are being told that there is no room at the inn. In the name of practicality, we reward mediocrity.

There are consequences of these actions. Just as we learned that natural disasters require competent people and institutions (and not simply political hacks at the helm), there will be real and serious consequences for mathematics and mathematics education because of the present funding environment. Of course, these consequences are several years away and so safe from existing politicians’ blame or attention. Nevertheless, we are headed for disaster unless we have the courage to stand up and fight—today. This is precisely equivalent to the global warming debate. We are poisoning our profession just as we poison our atmosphere. And we are running out of time, because systems take as long to fix as they do to break.

I call on the staff of NSF to take credit for their own successes and tell the community about what they know works—even if the current administration wants to tell a different story. I call on the private foundations to step into the coming void and fill in until the current federal policies turn around. And I call on members of our community who understand what’s at stake to stand up and be counted.

About the Author

Sol Garfunkel received his Ph.D. in mathematical logic from the University of Wisconsin in 1967. He was at Cornell University and at the University of Connecticut at Storrs for 11 years and has dedicated the last 25 years to research and development efforts in mathematics education. He has been the Executive Director of COMAP since its inception in 1980.

He has directed a wide variety of projects, including UMAP (Undergraduate Mathematics and Its Applications Project), which led to the founding of this *Journal*, and HiMAP (High School Mathematics and Its Applications Project), both funded by the NSF. For Annenberg/CPB, he directed three telecourse projects: *For All Practical Purposes* (in which he also appeared as the on-camera host), *Against All Odds: Inside Statistics* (still showing on late-night TV in New York!), and *In Simplest Terms: College Algebra*. He is currently co-director of the Applications Reform in Secondary Education (ARISE) project, a comprehensive curriculum development project for secondary school mathematics.

Important Note from the Editor

About This Issue (and Others to Come)

Paul J. Campbell

Editor

This issue of *The UMAP Journal* represents a departure from past practice and a further step toward electronic publishing.

For its first five years, the *Journal* published 512 pp/yr with a supplementary volume of *UMAP Modules: Tools for Teaching* (at extra cost to subscribers) that ran between 1044 and 1258 pp. Those were typescript pages that held only half the content of a page of today's *Journal*.

In 1984, the Mathematical Contest in Modeling (MCM) was founded, the *Journal* began to be typeset, and the annual *UMAP Modules: Tools for Teaching* supplement was bundled into the COMAP membership option for receiving the *Journal*. That supplemental volume, which libraries shelve as a separate serial, collected together UMAP Modules—and later also ILAP Modules—from the year's issues of the *Journal*, together with additional Modules (particularly longer ones) for which there was no room in the *Journal*.

We aimed for four 92-page issues per year and devoted one issue to the MCM. The size of the MCM issue has varied with the number of Outstanding teams, the length of their papers (sometimes the size of a small telephone book), and my ability to edit the papers down to a modeling core. The last year that we had only 368 pp in the *Journal* was 1992; the MCM issue in fact became a double issue (and more). In 2000, we had 530 pp, and the combined total for the *Journal* and the *Tools* volume has varied over the past 10 years between 642 and 715 pp. This year, the MCM yielded a record 10 Outstanding teams.

Meanwhile, costs for publishing on paper have risen faster than the *Journal's* income.

Hence, spurred by the desire to control costs, but also by the intention to make the contents of the *Journal* and the *Tools* volume more usable by members, we have settled on the following plan:

*COMAP members will receive four 92-page issues of the Journal,
plus a CD-ROM bundled into the MCM issue.*

The UMAP Journal 26 (3) (2005) 187–188. ©Copyright 2005 by COMAP, Inc. All rights reserved. Permission to make digital or hard copies of part or all of this work for personal or classroom use is granted without fee provided that copies are not made or distributed for profit or commercial advantage and that copies bear this notice. Abstracting with credit is permitted, but copyrights for components of this work owned by others than COMAP must be honored. To copy otherwise, to republish, to post on servers, or to redistribute to lists requires prior permission from COMAP.

Here are the particulars:

- As with other COMAP electronic products, the files on the CD-ROM will be Adobe Acrobat PDF files. In particular, color images that are rendered only in black and white in the printed copy will appear in the PDF files in color.
- The ICM and MCM issues, like the other two issues, will be limited to 92 *print* pages each.
- If an issue runs longer than 92 pp, some articles will not appear in print but only on the CD-ROM. However, all articles on the CD-ROM will appear in the printed table of contents and are regarded as published in the *Journal*. Pagination will run continuously, including in sequence articles that do not appear in printed form. *So, if you notice that, say, page 350 in the printed copy is followed by page 403, your copy is not necessarily defective!* The articles corresponding to the intervening pages should be on the CD-ROM.
- The CD-ROM will contain an entire year of *Journal* issues.
- The *Tools* volume will no longer appear as a printed volume but only in electronic form on the CD-ROM.
- We remind readers of the COMAP's policy concerning usage of material appearing in the *Journal*, which applies to all material on the CD-ROM. The policy appears as a footnote on the first page of each article:

Permission to make digital or hard copies of part or all of this work for personal or classroom use is granted without fee provided that copies are not made or distributed for profit or commercial advantage and that copies bear this notice. Abstracting with credit is permitted, but copyrights for components of this work owned by others than COMAP must be honored. To copy otherwise, to republish, to post on servers, or to redistribute to lists requires prior permission from COMAP.

We hope that you will find this arrangement, if not entirely satisfying, at least satisfactory. It will mean that we will not have to procrusteanize the content of the *Journal* to fit a fixed number of allocated pages. For example, we might otherwise need to select only two or three of the MCM Outstanding papers to publish (a hard task indeed!). Instead, we can continue to bring you the full content as in the past.

Modeling Forum

Results of the 2005 Mathematical Contest in Modeling

Frank Giordano, MCM Director

Naval Postgraduate School

1 University Circle

Monterey, CA 93943-5000

frgiorda@nps.navy.mil

Introduction

A total of 664 teams of undergraduates, from 259 institutions and 306 departments in 10 countries, spent the second weekend in February working on applied mathematics problems in the 21st Mathematical Contest in Modeling (MCM).

The 2005 MCM began at 8:00 P.M. EST on Thursday, February 3 and ended at 8:00 P.M. EST on Monday, February 7. During that time, teams of up to three undergraduates were to research and submit an optimal solution for one of two open-ended modeling problems. Students registered, obtained contest materials, downloaded the problems at the appropriate time, and entered completion data through COMAP'S MCM Website. After a weekend of hard work, solution papers were sent to COMAP on Monday. The top papers appear in this issue of *The UMAP Journal*.

Results and winning papers from the first 20 contests were published in special issues of *Mathematical Modeling* (1985–1987) and *The UMAP Journal* (1985–2004). The 1994 volume of *Tools for Teaching*, commemorating the tenth anniversary of the contest, contains all of the 20 problems used in the first 10 years of the contest and a winning paper for each year. Limited quantities of that volume and of the special MCM issues of the *Journal* for the last few years are available from COMAP. That volume is available on COMAP'S special Modeling Resource CD-ROM (<http://www.comap.com/product/?idx=613>). In addition, COMAP will shortly release a new volume, *The MCM at 21*, which will contain

The UMAP Journal 26 (3) (2005) 189–216. ©Copyright 2005 by COMAP, Inc. All rights reserved. Permission to make digital or hard copies of part or all of this work for personal or classroom use is granted without fee provided that copies are not made or distributed for profit or commercial advantage and that copies bear this notice. Abstracting with credit is permitted, but copyrights for components of this work owned by others than COMAP must be honored. To copy otherwise, to republish, to post on servers, or to redistribute to lists requires prior permission from COMAP.

all of the 20 problems from the second 10 years of the contest and a winning paper for each year.

This year's Problem A asked teams to develop a model showing the consequences of a massive dam failure. Problem B asked teams to propose a model to help determine the optimal number of tollbooths in a barrier-toll plaza. The 10 Outstanding solution papers are published in this issue of *The UMAP Journal*, along with commentary from problem authors, contest judges, and outside experts.

In addition to the MCM, COMAP also sponsors the Interdisciplinary Contest in Modeling (ICM) and the High School Mathematical Contest in Modeling (HiMCM). The ICM, which runs concurrently with MCM, offers a modeling problem involving concepts in operations research, information science, and interdisciplinary issues in security and safety. Results of this year's ICM are on the COMAP Website at <http://www.comap.com/undergraduate/contests>; results and Outstanding papers appeared in Vol. 26 (2005), No. 2. The HiMCM offers high school students a modeling opportunity similar to the MCM. Further details about the HiMCM are at <http://www.comap.com/highschool/contests>.

Problem A: Flood Planning

Lake Murray in central South Carolina is formed by a large earthen dam, which was completed in 1930 for power production. Model the flooding downstream in the event there is a catastrophic earthquake that breaches the dam.

Two particular questions:

1. Rawls Creek is a year-round stream that flows into the Saluda River a short distance downriver from the dam. How much flooding will occur in Rawls Creek from a dam failure, and how far back will it extend?
2. Could the flood be so massive downstream that water would reach up to the S.C. State Capitol Building, which is on a hill overlooking the Congaree River?

Problem B: Tollbooths

Heavily-traveled toll roads such as the Garden State Parkway in New Jersey, Interstate 95, and so forth, are multilane divided highways that are interrupted at intervals by toll plazas. Because collecting tolls is usually unpopular, it is desirable to minimize motorist annoyance by limiting the amount of traffic disruption caused by the toll plazas. Commonly, a much larger number of tollbooths is provided than the number of travel lanes entering the toll plaza. Upon entering the toll plaza, the flow of vehicles fans out to the larger number of tollbooths, and when leaving the toll plaza, the flow of vehicles is required

to squeeze back down to a number of travel lanes equal to the number of travel lanes before the toll plaza. Consequently, when traffic is heavy, congestion increases upon departure from the toll plaza. When traffic is very heavy, congestion also builds at the entry to the toll plaza because of the time required for each vehicle to pay the toll.

Make a model to help you determine the optimal number of tollbooths to deploy in a barrier-toll plaza. Explicitly consider the scenario where there is exactly one tollbooth per incoming travel lane. Under what conditions is this more or less effective than the current practice? Note that the definition of “optimal” is up to you to determine.

The Results

The solution papers were coded at COMAP headquarters so that names and affiliations of the authors would be unknown to the judges. Each paper was then read preliminarily by two “triage” judges at either Appalachian State University (Flood Planning Problem) or at the National Security Agency (Tollbooths Problem). At the triage stage, the summary and overall organization are the basis for judging a paper. If the judges’ scores diverged for a paper, the judges conferred; if they still did not agree on a score, a third judge evaluated the paper.

This year, again an additional Regional Judging site was created at the U.S. Military Academy to support the growing number of contest submissions.

Final judging took place at Harvey Mudd College, Claremont, California. The judges classified the papers as follows:

	Outstanding	Meritorious	Honorable Mention	Successful Participation	Total
Flood Planning Problem	3	25	50	94	172
Tollbooths Problem	<u>7</u>	<u>60</u>	<u>145</u>	<u>280</u>	<u>492</u>
	10	85	195	374	664

The 10 papers that the judges designated as Outstanding appear in this special issue of *The UMAP Journal*, together with commentaries. We list those teams and the Meritorious teams (and advisors) below; the list of all participating schools, advisors, and results is in the **Appendix**.

Outstanding Teams

Institution and Advisor	Team Members
-------------------------	--------------

Flood Planning Papers

“From Lake Murray to a Dam Slurry”

Harvey Mudd College
Claremont, CA
Jon Jacobsen

Clay Hambrick
Katie Lewis
Lori Thomas

“Through the Breach: Modeling Flooding
from a Dam Failure in South
Carolina”

University of Saskatchewan
Saskatoon, SK, Canada
James Brooke

Jennifer Kohlenberg
Michael Barnett
Scott Wood

“Analysis of Dam Failure in the Saluda
River Valley”

University of Washington
Seattle, WA
Rekha Thomas

Ryan Bressler
Christina Polwarth
Braxton Osting

Tollbooths Papers

“The Booth Tolls for Thee”

Duke University
Durham, NC
William G. Mitchener

Adam Chandler
Matthew Mian
Pradeep Baliga

“A Single-Car Interaction Model of Traffic
for a Highway Toll Plaza”

Harvard University
Cambridge, MA
Clifford H. Taubes

Sheel Ganatra
Ivan Corwin
Nikita Rozenblyum

“Lane Changes and Close Following:
Troublesome Tollbooth Traffic”

Massachusetts Institute of Technology
Cambridge, MA
Martin Bazant

Andrew Spann
Daniel Kane
Dan Gulotta

“A Quasi-Sequential Cellular Automaton
Approach to Traffic Modeling”

Rensselaer Polytechnic Institute
Troy, NY
Peter Kramer

John Evans
Meral Reyhan

“Two Tools for Tollbooth Optimization”

University of California, Berkeley
Berkeley, CA
L. Craig Evans

Ephrat Bitton
Anand Kulkarni
Mark Shlimovich

“The Multiple Single-Server Queueing
System”

University of California, Berkeley
Berkeley, CA
Jim Pitman

Azra Panjwani
Yang Liu
Huan Qi

“For Whom the Booth Tolls”

University of Colorado
Boulder, CO
Anne Dougherty

Brian Camley
Bradley Klingenberg
Pascal Getreuer

Meritorious Teams

Flood Planning Papers (25 teams)

Albion College, Albion, MI (Darren Mason)
Bucknell University, Lewisburg, PA (Karl Voss)
Carroll College, Helena, MT (Sam Alvey)
China University of Mining and Technology, Xuzhou, Jiangsu, China (Zhang Xingyong)
College of Science, Southeast University, Nanjing, Jiangsu, China (Jia Xingang)
Duke University, Durham, NC (Owen Astrachan)
Fudan University, Shanghai, Shanghai, China (Cai Zhijie)
Harvey Mudd College, Claremont, CA (Jon Jacobsen)
James Madison University, Harrisonburg, VA (James Sochacki)
Lewis and Clark College, Portland, OR (Robert Owens)
McGill University, Montreal, Quebec, Canada (Nilima Nigam)
Midlands Technical College, West Columbia, SC (John Long)

Nanjing University, Nanjing, Jiangsu, China (Bo Wen)
National University of Defense Technology, Changsha, Hunan, China (Yi Wu)
NC School of Science & Mathematics, Durham, NC (Daniel Teague)
United States Military Academy, West Point, NY (John Jackson)
University of Delaware, Newark, DE (Louis Rossi)
University of Electronic Science and Technology of China, Chengdu, Sichuan, China
(Gao Qing)
University of Washington, Seattle, WA (James Morrow)
Western Washington University, Bellingham, WA (Saim Ural)
Wuhan University, Wuhan, Hubei, China (Deng Aijiao)
Wuhan University, Wuhan, Hubei, China (Hu Xinqi)
Youngstown State University, Youngstown, OH (Angela Spalsbury)
Zhejiang Gongshang University, Hangzhou, Zhejiang, China (Ding Zhengzhong)
Zhejiang University City College, Hangzhou, Zhejiang, China (Huang Huang)

Tollbooths Papers (60 teams)

Albertson College, Caldwell, ID (Michael Hitchman)
Asbury College, Wilmore, KY (David Coulliette)
Asbury College, Wilmore, KY (Kenneth Rietz)
Beijing Normal University, School of Mathematical Sciences, Beijing, China
(Huang Haiyang)
Bethel University, St. Paul, MN (William Kinney)
California Polytechnic State University, San Luis Obispo, CA (Jonathan Shapiro)
Central Washington University, Ellensburg, WA (Stuart Boersma)
Chongqing University, Chongqing, China (Li Fu)
Chongqing University, Chongqing, China (He Renbin)
College of Mount St. Joseph, Cincinnati, OH (Scott Sportsman)
Cornell University, Ithaca, NY (Alexander Vladimirovsky)
Davidson College, Davidson, NC (Malcolm Campbell)
Davidson College, Davidson, NC (Mark Foley)
Duke University, Durham, NC (Owen Astrachan)
Duke University, Durham, NC (William Mitchener)
Eastern Oregon University, La Grande, OR (Anthony Tovar)
Harbin Institute of Technology Science Faculty, Harbin, Heilongjian, China
(Shang Shouting)
Harvey Mudd College, Claremont, CA (Ran Libeskind-Hadas) (two teams) Hastings
College, Hastings, NE (Dave Cooke)
Jiangsu University, Zhenjiang, Jiangsu, China (Gang Xu)
Kansas State University, Manhattan, KS (David Auckly)
Lafayette College, Easton, PA (Ethan Berkove)
Luther College, Decorah, IA (Reginald Laursen) (two teams)
Nanchang University, Nanchang, Jiangxi, China (Liao Chuangrong)
Northern Kentucky University, Highland Heights, KY (Gail Mackin)
Northwest University, Xi'an, Shaanxi, China (Wang Liantang)
School of Economics & Management, Tsinghua University, Beijing, China (Xie Qun)
School of Financial Mathematics, Peking University, Beijing, China (Lan Wu)
School of Mathematical Sciences, Peking University, Beijing (Liu Xufeng)
School of Science, Beijing University of Posts and Telecommunications, Beijing, China
(Sun Hongxiang)
Shanghai Jiao Tong University, Shanghai, China (Song Baorui)

Shanghai Jiao Tong University, Shanghai, China (Huang Jianguo)
South China University of Technology, Guangzhou, Guangdong, China (Liu Shen Quan)
South-China Normal University, Guangzhou, Guangdong, China (Wang Henggeng)
Southeast University, Nanjing, Jiangsu, China (Dan He)
Southeast University, Nanjing, Jiangsu, China (Wang Liyan)
Truman State University, Kirksville, MO (Steve Smith)
Tsinghua University, Beijing, China (Hu Zhiming)
Tsinghua University, Beijing, China (Lu Mei)
University College Cork, Cork, Ireland (Donal Hurley)
University of California, Berkeley, Berkeley, CA (Lawrence Evans)
University of Colorado at Boulder, Boulder, CO (Michael Ritzwoller)
University of Delaware, Newark, DE (Louis Rossi)
University of Pittsburgh, Pittsburgh, PA (Christopher Earls)
University of Pittsburgh, Pittsburgh, PA (Jonathan Rubin)
University of Puget Sound, Tacoma, WA (DeWayne Derryberry)
University of Richmond, Richmond, VA (Kathy Hoke) (two teams)
University of Saskatchewan, Saskatoon, SK, Canada (James Brooke)
University of Western Ontario, London, ON, Canada (Allan MacIsaac)
Wake Forest University, Winston-Salem, NC (Miaohua Jiang) (two teams)
Wesleyan College, Macon, GA (Joseph Iskra)
Western Washington University, Bellingham, WA (Saim Ural)
Worcester Polytechnic Institute, Worcester, MA (Suzanne Weekes)
Wuhan University, Wuhan, Hubei, China (Chen Wenyi)
Wuhan University of Technology, Wuhan, Hubei, China (Huang Wei)
Zhejiang University, Hangzhou, Zhejiang, China (Yong He)

Awards and Contributions

Each participating MCM advisor and team member received a certificate signed by the Contest Director and the appropriate Head Judge.

INFORMS, the Institute for Operations Research and the Management Sciences, recognized the teams from the University of Washington (Flood Planning Problem) and University of California, Berkeley (Advisor: Jim Pitman) (Toll-booths Problem) as INFORMS Outstanding teams and provided the following recognition:

- a letter of congratulations from the current president of INFORMS to each team member and to the faculty advisor;
- a check in the amount of \$300 to each team member;
- a bronze plaque for display at the team's institution, commemorating their achievement;
- individual certificates for team members and faculty advisor as a personal commemoration of this achievement;

- a one-year student membership in INFORMS for each team member, which includes their choice of a professional journal plus the *OR/MS Today* periodical and the INFORMS society newsletter;
- a one-year subscription access to the COMAP modeling materials Website for the faculty advisor.

The Society for Industrial and Applied Mathematics (SIAM) designated one Outstanding team from each problem as a SIAM Winner. The teams were from Harvey Mudd College (Flood Planning Problem) and Rensselaer Polytechnic Institute (Tollbooths Problem). Each of the team members was awarded a \$300 cash prize and the teams received partial expenses to present their results in a special Minisymposium at the SIAM Annual Meeting in New Orleans in July. Their schools were given a framed hand-lettered certificate in gold leaf.

The Mathematical Association of America (MAA) designated one Outstanding team from each problem as an MAA Winner. The teams were from the University of Saskatchewan (Flood Planning Problem) and Duke University (Tollbooths Problem). With partial travel support from the MAA, both teams presented their solutions at a special session of the MAA Mathfest in Albuquerque, NM in August. Each team member was presented a certificate by Richard S. Neal, Co-Chair of the MAA Committee on Undergraduate Student Activities and Chapters.

Ben Fusaro Award

Two Meritorious papers were selected for the Ben Fusaro Award, named for the Founding Director of the MCM and awarded for the second time this year. It recognizes an especially creative approach; details concerning the award, its judging, and Ben Fusaro are in *The UMAP Journal* 25 (3) (2004): 195–196. The Ben Fusaro Award teams were from McGill University (Flood Planning Problem) and University of California, Berkeley (Advisor: Lawrence Evans) (Tollbooths Problem). Each team received a plaque from COMAP.

Judging

Director

Frank R. Giordano, Naval Postgraduate School, Monterey, CA

Associate Directors

Robert L. Borrelli, Mathematics Dept., Harvey Mudd College, Claremont, CA

Patrick J. Driscoll, Dept. of Systems Engineering, U.S. Military Academy,
West Point, NY

Contest Coordinator

Kevin Darcy, COMAP Inc., Lexington, MA

Flood Planning Problem

Head Judge

Marvin S. Keener, Executive Vice-President, Oklahoma State University,
Stillwater, OK (MAA)

Associate Judges

Peter Anspach, National Security Agency, Ft. Meade, MD (Triage)

Courtney Coleman, Mathematics Dept., Harvey Mudd College,
Claremont, CA (SIAM)

Ben Fusaro, Mathematics Dept., Florida State University, Tallahassee, FL

Jerry Griggs, Mathematics Dept., University of South Carolina, Columbia, SC

John Kobza, Mathematics Dept., Texas Tech University, Lubbock, TX
(INFORMS)

Michael Moody, Olin College of Engineering, Needham, MA

Kathleen M. Shannon, Dept. of Mathematics and Computer Science,
Salisbury University, Salisbury, MD (MAA)

Daniel Zwillinger, Newton, MA (SIAM)

Tollbooths Problem

Head Judge

Maynard Thompson, Mathematics Dept., University of Indiana,
Bloomington, IN

Associate Judges

William C. Bauldry, Chair, Dept. of Mathematical Sciences,
Appalachian State University, Boone, NC (Triage)

Kelly Black, Mathematics Dept., University of New Hampshire,
Durham, NH (SIAM)

Karen D. Bolinger, Mathematics Dept., Clarion University of Pennsylvania,
Clarion, PA (SIAM)

J. Douglas Faires, Youngstown State University, Youngstown, OH (SIAM)

William P. Fox, Mathematics Dept., Francis Marion University, Florence, SC

Mario Juncosa, RAND Corporation, Santa Monica, CA (retired)

Don Miller, Mathematics Dept., St. Mary's College, Notre Dame, IN

John L. Scharf, Mathematics Dept., Carroll College, Helena, MT

Dan Solow, Mathematics Dept., Case Western Reserve University,
Cleveland, OH (INFORMS)

Michael Tortorella, Dept. of Industrial and Systems Engineering,
Rutgers University, Piscataway, NJ

Marie Vanisko, Dept. of Mathematics, California State University,
Stanislaus, CA (MAA)

Richard Douglas West, Francis Marion University, Florence, SC

Regional Judging Session

Head Judge

Patrick J. Driscoll, Dept. of Systems Engineering

Associate Judges

Darrall Henderson, Dept. of Mathematical Sciences

Steven Henderson, Dept. of Systems Engineering

Steven Horton, Dept. of Mathematical Sciences

Michael Jaye, Dept. of Mathematical Sciences

—all of the U.S. Military Academy, West Point, NY

Triage Sessions:

Flood Planning Problem

Head Triage Judge

Peter Anspach, National Security Agency (NSA), Ft. Meade, MD

Associate Judges

Dean McCullough, High Performance Technologies, Inc.

Robert L. Ward (retired)

Blair Kelly,

Craig Orr,

Brian Pilz,

Eric Schram,

and other members of NSA.

Tollbooths Problem

Head Triage Judge

William C. Bauldry, Chair

Associate Judges

Terry Anderson,

Mark Ginn,

Jeff Hirst,

Rick Klima,

Katie Mawhinney,

and

Vickie Williams

—all from Dept. of Math'l Sciences, Appalachian State University, Boone, NC

Fusaro Award Committee

Flood Planning Problem:

Peter Anspach, National Security Agency, Ft. Meade, MD

Michael Moody, Olin College of Engineering, Needham, MA

Tollbooths Problem:

William C. Bauldry, Chair, Dept. of Mathematical Sciences,
Appalachian State University, Boone, NC

Kathleen M. Shannon, Dept. of Mathematics and Computer Science,
Salisbury University, Salisbury, MD

Sources of the Problems

The Flood Planning Problem was contributed by Jerry Griggs (Mathematics Dept., University of South Carolina, Columbia, SC).

The Tollbooths Problem was contributed by Michael Tortorella (Dept. of Industrial and Systems Engineering, Rutgers University, Piscataway, NJ).

Acknowledgments

Major funding for the MCM is provided by the National Security Agency and by COMAP. We thank Dr. Gene Berg of NSA for his coordinating efforts. Additional support is provided by the Institute for Operations Research and the Management Sciences (INFORMS), the Society for Industrial and Applied Mathematics (SIAM), and the Mathematical Association of America (MAA). We are indebted to these organizations for providing judges and prizes.

This year we have two new sponsors, whom we thank for their involvement and support:

- IBM Business Consulting Services, Center for Business Optimization; and
- Two Sigma Investments. (This group of experienced, analytical, and technical financial professionals based in New York builds and operates sophisticated quantitative trading strategies for domestic and international markets. The firm is successfully managing several billion dollars using highly automated trading technologies. For more information about Two Sigma, please visit <http://www.twosigma.com>.)

We thank the MCM judges and MCM Board members for their valuable and unflagging efforts. Harvey Mudd College, its Mathematics Dept. staff, and Prof. Borrelli were gracious hosts to the judges.

Cautions

To the reader of research journals:

Usually a published paper has been presented to an audience, shown to colleagues, rewritten, checked by referees, revised, and edited by a journal editor. Each of the student papers here is the result of undergraduates working on a problem over a weekend; allowing substantial revision by the authors could give a false impression of accomplishment. So these papers are essentially *au naturel*. Editing (and sometimes substantial cutting) has taken place: Minor errors have been corrected, wording has been altered for clarity or economy, and style has been adjusted to that of *The UMAP Journal*. Please peruse these student efforts in that context.

To the potential MCM Advisor:

It might be overpowering to encounter such output from a weekend of work by a small team of undergraduates, but these solution papers are highly atypical. A team that prepares and participates will have an enriching learning experience, independent of what any other team does.

COMAP's Mathematical Contest in Modeling and Interdisciplinary Contest in Modeling are the only international modeling contests in which students work in teams. Centering its educational philosophy on mathematical modeling, COMAP uses mathematical tools to explore real-world problems. It serves the educational community as well as the world of work by preparing students to become better-informed and better-prepared citizens.

Appendix: Successful Participants

KEY:

P = Successful Participation

H = Honorable Mention

M = Meritorious

O = Outstanding (published in this special issue)

INSTITUTION	CITY	ADVISOR	A	B
CALIFORNIA				
Cal Poly Pomona	Pomona	Hubertus von Bremen	P	
		Ioana Mihaila		P
		Peter Siegel		P
California Baptist U.	Riverside	Catherine Kong		P
Calif. Poly. State U.	San Luis Obispo	Jonathan Shapiro		M,P
Calif. State Poly. U.	Pomona	Kurt Vandervoort		P
Calif. State U.	Seaside	Hongde Hu	P	
		Jeffrey Groah		P
Hartnell College	Salinas	Kelly Locke		P
Harvey Mudd College (CS)	Claremont	Jon Jacobsen	O,M	
		Ran Libeskind-Hadas		M,M
Pomona College	Claremont	Ami Radunskaya		P
Univ. of California (Stat)	Berkeley	L. Craig Evans		O,M
		Jim Pitman		O
COLORADO				
Colorado College	Colorado Springs	David Brown		P
Colorado State Univ.	Pueblo	Bruce Lundberg		P
Regis University	Denver	David Bahr		H,P
USAF Academy	USAF	Timothy Cooley	P	H
		James Rolf	P	
Univ. of Colorado	Boulder	Anne Dougherty		O
		Bengt Fornberg		H
		Michael Ritzwoller		M
U. of Northern Colo.	Denver	Lynn Bennethum		H
		Michael Jacobson		H
		Nathaniel Miller	P	
CONNECTICUT				
Southern Conn. State U.	New Haven	Ross Gingrich	H	
Western Conn. State U.	Danbury	Josephine Hamer		P
DELAWARE				
Univ. of Delaware	Newark	Louis Rossi	M	M

INSTITUTION	CITY	ADVISOR	A	B
FLORIDA				
Embry-Riddle University	Daytona Beach	Greg Spradlin		H
Jacksonville University	Jacksonville	Robert Hollister	H	
GEORGIA				
Georgia Southern Univ.	Statesboro	Laurene Fausett	H	P
State Univ. of West Georgia	Carrollton	Scott Gordon		H
Wesleyan College	Macon	Charles Benesh		P
		Joseph Iskra		M,H
IDAHO				
Albertson College	Caldwell	Michael Hitchman	P	M
Idaho State University	Pocatello	Robert Van Kirk		P
ILLINOIS				
Greenville College	Greenville	George Peters	P	
Illinois Institute of Tech.	Chicago	Michael Pelsmajer		P
Monmouth College	Monmouth	Howard Dwyer	H	
		Christopher Fasano		H
Northern Illinois Univ.	DeKalb	Chris Hurlburt		H,H
Wheaton College	Wheaton	Paul Isihara		P
INDIANA				
Earlham College	Richmond	Mic Jackson	P	P
(CS)		Charlie Peck	P	
Franklin College	Franklin	John Boardman		P
Rose-Hulman Inst. of Tech.	Terre Haute	David Rader		H,H
Saint Mary's College	Notre Dame	Joanne Snow		H,P
IOWA				
Grinnell College	Grinnell	Charles Cunningham	P	
		Karen Shuman		P,P
Luther College	Decorah	Steve Hubbard	P	
		Reginald Laursen		M,M
Mt. Mercy College	Cedar Rapids	K.R. Knopp		P
Simpson College	Indianola	James Bohy	H	
		Jeff Parmelee		P
		Murphy Waggoner		H,P
Wartburg College	Waverly	Brian Birgen		P
KANSAS				
Emporia State University	Emporia	Brian Hollenbeck		P
Kansas State University	Manhattan	David Auckly		M,P

INSTITUTION	CITY	ADVISOR	A	B
KENTUCKY				
Asbury College	Wilmore	David Coulliette		M
		Kenneth Rietz		M
Brescia University	Owensboro	Chris Tiahr		P
Morehead State University	Morehead	Michael Dobranski		P
Northern Kentucky University	Highland Heights	Gail Mackin	P	M
Thomas More College	Crestview Hills	Robert Riehemann	P	
MAINE				
Colby College	Waterville	Jan Holly		P
MARYLAND				
Hood College	Frederick	Betty Mayfield		H
Johns Hopkins University	Baltimore	Greg Eyink		H
		Fred Torcaso		H,P
Loyola College	Baltimore	Jiyuan Tao		P
Mount St. Mary's University	Emmitsburg	Fred Portier	P	P
Salisbury University	Salisbury	Michael Bardzell		P
Villa Julie College	Stevenson	Eileen McGraw		P
Washington College	Chestertown	Eugene Hamilton		P
MASSACHUSETTS				
College of the Holy Cross	Worcester	Gareth Roberts		P
Harvard University	Cambridge	Clifford Taubes		O
MIT	Cambridge	Martin Bazant		O
Olin College of Engineering	Needham	Burt Tilley		H
Salem State College	Salem	Kenny Ching		P
Simon's Rock College	Great Barrington	Allen Altman		P,P
		Michael Bergman	P	P
Smith College	Northampton	Ruth Haas	H	
University of Massachusetts	Lowell	James Graham-Eagle		P
Western New England College	Springfield	Lorna Hanes		P
Worcester Polytechnic Institute	Worcester	Suzanne Weekes		M,P
MICHIGAN				
Albion College	Albion	Darren Mason	M	P
Ferris State University	Big Rapids	Holly Price		H
Lawrence Technological University	Southfield	Ruth Favro	H	P
		Valentina Tobos		H
Siena Heights University	Adrian	Pamela Warton	P,P	
		Tim Husband		H
MINNESOTA				
Bethel University	St. Paul	William Kinney		M,P
Minnesota State University	Moorhead	Ellen Hill	P	
Saint John's University	Collegeville	Robert Hesse		H

INSTITUTION	CITY	ADVISOR	A	B
MISSOURI				
Drury University	Springfield	Bruce Callen		P
		Bob Robertson	H	P
Northwest Missouri State University	Maryville	Russell Euler		H
Saint Louis University	St. Louis	James Dowdy	H	
Southeast Missouri State University	Cape Girardeau	Robert Sheets		P
Truman State University	Kirksville	Steve Smith		M
MONTANA				
Carroll College	Helena	Sam Alvey	M	P
		Kelly Cline		H,P
NEBRASKA				
Hastings College	Hastings	Dave Cooke		M
NEW JERSEY				
New Jersey Institute of Technology	Newark	Roy Goodman		P
Rowan University	Glassboro	Hieu Nguyen		H,H
NEW MEXICO				
New Mexico Tech	Socorro	Brian Borchers		P
NEW YORK				
Clarkson University	Potsdam	Kathleen Fowler	H	H
		William Hesse		P
Colgate University	Hamilton	Warren Weckesser	H	
Concordia College	Bronxville	John Loase		H,P
Cornell University	Ithaca	Alexander Vladimirovsky	P	M
Hobart and William Smith Colleges	Geneva	Scotty Orr		P
Ithaca College	Ithaca	John Maceli		H
Nazareth College	Rochester	Daniel Birmajer		H
Rensselaer Polytechnic Institute	Troy	Peter Kramer		O,P
Roberts Wesleyan College	Rochester	Gary Raduns	P	
United States Military Academy	West Point	J. Billie		H
		John Jackson	M	
		Sakura Therrien		P
Westchester Community College	Valhalla	Marvin Littman	P	
NORTH CAROLINA				
Appalachian State University	Boone	Holly Hirst	P	
Davidson College	Davidson	Malcolm Campbell		M
		Tim Chartier		H,H
		Mark Foley		M
Duke University (CS)	Durham	William Mitchener		O,M
		Owen Astrachan	M	M

INSTITUTION	CITY	ADVISOR	A	B
Meredith College	Raleigh	Cammev Cole		P
NC School of Science & Math.	Durham	Daniel Teague	M	P
Wake Forest University	Winston-Salem	Miaohua Jiang		M,M
OHIO				
Bowling Green State Univ.	Bowling Green	Juan Bes	P	
College of Mount St. Joseph	Cincinnati	Scott Sportsman		M
Malone College	Canton	David Hahn		P
Miami University	Oxford	Doug Ward		P
University of Dayton	Dayton	Youssef Raffoul		H
Youngstown State University (CS)	Youngstown	Angela Spalsbury	M	H
		Michael Crescimanno	P	
OKLAHOMA				
Oklahoma State University	Stillwater	Lisa Mantini	H	
OREGON				
Eastern Oregon University	La Grande	David Allen		P
		Anthony Tovar		M
Lewis and Clark College	Portland	Robert Owens	M	P
Linfield College	McMinnville	Jennifer Nordstrom		P,P
Pacific University	Forest Grove	Christine Guenther		P
Southern Oregon University	Ashland	Kemble Yates		H
Western Oregon University	Monmouth	Maria Fung		P
PENNSYLVANIA				
Bloomsburg University	Bloomsburg	Kevin Ferland	H	P
Bucknell University	Lewisburg	Karl Voss	M	
Clarion Univ. of Pennsylvania	Clarion	Dana Madison		H
Drexel University	Philadelphia	Hugo Woerdeman		P
Gannon University	Erie	Michael Caulfield		H,P
Gettysburg College	Gettysburg	Bogdan Doytchinov	P	
Juniata College	Huntingdon	John Bukowski	H	
Lafayette College	Easton	Ethan Berkove		M,P
Slippery Rock University	Slippery Rock	Richard Marchand		P
University of Pittsburgh (Eng)	Pittsburgh	Jonathan Rubin	H	M
		Christopher Earls		M
Westminster College	New Wilmington	Barbara Faires		H
SOUTH CAROLINA				
Benedict College	Columbia	Balaji Iyengar		P
Francis Marion University	Florence	Thomas Fitzkee	P	
Midlands Technical College	West Columbia	John Long	M,H	

INSTITUTION	CITY	ADVISOR	A	B
SOUTH DAKOTA				
Mount Marty College	Yankton	Bonita Gacnik		P
		Stephanie Gruver	P	P
		James Miner	P	
SD School of Mines and Technology	Rapid City	Robert Kowalski		P
		Kyle Riley		H
TENNESSEE				
Austin Peay State University	Clarksville	Nell Rayburn	P	
TEXAS				
Angelo State University	San Angelo	Karl Havlak	P	
Austin College	Sherman	John Jaroma		P
Trinity University	San Antonio	Richard Cooper		P
		Allen Holder		P
VIRGINIA				
Eastern Mennonite University	Harrisonburg	Charles Cooley		P
		Leah Boyer	H,H	
James Madison University	Harrisonburg	Hasan Hamdan		H
		Caroline Smith	P	
		James Sochacki	M	
Maggie Walker Governor's School	Richmond	John Barnes		P,P
		Harold Houghton		P,P
Roanoke College	Salem	Jeffrey Spielman		P
University of Richmond	Richmond	Kathy Hoke		M,M
Virginia Western Community College	Roanoke	Steve Hammer	P	
		Ruth Sherman	P	
WASHINGTON				
Central Washington University	Ellensburg	Stuart Boersma		M
Heritage University	Toppenish	Richard Swearingen	P	H
Pacific Lutheran University	Tacoma	Daniel Heath		P,P
University of Puget Sound	Tacoma	DeWayne Derryberry		M
University of Washington	Seattle	James Morrow	M	H
		Rekha Thomas	O	H
Western Washington University	Bellingham	Saim Ural	M	M
		Tjalling Ypma		P,P
WISCONSIN				
Northland College	Ashland	William Long	P,P	

INSTITUTION	CITY	ADVISOR	A	B
CANADA				
Dalhousie University	Halifax	Dorothea Pronk		P,P
McGill University	Montreal	Antony Humphries		H
		Nilima Nigam	M	
University of Saskatchewan	Saskatoon	James Brooke	O	M
University of Western Ontario	London	Allan MacIsaac		M
York University	Toronto	Hongmei Zhu		P
		Huaiping Zhu	H	P
CHINA				
Anhui				
Anhui University	Hefei	Wang Xuejun		H
		Zhu Xiaobao		P
		Zhang Quanbing		P
		Wu Yunqi		P
Anhui Univ. of Technology and Science	Wuhu	Wang Chuanyu		P
Hefei University of Technology	Hefei	Gu Junli		H
		Zheng Qi		P
		Du Xueqiao		P
		Huang Youdu	P	
Univ. of Science and Technology of China	Hefei	Liu Yanjun		P
		Huang Zhangjin		P
		Yang Zhouwang	P	
		Sun Guangzhong		P
	(CS)			
Beijing				
BeiHang University	Beijing	Wu Sanxing		H
Beijing Institute of Science and Technology	Beijing	Sun Huafei		H
Beijing Institute of Technology	Beijing	Wang Hongzhou	H	P
		Yan Guifeng	H	P
Beijing Jiaotong University	Beijing	Wu Faen		P
		Wang Xiujuan		P,P
	(Eng)	Deng Xiaoqin	P	
	(Info)	Wang Bingtuan		P,P
	(Sci)	Feng Guochen		P
		Liu Minghui	H	P
		Wang Xiaoxia		H
Beijing Language and Culture University (CS)	Beijing	Liu Guilong	P	P
Beijing Materials Institute	Beijing	Li Zhenping	P	P
		Cheng Xiaohong		P,P

INSTITUTION	CITY	ADVISOR	A	B
Beijing Normal University	Beijing	Cui Hengjian	P	H
		Shen Fuxing		H
		He Qing		P,P
		Peng Fanglin		P
		Wang Jiayin		H
		Huang Haiyang		M
		Liu Laifu		P
Beijing University of Chemical Technology	Beijing	Liu Damin	P	
		Jiang Guangfeng	H	
		Yuan Wenyan		P
Beijing University of Posts and Telecomm.	Beijing	Jiang Xinhua		P
		Ding Jinkou		H
(Sci)	Beijing	Zhang Wenbo		P
		Wu Yunfeng		H
		Sun Hongxiang		M
		He Zuguo	H	H
		Xue Yi		P
Beijing University of Technology	Beijing	Chang Jingang	P	
		Guo Sili		P
		Yang Shilin	P	P
Central University of Finance and Economics	Beijing	Ge Binhua	H	H
		Huang Huiqing		H,P
China Agricultural University	Beijing	Zou Hui		H,P
Peking University	Beijing	Wang Ming		P
		Deng Minghua		H,P
		Tang Huazhong	P	
		Lan Wu		M
		Liu Xufeng		M,P
Renmin University of China (Statistics)	Beijing	Jin Yang		P
Tsinghua University	Beijing	Hu Zhiming		M,H
		Lu Mei		M,H
		Xie Qun		M
(Econ)	Beijing			
Chongqing				
Chongqing University	Chongqing	Li Chuandong	P	
		Liu Qiongfang	P	
		He Renbin		M
		Duan Zhengmin		H
		Wang Zongli		P
		Li Zhiliang	H	
		Fu Li		M
(Chem)	Chongqing			
(CS)	Chongqing			
Fujian				
Xiamen University (Info)	Xiamen	Zheng Xiaolian		H

INSTITUTION	CITY	ADVISOR	A	B
Guangdong				
Jinan University	Guangzhou	Hu Daiqiang		H
		Fan Suohai		P
(CS)		Luo Shizhuang	H	
(Electronics)		Ye Shiqi		P
Shandong University	Jinan	Ma Jianhua		P
South-China Normal University	Guangzhou	Wang Hengheng		M
(CS)		Li Hunan	P	P
(Info)		Yu Jianhua	H	
(Phys)		Liu Xiuxiang		H,P
South China University of Technology	Guangzhou	Liang Man Fa		P
		Liu Shen Quan		M
		Qin Yong An		P
		Liu Xiao Lan		H
Sun Yat-Sen University	Guangzhou	Feng Guo		H
		Jiang Xiao Long	H	
		Chen Ze Peng		P
		Yuan Zhou	H	
Hebei				
Hebei Polytechnic University	Tangshan	Wan Xinghuo		H
		Xiao Jixian	P	
		Tan Yili		H
North China Electric Power University	Baoding	Gu Gendai		H
		Liu Jinggang		H
		Shi Huifeng		H
		Zhang Po	P	
Shijiazhuang University of Economics	Shijiazhuang	Peng Jianping		P
		Kang Na		P
Heilongjiang				
Jia Mu-Si University	Jia Mu-si	Fan Wei		H
		Zhang Hong	P	P
Harbin Engineering University	Harbin	Yu Fei		P
		Zhang XiaoWei		P
		Luo Yue Sheng		P
Harbin Institute of Technology	Harbin	Shang Shouting	H	M
		Zhang Chiping		P,P
		Jiao Guanghong		P,P
		Liu Kean	P	H
		Wang Xilian	H	P
(Econ)		Wei Shang	H	
(Sci)		Hong Ge		P,P

INSTITUTION	CITY	ADVISOR	A	B
Harbin Medical University	Harbin	Wang QiangHu		P,P
Harbin University of Science and Technology	Harbin	Li Dongmei		H
		Chen Dongyan		H
		Tian Guangyue		H
		Wang Shuzhong		H
Northeast Agricultural University	Harbin	Li Fangge		P
Hubei				
China University of Geosciences (CS)	Wuhan	Luo Wenqiang		P
		Cai Zhihua		P
Huazhong University of Science & Technology	Wuhan	Yuan Linjie		P
		Wang Yongji		P
Wuhan University	Wuhan	Deng Aijiao	M	H
		Zhong Liuyi	H	
		Chen Wenyi		M,H
		Hu Xinqi	M	
		Yi Xuming		P
(Eng)		Luo Zhuangchu	P	
Wuhan University of Technology	Wuhan	Chen Ye		H
		Chu Jie	P	
		He Lang		H
		Huang Wei		M
		Li Guang		H,P
Hunan				
Central South University	Changsha	He Wei	H	
		Yi Kunnan		P
		Zhang Hongyan		P
(Bio)		Zhang Dianzhong		P
Hunan University	Changsha	Li Xiaopei		P
(Applied Math.)		Ma Bolin		P
(Info)		Ma Chuanxiu		P
(Stat)		Luo Han	P	
National University of Defense Technology	Changsha	Duan Xiaojun		P
		Mao Ziyang		P
(Math. & System Science)		Cheng Lizhi		P
		Wu Yi	M	
Inner Mongolia				
Inner Mongolia University	Hohhot	Wang Mei		P
		Ma Zhuang	P	

INSTITUTION	CITY	ADVISOR	A	B
Jiangsu				
China Univ. of Mining and Technology	Xuzhou	Wu Zongxiang		H
		Zhang Xingyong	M	
		Zhu Kaiyong		H,P
HoHai University	Suzhou	Rong Shen		P
Jiangsu University	Zhenjiang	Xu Gang		M,H
		Li Yimin		H,P
Nanjing University	Nanjing	Wu Zhaoyang	P	
		Chunying Duan		P
		Yao Tianxing		H,H
		Wen Bo	M	
(Phys)				
Nanjing Univ. of Finance and Economics	Nanjing	Wang Geng		P
Nanjing Univ. of Posts and Telecomm.	Nanjing	He Ming		H,H
Nanjing University of Sci. & Tech.	Nanjing	Xu Chungun	H	
		Liu Liwei		P
		Chen Peixin		H
		Zhang Zhengjun		P
		He Dan		M
		Wang Liyan		M
		Zhang Zhiqiang	P	P
(Sci)				
		Jia Xingang	M,P	
		Sun Zhizhong		P,P
Xuzhou Institute of Technology	Xuzhou	Jiang Yingzi	H	H
Jiangxi				
East China Inst. of Tech. (Foreign Lang.)	Fuzhou	Cai Ying		P
Jiangxi Normal University	Nanchang	Wu Gengxiu		H
		Xiongjun		P
Nanchang University	Nanchang	Chen Tao		H
		Chen Yuju	P	
		Liao Chuangrong		M
		Ma Xincheng Ma		P
Jilin				
Jilin University	Changchun	Zou Yongkui	H,P	
		Zhou Lai		H
		Fang Peichen		H,H
		Pei Yongchen		P,P
Northeast Normal University	Changchun	Li Zuofeng	P	P

INSTITUTION	CITY	ADVISOR	A	B
Liaoning				
Dalian Maritime University (CS)	Dalian	Zhang Yunjie Yang Shuqin	P	P P,P
Dalian Nationalities University (CS)	Dalian	Guo Qiang Li Xiaoniu	P	H H,H
Dalian University (Info)	Dalian	Tan Xinxin Gang Jiatai	H,P	P
Dalian University of Technology	Dalian	Yu Hongquan Liu Jianguo Zhao Lizhong Wang Yi Li Lianfu Gao Xubin		H,P P H,H H P P,P
(Inst. of Univ. Students' Innovation)		Zhou Qi Pan Qiuhui		H,H H
Liaoning High Police Academic School	Dalian	Shen Cong		P,P
Northeastern University (Info)	Shenyang	Sun Ping Hao Peifeng He Xuehong		H,P H,P H,H
(Eng)		Cui Jianjiang	P	H
(CS)		Liu Huilin	P	H
Shenyang Institute of Aero. Engineering	Shenyang	Shan, Feng Zhu Limei		P,P H,H
Shaanxi				
Northwestern Polytechnical University	Xi'an	Zhao Xuanmin Sun Hao Liu Xiaodong Peng Guohua Zhang Shenggui	H P	 P P P
(Chem)		Shi Yimin		H
(Phys)		Xiao Huayong		H
Northwest University	Xi'an	Dou Jihong He Ruichan Wang Liantang		P P M
Xi'an Communication Institute (Info)	Xi'an	Wang Hong Kang Jinlong Song Xiaofeng		P P P
(Sci)	Xi'an	Li Guo Yang Dongsheng Zhang Jianhang Jiang Yan		P P P P

INSTITUTION	CITY	ADVISOR	A	B
Xi'an Jiaotong University (Applied Math.)	Xi'an	He Xiaoliang		H,H
		Dai Yonghong		H
		Zhou Yicang	P	
		Liu Hongwei	P	
Xidian University	Xi'an	Bo Liefeng		P
		Ye Feng	P	
		Tang Houjian		P
Shandong				
Shandong University (CS)	Jinan	Liu Baodong	P	
		Huang Shuxiang	P	
		Huang Shuxiang		P,P
		Ma Jianhua		P,P
		Huang Shuxiang	P	
		Liu Dong	P	
Shanghai				
Donghua University	Shanghai	You Surong		P
		Chen Chao		P
		He Guoxin		P
		Wang ZhiJie		P
East China University of Sci. and Technology (Bio)	Shanghai	Liu Zhaohui		P
		Qin Yan	H	
		Su Chunjie		P
		Sun Jun	P	
		Wang Haitao		P
		Chen Haoming		P
Fudan University	Shanghai	Cao Yuan		P
		Cai Zhijie	M	
Jiading No. 1 Middle School	Shanghai	Xie Xilin and Fang Yunping		P,P
Shanghai Foreign Language School	Shanghai	Pan Liqun		H,H
		Sun Yu		H,P
Shanghai Jiao Tong University (Minhang Branch)	Shanghai	Song Baorui		M
		Huang Jianguo		M,P
		Zhou Gang	P	P
Shanghai Normal University	Shanghai	Zhou Guobiao		P,P
		Liu Rongguan		P
		Guo Shenghuan		P
		Shi Yongbing		H
		Zhang Jizhou and Zhu Detong		P

INSTITUTION	CITY	ADVISOR	A	B		
Shanghai University of Finance and Economics	Shanghai	Dong Dong-cheng	P			
		Yu Juntao		H		
		Yin Chenyuan		H		
		Li Tao		H		
		Shanghai Xiangming High School	Shanghai	Feng Qiang		P,P
		Shanghai Youth Centre of Sci. and Tech. Educ.	Shanghai	Chen Gan		P
Shanghai Yucai High School	Shanghai	Li Zhengtai		P		
Tongji University	Shanghai	Zhang Hualong		P		
		Chen Xiongda	H			
		Gui Zipeng	P			
Sichuan						
Chengdu University of Technology	Chengdu	Yuan Yong	P			
		Wei Youhua		P		
Sichuan University	Chengdu	Niu Hai		P		
		Zhou Jie	H			
Univ. of Electronic Sci. and Tech. of China	Chengdu	Gao Qing	M	H		
		Qin Siyi		H		
		Xu Quanzi		H		
Southwest Jiaotong University	E'mei	Zhao Lianwen	P	P		
Tianjin						
Nankai University	Tianjin	Wang Yi		P		
		Zhang Chunsheng	P			
		Chen Dianfa		P		
		Zhou Xingwei		H		
		Wang Zhaojun		P		
Tianjin University	Tianjin	Liang Fengzhen		H		
		Xu Genqi		P,P		
		Lan Guoliang		H		
		Rong Ximin		H		
Zhejiang						
Zhejiang Gongshang University	Hangzhou	Ding Zhengzhong	M	P		
		Hua Jiukun		H,P		
Zhejiang Sci-Tech Univ. (Academy of Science)	Hangzhou	Hu Jueliang		H		
		Luo Hua	H			
Zhejiang University (City College)	Hangzhou	Yang Qifan	H			
		He Yong		M,H		
		Tan Zhiyi	P			
		Huang Waibin	M			
		Wang Gui		P		
		Kang Xusheng	P			
		Zhao Yanan		P,P		

INSTITUTION	CITY	ADVISOR	A	B
(Chu Kechen Honors College)		Wu Jian		H
		Chen Lingxi		H,P
		Zhou Yongming	H	
(Ningbo Institute of Technology)	Ningbo	Sun Haina	P	
		Tu Lihui	P	P
		Li Zhening		P
Zhejiang Univ. of Finance and Economics	Hangzhou	Wang Fulai		P
		Luo Ji		P
Zhejiang University of Technology	Hangzhou	Zhou Minghua		P
		Wu Xuejun		P
(Jianxing College)		Wang Shiming		P,P
FINLAND				
Helsinki Mathematical High School	Helsinki	Terhi Olkkonen	P	P
Päivölä College	Tarttila	Merikki Lappi		P,P
GERMANY				
International University Bremen	Bremen	Peter Oswald		H
Universität Karlsruhe	Karlsruhe	Lars Behnke	P	
HONG KONG				
City University of Hong Kong	Hong Kong	Ho To Ming		P
Hong Kong Baptist University	Kowloon	C.S. Tong		P
		Wai Chee Shiu		P
KOREA				
Korea Adv. Inst. of Sci. and Tech. (KAIST)	Daejeon	Chang-Ock Lee		H,H
INDONESIA				
Institute of Technology Bandung	Bandung	Kuntjoro Sidarto	H	
		Rieske Hadianiti		P
IRELAND				
Trinity College Dublin	Dublin	Conor Houghton		P
University College Cork	Cork	Andrew Usher		H
		Donal Hurley		M
		James Grannell		H
SOUTH AFRICA				
University of Stellenbosch	Stellenbosch	Jan van Vuuren		H,P

Abbreviations for Organizational Unit Types (in parentheses in the listings)

(none)	Mathematics	M; Pure M; Applied M; Computing M; M and Computer Science; M and Computational Science; M and Information Science; M and Statistics; M, Computer Science, and Statistics; M, Computer Science, and Physics; Mathematical Sciences; Applied Mathematical and Computational Sciences; Natural Science and M; M and Systems Science; Applied M and Physics
Bio	Biology	B; B Science and Biotechnology; Biomathematics; Life Sciences
Chm	Chemistry	C; Applied C; C and Physics; C, Chemical Engineering, and Applied C
CS	Computer	C Science; C and Computing Science; C Science and Technology; C Science and (Software) Engineering; Software; Software Engineering; Artificial Intelligence; Automation; Computing Machinery; Science and Technology of Computers
Econ	Economics	E; E Mathematics; Financial Mathematics; Financial Mathematics and Statistics; Management; Business Management; Management Science and Engineering
Eng	Engineering	Civil E; Electrical Eng; Electronic E; Electrical and Computer E; Electrical E and Information Science; Electrical E and Systems E; Communications E; Civil, Environmental, and Chemical E; Propulsion E; Machinery and E; Control Science and E; Mechanisms; Operations Research and Industrial E; Automatic Control
Info	Information	I Science; I and Computation(al) Science; I and Calculation Science; I Science and Computation; I and Computer Science; I and Computing Science; I Engineering; Computer and I Technology; Computer and I Engineering; I and Optoelectronic Science and Engineering
Phys	Physics	P; Applied P; Mathematical P; Modern P; P and Engineering P; P and Geology; Mechanics; Electronics
Sci	Science	S; Natural S; Applied S; Integrated S
Stat	Statistics	S; S and Finance; Mathematical S; Probability and S

EDITOR'S NOTE: For team advisors from China, I have endeavored to list family name first. For their advice in that connection, I thank Wang Meng and Jiang Liming of Fudan University, exchange students at Beloit College.

From Lake Murray to a Dam Slurry

Clay Hambrick

Katie Lewis

Lori Thomas

Harvey Mudd College

Claremont, CA

Advisor: Jon Jacobsen

Summary

We predict the extent of flooding in the Saluda river if a large earthquake causes the Lake Murray dam to break. In particular, we predict how high the water would be when it reached Columbia and how far the flooding would spread up tributaries of the Saluda like Rawls Creek. We base our model on the Saint-Venant equations for open-channel water flow. We use a discrete version of them to predict the water level along the length of the river. Our model takes into account the width of the floodplain, the slope of the river, the size of the break in the dam, and other factors. We estimate parameters for Lake Murray, its dam, and the Saluda River and calculate the flood results.

The South Carolina State Capitol is safe under even the most extreme circumstances, since it sits on a hill well above the highest possible water level. However, flood waters could still reach 17 m at Columbia and even higher upstream. Buildings in Columbia close to the water would be inundated, but there should be enough warning time for residents to escape. Both our model and local evacuation plans suggest that low-lying areas for miles around would be covered with water.

The text of this paper appears on pp. 229–244.

The UMAP Journal 26 (3) (2005) 217. ©Copyright 2005 by COMAP, Inc. All rights reserved. Permission to make digital or hard copies of part or all of this work for personal or classroom use is granted without fee provided that copies are not made or distributed for profit or commercial advantage and that copies bear this notice. Abstracting with credit is permitted, but copyrights for components of this work owned by others than COMAP must be honored. To copy otherwise, to republish, to post on servers, or to redistribute to lists requires prior permission from COMAP.

Through the Breach: Modeling Flooding from a Dam Failure in South Carolina

Jennifer Kohlenberg

Michael Barnett

Scott Wood

University of Saskatchewan

Saskatoon, SK, Canada

Advisor: James Brooke

Summary

The Saluda Dam, separating Lake Murray from the Saluda River in South Carolina, could breach in the event of an earthquake.

We develop a model to analyze the flow from four possible types of dam breaches and the propagation of the floodwaters:

- instant total failure, where a large portion of the dam erodes instantly;
- delayed total failure, where a large portion of the dam slowly erodes;
- piping, where a small hole forms and eventually opens into a full breach; and
- overtopping, where the dam erodes to form a trapezoidal breach.

We develop two models for the spread of the downstream floodwaters. Both use a discrete-grid approach, modelling the region as a set of cells, each with an elevation and a volume of water. The Force Model uses cell velocities, gravity, and the pressure of neighbouring cells to model water flow. The Downhill Model assumes that flow rates are proportional to the height differences between the water in adjacent cells.

The Downhill Model is efficient, intuitive, flexible, and could be applied to any region with known elevation data. Its two parameters smooth and regulate water flow, but the model's predictions depend little on their values.

For a Saluda Dam breach, the total extent of the flooding is 106.5 km²; it does not reach the State Capitol. The flooding in Rawls Creek extends 4.4 km upstream and covers an area of 1.6–2.4 km².

The text of this paper appears on pp. 245–261.

Analysis of Dam Failure in the Saluda River Valley

Ryan Bressler
Christina Polwarth
Braxton Osting
University of Washington
Seattle, WA

Advisor: Rekha Thomas

Summary

We identify and model two possible failure modes for the Saluda Dam: gradual failure due to an enlarging breach, and sudden catastrophic failure due to liquefaction of the dam.

For the first case, we describe the breach using a linear sediment-transport model to determine the flow from the dam. We construct a high-resolution digital model of the downstream river valley and apply the continuity equations and a modified Manning equation to model the flow downstream.

For the case of dam annihilation, we use a model based on the Saint-Venant equations for one-dimensional flood propagation in open-channel flow. Assuming shallow water conditions along the Saluda River, we approximate the depth and speed of a dam break wave, using a sinusoidal perturbation of the dynamic wave model.

We calibrate the models with flow data from two river observation stations.

We conclude that the flood levels would not reach the Capitol Building but would intrude deeply into Rawls Creek.

The text of this paper appears on pp. 263–278.

Catastrophic Consequences of Earthquake Destruction of the Saluda Dam

Miika Klemetti
Colin McNally
Chris Payette
McGill University
Montréal, Québec, Canada

Advisor: Nilima Nigam

Summary

We model the flow of water in the Saluda river valley to determine the extent of flooding resulting from a failure of the Saluda Dam due to an earthquake. The model is divided into two parts: the flow of water in the river, and the evolution of the dam breach. We consider two questions in detail: How far up Rawls Creek, 3.3 km from the dam, will the flooding extend? And will the State Capitol in Columbia, 14 km downriver from the dam, get wet?

We assume that the dam fails as a result of overtopping after the dam slumps due to soil liquefaction. We model the shape of the breach as an enlarging trapezoid. This model provides the essential time-varying boundary conditions for the flow in the river and results in the dam collapsing in 3 to 4 min.

The model for the water flow is based on dividing the river into sections of varying sizes. Tunable parameters for each section allow shaping of the valley along the river. The geometry of each cross section is modeled as a piecewise-linear function with three parameters (two for the slopes, one for the length). In addition, the length of each section of the river can be adjusted to obtain greater resolution for regions of interest. We model the flow of the water by the transfer of momentum and volume between the sections of the river. The equations governing these exchanges comprise a low-order finite-volume advection scheme. For our geometry, the flow is sub-critical and momentum-dominated, allowing the above simplified physics model for the flow.

The UMAP Journal 26 (3) (2005) 220–221. ©Copyright 2005 by COMAP, Inc. All rights reserved. Permission to make digital or hard copies of part or all of this work for personal or classroom use is granted without fee provided that copies are not made or distributed for profit or commercial advantage and that copies bear this notice. Abstracting with credit is permitted, but copyrights for components of this work owned by others than COMAP must be honored. To copy otherwise, to republish, to post on servers, or to redistribute to lists requires prior permission from COMAP.

We check convergence and stability of the results by varying the time resolution.

The simulations of the model indicate major flooding in Rawls Creek up to 2.4 km from the Saluda River, but flooding will not extend to the State Capitol.

[EDITOR'S NOTE: This Meritorious paper won the Ben Fusaro Award for the Flood Planning Problem. Only this abstract of the paper appears in this issue of the *Journal*.]

The Booth Tolls for Thee

Adam Chandler
Matthew Mian
Pradeep Baliga
Duke University
Durham, NC

Advisor: William G. Mitchener

Summary

We determine the optimal number of tollbooths for a given number of incoming highway lanes. We interpret optimality as minimizing “total cost to the system,” the time that the public wastes while waiting to be processed plus the operating cost of the tollbooths.

We develop a microscopic simulation of line-formation in front of the tollbooths. We fit a Fourier series to hourly demand data from a major New Jersey parkway. Using threshold analysis, we set upper bounds on the number of tollbooths. This simulation does not take bottlenecking into account, but it does inform a more general macroscopic framework for toll plaza design.

Finally, we formulate a model for traffic flow through a plaza using cellular automata. Our results are summarized in the formula for the optimal number B of tollbooths for L lanes: $B = \lfloor 1.65L + 0.9 \rfloor$.

The text of this paper appears on pp. 283–297.

A Single-Car Interaction Model of Traffic for a Highway Toll Plaza

Ivan Corwin
Sheel Ganatra
Nikita Rozenblyum
Harvard University
Cambridge, MA

Advisor: Clifford H. Taubes

Summary

We find the optimal number of tollbooths in a highway toll-plaza for a given number of highway lanes: the number of tollbooths that minimizes average delay experienced by cars.

Making assumptions about the homogeneity of cars and tollbooths, we create the Single-Car Model, describing the motion of a car in the toll-plaza in terms of safety considerations and reaction time. The Multi-Car Interaction Model, a real-time traffic simulation, takes into account global car behavior near tollbooths and merging areas.

Drawing on data from the Orlando–Orange Country Expressway Authority, we simulate realistic conditions. For high traffic density, the optimal number of tollbooths exceeds the number of highway lanes by about 50%, while for low traffic density the optimal number of tollbooths equals the number of lanes.

The text of this paper appears on pp. 299–315.

The UMAP Journal 26 (3) (2005) 223. ©Copyright 2005 by COMAP, Inc. All rights reserved. Permission to make digital or hard copies of part or all of this work for personal or classroom use is granted without fee provided that copies are not made or distributed for profit or commercial advantage and that copies bear this notice. Abstracting with credit is permitted, but copyrights for components of this work owned by others than COMAP must be honored. To copy otherwise, to republish, to post on servers, or to redistribute to lists requires prior permission from COMAP.

Lane Changes and Close Following: Troublesome Tollbooth Traffic

Andrew Spann

Daniel Kane

Dan Gulotta

Massachusetts Institute of Technology
Cambridge, MA

Advisor: Martin Zdenek Bazant

Summary

We develop a cellular-automaton model to address the slow speeds and emphasis on lane-changing in tollbooth plazas. We make assumptions about car-following, based on distance and relative speeds, and arrive at the criterion that cars maximize their speeds subject to

$$\text{gap} > \left\lfloor \frac{V_{\text{car}}}{2} \right\rfloor + \frac{1}{2}(V_{\text{car}} - V_{\text{frontcar}})(V_{\text{car}} + V_{\text{frontcar}} + 1).$$

We invent lane-change rules for cars to determine if they can turn safely and if changing lanes would allow higher speed. Cars modify these preferences based on whether changing lanes would bring them closer to a desired type of tollbooth. Overall, our assumptions encourage people to be a bit more aggressive than in traditional models when merging or driving at low speeds.

We simulate a 70-min period at a tollbooth plaza, with intervals of light and heavy traffic. We look at statistics from this simulation and comment on the behavior of individual cars.

In addition to determining the number of tollbooths needed, we discuss how tollbooth plazas can be improved with road barriers to direct lane expansion or by assigning the correct number of booths to electronic toll collection. We set up a generalized lane-expansion structure to test configurations.

Booths should be ordered to encourage safe behavior, such as putting faster electronic booths together. Rigid barriers affect wait time adversely.

Under typical traffic loads, there should be *at least twice as many booths as highway lanes*.

The text of this paper appears on pp. 317–330.

A Quasi-Sequential Cellular-Automaton Approach to Traffic Modeling

John Evans
Meral Reyhan
Rensselaer Polytechnic Institute
Troy, NY

Advisor: Peter Kramer

Summary

The most popular discrete models to simulate traffic flow are cellular automata, discrete dynamical systems whose behavior is completely specified in terms of its local region. Space is represented as a grid, with each cell containing some data, and these cells act in accordance to some set of rules at each temporal step. Of particular interest to this problem are sequential cellular automata (SCA), where the cells are updated in a sequential manner at each temporal step.

We develop a discrete model with a grid to represent the area around a toll plaza and cells to hold cars. The cars are modeled as 5-dimensional vectors, with each dimension representing a different characteristic (e.g., speed). By discretizing the grid into different regimes (transition from highway, tollbooth, etc.), we develop rules for cars to follow in their movement. Finally, we model incoming traffic flow using a negative exponential distribution.

We plot the average time for a car to move through the grid vs. incoming traffic flow rate for three different cases: 4 incoming lanes and tollbooths, 4 incoming lanes and 4, 5, and 6 tollbooths. In each plots, we noted at certain values for the flow rate, there is a boundary layer in our solution. As we increase the ratio of tollbooths to incoming lanes, this boundary layer shifts to the right. Hence, the optimum solution is to pick the minimum number of tollbooths for which the maximum flow rate expected is located to the left of the boundary layer.

The text of this paper appears on pp. 331–344.

The UMAP Journal 26 (3) (2005) 225. ©Copyright 2005 by COMAP, Inc. All rights reserved. Permission to make digital or hard copies of part or all of this work for personal or classroom use is granted without fee provided that copies are not made or distributed for profit or commercial advantage and that copies bear this notice. Abstracting with credit is permitted, but copyrights for components of this work owned by others than COMAP must be honored. To copy otherwise, to republish, to post on servers, or to redistribute to lists requires prior permission from COMAP.

The Multiple Single Server Queueing System

Azra Panjwani

Yang Liu

HuanHuan Qi

University of California, Berkeley
Berkeley, CA

Advisor: Jim Pitman

Summary

Our model determines the optimal number of tollbooths at a toll plaza in terms of that minimizing the time that a car spends in the plaza.

We treat the toll collection process as a network of two exponential queueing systems, the Toll Collection system and the Lane Merge System. The random, memoryless nature of successive car interarrival and service times allows us to conclude that the two are exponentially distributed.

We use properties of single server and multiple server queueing systems to develop our Multiple Single Server Queueing System. We simulate our network in Matlab, analyzing the model's performance in light, medium, and heavy traffic for tollways with 3 to 6 lanes. The optimal number of tollbooths is roughly double the number of lanes.

We also evaluate a single tollbooth vs. multiple tollbooths per lane. The optimal number of booths improves the processing time by 22% in light traffic and 61% in medium traffic. In heavy traffic, one tollbooth per lane results in infinite queues.

Our model produces consistent results for all traffic situations, and its flexibility allows us to apply it to a wide range of toll-plaza systems. However, the minimum time predicted is an average value, hence it does not reflect the maximum time that an individual may spend in the network.

The text of this paper appears on pp. 345–354.

Two Tools for Tollbooth Optimization

Ephrat Bitton

Anand Kulkarni

Mark Shlimovich

University of California, Berkeley

Berkeley, CA

Advisor: L. Craig Evans

Summary

We determine the optimal number of lanes in a toll plaza to maximize the transit rate of vehicles through the system. We use two different approaches, one macroscopic and one discrete, to model traffic through the toll plaza.

In our first approach, we derive results about flows through a sequence of bottlenecks and demonstrate that maximum flow occurs when the flow rate through all bottlenecks is equal. We apply these results to the toll-plaza system to determine the optimal number of toll lanes. At high densities, the optimal number of tollbooths exhibits a linear relationship with the number of toll lanes.

We then construct a discrete traffic simulation based on stochastic cellular automata, a microscopic approach to traffic modeling, which we use to validate the optimality of our model. Furthermore, we demonstrate that the simulation generates flow rates very close to those of toll plazas on the Garden State Parkway in New Jersey, which further confirms the accuracy of our predictions.

Having the number of toll lanes equal the number of highway lanes is optimal only when a highway has consistently low density and is suboptimal otherwise. For medium- to high-density traffic, the optimal number of toll lanes is three to four times the number of highway lanes. Both models demonstrate that if a tollway has lanes in excess of the optimal, flow will not increase or abate.

Finally, we examine how well our models can be generalized and comment on their applicability to the real world.

[EDITOR'S NOTE: This Outstanding paper won the Ben Fusaro Award for the Tollbooths Problem. The text of the paper appears on pp. 355–371.]

The UMAP Journal 26 (3) (2005) 227. ©Copyright 2005 by COMAP, Inc. All rights reserved. Permission to make digital or hard copies of part or all of this work for personal or classroom use is granted without fee provided that copies are not made or distributed for profit or commercial advantage and that copies bear this notice. Abstracting with credit is permitted, but copyrights for components of this work owned by others than COMAP must be honored. To copy otherwise, to republish, to post on servers, or to redistribute to lists requires prior permission from COMAP.

For Whom the Booth Tolls

Brian Camley
Bradley Klingenberg
Pascal Getreuer
University of Colorado
Boulder, CO

Advisor: Anne Dougherty

Summary

We model traffic near a toll plaza with a combination of queueing theory and cellular automata in order to determine the optimum number of tollbooths. We assume that cars arrive at the toll plaza in a Poisson process, and that the probability of leaving the tollbooth is memoryless. This allows us to completely and analytically describe the accumulation of cars waiting for open tollbooths as an $M|M|n$ queue. We then use a modified Nagel-Schreckenberg (NS) cellular automata scheme to model both the cars waiting for tollbooths and the cars merging onto the highway. The models offer results that are strikingly consistent, which serves to validate the conclusions drawn from the simulation.

We use our NS model to measure the average wait time at the toll plaza. From this we demonstrate a general method for choosing the number of tollbooths to minimize the wait time. For a 2-lane highway, the optimal number of booths is 4; for a 3-lane highway, it is 6. For larger numbers of lanes, the result depends on the arrival rate of the traffic.

The consistency of our model with a variety of theory and experiment suggests that it is accurate and robust. There is a high degree of agreement between the queueing theory results and the corresponding NS results. Special cases of our NS results are confirmed by empirical data from the literature. In addition, changing the distribution of the tollbooth wait time and changing the probability of random braking does not significantly alter the recommendations. This presents a compelling validation of our models and general approach.

The text of this paper appears on pp. 373–390.

From Lake Murray to a Dam Slurry

Clay Hambrick

Katie Lewis

Lori Thomas

Harvey Mudd College
Claremont, CA

Advisor: Jon Jacobsen

Summary

We predict the extent of flooding in the Saluda river if a large earthquake causes the Lake Murray dam to break. In particular, we predict how high the water would be when it reached Columbia and how far the flooding would spread up tributaries of the Saluda like Rawls Creek. We base our model on the Saint-Venant equations for open-channel water flow. We use a discrete version of them to predict the water level along the length of the river. Our model takes into account the width of the floodplain, the slope of the river, the size of the break in the dam, and other factors. We estimate parameters for Lake Murray, its dam, and the Saluda River and calculate the flood results.

The South Carolina State Capitol is safe under even the most extreme circumstances, since it sits on a hill well above the highest possible water level. However, flood waters could still reach 17 m at Columbia and even higher upstream. Buildings in Columbia close to the water would be inundated, but there should be enough warning time for residents to escape. Both our model and local evacuation plans suggest that low-lying areas for miles around would be covered with water.

Introduction

In central South Carolina, a lake is held back by a 75-year-old earthen dam. What would happen if an earthquake breached the dam? The concern is based on an earthquake in 1886 at Charleston that scientists believe measured 7.3 on the Richter Scale [Federal Energy Regulatory Commission 2002]. The location of fault lines almost directly under Lake Murray [SCIway 2000; South Carolina

The UMAP Journal 26 (3) (2005) 229–244. ©Copyright 2005 by COMAP, Inc. All rights reserved. Permission to make digital or hard copies of part or all of this work for personal or classroom use is granted without fee provided that copies are not made or distributed for profit or commercial advantage and that copies bear this notice. Abstracting with credit is permitted, but copyrights for components of this work owned by others than COMAP must be honored. To copy otherwise, to republish, to post on servers, or to redistribute to lists requires prior permission from COMAP.

Geological Survey 1997; 1998] and the frequency of small earthquakes in the area led authorities to consider the consequences of such a disaster.

Our task is to predict how water levels would change along the Saluda River, from Lake Murray Dam to Columbia, if an earthquake on the same scale as the 1886 breaches the dam. In particular, how far would the tributary Rawls Creek flow back and how high would the water rise near the State Capitol in Columbia, South Carolina.



Figure 1. Topographical map of the Saluda River from the base of Lake Murray to the Congaree River [Topozone 2004].

We lay out our assumptions and set up a submodel of Lake Murray and the Lake Murray dam to simulate the overflow when the dam breaks.

We then build a model based on the Saint-Venant equations [Moussa and Bocquillon 2000], using conservation of water and momentum to capture the nature of a flood where the main water channel overflows into the surrounding area. We convert the model to a system of difference equations and feed the dam outflow into the beginning of the river.

To increase accuracy, we measure along the river the ratio of the floodplain to the river width and use these values to modify the equations. We then use data from Lake Murray and the Saluda river to model several scenarios.

Finally, we discuss the implications of our model, analyze its strengths and weaknesses, and discuss how the model could be extended.

Background of Earthquake Effects

- Effect on the dam
 - How the dam is compromised (size and shape of the initial breach)
 - Interaction between the lake water and the initial breach
 - Breach size and shape over time

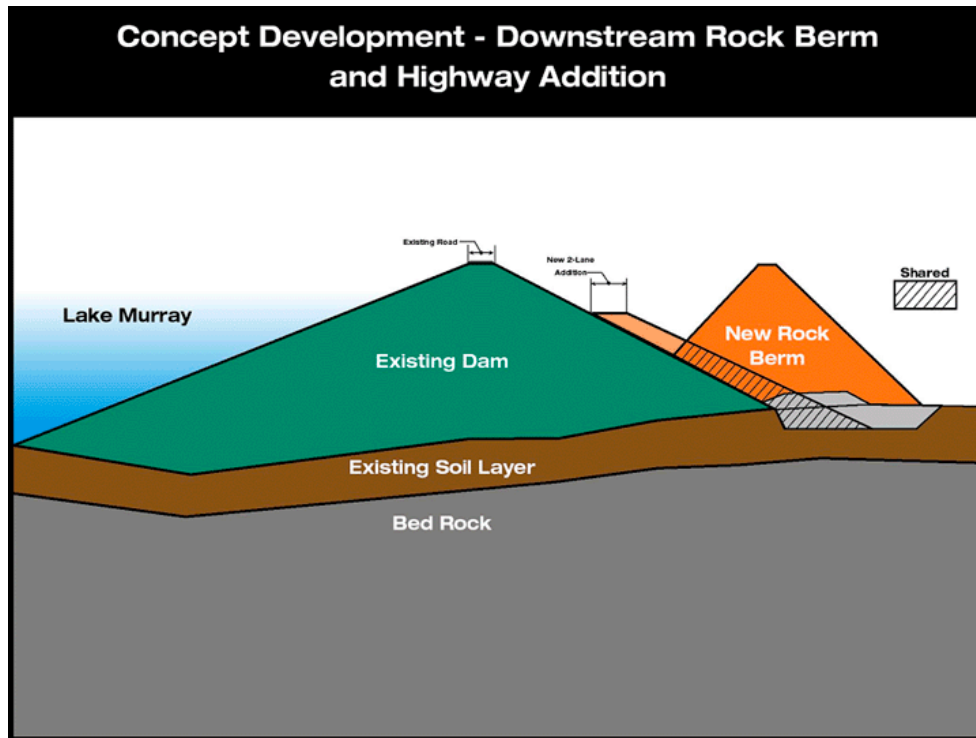


Figure 2. Schematic of the earth dam and the new planned dam at Lake Murray [Lake Murray 2005].

- Effect on the water
 - Earthquake’s effect on the lake in so far as it affects the dam
- Effect on the surrounding countryside
 - Whether earthquake alteration of the landscape opens or closes available floodplains
 - Whether earthquake damage could divert the Saluda river
 - Whether earthquake damage would make the Saluda’s path choppier and slow down the water

The situation looks something like this: A large earthquake compromises the Lake Murray dam. Earthen dams do not usually fail completely or instantaneously [U.S. Army Corps of Engineers 1997]. Instead, the dam begins to leak. Over time, the water causes further erosion, allowing more and more water to flow out of the lake, until the lake and dam reach a new equilibrium. Depending on the initial breach and the dam construction, the final equilibrium may take anywhere from a few minutes to a few hours [U.S. Army Corps of Engineers 1997] to reach. The fully formed breach usually has a width somewhere between half the height of the dam and three times the height of the dam [U.S. Army Corps of Engineers 1997; 1980]. At half a mile wide (1,609 m) and 208 ft (63 m) tall [SouthCarolinaLakes.net], the Lake Murray Dam is about 25 times

as wide as it is tall, which suggests a breach width much smaller than the dam width.

Below the dam, the increasing flow of water puts stress on the countryside, with flooding and hillside carving. Water back-flows up smaller creeks such as Rawls Creek and pools in the flatter sections. Far downstream, either the water pools enough to stay within normal channels, or excess water creates its own channel, or excess water continues flowing from river to river to the sea.

Assumptions

Earthquake

- *Aftershocks disregarded:* Earthquakes generally consist of a main shock and smaller aftershocks. Although an aftershock is itself a significant event and might cause a spike in dam destruction, for simplicity we neglect aftershocks.
- *Dam breach only:* The earthquake could affect the dam, the water involved, and the landscape. The earthquake's effect on the water matters only if the water damages the terrain or escapes from the lake or riverbed. Thus, by assuming that the earthquake affects only the dam, we bundle any effect of the earthquake on the water into the water's effect on other things. The earthquake could significantly affect the terrain, but such changes are unpredictable and we assume no significant terrain changes take place.

Weather and Terrain

- *No effect from wind:* The effects of wind here are minuscule in comparison with other forces.
- *Low land near river would flood:* We assume that the river would overflow its banks and fill the surrounding floodplain.

Lake Murray and Dam

- *Lake has a simple shape:* We assume that the lake has perfectly vertical sides and a flat bottom.
- *Dam breach is rectangular:* We can thus model a variety of dam breaches, since we can vary the height and width independently.
- *Washed-out dam materials are negligible compared to water flooding:* Since we already assume that the breach does not erode, there is no new source of earth after that initial point. This assumption should work well when the breach is small but less so when the breach is large.

Saluda River

- *River channel has constant width:* The Saluda river widens slightly after 11.4 km [Topozone 2004]; but to model it simply, we assume that it has a constant width.
- *River has steady elevation loss:* Due to limits of our topographical data, we assume that the height of the river drops off steadily.
- *River has constant initial depth:* Because we assume that the river drops off steadily, there are no pockets where water could pool. Since the river starts in equilibrium, we assume that the depth is uniform from start to finish.
- *River is straight:* The curvature of a river contributes somewhat to slow the flow of water, and some models include a curvature parameter; but given how straight the Saluda is [Topozone 2004], it is reasonable to approximate it as a linear river.

Dam Model

We use a submodel to simulate what happens on the lake and at the dam after an earthquake causes a breach. The submodel provides information about the volume and speed of water leaving the dam at any given time. This information depends on the volume of water in the lake, the surface area of the lake, and the size of the breach in the dam.

We model the breach as a rectangular opening in the dam. We assume that water would flow out of the bottom of this breach and that its energy would be conserved. The potential energy is converted into kinetic energy, and so from the equation

$$\frac{1}{2}ms^2 = mgh$$

we get

$$s = \sqrt{2gh},$$

where

s is the speed of the water,

m is the mass of the water,

g is acceleration due to gravity, and

h is the height of the water—the difference in height between the lake and the bottom of the breach.

We assume that all water leaves at the maximum speed, a slight overestimate. We can write this equation in terms of our model as

$$s_{\text{water leaving}} = \sqrt{2g(h_{\text{lake}} - h_{\text{dam}})}.$$

The volume of water leaving in each time step is the area of the breach times the velocity of the water times the size of the time step:

$$v_{\text{water leaving}} = w_{\text{breach}}(h_{\text{lake}} - h_{\text{dam}})s_{\text{water leaving}}t_{\text{time step}},$$

where v is volume, w is width, h is height, s is speed, and t is time.

We assume in effect that the lake is a large straight-sided holding tank, so its area doesn't change when the water height does. This means that the height of the lake is simply the volume divided by area, or

$$h_{\text{lake}} = \frac{v_{\text{lake}}}{a_{\text{lake}}}$$

where h is the height, v the volume, and a is the area. This assumption can be changed to make the area of the lake a function of the amount of water in it; for example, we could model the lake as a shallow cone.

We also assume that the breach in the dam stays the same size throughout the simulation, though it would be simple to make the width and depth of the breach increase as a function of the amount and speed of the water flowing through. Doing so would mimic erosion caused by the force of the water traveling through the gap.

Saint-Venant Model

Our primary model is based on the Saint-Venant system of (partial differential) equations. This choice was inspired by Moussa and Bocquillon [2000], who describes how to use them (slightly modified) to model floods. These equations govern open-channel fluid flow that is nonuniform and nonconstant, and they take into account variations in velocity, the topography of the river and surroundings, and friction with the ground. This makes the Saint-Venant system much preferable to simpler models, especially since friction is a dominant force in flood behavior (the floodwaters cover uneven ground with many obstacles—trees, houses, etc.).

The (modified) Saint-Venant system consists of a water conservation equation,

$$\eta \frac{\partial y}{\partial t} + y \frac{\partial V}{\partial x} + V \frac{\partial y}{\partial x} = 0,$$

and a linear momentum equation,

$$\frac{\partial V}{\partial t} + V \frac{\partial V}{\partial x} + g \left(\frac{\partial y}{\partial x} + S_f - S \right) = 0,$$

where

y is the height of the water;

x is the distance along the river;

t is time;

V is the speed of the water,

S is the river slope;

η , the new parameter introduced by Moussa and Bocquillon [2000], is the relative floodplain width (see below); and

S_f is the so-called *energy-line slope*.

The energy-line slope represents how much friction the flowing water must overcome; it is calculated from the velocity and flow radius of the water via the Manning formula [Moussa and Bocquillon 2000],

$$S_f = n^2 k V^2 R^{-4/3},$$

where R , the hydraulic or flow radius, is given by $R = W_1 y / (W_1 + 2y)$, where W_1 is the width of the channel. There are two constants: n is the dimensionless “roughness parameter” characterizing the land that the water flows over, while k is a constant equal to $1 \text{ s}^2/\text{m}^{2/3}$.

But what does the introduction of the parameter η do? The model assumes that outside the river channel there is a floodplain that has a very high fluid resistance (e.g., trees, houses). This means that the downstream flow of water in this area is negligible. However, the floodplain serves as a sink for water, so $\partial y / \partial t$ is modified by the factor η , the ratio of the floodplain width to the channel width. This way, when the water rises, the actual height change in the channel is attenuated by η , since some water is absorbed by the floodplain. We make η a function of the distance along the river by measuring the width of the floodplain at various points.

To model numerically, we turn this PDE system into a difference-equation system. As is common with numerical PDEs, and in particular fluid dynamics problems, special care must be taken to ensure the stability of the algorithm [Trefethen 1996]. We use the Lax-Wendroff difference formula,

$$u_j^{n+1} = u_j^n + \frac{1}{2} \lambda (u_{j+1}^n - u_{j-1}^n) - \frac{1}{2} \lambda^2 (u_{j+1}^n - 2u_j^n + u_{j-1}^n).$$

Here the upper indices represent time and the lower, space; λ is the ratio of the time to the space step size. (Our model converts distance and time to model units, so the step size in each is 1.) The second term acts to damp out spikes, since it looks at how much each point differs from the points on either side of it, and compensates.

We find that the model is highly sensitive to the roughness parameter n (note that this is the effective roughness in the channel only). When n is large (even at 0.03, the standard value for large rivers), there is high resistance to

the water flow, and the floodwater tends to pile up. This leads to excessive steepness in the water-depth profile and tends to make the model break down. Fortunately, we can assume a smaller value for n , since we are considering only the water in the channel area, which is bounded on the sides not by rocks and grass (as a river is normally), but by other floodwater (covering the floodplain), which is moving a bit slower (in fact, we assume that it is stationary) but should be smoother than stationary rocks. Therefore, we take $n = 0.01$.

Further, the model is increasingly unstable at higher rates of lake outflow. This is presumably because the Saint-Venant equations are essentially perturbations about steady flow, so they tend to break down in massive flooding. We resort to periodic averaging of neighboring water depths (every 20 time steps, for the most part). This does not seem to affect the results much.

Rawls Creek Back-Flooding

Our initial idea for computing the back-flooding at Rawls Creek was to use the same Saint-Venant modeling technique as for Saluda, adjusted for the different parameters of Rawls, and using the water depths calculated at the creek's mouth for the "dam". However, it is unclear what the initial speeds should be, since the back-flow water moves more or less perpendicularly to the main flood. Moreover, the model displays severe instability with the relevant data. Hence, we take the water height at the mouth and use the topographical map Topozone [2004] to find the matching place upstream. Though highly simplistic, this method is consistent with a modified Saint-Venant system, since it assumes that there is no flow outside the main channel and that the floodplain area is filled instantaneously along with the channel. The Rawls Creek valley is simply a wider section of floodplain (and we include it in calculating the floodplain widths).

Parameters

Lake Murray Dam

We use the following parameter values:

- $g = 9.8 \text{ m/s}^2$, the gravitational constant
- $h_{0_{\text{lake}}} = 60 \text{ m}$ [SouthCarolinaLakes.net]. This is the initial height of water in the lake.
- $v_{0_{\text{lake}}} = 3 \times 10^9 \text{ m}^3$ [Publications 2004]. This is the initial volume of water in the lake.
- $a_{0_{\text{lake}}}$, the area of the lake assuming that the sides are exactly vertical.

Saluda River

- $\text{length}_{\text{river}} = 16200 \text{ m}$, the length of the Saluda River as measured on the topographic map in **Figure 1**.
- $h_{\text{BedUpstream}} = 0 \text{ m}$, the height of the stream bed just after the dam, compared to the base of the dam.
- $h_{\text{BedDownstream}} = -10 \text{ m}$, the height of the stream bed as it joins the Congaree River outside Columbia. We obtain this value by comparing the height above sea level of the beginning and at the end of the Saluda river on the topographic map in **Figure 1**.
- $h_{0\text{water}} = 1.2 \text{ m}$ [South Carolina Department of Natural Resources], the initial water depth along the river, assumed uniform.

Floodplain

Water flowing out from the dam would not stay entirely within the Saluda River bed. To model accurately the ratio of the river channel to the floodplain surrounding it, we examine topographical maps. The river has an elevation of approximately 170 ft (52 m). The area near the river rises gradually to approximately 200 ft (61 m), before nearby hills start. We assume that this area between the river and the hills is the approximate floodplain. We measure the width of this plain every 600 m. We assume that the width varies linearly between these measurements and interpolate plain widths for distances downstream that we didn't measure directly. This assumption allows us a much more accurate model than if we simply assume that the floodplain has constant width.

Results

The Lake Murray Dam is roughly 800 m long (in the highest region) by 60 m high [Topozone 2004], so any breach up to this size is at least theoretically possible.

No Breach

Breach width: 0 m, breach height: 0 m

Tested with no breach, the model performs as expected, with the water level staying very nearly constant, since replacement water from the ordinary hydroelectric pipes is included in the model.

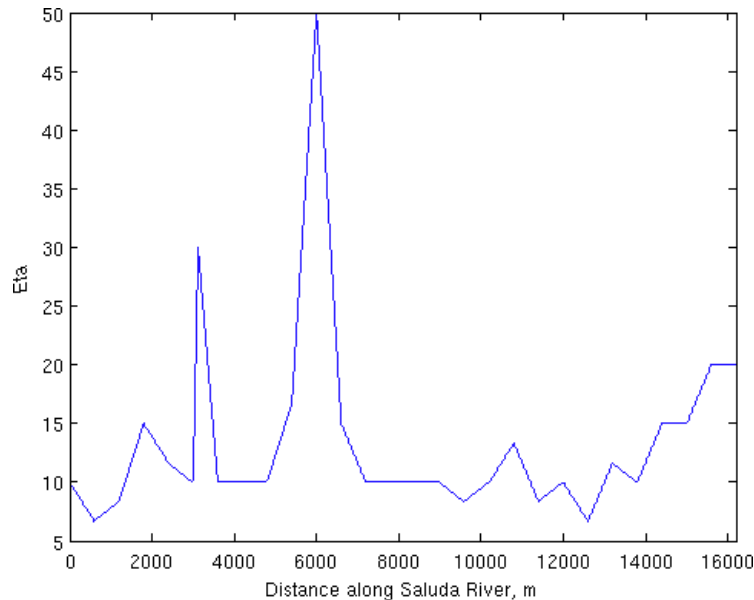


Figure 4. Ratio of the width of the river channel and the flood plain as a function of distance along the river. The two spikes are tributaries; the left one is Rawls Creek. The widening at the end is the mouth of the Saluda where it enters the Congaree.

Realistic Breach

Breach width 800 m, breach height 10 m

The most common earthquake failure mode for an earthen dam is for the underwater side to simply landslide down, producing a wide but shallow breach.

In this scenario, flooding crests in the Rawls after 1.1 h at a height of 7.1 m. This means that the creek backfloods for some 2.4 km along its course, as measured on the topographical map Topozone [2004]. Crest at Columbia (where the Saluda flows into the Congaree) is reached after 7.5 h at a height of 4.15 m. Since the Capitol sits some 50 m above the river, it is in no danger.

Alternative Breach

Breach width 133 m, breach height 60 m

To explore the effect of breach shape as well as size, we run a scenario with a breach of the same cross-section as the previous case but with the opposite rectangular shape. Since the breach is deeper, the speed of the escaping water is higher than before and more water escapes also, since the lake can drain to a lower level.

The water crests at the Rawls after 1.4 h at 9.11 m. The backflooding extends for 3.0 km. Crest at Columbia occurs after 7.0 h at 6.23 m.

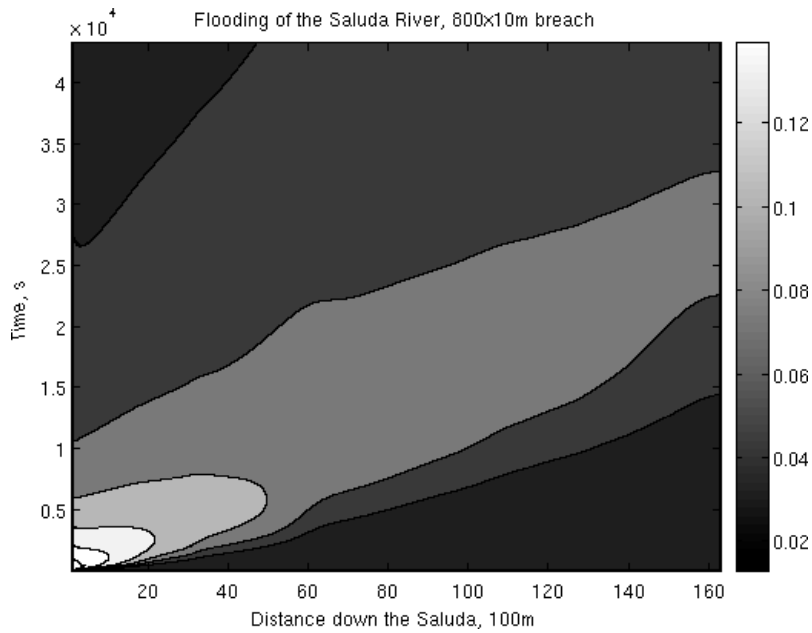


Figure 5. Contour map of the water level along the river from the start of the simulation to the end. The x -axis is distance (m) along the river and the y -axis is time (s) into the simulation. The color bar gives the scale for the height (100s of m) of the water.

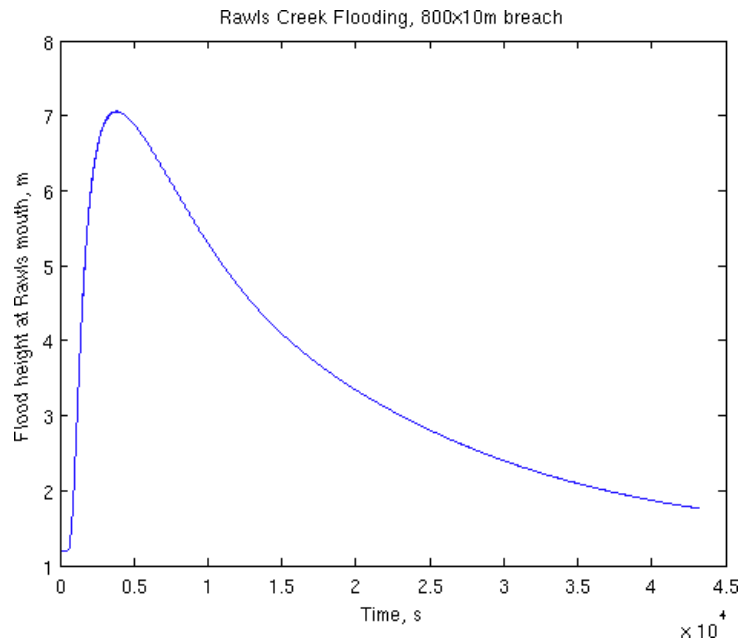


Figure 6. Water level where Rawls Creek joins the Saluda River, from the start of the simulation to the end. The x -axis is time (s) into the simulation and the y -axis is the height (m) of the water.

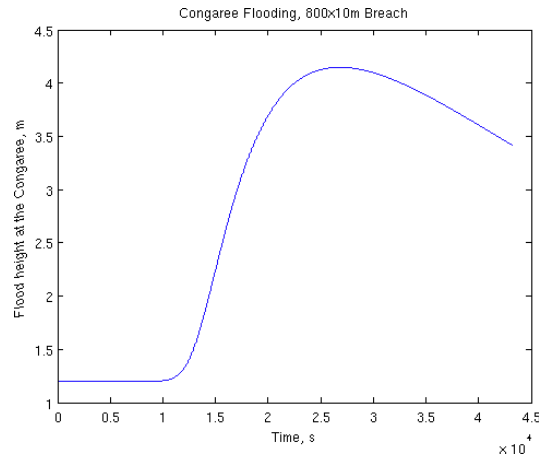


Figure 7. Water level where the Saluda River meets the Congaree River in Columbia, from the start of the simulation to the end. The x -axis is time (s) into the simulation (in seconds) and the y -axis is the height (m) of the water.

Maximum Breach

Breach width: 800 m, breach height: 60 m

What if the entire dam simply vanishes? Both the model and our assumptions are overextended by this scenario. Despite more frequent smoothing (every 5 time steps), the numbers consistently exploded after 3 h of simulated time. Fortunately, this was long enough for cresting at the Rawls and for a pretty good guess at the Columbia crest. Unfortunately, the water rises so high in the early sections of the river that our values for η are no longer valid—the flood simply expands outside the normal floodplain. This means that the water would not actually be as high as the model indicates.

The Rawls crest occurs after 0.4 h 34.35 m. This height of water causes backflooding as much as 5 km upstream (a strong indication that our η values are indeed too low for this level of flooding). The Columbia crest appears after 4 to 5 h and is no more than 17 m. The Capitol is still safe, by a large margin.

Interpretation

While the Capitol is safe in all scenarios, massive flooding nonetheless occurs in low-lying areas and in the homes and businesses along the Columbia. Happily, based on the flood scenarios above, if a warning system is in place, there should be enough time to escape before the flood water arrives.

Analysis of Model

Strengths and Weaknesses

Our model is built on trade-offs. One weakness is the transformation of PDEs into difference equations; the latter are prone to instability in extreme scenarios.

Our assumptions represent other trade-offs. The floodplain, though a vast improvement over an extremely simple model where all water stays in the channel, requires us to assume that the water instantaneously drains from the river and immediately stops moving. Extending the system to be fully three-dimensional, with water flowing both downstream and outward from the riverbed, would represent a great improvement (and indeed, is performed admirably by various commercial software packages).

On the other hand, we implement equations designed specifically to model situations like the one on the Saluda River and use data specific to Lake Murray and the Saluda River.

Comparison to Other Predictions

The company that owns the dam provides an evacuation map that shows where the water is expected to go during a flood. This map seems to agree roughly with our worst-case model predictions.

Future Work

- We could model an expanding trapezoidal breach, representing erosion of the original breach, using values from the literature [U.S. Army Corps of Engineers 1980] to select appropriate slope and time intervals.
- We could acquire data on the normal width of the Saluda River at intervals along its course between Lake Murray and the Congaree, rather than assuming a constant stream width.
- We could collect data on the elevation of the stream at regular intervals. For instance, the river might have a waterfall, which could affect the flood pattern.
- We could consider information on the distribution of the lake's water. In real life, the lake has large areas that are shallow, with a smaller deep region.
- We could move from the straight-stream assumption to a two-dimensional analysis; some momentum is lost in bends in the river.

- Our assumptions (the earthquake affects just the dam, aftershocks can be disregarded, wind has no effect, and washed-out dam materials can be disregarded) are sturdy enough that an upgrade of the water-flow modeling technique used (Saint-Venant) should be attempted before correcting these assumptions.

Conclusion

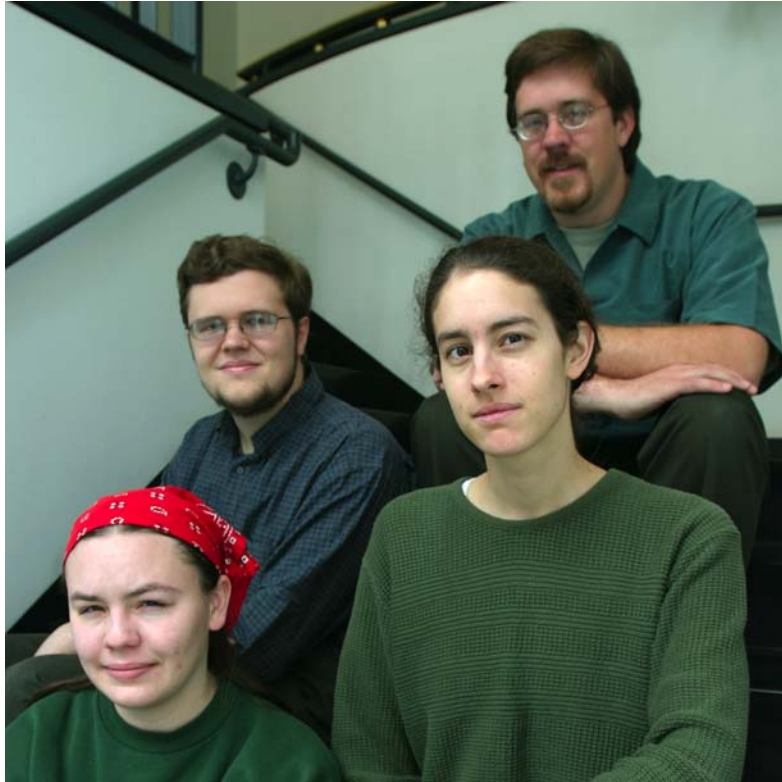
Dam-breach flooding is a rare but very serious problem, especially when the dam sits less than 20 km above a major city. We create a hydrodynamical model that gives the downstream results of both likely and possible earthquake-driven dam breach scenarios. Since the city of Columbia sits mainly on a hill, the predicted flood levels of 4 m to 17 m would flood only the few blocks closest to the river. However, upstream areas such as Rawls Creek would experience levels 7 m to 34 m higher. The water could arrive at Rawls in as little as half an hour, and flood 2.5–5 km upstream; so an early-warning system for dam breaches along the Saluda is a vital protective measure.

Our model produces results that make intuitive sense when we vary the parameters: The flooding increases with a larger breach, and a deeper breach floods more than a shallower one of the same area. The water height falls off downstream, as some of the water is held in the floodplain, and this attenuation varies with the width of the floodplain.

References

- Castro, Gonzalo. 1999. Seismic stability and deformations of embankment dams. *2nd US-Japan Workshop on Dam Earthquake Engineering* <http://www.geiconsultants.com/images/library/sub31.pdf> .
- Dutch, Steven. 2003. Faults and earthquakes. <http://www.uwgb.edu/dutchs/EarthSC202Notes/quakes.htm> .
- Federal Energy Regulatory Commission. 2002. News release: Commission moves to protect public near south carolina dam. <http://www.ferc.gov/press-room/pr-archives/2002/2002-2/4-9-saludazz.pdf> .
- Jones, Lucile M. 1995. Foreshocks, mainshocks, and aftershocks. Southern California Earthquake Center. <http://www.data.scec.org/eqcountry/aftershock.html> .
- Lake Murray. 2005. The lake murray home page. <http://www.lakemurray.com/> . Accessed 12 Feb 2005.
- Moussa, Roger, and Claude Bocquillon. 2000. Approximation zones of the saint-venant equations for flood routing with overbank flow. *Hydrology and Earth System Sciences* 4 (2): 251–261.

- Publications, Gardener. 2004. Lakeside living. <http://www.gardenerguides.com/ColumbiaPage-Neighborhoods-LakeM.htm>.
- Scana. 2005. Emergency information: Lake murray evacuation map. http://www.scana.com/SCEG/For+Living/Lake+Murray/emergency_information.htm.
- SCIway. 2000. South carolina county maps. <http://www.sciway.net/maps/cnty/>.
- of Natural Resources, South Carolina Department. Lake and stream data. <http://www.dnr.state.sc.us/pls/hydro/river.home>.
- South Carolina Geological Survey. 1997. Simplified map showing faults and related geologic structures. <http://www.dnr.state.sc.us/geology/earthqua2.htm>.
- _____. 1998. Structural features of South Carolina. <http://water.dnr.state.sc.us/geology/structur.htm>.
- SouthCarolinaLakes.net. Lake murray. <http://www.southcarolinialakes.net/murray.htm>.
- Topozone. 2004. <http://www.topozone.com/map.asp?lat=34.042&lon=-81.2&s=50&size=1&symshow%=n&datum=nad83&layer=DRG25>.
- Trefethen, Lloyd N. 1996. *Finite Difference and Spectral Methods for Ordinary and Partial Differential Equations*. Unpublished textbook available at <http://web.comlab.ox.ac.uk/oucl/work/nick.trefethen/pdetext.html>.
- U.S. Army Corps of Engineers. 1997. Engineer Manual 1110-2-1420. *Engineering and Design—Hydrologic Engineering Requirements for Reservoirs*. <http://www.usace.army.mil/inet/usace-docs/eng-manuals/em1110-2-1420/>.
- _____, Hydrologic Engineering Center. 1980. *Flood Emergency Plans: Guidelines for Corps Dams*. RD-13, HEC. http://www.hec.usace.army.mil/publications/pub_download.html.



Lori Thomas, Clay Hambrick, Katie Lewis, and Jon Jacobsen (advisor).

Through the Breach: Modeling Flooding from a Dam Failure in South Carolina

Jennifer Kohlenberg
Michael Barnett
Scott Wood
University of Saskatchewan
Saskatoon, SK, Canada

Advisor: James Brooke

Summary

The Saluda Dam, separating Lake Murray from the Saluda River in South Carolina, could breach in the event of an earthquake.

We develop a model to analyze the flow from four possible types of dam breaches and the propagation of the floodwaters:

- instant total failure, where a large portion of the dam erodes instantly;
- delayed total failure, where a large portion of the dam slowly erodes;
- piping, where a small hole forms and eventually opens into a full breach; and
- overtopping, where the dam erodes to form a trapezoidal breach.

We develop two models for the spread of the downstream floodwaters. Both use a discrete-grid approach, modelling the region as a set of cells, each with an elevation and a volume of water. The Force Model uses cell velocities, gravity, and the pressure of neighbouring cells to model water flow. The Downhill Model assumes that flow rates are proportional to the height differences between the water in adjacent cells.

The Downhill Model is efficient, intuitive, flexible, and could be applied to any region with known elevation data. Its two parameters smooth and regulate water flow, but the model's predictions depend little on their values.

The UMAP Journal 26 (3) (2005) 245–261. ©Copyright 2005 by COMAP, Inc. All rights reserved. Permission to make digital or hard copies of part or all of this work for personal or classroom use is granted without fee provided that copies are not made or distributed for profit or commercial advantage and that copies bear this notice. Abstracting with credit is permitted, but copyrights for components of this work owned by others than COMAP must be honored. To copy otherwise, to republish, to post on servers, or to redistribute to lists requires prior permission from COMAP.

For a Saluda Dam breach, the total extent of the flooding is 106.5 km²; it does not reach the State Capitol. The flooding in Rawls Creek extends 4.4 km upstream and covers an area of 1.6–2.4 km².

Variables and Assumptions

Table 1 shows the variables used in the design and simulation of the flooding model, and **Table 2** lists the parameters in the simulation program.

Table 1.
Variables used in the model.

Variable	Definition
Voume flow rates from the dam	
Q_{TF1}	For instant total failure
Q_{TF2}	For delayed total failure
Q_{PIPE}	For piping failure
Q_{OT}	For overtopping failure m
Q_{peak}	Maximum flow rate
Times when water ceases to flow through the dam	
t_{TF1}	For instant total failure
t_{TF2}	For delayed total failure
t_{PIPE}	For piping failure
t_{OT}	For overtopping failure
ΔV	Total volume of water displaced from Lake Murray by flooding
Vol_{LM}	Normal volume of Lake Murray
$Area_{LM}$	Normal area of Lake Murray
d_{breach}	Depth of the breach from the top of the dam
t_{breach}	Time from when the breach begins to form until its final formation
m	Slope of the sides of the cone approximating Lake Murray

General Assumptions

- Normal water level is present in the lake prior to a dam breach.
- No seasonal variation of flows occurs in waterways.
- Volume of water in Lake Murray can be accurately approximated by a right circular cone (**Figure 1**).

Dam Assumptions

- Saluda Dam fails in one of four ways:
 - instant total failure,
 - delayed total failure,

Table 2.
Parameters used in the simulation program.

Parameter	Typical value	Meaning
BREACH_TYPE	varies	one of INSTANT_TOTAL_FAILURE, DELAYED_TOTAL_FAILURE, PIPING, or OVERTOPPING
ΔT	10.0	Length of one time step (s)
MIN_DEPTH	0.0001	Depth below which a cell is considered empty (m)
T_{FINAL}	100000	Time for the breach to empty completely the affected portion of the reservoir (s)
T_b	3600	Time until breach reaches maximum size (s)
Q_{peak}	25000	Maximum flow rate of the breach (m^3/s)
d_{breach}	30	Maximum depth of breach below initial reservoir level (m)
Volume _{LM}	2.714×10^9	Initial volume of Lake Murray (m^3)
Area _{LM}	202×10^6	Initial area of Lake Murray (m^2)
k	0.504	Spreading factor (regulates amount of water exchanged between two cells)
MAX_LOSS_FRAC	0.25	Maximum fraction of a cell's water that it can donate in a single time step

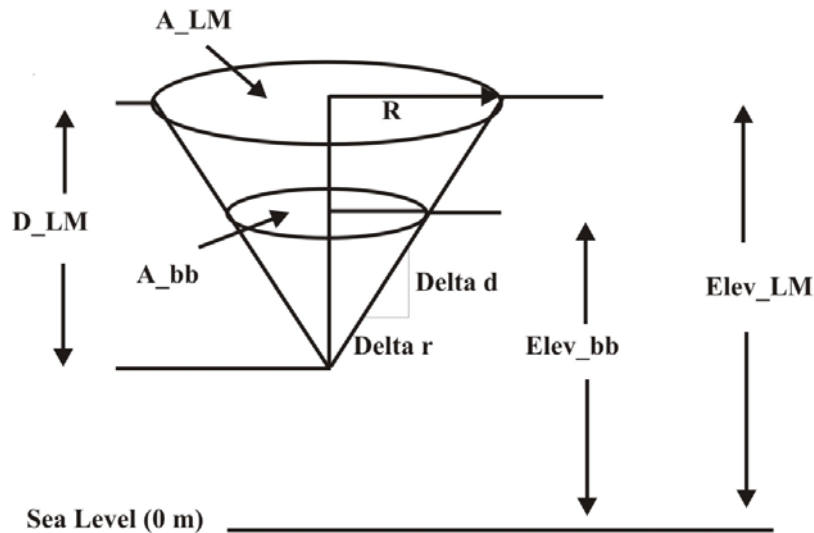


Figure 1. Reservoir approximation using a right circular cone.

- piping, or
- overtopping.
- Composition of the earthen dam is uniform throughout.
- Width of the base of the breach is between the height of the dam and three times the height of the dam [U.S. Army Corps of Engineers 1997].
- No human attempt is made to prevent dam breaching.

Downstream Assumptions

- Resistance to water flow due to structures such as bridges and buildings is negligible.
- Water does not alter the terrain significantly as it flows over the floodplain.
- Water does not make alluvial deposits as it flows over the floodplain.
- A negligible amount of water is present in the valley before flooding.
- Negligible water inflow occurs from sources other than the dam breach.
- No human attempt will be made to prevent flooding.

Accepted Facts

- Area of Lake Murray: 200 km²
- Volume of Lake Murray: 2.710×10^6 m³
- Height of dam: 63.4 m (crest at 370 ft above sea level)
- Length of dam: 2.4 km
- Elevation of surface of Lake Murray: 106.5—110 m above sea level

Model Design

Dam Breach

Each type of dam breach is described by flow rate as a function of time, with corresponding parameters.

Instant Total Failure

A model of flow rate for instant total failure is right triangular [U.S. Army Corps of Engineers 1997] (**Figure 2**). The parameters are breach depth and peak volume outflow, with values

$$d_{\text{breach}} = 20 \text{ m}, \quad Q_{\text{peak}} = 30,000 \text{ m}^3/\text{s}.$$

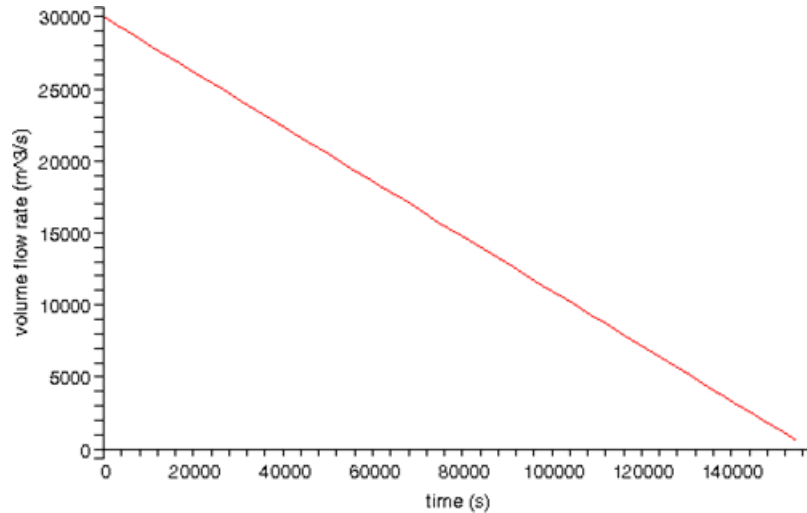


Figure 2. Flow rate for an instant total failure.

Delayed Total Failure

An isosceles triangle model makes sense for delayed failure because it takes half of the total volume of water removed from the lake to erode the dam and the flow rate does not peak until the erosion is complete [U.S. Army Corps of Engineers 1997] (Figure 3). Also, for an earthen dam, the erosion time may be longer than for other types of dams, such as concrete.

This model has the same parameters and same values:

$$d_{\text{breach}} = 20 \text{ m}, \quad Q_{\text{peak}} = 30,000 \text{ m}^3/\text{s}.$$

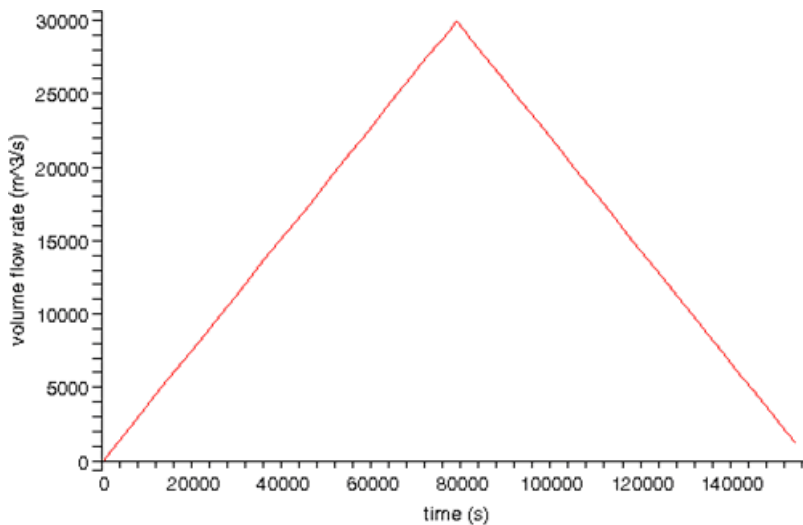


Figure 3. Flow rate for a delayed total failure.

Piping Failure

For a piping failure, the breach begins in the middle of the dam face and grows until the material above the pipe collapses [Sedimentation and River Hydraulics Group 2004]. As the breach grows, the flow rate increases exponentially; the peak flow rate occurs when the material above the pipe collapses. From that point, the flow through the breach is similar to a total failure. We select an exponential decay so as to observe a different effect from the linear decay of the total failure models (**Figure 4**).

We choose the growth rate so that the peak flow rate occurs at the breach time, and the decay rate so that the flow rate is less than 1% of the peak flow rate at the final time. The parameters are the breach depth, the peak volume outflow of the dam, and the breach time, with values

$$d_{\text{breach}} = 20 \text{ m}, \quad Q_{\text{peak}} = 30,000 \text{ m}^3/\text{s}, \quad t_{\text{breach}} = 50,000 \text{ s}.$$

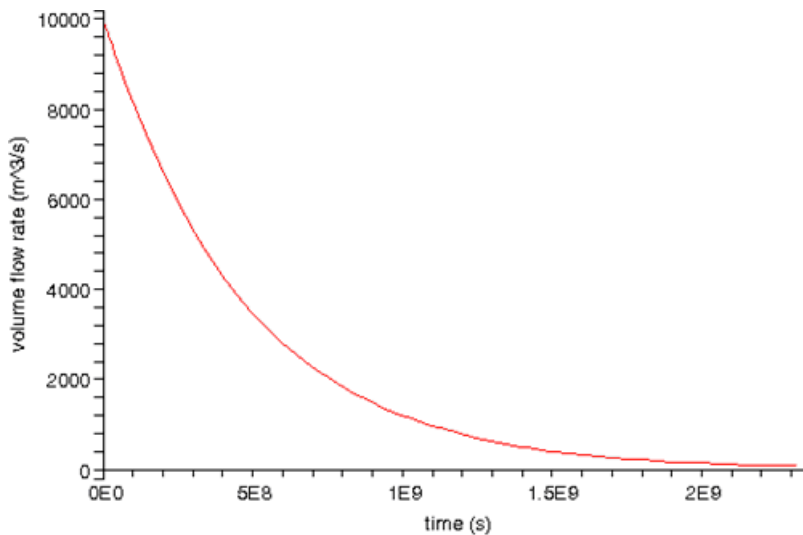


Figure 4. Flow rate for a piping failure.

To demonstrate better the change in flow rate with time when the breach begins to form, we plot over a shorter range of time in **Figure 5**.

Overtopping Failure

For an overtopping failure, the water begins flowing over the top of the breach, eroding the dam from above. We found little information about overtopping failures. From the piping failure, we estimate that the flow rate increases according to a parabolic shape until dam erosion is complete (**Figure 6**). After this point, which corresponds to the breach time, the flow rate behaves as in a total failure.

The parameters are again breach depth, peak volume outflow of the dam, and breach time, with values

$$d_{\text{breach}} = 20 \text{ m}, \quad Q_{\text{peak}} = 30,000 \text{ m}^3/\text{s}, \quad t_{\text{breach}} = 30,000 \text{ s}.$$

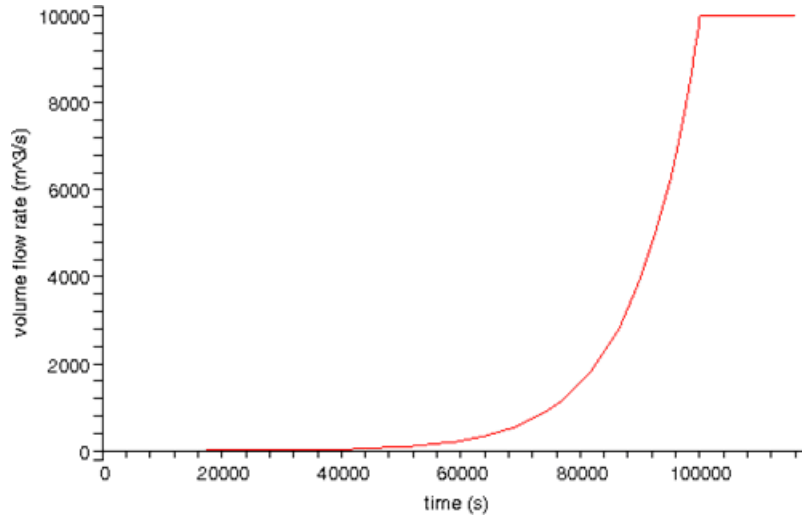


Figure 5. Flow rate for beginning of a piping failure.

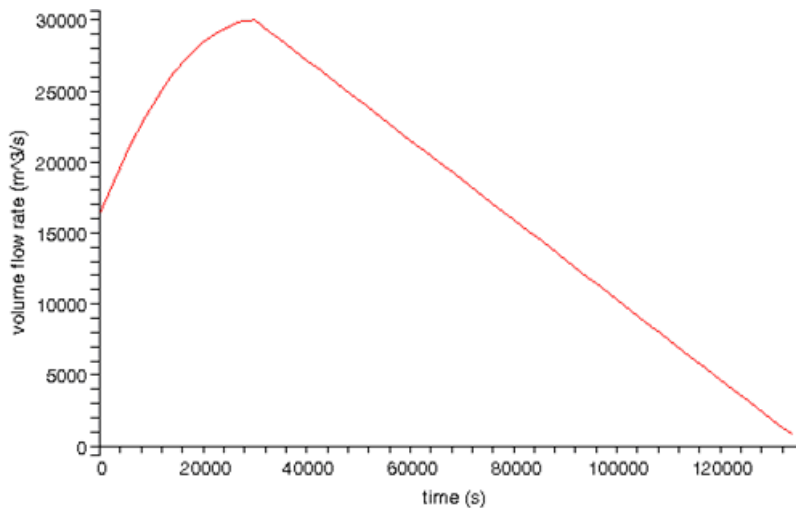


Figure 6. Flow rate for an overtopping failure.

Downstream Flow

We model the behaviour of the water in the region downstream of the breach using a discrete approach. The Force Model uses a physical analogy based on the Bernoulli equation for fluid flow; the Downhill Model uses a simpler, more intuitive mechanism for water flow. The Force Model produces unphysical results; therefore, we use Downhill Model in analysis of the flooding.

For both models, the region surrounding the Saluda Dam is divided into a grid of square cells. Each cell covers a surface area of 210 m by 210 m and has an associated elevation above sea level and a volume of water (based on the mean depth of water in the cell). The elevation data are adapted from the U.S. Geological Survey's National Elevation Data [2004] by (to reduce processing time) averaging together groups of 7×7 cells. Each model simulates the

propagation of water among cells; the models differ in how neighbouring cells determine how much water to exchange per unit time.

Force Model

Design

This model performs a force analysis on the water contained in the model cells. Each cell has an associated elevation above sea level, mean depth of water contained in the cell, and mean velocity (x - and y -components) of water within the cell. The force acting on a particular cell is assumed to be due to two effects only: the pressure force exerted by the four cells in direct contact with it, and the gravitational force that accelerates the water to places of lower elevation (that is, downhill).

The main principles of the model are:

- Volume flow between cells is proportional to the difference in pressure between the four adjacent cells with a common face.
- Pressure difference in cells is proportional to the difference in mean depth of each cube.

As demonstrated in the **Figures 7 and 8**, the mean pressure exerted by a cell is assumed to be the pressure at half the depth of the cell, or $P = \frac{1}{2}\rho g d$.

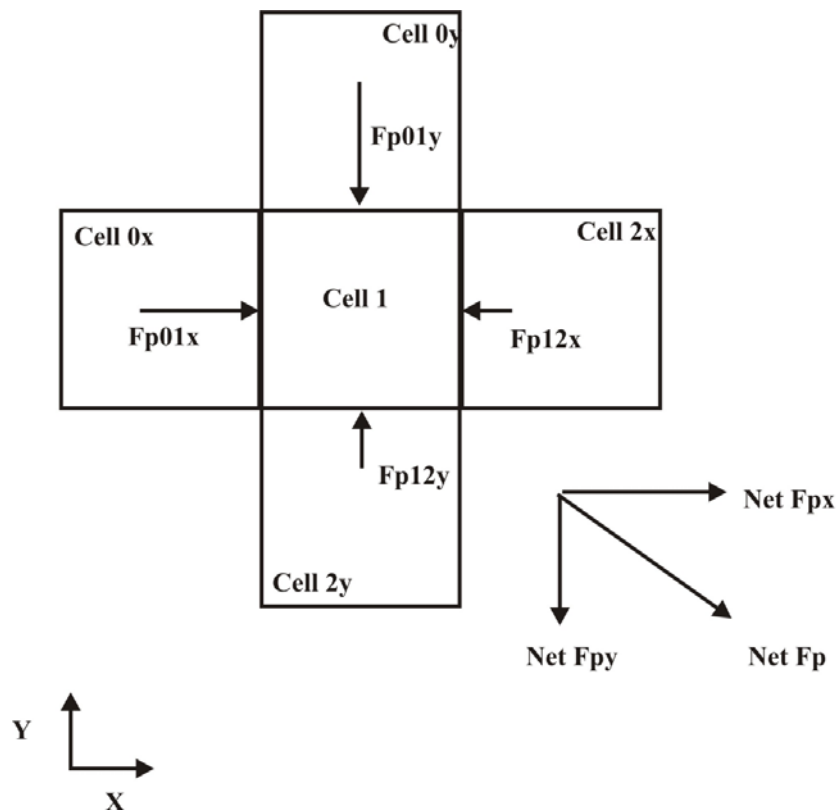


Figure 7. Pressure forces acting on cell matrix.

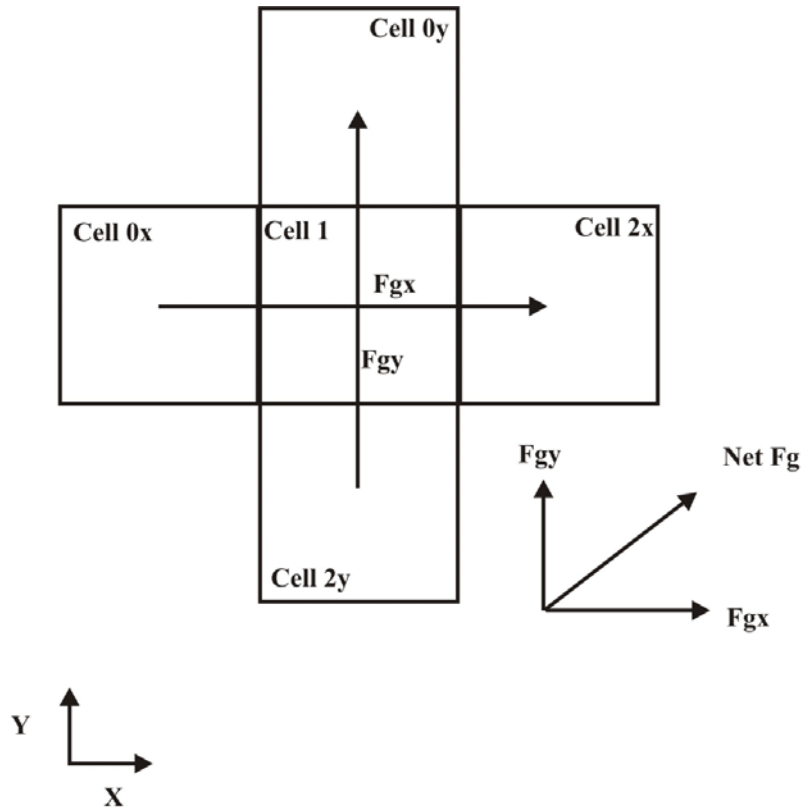


Figure 8. Gravitational forces acting on cell matrix.

We assume that the area over which the pressure acts is the mean depth of the two adjacent cells, so that the depth of water varies linearly between them, with the depth at the boundary the average depth of the two. The force exerted by a neighbouring cell is the mean pressure times the area between the two cells. To find acceleration, we divide the force by the mass of water in the cell, taken to be the volume of the cell times the water density:

$$a_x = \frac{g(d_{0x}^2 - d_{2x}^2)}{4wd_1}.$$

We calculate the acceleration due to gravity by estimating the gradient of the ground of the current cell and its four immediate neighbours. We determine the horizontal component of the acceleration geometrically (Figure 9) to be

$$a_g = \frac{2\Delta h w g}{4w^2 + \Delta h^2}.$$

The model iterates through a large number of time steps, typically each of 1 s duration. At the beginning of each time step, water is injected into the cells containing the dam breach; the amount is determined by the breach models described above. For each time step, the acceleration (x - and y -components) is calculated for each cell in the region, and the velocity of water in the region is updated according to

$$v_{\text{new}} = v_{\text{old}} + a\Delta t.$$

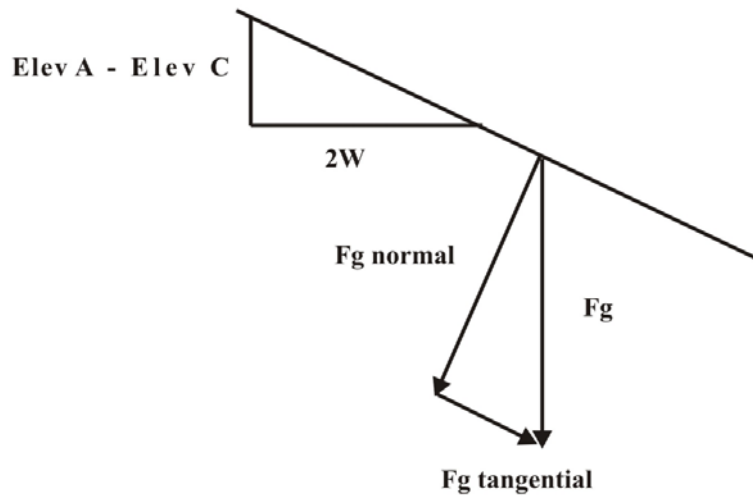
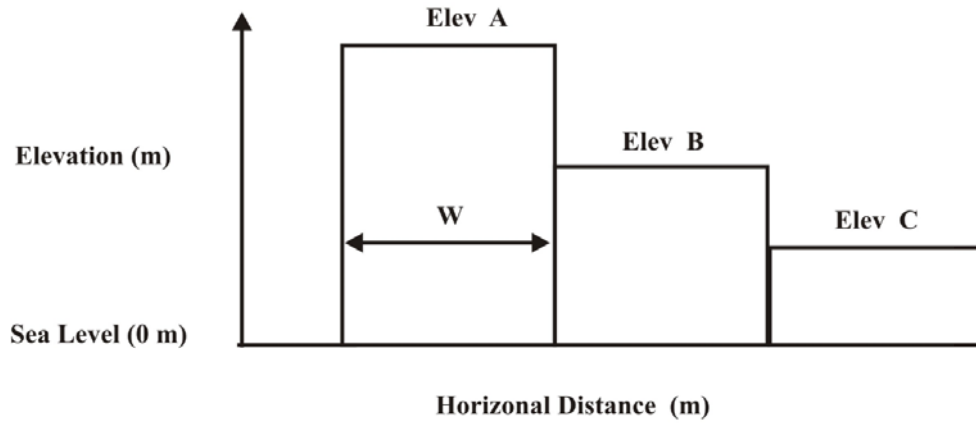


Figure 9. Determination of tangential component of gravity.

The direction of the velocity determines in which direction each cell donates: For $v_x > 0$, the cell donates to the right; for $v_x < 0$, the cell donates to the left. The amount of water donated is proportional to the speed in that direction, so that the change in water depth of the current cell is

$$d_{\text{donated}} = \frac{d_{\text{avg}} \Delta t}{2w}.$$

The water depth of the neighbouring cell receiving the donation is also updated, so that the total amount of water in the model is conserved (except for donations off the edges of the map and the water injected at the breach cell).

For very large velocities, a cell can donate more water than it has. Specifically, if the speed times the time step size is larger than the cell width, the donation would be greater than the cell's current volume. If this occurs, the cell

is assumed to donate all its water, and the donations in the x - and y -directions are scaled to account for this.

Justification

This model is intuitively appealing: It models the behaviour of the water using a simple but meaningful physical analogy. The force analysis used is equivalent to taking the gradient of the Bernoulli equation and modeling the fluid discretely.

The model computes and saves velocity information, allowing modeling of the manner in which regions are flooded. For example, the model could predict the speed of the water as it struck a particular building in Columbia, such as the State Capitol.

Reasons for Rejecting the Model

The results from the model are unrealistic. Since cells with large volumes of water have small accelerations, these cells tend to empty very slowly, even if adjacent to completely empty cells; for the same reason, small cells tend to empty too quickly. The result is a checkerboard pattern: Large cells grow larger and their small neighbours grow smaller. This error relates to our assumption that all water within a cell has the same velocity: A single cell cannot spread out in all directions. For a simpler terrain (such as a simple downhill channel), this would not be a problem; however, this terrain is highly complicated and requires the water to propagate in several directions.

Another problem with this model is its complexity. The model juggles a large number of parameters for each cell, making tuning and troubleshooting difficult.

Downhill Model

Design

The Downhill Model assumes that the flow rate between two cells is proportional to the height difference between the centers of mass of those cells multiplied by the effective area between them. The model allows water to be donated in multiple directions by a single cell, if it is higher than several of its neighbours. As in the Force Model, the program iterates through time steps, adding water each step to the cells containing the dam breach.

For each time step, each cell (except those on the bottom and right boundaries of the map, which are handled later) exchanges water with the two cells immediately below and to the right. This ensures that each cell exchanges water with its four neighbours exactly once per time step. To exchange with a neighbour, a cell changes its height according to the formula

$$d_{\text{donated}} = kd_{\text{avg}}(h_0 - h_2).$$

The value of k is based on the assumption that the water speed at the breach during the peak flow rate is 30 m/s. We later describe the model's response to a change in k .

The neighbouring cell then changes its height by the negative of this value. To ensure consistency, the changes in height are not applied until the end of the time step, after all cell height changes have been calculated. If a cell had donated more than `MAX_LOSS_FRAC` of the water that it originally contained, then its donations are scaled down so that it donates exactly this amount. The factor `MAX_LOSS_FRAC` is used to prevent sloshing: Large cells tend to empty completely into empty neighbours, which then donate back on the next turn, so that half of the cells are empty at any one time.

For cells along the boundary, donations on their side(s) against the edges of the map are assumed to be equal to their donations on the opposite sides. Since these cells are far away from the breach or areas of interest, their precise behaviour is less important. Our approach ensures that water reaching the edges of the map leaves smoothly, without piling up unphysically.

Justification

This model affords rapid computation and uses a simple principle that is easy to troubleshoot. Although the equation governing the water exchange between cells lacks a direct physical analogy, it produces results consistent with physical expectations. Water travels most quickly downhill or across the nearly flat floodplain, and creeps uphill only as water levels rise.

Testing and Results

Testing

To test our models, we use National Elevation Data from the U.S. Geological Survey [USGS 2004]. The data are a set of elevation values (in meters above sea level) arranged into rows and columns. Each element represents a square with sides 30 m in length. To reduce computation, we averaged groups of 7×7 cells together, so that the cells that we used were squares 210 m on a side.

We tested both the Force Model and the Downhill Model by placing the breach cell just in front of the dam face and modeling the spread of water for several choices of breach type (instant total failure, delayed total failure, piping, overtopping) and time period (360, 1800, 6240 s). We tested the k dependence and `MAX_LOSS_FRAC` dependence by using the instant total failure breach model.

To prevent errors from very small volumes in cells, we treated a cell as empty if its mean depth was less than 0.0001 m. This cutoff was especially important in the Force Model, where such small cells acquire enormous velocities ($> 10^6$ m/s) when placed next to a cell with a significant amount of water.

We tested the Downhill Model for robustness by running the instant total failure model for 50,000 time steps. The model behaves poorly beyond 40,000 time steps, when the flow rate out of the map becomes much greater than the flow rate of the dam breach (which has slowed by this point). We also tested the model for very large flow rates. For rates that increased the height of the breach cell by more than 10 m per time interval (more than 30 times as large as any flow rate in the simulation), the simulation lasts only 1000 time steps before becoming unstable.

Results

Flooding Extent

The extent of the flooding is largely independent of the type of breach (**Figure 10**); the difference between breach types is in how quickly flooding spreads. For instant total failure breach, the flooding has a maximum extent of 106.5 km². The flooding is greatest in the Saluda and Congaree valleys, which are quite flat and broad. The flooding in the city of Columbia itself, which is elevated from these valleys, is very minimal. We did not model the effects of the flooding farther down the Congaree, but we expect those to be comparable to the flooding within the region simulated.

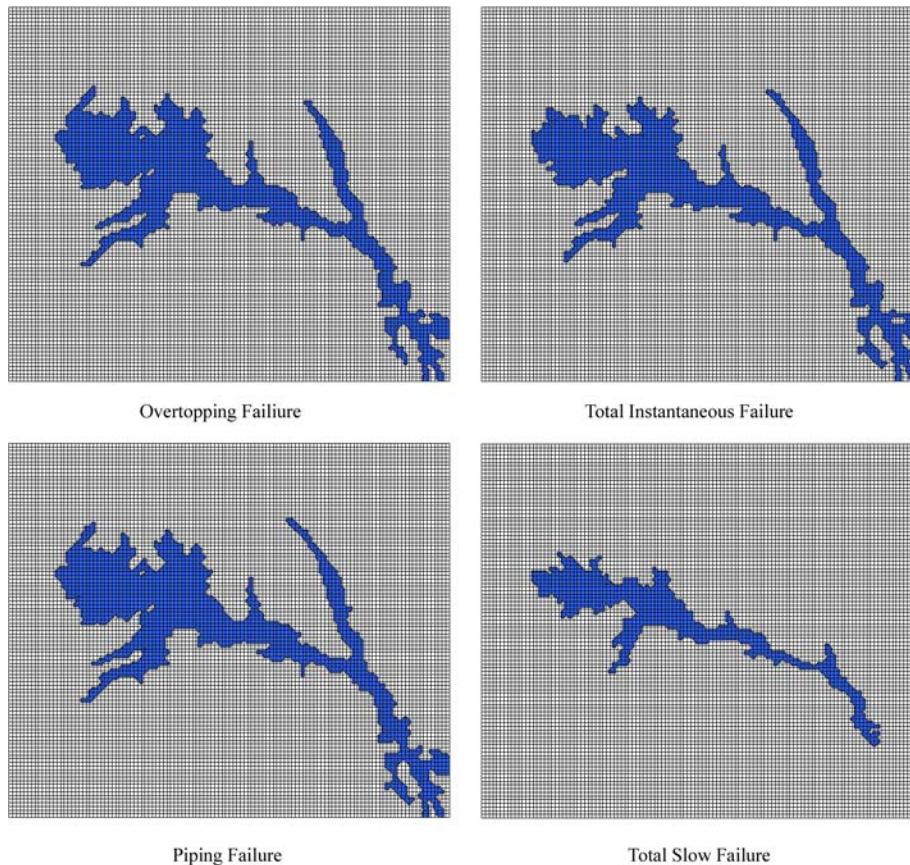


Figure 10. Comparison of dam breach scenarios: flooding area after 24 h.

Rawls Creek

The flooding in Rawls creek is extensive in area but not in upstream extent. Although it is difficult to establish where the flooding of the Saluda river ends and the flooding of Rawls Creek begins, the area around Rawls Creek that becomes flooded we estimate as between 1.6 and 2.4 km². The farthest flooded point is 4.4 km upstream.

State Capitol

Flooding does not reach the State Capitol, even for the most extreme case, instant total failure

Error Analysis, Sensitivity, and Robustness

The model depends on the factor k to scale the amount of water donated. Its value is based on the assumption that the water speed at the breach during the peak flow rate is 30 m/s. However, the value of k does not affect the simulation greatly; the total flooded area after 1800 time steps varies by just 17% when k is varied by a factor of 100.

The `MAX_LOSS_FRAC` is used to prevent each cell from donating too much water. However, the extent of the flooding is not strongly dependent on its value, which we took as 0.25 to produce reasonably smooth water distributions.

Strengths and Weaknesses

Strengths

The model is independent of the site simulated: Given elevation data for a region and an equation governing the flow rate of water from a dam breach, it calculates the behaviour of flooding.

The Downhill Model is intuitive. It relies on a simple exchange rule between cells, making it easy to tune and troubleshoot. Tuning may be needed to account for problems associated with more extreme flooding cases, a need to extract additional results from the model, or other unforeseen demands.

The algorithm is efficient; the computation of a single time step is linear in the number of cells in the region. This efficiency makes it possible to model many variations on breach types and flow rates in a short period of time.

The model produces three data sets of grids: 0/1 values describing which cells are flooded; the water depth in each cell to determine the severity of the flooding in a region; and the water depth plus elevation for each cell. From plots of these data sets, the extent and severity of the flooding are easy to see.

Weaknesses

The primary weakness of this model is the tendency of water in the deeper regions of the flooded area to slosh. It should be possible to eliminate this, perhaps by introducing a depth dependence into `MAX_LOSS_FRAC`.

Another weakness that could be corrected with more analysis is the time scale. Since the k -dependence—the only place where the duration of the time step is used explicitly—is weak, the model's time scale is not easily changeable. The time scale could be calibrated by running simulations of an analytical system, such as the propagation of water down a channel, and determining the speed of the water and hence the time scale. Since the time scale was not needed to analyze the extent of the flooding, we did not perform this calibration.

References

- Chauhan, Sanjay S., et al. 2004. Do current breach parameter estimation techniques provide reasonable estimates for use in breach modeling? Utah State University and RAC Engineers & Economists. www.engineering.usu.edu/uwrl/www/faculty/DSB/breachparameters.pdf . Accessed 3 February 2005.
- Cheremisinoff, Nicholas P. 1981. *Fluid Flow: Pumps, Pipes, and Channels*. England: Butterworth.
- Federal Energy Regulatory Commission (FERC). 2002. Saluda Dam remediation: Updated frequently-asked questions and answers. www.ferc.gov/industries/hydropower/safety/saluda/saluda_qa.pdf . Accessed 4 February 2005.
- Fread, D.L. 1998. *Dam-Breach Modeling and Flood Routing: A Perspective on Present Capabilities and Future Directions*. Silver Spring, MD: National Weather Service, Office of Hydrology.
- Mayer, L. 1987. *Catastrophic Flooding*. Boston, MA: Allen & Unwin.
- Munson, Bruce R., et al. 2002. *Fundamentals of Fluid Mechanics*. 4th ed. New York: John Wiley & Sons.
- Sedimentation and River Hydraulics Group. 2004. Comparison between the methods used in MIKE11, FLDWAV 1.0, and HEC-RAS 3.1.1 to compute flows through a dam breach. U.S. Department of the Interior.
- Smith, Alan A. Hydraulic theory: Kinematic flood routing. Alan A. Smith Inc. <http://www.alanasmith.com/theory-Kinematic-Flood-Routing.htm> . Accessed 3 February 2005.
- U.S. Army Corps of Engineers. 1997. Engineering and design—Hydrologic engineering requirements for reservoirs. Department of the Army Publication EM 1110-2-1420, Ch. 16.
- U.S. Geological Survey (USGS). 2004. Seamless Data Distribution System, National Center for Earth Resources Observation and Science. seamless.usgs.gov . Accessed 4 February 2005.
- Wahl, Tony L. 1997. Predicting embankment dam breach parameters—A needs assessment. Denver, CO: U.S. Bureau of Reclamation. http://www.usbr.gov/pmts/hydraulics_lab/twahl/publications.html . Accessed 3 February 2005.
- Williams, Garnett P. 1978. Hydraulic geometry of river cross sections—Theory of minimum variance. Geological Survey Professional Paper. Washington, DC: U.S. Government Printing Office.

Appendix: Dam Breach Model Equations

For an instant total failure:

$$Q_{TF1}(t) = \begin{cases} -\frac{Q_{\text{peak}}(t - t_{TF1})}{t_{TF1}}, & t < t_{TF1}; \\ 0 & t_{TF1} < t, \end{cases}$$

where $t_{TF1} = \frac{2\Delta V}{Q_{\text{peak}}}$.

For a delayed total failure:

$$Q_{TF2}(t) = \begin{cases} \frac{2Q_{\text{peak}}t}{t_{TF2}}, & t \leq \frac{1}{2}t_{TF2}; \\ \frac{2(t_{TF2} - t)Q_{\text{peak}}}{t_{TF2}}, & \frac{1}{2}t_{TF2} - t < 0 \text{ and } t - t_{TF2} < 0; \\ 0, & t_{TF2} \leq t, \end{cases}$$

where $t_{TF2} = \frac{2\Delta V}{Q_{\text{peak}}}$.

For a piping breach that turns into a total failure:

$$Q_{\text{PIPE}}(t) = \begin{cases} (Q_{\text{peak}} + 1)^{t/t_b} - 1, & t \leq t_b; \\ Q_{\text{peak}} \exp\left[\frac{5(t - t_b)}{t - t_b}\right], & t_b - t < 0 \text{ and } t + t_b < 0; \\ 0, & t \leq t, \end{cases}$$

where

$$t_{\text{PIPE}} = \Delta V - t_{\text{breach}} \left[\frac{5 \left(\frac{2 + Q_{\text{peak}}}{\ln(Q_{\text{peak}} + 1)} - 1 \right)}{Q_{\text{peak}}(1 - e^{-5})} + 1 \right].$$

For an overtopping breach:

$$Q_{\text{OT}} = \begin{cases} Q_{\text{peak}} + 15(t^2 + 2tt_{\text{breach}} - t_{\text{breach}}^2) \times 10^{-6}, & t \leq t_{\text{breach}}; \\ \frac{Q_{\text{peak}}(t - t_{\text{OT}})}{t_{\text{breach}} - t_{\text{OT}}}, & t_{\text{breach}}t < 0 \text{ and } t - t_{\text{OT}} < 0; \\ 0, & \text{otherwise,} \end{cases}$$

where

$$t_{\text{OT}} = \frac{2(\Delta V + 0.000005t_{\text{breach}}^3 - t_{\text{breach}}Q_{\text{peak}})}{Q_{\text{peak}}} + t_{\text{breach}}.$$



Michael G. Barnett, Dr. James Brooke (advisor), Scott J. Wood, and Jennifer Dale Kohlenberg.

Analysis of Dam Failure in the Saluda River Valley

Ryan Bressler
Christina Polwarth
Braxton Osting
University of Washington
Seattle, WA

Advisor: Rekha Thomas

Summary

We identify and model two possible failure modes for the Saluda Dam: gradual failure due to an enlarging breach, and sudden catastrophic failure due to liquefaction of the dam.

For the first case, we describe the breach using a linear sediment-transport model to determine the flow from the dam. We construct a high-resolution digital model of the downstream river valley and apply the continuity equations and a modified Manning equation to model the flow downstream.

For the case of dam annihilation, we use a model based on the Saint-Venant equations for one-dimensional flood propagation in open-channel flow. Assuming shallow water conditions along the Saluda River, we approximate the depth and speed of a dam break wave, using a sinusoidal perturbation of the dynamic wave model.

We calibrate the models with flow data from two river observation stations.

We conclude that the flood levels would not reach the Capitol Building but would intrude deeply into Rawls Creek.

Introduction

The Saluda Dam, located 20 km above Columbia, South Carolina, impounds the almost 3-billion-cubic-meter Lake Murray [South Carolina Electric & Gas Company 1995]. It is a large earthen dam of a type that has failed in earthquakes before [Workshop 1986]. In such a failure, the water in Lake Murray would

The UMAP Journal 26 (3) (2005) 263–278. ©Copyright 2005 by COMAP, Inc. All rights reserved. Permission to make digital or hard copies of part or all of this work for personal or classroom use is granted without fee provided that copies are not made or distributed for profit or commercial advantage and that copies bear this notice. Abstracting with credit is permitted, but copyrights for components of this work owned by others than COMAP must be honored. To copy otherwise, to republish, to post on servers, or to redistribute to lists requires prior permission from COMAP.

rush down the Saluda River Valley towards Columbia, its 100,000 residents, and the State Capitol.

We present a comprehensive mathematical description of the resulting flood, including its intrusion into Columbia and the tributaries of the Saluda. See **Figure 1** for an overview of the local topography.

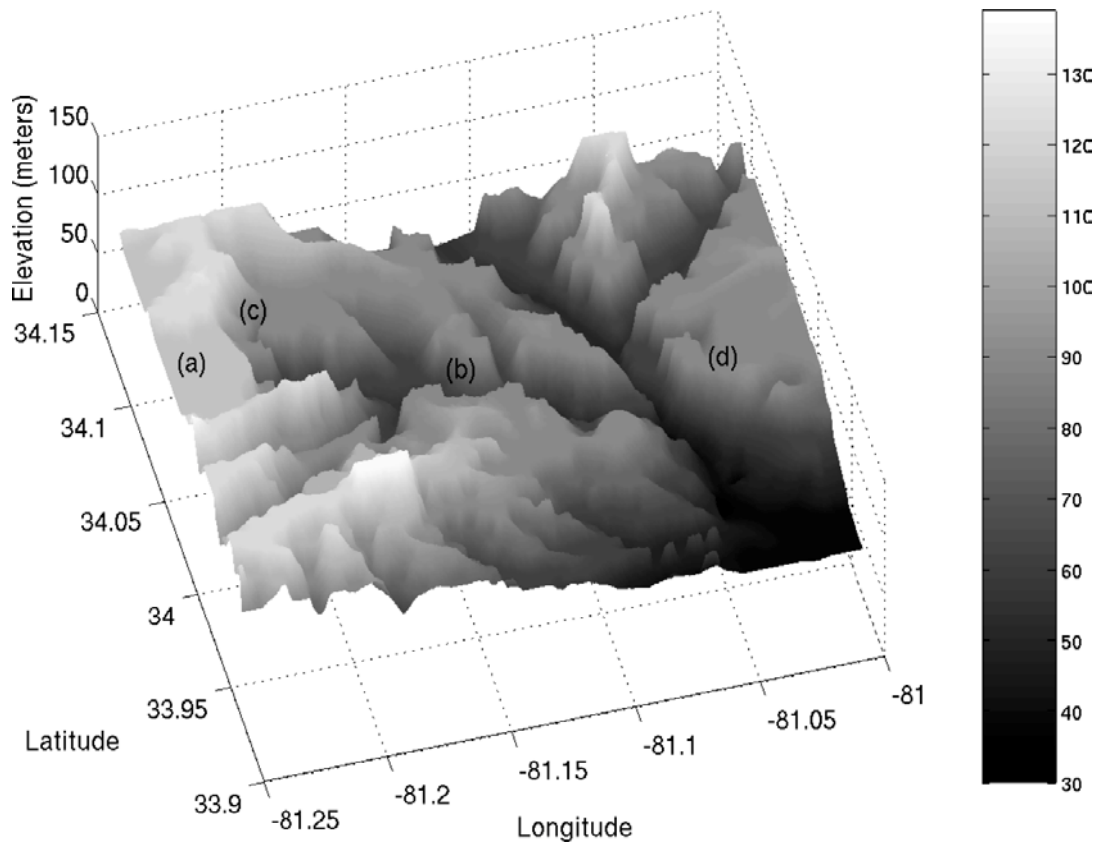


Figure 1. An overview of Lake Murray and the Saluda River Valley generated from the NCRS topographical data [National Geophysical Data Center 2005]. (a) Lake Murray. (b) Saluda River. (c) Rawls Creek. (d) State Capitol Building.

A brief survey of earthquake-related earthen dam incidents [Workshop 1986] reveals that failure can follow two distinct courses:

- A crack or breach forms in the dam, causing gradual failure due to erosion.
- The dam is completely annihilated, resulting in the formation of a surge.

To describe both of these situations accurately, we apply two different models.

Gradual Failure The relatively gradual rate at which water is introduced into the downstream valley suggests that the dispersion of the flood may be modeled using classical open-channel hydraulics. We divide the downstream river course into basins or reaches and then use the Manning formula and the continuity equation to describe the movement of water between them.

We determine the flow into the first basin using a model for the destruction of the dam due to breach erosion.

We create a three-dimensional topographical model of each basin using 3' resolution data from the NGDC Coastal Relief Model [National Geophysical Data Center 2005]. (**Figure 1** was generated using these models.) This lets us estimate the relationship between the volume in each basin and the cross-sectional area of its outflow channel. The Manning formula and the continuity equation yield a system of coupled first-order differential equations. We integrate this system numerically and calibrate it using data for normal flow in the Saluda River from river observation stations just below the Saluda Dam and just above Columbia City [USGS 2005].

Rapid Failure The flood wave is described as a sinusoidal perturbation to the steady-state solution of the Saint-Venant equation. We apply the dynamic wave model of Ponce et al. [1997] to determine the surge's propagation.

We represent the Saluda River Valley as a prismatic channel of rectangular cross section. We use a small surge recorded by the USGS river observation station in the Saluda Valley [USGS 2005] to calibrate the frictional constant governing the rate of attenuation of the flood waves.

Finally, we address the results of the two models and their consequences for Rawls Creek, the Capitol, and the residents of Columbia.

Gradual Failure

Our model for downstream flooding depends on the conservation of matter as described by the continuity equation, which states that for any given reach of the river, the change in volume equals the difference between flow in and flow out:

$$\frac{dV}{dt} = Q_{\text{in}} - Q_{\text{out}}, \quad (1)$$

where V is the volume of the reach, t is time, and Q_{in} and Q_{out} are the flows.

We divide the Saluda River Valley into four reaches. Since the amount of water involved in a dam failure flood would be significantly greater than that contributed by any other source, we simplify our model by assuming that all flow into and out of a reach would occur along the Saluda. For each reach, we set Q_{in} of each reach equal to Q_{out} of the reach above it, ignoring all tributaries. Eq. (1) becomes:

$$\frac{dV_n}{dt} = Q_{n-1} - Q_n, \quad n = 1, \dots, 4, \quad (2)$$

where V_n is the volume in the n th reach (numbered downstream from the dam) and Q_n is the flow out of the n th reach; Q_0 is the flow into the reach 1 through the breach in the dam.

To evaluate (2), we must estimate several parameters and relations:

- the flow out of the reservoir (into the first reach) resulting from a dam breach,
- the flow through each reach, and
- the topographical profiles of the reaches.

Flow Through the Breach

Dam-breach erosion is an interaction between the flooding water and the material of the dam. Once a breach has formed, the discharging water further erodes the breach. Enlargement of the breach increases the rate of discharge, which in turn increases the rate of erosion. This interaction continues until the reservoir water is depleted or until the dam resists further erosion.

We assume that the pre-breach flow into and out of the reservoir can be ignored, since they are of opposite sign and of negligible magnitude compared to the flooding waters. The breach outflow discharge Q_0 equals the product of the rate at which the water is lowering and the surface area at that height, $A_s(H)$. Also, the breach outflow discharge is related to the mean water velocity u and the breach cross-sectional area A_b by the continuity equation:

$$A_s(H) \frac{dH}{dt} = -Q_0 = -uA_b. \quad (3)$$

Experimental observations show that the flow of water through a breach can be simulated by the hydraulics of broad-crested weir flow [Chow 1959; Pugh et al. 1984]:

$$u = \alpha(H - Z)^\beta, \quad (4)$$

where Z is the breach bottom height measured from the bottom of the lake. For critical flow conditions, $\alpha = [(2/3)^3 g]^{1/2} = 1.7 \text{ m/s}$ and $\beta = 1/2$ [Singh 1996].

We further assume that the surface area of the reservoir, A_s , is independent of the height (i.e., the reservoir is rectangular). Combining (3) and (4) yields

$$A_s \frac{dH}{dt} = -uA_b = -\alpha(H - Z)^{\frac{1}{2}} A_b. \quad (5)$$

We describe erosion in the breach using the simplest method that has been used to model dam breaks accurately in the past [Singh 1996] and assume that

$$\frac{dZ}{dt} = -\gamma u^\phi = -\gamma \alpha^\phi (H - Z)^{\phi\beta}, \quad (6)$$

where γ and ϕ are determined from experimental analysis of the dam material and u is given by (4). Because we do not have access to the dam, we assume that $\phi = 1$ (linear erosion) and approximate γ as 0.01. This value of γ has given good results for linear erosion in the past [Singh 1996]. Eqs. (5)–(6) are coupled

first-order differential equations governing the elevation of the water surface and the elevation of the breach bottom as functions of time. To evaluate them, we must determine the shape of the breach.

Breaches in dams are typically modeled as triangles, trapezoids, or rectangles; but rectangles are used most often, since the resulting ODEs (5)–(6) are solved relatively easily [Singh 1996]. For simplicity, we model the breach as a rectangle with constant width b such that it erodes only in the vertical direction. Thus, the area of the breach is given by

$$A_b = b(H - Z). \quad (7)$$

Substituting (7) into (5) and rewriting (6) with $\phi = 1$ and $\beta = 1/2$ gives

$$\frac{dH}{dt} = -\frac{\alpha b}{A_s}(H - Z)^{\frac{3}{2}}, \quad \frac{dZ}{dt} = -\gamma\alpha(H - Z)^{\frac{1}{2}}. \quad (8)$$

Equations (8) admit the solution

$$H(Z) = Z + q + C \exp\left(\frac{-(Z_0 - Z)}{q}\right), \quad (9)$$

$$t(Z) = \frac{2\sqrt{q} \operatorname{arctanh}\left(\sqrt{\frac{H(Z) - Z}{q}}\right)}{\gamma\alpha} - D,$$

where $q = A_s\gamma/b$ and $C = H_0 - Z_0 - q$, H_0 and Z_0 are the initial values of H and Z at $t = t_0$, and D is a constant of integration determined from the initial conditions. The quantity $Z(t)$ is defined implicitly by (9), and $H(t)$ can then be recovered from (9). Then the flow through the breach, Q_0 can be determined from (3) and (5):

$$Q_0 = -\alpha \left[q + C \exp\left(\frac{-(Z_0 - Z)}{q}\right) \right]^{1/2} A_b. \quad (10)$$

When $Z(t) = 0$ at some time \tilde{t} , the dam must stop eroding and from (8) we obtain

$$\frac{dH}{dt} = -\frac{\alpha b}{A_s}H^{3/2}, \quad (11)$$

resulting in

$$H(t) = \left(\frac{1}{\sqrt{H_0}} + \frac{\alpha b}{2A_s}(t - t_0) \right)^{-2} \quad \text{for } t \geq \tilde{t}. \quad (12)$$

Figure 2 graphs Q and Z vs. time. The discontinuity of the derivative at time $t \approx 2$ h is the transition between these two solutions.

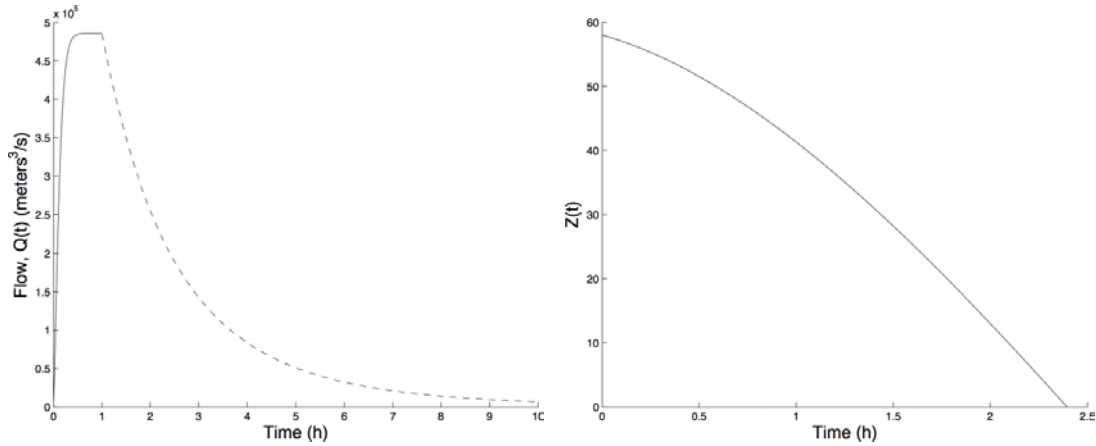


Figure 2. Flow through dam and height of breach bottom as breach enlarges.

Flow Between Reaches and the Manning Equation

We select reaches so that the river valley at their junctions is relatively prismatic and narrow. Assuming that the flow in a flood would be regulated by the rate at which water can flow through these narrows, we model the river as a series of pools, one flowing into the next.

Traditionally, flow in a floodplain is analyzed as the flow in a prismatic channel using the Manning equation

$$u = \frac{1}{n_m} \left(\frac{A}{P_w} \right)^{2/3} \sqrt{S}, \quad (13)$$

where

u is the mean flow velocity,

n_m is determined experimentally for each channel,

A is the cross-sectional area of the flow channel,

P_w is the wet perimeter of the channel cross section, and

S is the slope of the energy line.

There is no theoretical basis for the Manning equation; however, it has been extensively verified experimentally. Its primary advantage is the amount of information available on estimating Manning coefficients, n_m [Chanson 2004]. We apply it in our model because we can estimate n_m for the Saluda from data for other floodplains. The prismatic nature of the narrows means that we can apply the Manning equation without correcting for channel irregularities. Typical values of n_m are 0.5 for a brush-covered floodplain and 1.5 for a tree-covered one [Chanson 2004]. Assuming that our floodplain is somewhere between, we choose a moderate value of $n_m = 1$.

We set S , the slope of the energy line, equal to the slope of the valley floor. This is equivalent to assuming that the depth and speed of the water are constant with respect to flow direction in each narrows. Because of this, our model will be most accurate when radical changes in volume occur on a time scale greater than the time required to pass through the narrows. From the propagation rates observed, the time required for the water to pass through each of the narrows is on the order of 0.1 h. The flood that we wish to consider rises sharply for 0.5 h, stays steady for 1.5 h, and then trails off gradually (see **Figure 2**). Our model is least accurate for the steepest part of the initial rise but ultimately describes most of the flood well.

We estimate the slope of the channel out of each reach from USGS topographical maps [USGS 1971; 1994; 1997]:

$$S_1 = \frac{1}{1200}, \quad S_2 = \frac{1}{800}, \quad S_3 = \frac{1}{600}, \quad S_4 = \frac{1}{800}. \quad (14)$$

We estimate S_4 , the slope of the final outflow channel, conservatively so as to produce a worst-case scenario of the flooding of the basin that contains Columbia.

Our topographical models of the river basin allow us to establish one-to-one correspondences between the volume of water in each reach, the cross-sectional area and wet perimeter of its outlet, and the height of the water in the reach. These correspondences define the cross-sectional area and wet perimeter of the outflow narrows as functions of volume; we designate these functions as $A_n(V)$ and $P_n(V)$. Noting that for a given channel cross section, the flow Q satisfies

$$Q = uA_n, \quad (15)$$

where u is the mean water velocity, (13) can be stated as a constraint on (2):

$$Q_n = A_n u_n = \frac{A_n}{n_m} \left(\frac{A_n}{P_n} \right)^{2/3} \sqrt{S_n}, \quad (16)$$

where $A_n = A_n(\rho V)$, $P_n = P_n(\rho V)$, and $V = V(t - \zeta)$.

We introduce parameters ρ and ζ to calibrate of the model; we determine them subsequently from observational data.

ρ describes how friction and surface features of the reach prevent the entire volume of water from flowing downstream.

ζ describes the amount of time that it takes water to pass through a reach. We assume ζ to be constant because of the constant length of our reaches.

Selection and Analysis of Reaches

We use 3' topographical data [National Geophysical Data Center 2005] to construct a topographical model. To establish correspondences between the

volume V_n of water contained in each basin and the area A_n and wet perimeter P_w of their outflow channels, we intersect the topographical model of each basin with a plane representing the water level and integrate numerically over the appropriate regions. We construct a database of these values in terms of height, to be used as we simulate (2). **Figure 3** displays one such profile, for reach 4, with volume and area next to the topographical map of the basin.

Our accuracy is limited by the 0.2-m height resolution of the NGDC data. This does not significantly effect the accuracy of our volume estimates, but the area and wet perimeter estimates display noticeable discontinuities for small volumes. (The oscillatory behavior seen later in **Figure 4** is caused by this.) Our model could be improved by conducting better surveys of the outflow channel of each reach; since we are primarily interested in large volumes, we proceed.

To summarize, our model places the following requirements on the selection of the reaches:

- The inflow and outflow channels must be narrower than the rest of the reach.
- The channels must also be prismatic.
- Water should take approximately the same amount of time to flow down each reach.

To satisfy these conditions, we construct reaches as follows:

- Reach 1: The 6-km section from Saluda Dam to the narrows at Correly Island.
- Reach 2: The 6-km section from Correly Island to the narrows just below Interstate 20.
- Reach 3: The 6-km section from just below Interstate 20 to the narrows just above the Saluda's outlet into the Congaree river.
- Reach 4: A large section of the Congaree River Basin including the area around the Capitol and a 6-km stretch of downstream channel.

Reaches 1, 2, and 3 satisfy our requirements extremely well. The Congaree River valley widens rapidly into a floodplain below Columbia and there are no natural narrows. We end our basin at a point that is somewhat narrow and satisfies the requirement for water flow time. A large portion of the broad river valley is included to allow for upstream flooding.

Calibration and Sensitivity Analysis

The US Geological Survey (USGS) has river observation stations just below the dam (at $34^{\circ}03'03''$ N $81^{\circ}12'35''$ W) and just above Columbia (at $34^{\circ}00'50''$ N $81^{\circ}05'17''$ W). Each logs the last 31 days' flows [USGS 2005]. On 6 January 2005, the station at Saluda Dam registered a surge of $30,000 \text{ m}^3$. Flow rates jumped from $27 \text{ m}^3/\text{s}$ to $700 \text{ m}^3/\text{s}$ and then receded over a 5-h period. A similar surge

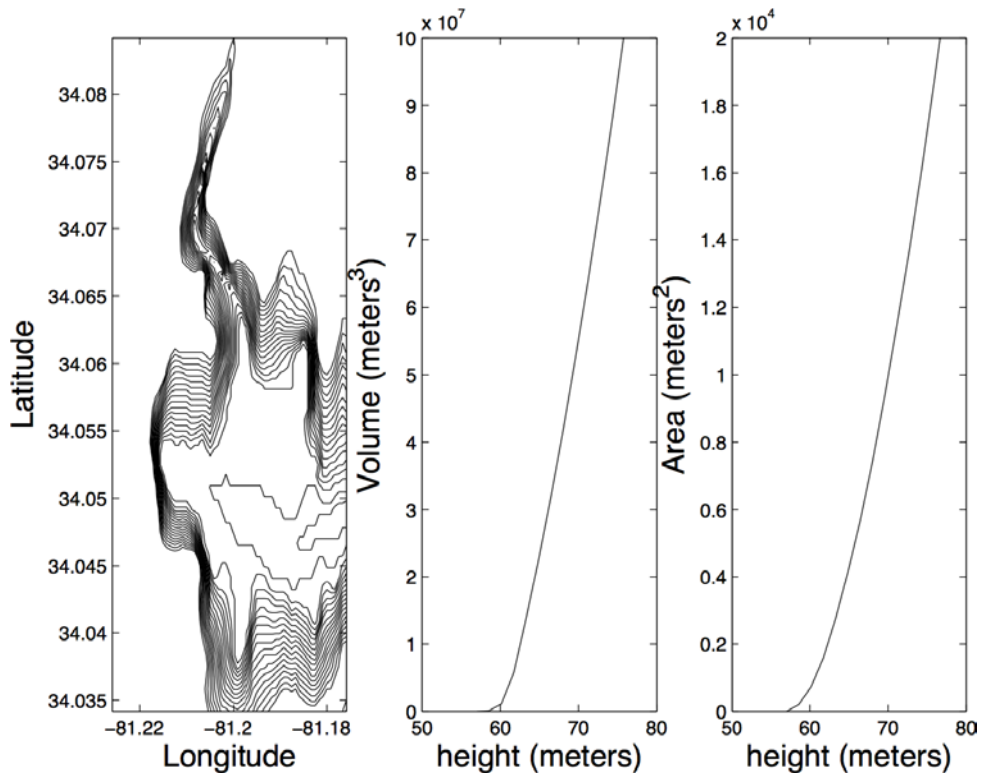
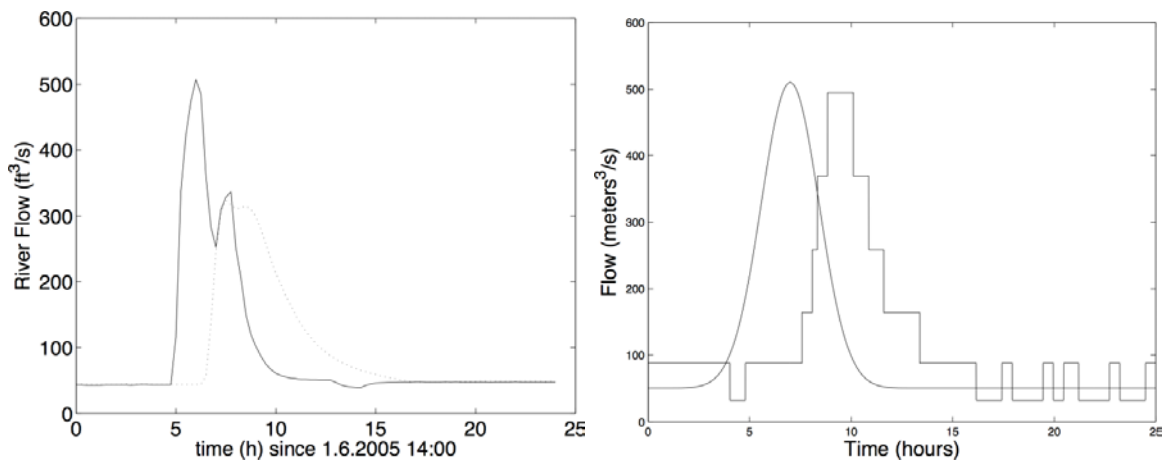


Figure 3. Topographical map and volume and outlet channel area profiles for Reach 4.



Surge down the Saluda River on 6 January 2005. The solid line is flow at the upstream station and the dotted line is flow at the downstream station.

Our simulation of a similar surge.

Figure 4. Actual surge and simulated surge.

was recorded by the Columbia observation station 1.5 h later (see **Figure 4**). We use this event to calibrate our model.

We first calibrate the model to produce a typical river flow at the dam to a value of $60 \text{ m}^3/\text{s}$ and systematically vary ρ . We find that our model displays stable but oscillatory behavior for $\rho < 0.1$. The oscillations can be traced to jumps in the flow rates between the breaches, and we attribute them to inaccuracy of our channel profiles for small volumes.

For $\rho = 0.1$, our system becomes unstable when large volumes are introduced. Since we are indeed interested in a large flood, we set $\rho = 0.01$. This value is consistent with the idea that the ground cover density, and thus the amount of water stored in the ground cover, increases with distance from the main river channel. The small size of ρ corresponds to the fact that in our equation it scales volume.

Once our model is stable for typical flow volumes, we introduce a “flood” in the form of a Gaussian bump in Q_0 of similar shape to the Jan. 6th event. We adjust ζ until this event arrives at the bottom of reach 3 in 1.5 hours. This occurs when $\zeta = -0.5$, consistent with the three reaches that must be traversed. In calibrating our model for a large flood by using a small one, we assume that the effect of ζ is independent of flood size. A better calibration could be achieved by analyzing observations of a larger flood, but such data are not available from the observation stations [USGS 2005].

Predictions

Our model predicts that the flood waters would travel slowly down the Saluda River Valley, producing extremely high levels of flooding in the upper reaches of the Saluda near Rawls Creek (reach 1) and near Columbia (reach 4). Our results are summarized in **Figure 5** and in **Tables 1–2**. Our numerical simulations suggest that Rawls Creek would flood approximately 32 m but the State Capitol building would remain dry.

Table 1.

The maximum flood volumes in each reach and their corresponding elevations above sea level.

Reach	Max. Flood Vol. ($\times 10^8 \text{ m}^3$)	Max Flood Elev. (m)	Avg. River Elev. (m)
1	19	87	58
2	15	79	55
3	3.5	68	50
4	2.4	68	45

Table 2.

Elevation above sea level of points of interest.

Point of Interest	Elevation (m)
Lake Murray	120
Saluda River (Just Below Dam)	60
Rawls Creek (Reach 1)	55
Saluda River (Bottom of River)	45
Capitol (Reach 4)	100

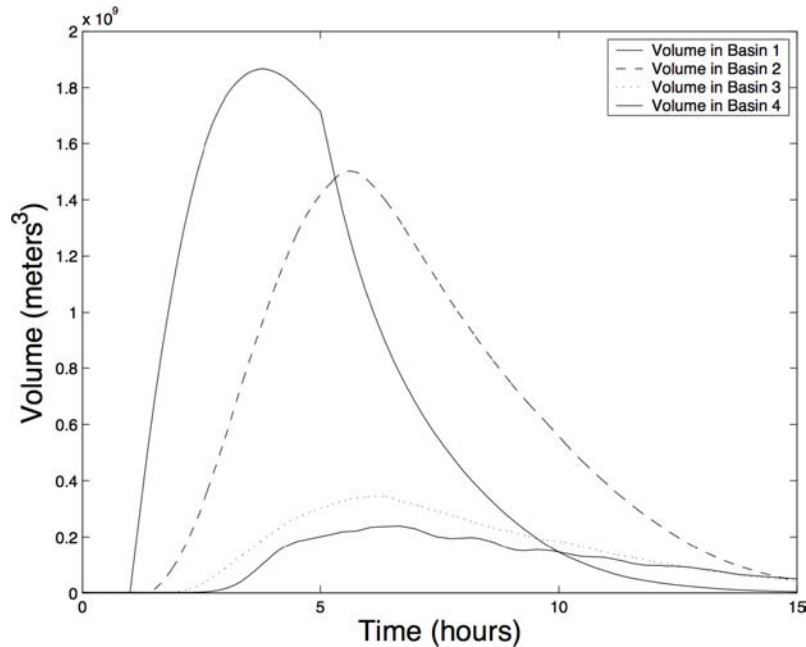


Figure 5. Volumes predicted in each reach as a gradual flood propagates.

Rapid Failure: Dam Break Wave

The complete annihilation of a dam results in a highly turbulent, unsteady flow that is commonly known as a *dam break wave*. The removal of the dam results in the creation of a retreating (negative surge) wave front in response to the sudden reduction in flow depth [Chanson 2004]. In the case of a dam separating two bodies of water, the intersection of the resulting negative surge with a relatively slow moving body of water results in a discontinuity of velocity. Since momentum must be preserved, these two bodies of water cannot intersect without the creation of a second wave moving in a direction opposite to that of the first wave; this second wave is a positive surge (see **Figure 6**).

The propagation properties of the wave resulting from the intersection of the positive and negative surges can be described using equations developed by Saint-Venant. These equations form a coupled system of one-dimensional quasi-linear hyperbolic partial differential equations describing varied unsteady

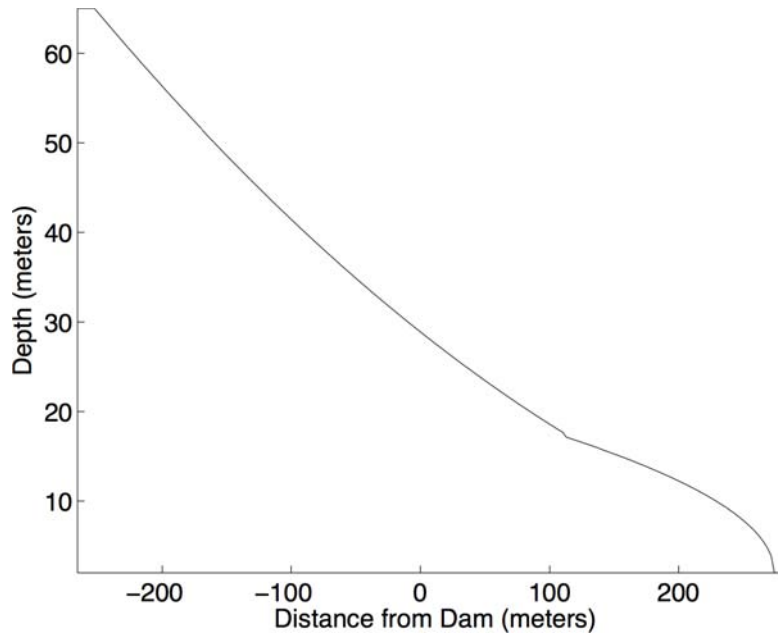


Figure 6. The shape of the wave just after the dam fails. The dam is located at $x = 0$. Note the discontinuity between the positive and negative surges at $x = 100$ m.

channel flow [Freed 1971]:

$$\begin{aligned} \frac{1}{g} \frac{\partial u}{\partial t} + \frac{u}{g} \frac{\partial u}{\partial x} + \frac{\partial d}{\partial x} + (S_f - S_0) &= 0, \\ \frac{\partial d}{\partial t} + \frac{\partial du}{\partial x} &= \frac{\partial d}{\partial t} + d \frac{\partial u}{\partial x} + u \frac{\partial d}{\partial x} = 0, \end{aligned} \quad (17)$$

where u is the mean velocity of the wave, d is the flow depth, x is the direction of propagation, t is time, and g is the acceleration due to gravity. S_f is the friction slope and S_0 is the slope of the canal.

The first equation is known as the *equation of motion* and describes the contribution of various forces to wave propagation, each of which is represented by a separate term:

- the first term describes the local inertia of the wave,
- the second term describes the convective inertia of the wave,
- the third term describes the pressure differential, and
- the fourth term describes the friction and bed slope.

The second equation, known as the *equation of continuity*, expresses conservation of mass.

The Saint-Venant equations assume the following [Chanson 2004; Freed 1971]:

- The flow is one dimensional; motion occurs only in the direction of propagation.

- Vertical acceleration is negligible, resulting in a hydrostatic pressure distribution.
- Water is incompressible.
- Flow resistance is the same as for uniform flow, $S_f = S_0$.

We are interested in describing the flood wave attenuation. In our model, we assume that the total volume of water impounded by the Saluda Dam is released as a single giant surge. The final value to which the peak discharge is attenuated is independent of the magnitude of the initial peak discharge [Ponce et al. 2003]. This allows for generalization of results calculated by our model to waves of arbitrary size.

Solutions to the Saint-Venant Equations

Ponce et al. [2003] derives a solution to (17) in the case of a dam failure through sinusoidal perturbation of the steady-state solution. Using spectral analysis, it can be shown that the peak discharge at position X has magnitude

$$q_p = q_{p0} \exp\left(\frac{-\alpha X}{L_0}\right), \quad (18)$$

where

$$\alpha = \frac{2\pi}{m^2} \left(\frac{L_0 d_0 B}{V_w} \right) \left[\zeta - \left(\frac{C - A}{2} \right)^{1/2} \right], \quad A = \frac{1}{F_0^2} - \zeta^2, \quad C = \left[A^2 + \zeta^2 \right]^{1/2},$$

$$\zeta = \frac{1}{\sigma F_0^2}, \quad \sigma = \left(\frac{2\pi}{L} \right) L_0, \quad F_0 = \frac{u_0}{\sqrt{g d_0}},$$

with

F_0 the Froude number F_0 ,

u_0 the steady equilibrium mean flow velocity,

L the perturbation wavelength,

L_0 the reference channel length,

d_0 the steady equilibrium flow depth,

B the average reach width,

V_w the reservoir volume,

g the acceleration due to gravity, and

m the Manning friction coefficient.

The equation for unit width discharge (speed \times depth) is

$$q = \frac{N}{N+1} V_{\max} d \quad (19)$$

where $N = 0.4\sqrt{8/f}$, f is the Darcy friction factor, V_{\max} is the maximum reservoir volume, and d is the flow depth.

We compute the wave speed using the empirical data in **Figure 4** and from it estimate the Darcy friction factor f for the Saluda River Valley. From (19), we also estimate the depth of the wave.

Predictions

Using estimated values of the depth of the water impounded by the dam, the depth of the Saluda River in close proximity to the dam, and the volume of the Saluda River Basin, we approximate the depth of a dam break wavefront as a function of distance from the dam site. **Figure 7** displays the results. The depth of the dam break wave decreases exponentially from an initial value of 65 m to a final value of approximately 4 m at a distance of 20 km from the dam site. This distance roughly corresponds to the distance between the Saluda Dam and the Capitol Building.

Since the Capitol Building sits approximately 50 m above the Saluda River, the possibility of the wave reaching the Capitol Building is extremely small. The probability is further decreased by the simplistic geometry of our model, which approximates the river bed approximated as rectangular and of uniform width and texture. In reality, the river exhibits numerous contractions and expansions and is far from uniform in texture. These qualities would further attenuate the flow depth of the propagating wave.

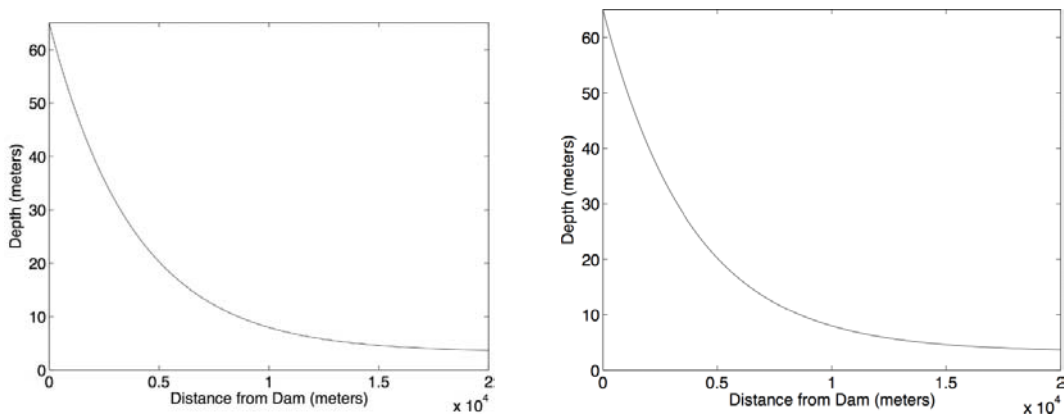


Figure 7. Predicted maximum depth of the floodwave for the upper Saluda River (left) and the entire Saluda River (right).

Our model predicts a wave 40 m high in the vicinity of Rawls Creek. A rapid dam failure would cause significant intrusion of flood waters into the Rawls Creek basin.

Conclusions

In either gradual or rapid failure of the Saluda dam, the effect on the downstream areas would be severe. Our models predict that the waters near Rawls Creek could rise by as much as 40 m (rapid dam failure) or 32 m (gradual dam failure), protruding far into the Rawls Creek basin and other drainages. The waters would not be as high near Columbia and would not reach the Capitol Building. However damage to low-lying areas would be severe, since the water might rise as much as 23 m.

Several improvements could be made to the models:

Gradual Failure Model

- This model successfully describes small surges in the Saluda River. However, extrapolating small events to larger events is inherently problematic; so for a flood of the magnitude that we are considering, we should test the model against larger events in the Saluda and/or large events in comparable rivers.
- Estimates in our erosion model could be strengthened with better information about the material from which the dam is constructed.
- Better profiles of the outlet channel of each reach would allow us to apply the Manning Equation more accurately.

Rapid Failure Model

- We calibrate this model too from a small surge in the Saluda River. A more comprehensive study of waves from other breached dams would provide better data for calibration of this model for large events.
- Access to the river site would provide better estimates for friction factors of the floodplain.
- This model is intended to place an upper bound on the magnitude of the flood wave. Further consideration of factors such as turns in the flood course would increase the accuracy of this model.

References

- Chanson, Herbert. 2004. *The Hydraulics of Open Channel Flow: An Introduction*. 2nd ed. Amsterdam, Holland: Elsevier.
- Chow, V.T. 1959. *Open-Channel Hydraulics*. New York: McGraw-Hill.
- Fread, D.L. 1971. Transient hydraulic simulation: Breached earth dams. Doctoral Dissertation, University of Missouri–Rolla.
- National Geophysical Data Center Coastal Relief Model. 2005. GEODAS Grid Translator—Design-a-Grid. http://www.ngdc.noaa.gov/mgg/gdas/gd_designagrid.html.

Ponce, V.M., and D.B. Simons. 1977. Shallow wave propagation in open channel flow. *Journal of the Hydraulics Division* 103 (12): 1461–1476.

Ponce, V.M., A. Taher-shamsi, and A.V. Shetty. 2003. Dam-breach flood wave propagation using dimensionless parameters. *Journal of the Hydraulics Division* 129 (10): 777–782.

Pugh, C.A., and F.W. Gray, Jr. 1984. *Fuse Plug Embankments in Auxillary Spillways—Developing Design Guidelines and Paramaters*. Bureau of Reclamation Reports. Denver, CO: U.S. Dept. of the Interior.

Singh, Vijay P. 1996. *Dam Breach Modeling Technology*. Dordrecht, Holland: Kluwer Academic Publishers.

South Carolina Electric & Gas Company. 1995. Lake Murray Shoreline Management Program. <http://www.scana.com/NR/rdonlyres/e56porb5wxxxtjqfz3i4dci3pc7j3o2ans3t7c2ydaoh5m7myuigj5dz3cnmdw7qpplewtvnq4j3qy3lhhrmjvmqawh/shorelinemanagementplan.pdf> .

Workshop on Seismic Analysis and Design of Earth and Rockfill Dams. 1986. Lecture notes. 2 vols. New Delhi, India: Central Board of Irrigation and Power.

USGS (Department of the Interior, U.S. Geological Survey). 1971. Irmo Quadrangle South Carolina 7.5 Minute Series (Topographic). Photorevised 1990. Denver, CO: Department of the Interior, U.S. Geological Survey.

_____. 1994. South West Columbia Quadrangle South Carolina 7.5 Minute Series (Topographic). Denver, CO: Department of the Interior, U.S. Geological Survey.

_____. 1997. Columbia North Quadrangle South Carolina 7.5 Minute Series (Topographic). Denver, CO: Department of the Interior, U.S. Geological Survey.

_____. 2005. USGS Real-Time Water Data for the Nation. Stations 02168504 (Saluda River below Lake Murray Dam . . .) and 02169000 (Saluda River near Columbia, SC). NWISWeb Data for the Nation. <http://waterdata.usgs.gov/nwis/current/?type=flow> .



Prof. Rekha Thomas, Ryan Bressler, Christina Polwarth, Braxton Osting, and Prof. Jim Morrow. Prof. Morrow coached the other MCM team from the University of Washington.

Judge's Commentary: The Outstanding Flood Planning Papers

Daniel Zwillinger
Raytheon
528 Boston Post Road
Sudbury, MA 01776

Introduction

Flood planning for dams is a real-life activity. An analysis of the Saluda Dam at Lake Murray determined that the area below the dam needed to be protected in the event of dam failure, and a second dam is being built. Investigation conclusions can be found on the Web.

Since flood plan analysis is complex, mathematical modeling is appropriate and useful. A sequence of models is typically used to understand a phenomena. For the Saluda Dam, a first model might have a straight river, the dam disappearing instantaneously, and a simple model of water flow. More detailed effects could then be added: the riverbed bends, the riverbed gradient is not uniform, perhaps the dam breaks slowly, perhaps the dam is breached in the center, etc. Starting with a complicated model may make it difficult to determine if the results are reasonable, since there may be little to validate against. A series of models that allows additional effects to be incorporated sequentially is preferable; it may facilitate creation of a sensitivity analysis.

Water flow in open channels has traditionally been modeled by the Saint-Venant equations, which are nonlinear partial differential equations. Many teams started by numerically solving these equations and got immersed in details. (The MCM is not a contest in computation!) Often these teams focused only on the water flow and spent little effort modeling the dam break itself. Although there are many models for dam failure, a dam "vanishing" completely is rather simplistic. (There are a few well-defined dam failure mechanisms. Teams that considered different mechanisms tended to do better than those teams that used simplistic assumptions.)

The UMAP Journal 26 (3) (2005) 279–281. ©Copyright 2005 by COMAP, Inc. All rights reserved. Permission to make digital or hard copies of part or all of this work for personal or classroom use is granted without fee provided that copies are not made or distributed for profit or commercial advantage and that copies bear this notice. Abstracting with credit is permitted, but copyrights for components of this work owned by others than COMAP must be honored. To copy otherwise, to republish, to post on servers, or to redistribute to lists requires prior permission from COMAP.

Many teams started with static models, but most recognized that these models do not yield reasonable results. The dam-break problem seemed to require a dynamic approach. The approaches varied considerably, but included:

- Continuous technique: use of sophisticated equations, such as Saint-Venant's equation. (Note: Copying an equation derivation achieves little. Pointing out assumptions needed to obtain an equation may be useful.)
- One-dimensional discrete techniques: breaking the Saluda River up into prisms and computing flow from one to the next. Rectangles and trapezoids were popular choices.
- Two-dimensional discrete techniques: cellular automata using USGS data and computing flows from neighboring cells. The cellular approach can be difficult to understand and to implement correctly.

Widely varying techniques obtained approximately the same result. Teams that used more than one approach tended to do better. The usual answers to the specific test questions are: No, the State Capitol doesn't flood, and Rawls Creek backs up about 2.5 miles.

The outstanding papers are remarkable in that each used a fundamentally different technique:

- The University of Washington team pursued an analytic approach. They considered two models, obtained real data, and calibrated their model.
- The Harvey Mudd team numerically solved the Saint-Venant equations.
- The University of Saskatchewan team considered a model, rejected it as being unrealistic, and then numerically solved a dynamic model that they created themselves.

Some overall comments on the submissions:

- Several teams validated their results from evacuation plans and recorded flood events. Many others did not do enough reality checking; a back-of-the-envelope computation frequently would have helped.
- Many teams had perhaps overly complicated models, involving many variables and parameters.
- The reference for a Web page should list the date of access.

About the Author

Daniel Zwillinger attended MIT and Caltech, where he obtained a Ph.D. in applied mathematics. He taught at Rensselaer Polytechnic Institute, worked in industry (Sandia Labs, Jet Propulsion Lab, Exxon, IDA, Mitre, BBN), and has been managing a consulting group for the last dozen years. He has worked in many areas of applied mathematics (signal processing, image processing, communications, and statistics) and is the author of several reference books.

The Booth Tolls for Thee

Adam Chandler
 Matthew Mian
 Pradeep Baliga
 Duke University
 Durham, NC

Advisor: William G. Mitchener

Summary

We determine the optimal number of tollbooths for a given number of incoming highway lanes. We interpret optimality as minimizing “total cost to the system,” the time that the public wastes while waiting to be processed plus the operating cost of the tollbooths.

We develop a microscopic simulation of line-formation in front of the tollbooths. We fit a Fourier series to hourly demand data from a major New Jersey parkway. Using threshold analysis, we set upper bounds on the number of tollbooths. This simulation does not take bottlenecking into account, but it does inform a more general macroscopic framework for toll plaza design.

Finally, we formulate a model for traffic flow through a plaza using cellular automata. Our results are summarized in the formula for the optimal number B of tollbooths for L lanes: $B = \lfloor 1.65L + 0.9 \rfloor$.

Previous Work in Traffic Theory

Most models for traffic flow fall into one of two categories: microscopic and macroscopic.

Microscopic models examine the actions and decisions made by individual cars and drivers. Often these models are called *car-following models*, since they use the spacing and speeds of cars to characterize the overall flow of traffic.

Macroscopic models view traffic flow in analogy to hydrodynamics and the flow of fluid streams. Such models assess “average” behavior, and commonly-used variables include steady-state speed, flux of cars per time, and density of traffic flow.

The UMAP Journal 26 (3) (2005) 283–297. ©Copyright 2005 by COMAP, Inc. All rights reserved. Permission to make digital or hard copies of part or all of this work for personal or classroom use is granted without fee provided that copies are not made or distributed for profit or commercial advantage and that copies bear this notice. Abstracting with credit is permitted, but copyrights for components of this work owned by others than COMAP must be honored. To copy otherwise, to republish, to post on servers, or to redistribute to lists requires prior permission from COMAP.

Some models bridge the gap between the two kinds, including the gas-kinetic model, which allows for individual driving behaviors to enter into a macroscopic view of traffic, much as ideal gas theory can examine individual particles and collective gas [Tampere et al. 2003].

The tollbooth problem involves no steady speed, so macroscopic views may be tricky. On the other hand, bottlenecking is complex and tests microscopic ideas.

An $M|M|n$ queue seems appropriate at first: Vehicles arrive with gaps (determined by an exponential random variable) at n tollbooths, with service at each tollbooth taking an exponential random variable amount of time [Gelenbe 1987]. We incorporate aspects of the situation from a small scale into a larger-scale framework.

Properties of a Successful Model

A successful toll-plaza configuration should

- maximize efficiency by reducing customer waiting time;
- suggest a reasonably implementable policy to toll plaza operators; and
- be robust enough to handle efficiently the demands of a wide range of operating capacities.

General Assumptions and Definitions

Assumptions

- All drivers act according to the same set of rules. Although the individual decisions of any given driver are probabilistic, the associated probabilities are the same for all drivers.
- Bottlenecking downstream of the tollbooths does not hinder their operation. Vehicles that have already passed through a tollbooth may experience a slowing down due to the merging of traffic, but this effect is not extreme enough to block the tollbooth exits.
- The number of highway lanes does not exceed the number of tollbooths.
- All tollbooths offer the same service, and vehicles do not distinguish among them.
- The amount of traffic on the highway is dictated by the number of lanes on the highway and not by the number of tollbooths. Changing the number of tollbooths does not affect “demand” for the roadway.
- The number of operating tollbooths remains constant throughout the day.

Terms and Definitions

- A “highway lane” is a lane of roadway in the original highway before and after the toll plaza.
- *Influx* is the rate (in cars/min) of cars entering all booths of the plaza.
- *Outflux* is the rate (in cars/min) of cars exiting all booths of the plaza.

Optimization

We seek to balance the cost of customer waiting time with toll plaza operating costs.

- The daily cost C of a tollbooth is the total time value of the delays incurred for all individuals (driver plus any passengers) plus the cost of operation of the booth. The tolls and the startup cost of building the plaza are not part of this cost.
- a is the average time-value of a minute for a car occupant.
- γ is the average car occupancy.
- N is the total number of (indistinct) tolls paid over the course of one day.
- L is the number of lanes entering and leaving a plaza.
- W is the average waiting time at a tollbooth, in minutes.
- B is the number of booths in the plaza.
- Q is the average daily operating cost of a human-staffed tollbooth.

We seek a number of toolbooths B that minimizes cost C .

The total waiting time per car is WN , so the total cost incurred by waiting time is $WaN\gamma$. General human time-value is cited as \$6/hour or $a = \$0.10/\text{min}$ [Boronico 1998]. The cost to operate a booth for a day is QB . The average annual operation cost for a human-staffed tollbooth is \$180,000, so we set $Q = \$180000/365.25$ days [Sullivan et al. 1994].

Reasoning that W depends on B , we have

$$C(B) = WaN\gamma + QB.$$

Car Entry Rate

We fit a curve to mean hourly traffic-flow data from Boronico [1998]. To interpolate an influx rate for every minute during the day, we fit a Fourier series approximation, whose advantage is its periodicity, with period of one day. [EDITOR'S NOTE: We omit the table of data from Boronico [1998] and the 17-term expression for the approximating series.]

Model 1: Car-Tracking Without Bottlenecks

Approach

We seek an upper bound on the optimal number of booths for a particular number of lanes.

Assumptions

- Each vehicle is looking to get through the toll plaza as quickly as possible, and the only factor that may cause Car A, which arrives earlier than Car B, to leave later than B is the random variable of service time at a tollbooth. In other words, cars do not make bad decisions about their wait times
- Customers are served at a tollbooth at a rate defined by an exponential random variable (a common assumption in queueing theory [Gelenbe 1987]) with mean 12 s/vehicle, or 5 cars/min.
- Traffic influx occurs on a “per lane” basis, meaning that influx per lane is constant over all configurations with varying number of lanes.
- Bottlenecking occurs more frequently when there are more tollbooths, given a particular number of lanes. This implies that omitting bottlenecking from our model will cause us to overestimate the optimal number of tollbooths.
- There exists a time-saving threshold such that if the waiting time saved by adding another tollbooth is under this threshold, it is not worth the trouble and expense to add the tollbooth. We assume that if an additional tollbooth does not reduce the maximum waiting time over all cars by the same amount as the average time that it takes to serve a car at a tollbooth (12 s = 0.2 m), then it is unnecessary.
- An incoming car chooses the tollbooth that will be soonest vacated, if all are currently occupied. If only one is vacant, the car chooses that tollbooth. If multiple tollbooths are vacant, the car chooses the one vacated the earliest.
- Cars make rational decisions with the goal of minimizing their wait times.

Expectations of the Model

- An additional booth should not increase waiting time.
- Each additional tollbooth offers diminishing returns of time saved.

Development of Model

Cars arrive at the toll plaza at a rate described by the Fourier series approximation of the data from Boronico [1998]. Cars are considered inside the toll plaza (meaning that we begin to tabulate their waiting times) when they are either being served or waiting to be served.

Service time does not count as waiting time; so if a car enters the toll plaza and there is a vacant tollbooth, its waiting time is 0. If there are no vacant tollbooths, cars form a queue to wait for tollbooths, and they enter new vacancies in the order in which they entered the toll plaza. Once a car has been served, it is considered to have exited its tollbooth and the toll plaza as a whole.

Our car-tracking model does not factor in the cost of tollbooth operation.

Simulation and Results

For L highway lanes, $L \in \{1..8, 16\}$, we ran the simulation for numbers B of tollbooths up to a point where additional booths no longer have any noticeable effect on waiting time. We exhibit results for a 6-lane highway in **Table 1**.

Table 1.
Waiting times (in minutes) for six-lane simulations.

Booths	Ave. wait	Ave. wait for wait > 0	Max. wait	Marginal utility
6	28	43	99	N/A
7	12	28	55	44
8	6	17	32	23
9	2	8	16	16
10	0.25	1.22	2.78	13
11	0.02	0.17	0.75	2
12	0.004	0.07	0.31	0.44
13	0.001	0.04	0.27	0.04

The column “Marginal Utility” shows how much each additional booth reduces maximum waiting time. For the 13th booth, this value is 0.04 min. To choose an optimal number of booths by threshold analysis, we seek the first additional booth that fails to reduce the maximum waiting time for a car by at least the length of the average tollbooth service time (0.2 min). So, based on our assumptions, it is unnecessary to build a 13th tollbooth for a toll plaza serving 6 lanes of traffic. Thus, we set $B = 12$ for $L = 6$. **Table 2** shows the optimal number of tollbooths for other various numbers of lanes.

Table 2.
Optimized number of booths.

Lanes	1	2	3	4	5	6	7	8	16
Booths	4	5	7	8	10	12	13	16	29

We also explore the situation of one booth per lane. Regardless of the number of lanes, we find average wait times of around 30 min (over 40 min for cars that wait at all), and maximum wait time of around 100 min.

Discussion

Our results match our expectations. The optimal number of booths increases with the number of lanes, each additional booth reduces waiting time, and additional booths yield diminishing returns in reducing waiting time.

The benefits of this rather simplistic model are its speed and the definite upper bounds that it offers.

Model 2: Cost Minimization

Approach

This model is concerned less with the details of individual vehicular motion and decision-making than with the general aggregate effect of the motions of the cars. We monitor traffic over the course of one day.

For instance, there is no need for this model to decompose analytically the situation of two cars trying to merge into the same lane. Instead, it recognizes that beyond a certain threshold of outflux from the booths, some bottlenecking will occur.

Also, this model addresses the cost of daily operation of the plazas.

Assumptions, Variables, and Terms

- The average waiting time per car in the toll plaza, W , is comprised of time in line (W_1), service time (W_2), and bottlenecking (W_3).
- F_i (a function of time) is the influx (cars/min) to the plaza from one lane, F_o is the outflux (cars/min) from the booth.
- r is the maximum potential service rate (cars/min).
- There is an outflux barrier, K (cars/min), above which bottlenecking takes place. We take it to be linear in L and independent of B , and we call it the *bottlenecking threshold*.

Development

From the definitions, we have $W_2 = 1/r$. Both W_1 and W_3 depend on B .

The average time in line, W_1 , begins to accumulate when the influx of traffic exceeds the toll plaza capacity (see **Figure 1**). The influx is $LF_i(t)$ and the

maximal rate of service is Br . We integrate over time to calculate how many cars were forced to wait in line.

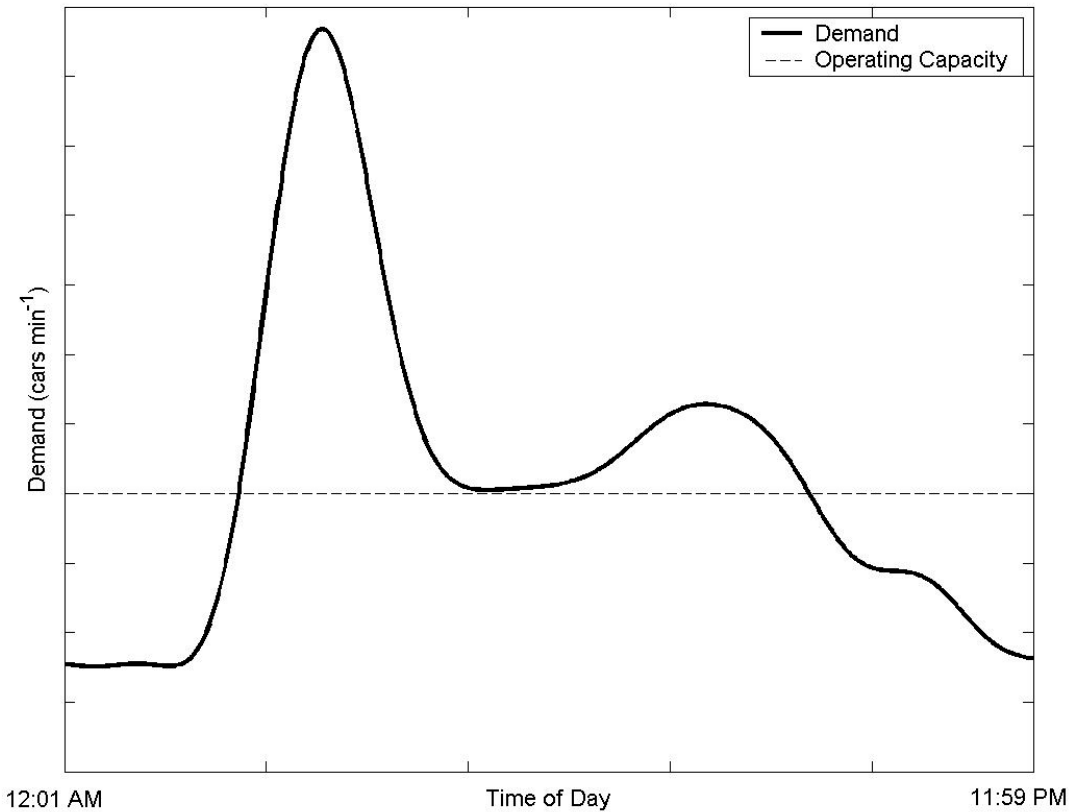


Figure 1. The area below the curve and above the line represents cars in line.

Integrating again (over time) gives us the total waiting time for all those cars (with 3600 as a scale factor for time units), and dividing by the total number of cars gives the average waiting time:

$$W_1 = \frac{3600}{N} \int_0^{24} \int_0^t \max(LF_1(\tau) - Br, 0) d\tau dt.$$

We obtain W_3 in similar fashion:

$$W_3 = \frac{3600}{N} \int_0^{24} \int_0^t \max(F_o(\tau, B) - K, 0) d\tau dt.$$

The problem is to determine the variable(s) that K depends on. First, K is not directly dependent on B , since bottlenecking should only be a result of general outflux from the booths into L lanes. Instead, K depends indirectly on the number of booths, because K depends on outflux F_o , which in turn depends on B . Also, K also can be considered a linear function of L , because L is directly proportional to influx, which, by the law of conservation of traffic, must equal outflux in the aggregate.

Simulation and Results

We use the same data and Fourier series for traffic influx as in Model 1. We focus our attention on the case $L = 6$; other values are analogous.

We use Mathematica to integrate numerically the expression for W_1 for a given L and $r = 5$ cars/min. (N comes from integration of the influx expression.) We do the calculation for values of B ranging from L to $L + 7$ (since $L + 7$ is usually greater than the upper bound from Model 1) with step size 0.25. We fit a quartic polynomial fit to the resulting points $(B, W_1(B))$ to get W_1 as a function of B .

We illustrate for $L = 6$. We find $N = 92,355$. We plot W_1 for values of B from 6 to 13, in steps of 0.25, together with the best-fit quartic, in **Figure 2**.

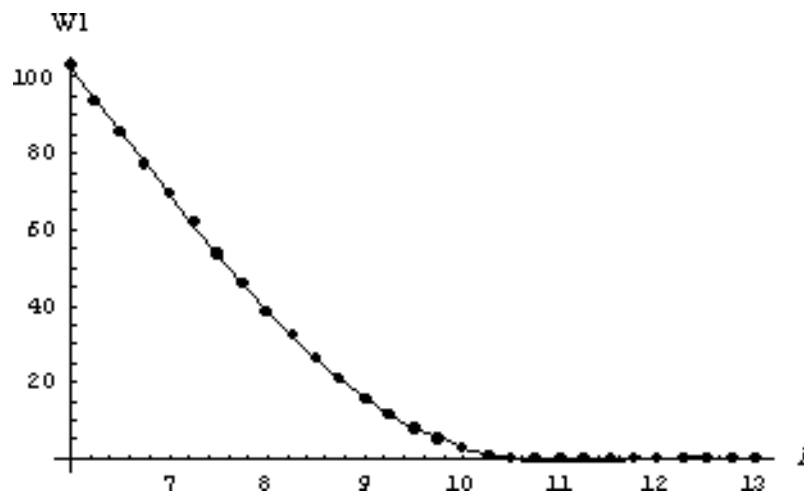


Figure 2. $W_1(B)$ for B ranging from 6 to 13 (actual points with quartic fit).

The recipe for $W_3(B)$ is somewhat less straightforward, since $F_0(t)$ is generated from a stochastic distribution, unlike the deterministic $F_1(t)$. Also, $F_0(t)$ depends on B , a significant complication. We ran at least 20 trials of each case (L, B) under the first model; the averaged outcomes of their outflux functions are the function that we use for outflux in this model's simulation, henceforth referred to just as $F_0(t, B)$.

We use surface-fitting software (Systat's TableCurve3D) to generate an expression for outflux as a function of time and the number of booths and use this expression in the compound integral for W_3 in integrating numerically. As before, we generate a scatter plot of points $(B, W_3(B))$ and fit a quartic polynomial.

The values of R^2 for the surface fits all fall between .84 and .95, which are acceptable values. All of the quartic fits have R^2 near 1.

For the case $L = 6$, **Figure 3** shows the surface fit and **Figure 4** shows the function W_3 .

With W_3 a quartic polynomial in B , minimization via calculus yields a solution. For 6 lanes, Mathematica's numeric solver gives the minimum at $B = 10.84$. Values for various numbers of lanes are summarized in **Table 3**.

Outflux (cars/min) -- 6 Lane

Rank 4 Eqn 317016996 $z^{(-1)}=a+bx^{(1.5)}+cx^2+dx^2\ln x+ex^{(2.5)}+fx^3+ge^{(x/wx)}+h/\ln y$
 $r^2=0.89795631$ DF Adj $r^2=0.89349539$ FitStdErr=3.5049628 Fstat=231.30704
 $a=-220.32191$ $b=-2.9096518$ $c=1.5952541$ $d=-0.63655404$
 $e=0.23714718$ $f=-0.0079954663$ $g=220.43421$ $h=0.010602912$

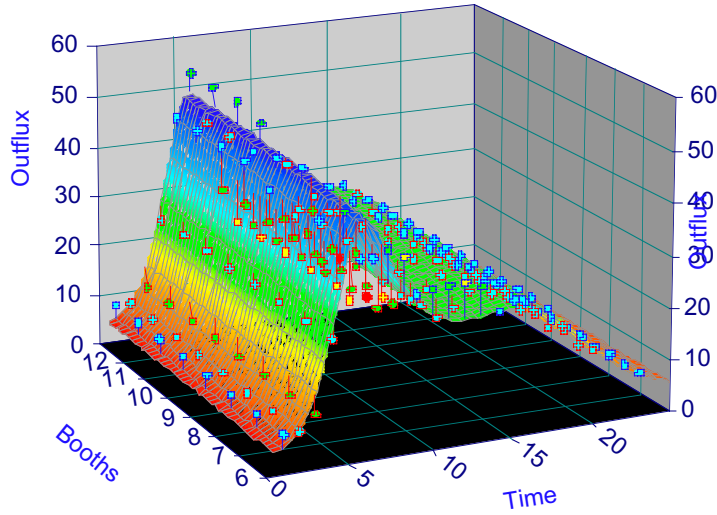


Figure 3. $L = 6$: Surface fit for outflux function in terms of time (h) and number of booths.

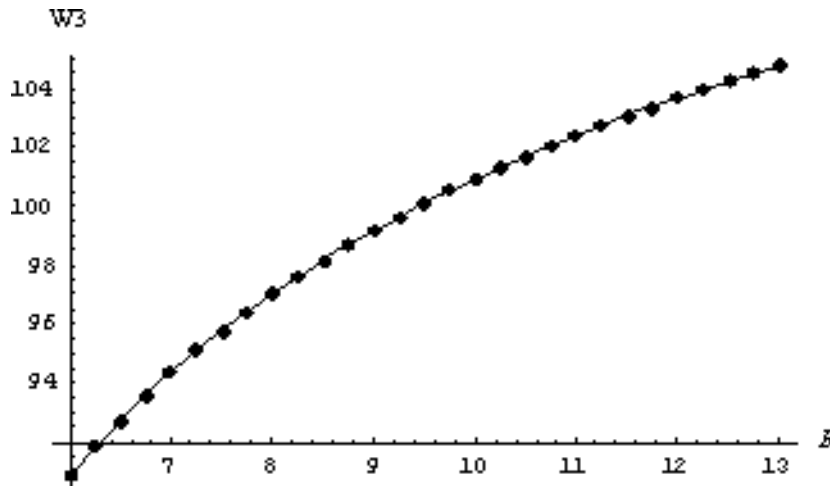


Figure 4. $L = 6$: Plot of $W_3(B)$ for B ranging from 6 to 13 (actual points plus quartic fit).

Table 3.

Optimized number of booths—final recommendations from Model 2.

Lanes	1	2	3	4	5	6	7	8	16
Booths	3	5	6	7	9	11	12	14	27

Discussion

This model calculates total waiting time for drivers based on general ideas of traffic flow. The results are reasonable and satisfy many of our expectations for a successful model. The recommended B -values increase monotonically with L and are all less than the upper bounds produced in Model 1. One booth per lane is nowhere near optimal, because (as we can see from the graphs of W_1 and W_3), while bottlenecking is zero, waiting time in line is much higher, thus diminishing the effect of bottlenecking.

Given the model's success, it may be disheartening to acknowledge its lack of robustness. Any adjustments to fine-scale aspects of traffic, such as the addition of a potential E-ZPass lane (to be discussed later), would be impossible to implement. Perhaps the rate of service r could be adjusted higher for such a scenario, but changing lanes before the tollbooths would be difficult to capture with this model.

Model 3: Cellular Automata

Motivation

What effect does the discreteness of traffic have on the nature and solution of the problem? A continuous model of traffic may neglect the very factors that give rise to traffic congestion and jamming. To address this possibility, we turn to cellular automata theory to develop a discrete, microscopic model.

Approach

Each cell is designated as a vehicle, a vacancy, or a barrier to traffic flow. The model follows individual vehicles through the plaza and computes the waiting time for each. The total waiting time measures the plaza's efficiency.

In any particular time step, a vehicle advances, changes lanes, or sits still. Vehicles enter the plaza from a stretch of road containing a specific number of lanes. As a vehicle approaches the string of tollbooths, the road widens to accommodate the booths (given that there are more tollbooths than lanes). There is a specific delay associated with using a tollbooth. Once a vehicle leaves a booth, it merges into a roadway with the original number of lanes.

Assumptions

- The plaza consists of occupied cells, vacant cells, and "forbidden" cells.
- Cells represent a physical space that accommodates a standard vehicle with buffer regions on both sides.
- All vehicles are the same size.

Governing Dynamics

Cars move through the toll plaza according to rules. Each vehicle has options, each with an associated probability. For each time step, the following rules are applied in sequential order:

1. Starting at the front of the traffic and moving backward (with respect to the flow), vehicles advance to the cell directly in front of them with probability p ; if the next cell is not vacant, the vehicle does not advance and is flagged. This probability is meant to simulate the stop-and-go nature of slowly moving traffic. We can think of p as a measure of driver attentiveness; $p = 1$ corresponds to the case where drivers are perfectly attentive and move forward at every opportunity, while $p = 0$ represents the extreme case where drivers have fallen asleep and fail to move forward at all.
2. Using an influx distribution function, the appropriate number of new vehicles is randomly assigned to lanes at the initial boundary (see next section).
3. Starting at the front of traffic and moving backward, vehicles flagged in step 1 are given the opportunity to switch lanes. For each row of traffic, the priority order for switching is determined by a random permutation of lanes. Switching is attempted with probability q . If switching is attempted, left and right merges are given equal probability to be attempted first. If a merge in one direction (i.e. left or right) is impossible (meaning that the adjacent cell is not vacant), then the other direction is attempted. If both adjacent cells are unavailable, the vehicle is not moved.
4. Total waiting time for the current time step is computed by determining the number of cells in the system containing a vehicle.
5. The number of vehicles advancing through the far boundary (end of the simulation space) are tabulated and added to the total output. This number is later used to confirm conservation of traffic.

Population Considerations

The Fourier series for daily influx distribution of cars is still valid for the automata model, but the influx values must be scaled to reflect the effective influx over a much smaller time interval (a single time step). The modified influx function, F_{in} , is computed as follows:

$$F_{in}(\tau) = \min \left(\left\lfloor \frac{F_{in}(t)}{\eta} \right\rfloor, L \right),$$

where η is a constant factor required for the conversion from units of t to those of τ and L is the number of initial travel lanes.

Computing Wait Time

Wait time is determined by looking through the entire matrix at each time step and noting the number of cells with positive values. The only cells containing positive values are those representing vehicles. Thus, by counting the number of vehicles in the plaza at any given time, we are also counting the amount of time spent by vehicles in the plaza (in units of time steps).

At time step i , total cumulative waiting time is computed as follows:

$$W_i = W_{i-1} + 1(\text{plaza}(x, y) > 0),$$

where $1()$ denotes an indicator function and plaza denotes the matrix of cells.

Simulation and Results

The cost optimization method defines total cost as

$$C_{\text{total}} = \alpha\gamma NW(B, L) + BQ.$$

Using the cellular automata model, we compute waiting time as a function of both the number of lanes and the number of tollbooths. For fixed L , we compare all values of C_{total} and choose the lowest one. The results are presented in **Table 4**.

Table 4.
Optimization for cellular automata model.

Highway lanes	Optimal number of booths	
	Typical day	Rush hour
1	1	2
2	4	4
3	5	6
4	7	7
5	8	9
6	10	11
7	12	13
8	14	15
16	27	29

Each value in **Table 4** represents approximately 20 trials. Through these trials, we noted a remarkable stability in our model. Despite the stochastic nature of our algorithm, each number of lanes was almost always optimized to the same number of tollbooths. There were a handful of exceptions; they occurred exclusively for small numbers of highway lanes (< 3 lanes).

Sensitivity Analysis

Our cellular automata model is relatively insensitive to both p and q . Changes of $\pm 11\%$ in p and $\pm 5.2\%$ in q have no effect on the optimal number of tollbooths

for a six-lane highway. On the other hand, increasing the delay time by 25% shifts the optimal number of booths from 10 to 11 (10%). Decreasing the delay by 25% has no effect on the solution. Perhaps additional work could lead to an elucidation of the relation between delay and optimal booth number that could help stabilize the cellular automata model.

Comparison of Results from the Models

Table 5 show the optimal number of booths.

Table 5.
Comparison of final recommendations for three models.

Lanes	Model		
	Car-tracking	Macroscopic	Automata
1	4	3	2
2	5	5	4
3	7	6	5
4	8	7	7
5	10	9	8
6	12	11	10
7	13	12	12
8	16	14	14
16	29	27	27

The car-tracking model serves as an upper bound for the optimal number of booths, due to its omission of bottlenecking, a fact confirmed in the table. The cellular automata model, on the other hand, incorporates bottlenecking. Due to its examination of each car and each period waited, we lean more toward the cellular automata model for a determination of the optimal number of booths that is more accurate than those of the other two models.

The optimal values for each model are fit very well ($r^2 > .996$) by a straight line, with slopes between 1.6 and 1.7.

Conclusion

We use three models—the car-tracking model, the macroscopic model for total cost minimization, and the cellular automata model—to determine the optimal (per our definition) number B of tollbooths for a toll plaza of L lanes.

The car-tracking model uses a simple orderly lineup of cars approaching tollbooths and ignores bottlenecking after the tollbooths; it provides a strong upper bound on B for any given L .

The macroscopic model looks at the motion of traffic as a whole. It tabulates waiting time in line before the tollbooths by considering times when traffic influx into the toll plaza is greater than tollbooth service time. It also

finds bottlenecking time by assuming there exists a threshold of outflux, above which bottlenecks will occur, and notices when outflux is greater than said threshold. This is a much more accurate model than the Car-Tracking Model, and it provides us with reasonable solutions for B in terms of L .

The cellular automata model looks at individual vehicles and their “per lane length” motion on a toll plaza made up of cells. With a probabilistic model of how drivers advance and change lanes, this model details far better than the other models the waiting time in line and the bottlenecking after the tollbooths.

Thus, we recommend values closer to those provided by the automata model than the macroscopic one. In order to write B explicitly in terms of L , we invoke the linearity of the results. Also, to preserve integral values for B , we use the floor function and determine that

$$B = \lfloor 1.65L + 0.9 \rfloor.$$

Potential Extension and Further Consideration

Our models assume that all booths are identical. However, systems such as E-ZPass allow a driver to pay a toll electronically from an in-car device without stopping at a tollbooth. If all E-ZPass booths also double as regular teller-operated booths, much of our models remain the same, except that the average service rate might increase. The trouble comes when all the booths are not the same and drivers may need to change lanes upon entering the plaza. This directed lane changing was not implemented in any of the models presented here, but could easily become a part of the automata model. Exclusive E-ZPass booths also would drastically reduce the operating cost for the booth, since an operator’s salary would not need to be paid (from \$16,000 to \$180,000 annually) [Sullivan 1994].

References

- Boronico, Jess S., and Philip H. Siegel. Capacity planning for toll roadways incorporating consumer wait time costs. *Transportation Research A* (May 1998) 32 (4): 297–310.
- Daganzo, C.F., et al. 1997. Causes and effects of phase transitions in highway traffic. ITS Research Report UCB-ITS-RR-97-8 (December 1997).
- Gartner, Nathan, Carroll J. Messer, and Ajay K. Rathi. 1992. *Traffic Flow Theory: A State of the Art Report*. Revised monograph. Special Report 165. Oak Ridge, TN: Oak Ridge National Laboratory. <http://www.tfhr.gov/its/tft/tft.htm>.
- Gelenbe, E., and G. Pujolle. 1987. *Introduction to Queueing Networks*. New York: John Wiley & Sons.

Jost, Dominic, and Kai Nagel. 2003. Traffic jam dynamics in traffic flow models. Swiss Transport Research Conference. <http://www.strc.ch/Paper/jost.pdf> . Accessed 4 February 2005.

Kuhne, Reinhart, and Panos Michalopoulos. 1992. Continuum flow models. Chapter 5 in Gartner et al. [1992].

Schadschneider, A., and M. Schreckenberg. Cellular automaton models and traffic flow. *Journal of Physics A: Mathematical and General* (1993) 26: L679–L683.

Sullivan, R. Lee. Fast lane. *Forbes* (4 July 1994) 154: 112–115.

Tampere, Chris, Serge P. Hoogendoorn, and Bart van Arem. Capacity funnel explained using the human-kinetic traffic flow model. <http://www.kuleuven.ac.be/traffic/dwn/res2.pdf> . Accessed 4 February 2005.



Matthew Mian, William G. Mitchener (advisor), Pradeep Baliga, and Adam Chandler.

A Single-Car Interaction Model of Traffic for a Highway Toll Plaza

Ivan Corwin
 Sheel Ganatra
 Nikita Rozenblyum
 Harvard University
 Cambridge, MA

Advisor: Clifford H. Taubes

Summary

We find the optimal number of tollbooths in a highway toll-plaza for a given number of highway lanes: the number of tollbooths that minimizes average delay experienced by cars.

Making assumptions about the homogeneity of cars and tollbooths, we create the Single-Car Model, describing the motion of a car in the toll-plaza in terms of safety considerations and reaction time. The Multi-Car Interaction Model, a real-time traffic simulation, takes into account global car behavior near tollbooths and merging areas.

Drawing on data from the Orlando–Orange Country Expressway Authority, we simulate realistic conditions. For high traffic density, the optimal number of tollbooths exceeds the number of highway lanes by about 50%, while for low traffic density the optimal number of tollbooths equals the number of lanes.

Definitions and Key Terms

- A **toll plaza** with n lanes is represented by the space $[-d, d] \times \{1, \dots, n\}$, where members of the set $\{0\} \times \{1, \dots, n\}$ are called **tollbooths** and d is called the **radius** of the toll plaza. Denote the tollbooth $\{0\} \times \{i\}$ by τ_i . The subspace $[-d, 0) \times \{1, \dots, n\}$ is known as the **approach region** and $(0, d] \times \{1, \dots, n\}$ is known as the **departure region**.

The UMAP Journal 26 (3) (2005) 299–315. ©Copyright 2005 by COMAP, Inc. All rights reserved. Permission to make digital or hard copies of part or all of this work for personal or classroom use is granted without fee provided that copies are not made or distributed for profit or commercial advantage and that copies bear this notice. Abstracting with credit is permitted, but copyrights for components of this work owned by others than COMAP must be honored. To copy otherwise, to republish, to post on servers, or to redistribute to lists requires prior permission from COMAP.

- A **highway/toll plaza pair** is represented by the space $H = (-\infty, d) \times \{1, \dots, m\} \cup [-d, d] \times \{1, \dots, n\} \cup (d, \infty) \times \{1, \dots, m\}$, where the toll plaza is (as above) the subspace $[-d, d] \times \{1, \dots, n\}$ and the stretches of highway are the subspaces $(-\infty, d) \times \{1, \dots, m\}$ and $(d, \infty) \times \{1, \dots, m\}$. Elements of the sets $\{1, \dots, m\}$ and $\{1, \dots, n\}$ are **highway lanes** and **tollbooth lanes** respectively, and elements of \mathbb{R} are **highway positions**. In practice, we take $m \geq n$.
- The **fork point** of a highway/toll plaza pair, given by the highway position $-d$, is the point at which highway lanes turn into toll lanes. Similarly, the **merge point** of a highway/toll plaza pair, given by the highway position d , is the point at which toll lanes turn back into highway lanes (**Figure 1**).

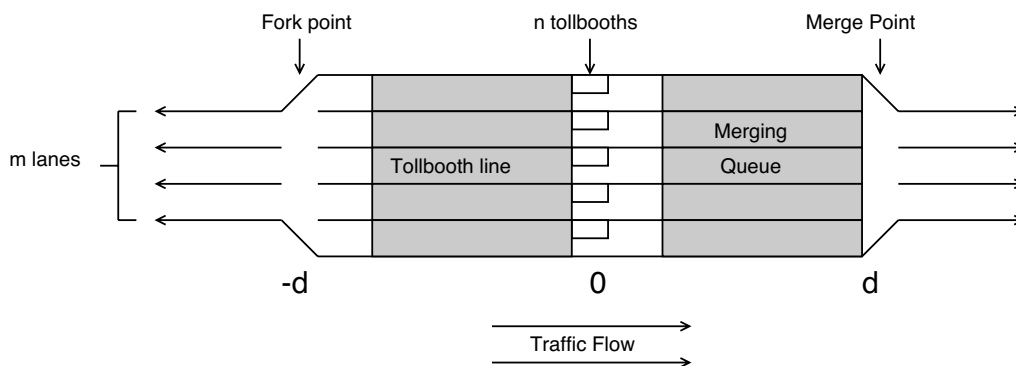


Figure 1. A depiction of the highway/toll plaza pair.

- A **car** C is represented by a 4-tuple $(L, a_+, a_-, a_{\text{brake}})$ and a position function $p = (x, k) : \mathbb{R} \rightarrow H$ where $x(t)$ is smooth for all t . Here, $x(t)$ gives the highway position of the front tip of C and $k(t)$ is the (tollbooth or highway) lane number of C . Let L be the length of C in meters, a_+ the constant comfortable positive acceleration, a_- the constant comfortable brake acceleration, and a_{brake} the maximum brake acceleration. At a fixed time, the region of H in **front** of C is the portion of H with greater highway position than C , while the **rear** of C is the region of H with highway position at most the position of C minus L .
- The **speed limit** v_{max} of H is the maximum speed at which any car in H can travel.
- The **traffic density** $\rho(t)$ of H at time t is the average number of cars per lane per second that would pass highway position 0 if there were no toll plaza.
- The **average serving rate** s of tollbooth τ_i is the average number of cars that can stop at τ_i , pay the toll, and leave, per second.

Table 1.
Variables, definitions, and units.

Variable	Definition	Units
n	Number of tollbooths	unitless
ρ	Traffic density	cars/s
T	Total delay time	s
x	Position	m
v	Velocity	m/s
x_o	Position of initial deceleration	m
t_o	Time of initial deceleration	s
x_f	Position upon returning to speed limit	m
t_f	Time upon returning to speed limit	s
x_1	Position of car C	m
x_2	Position of car C'	m
v_1	Velocity of car C	m/s
v_2	Velocity of car C'	m/s
x'_1	Position of car C after time step	m
x'_2	Position of car C' after time step	m
v'_1	Velocity of car C after time step	m/s
v'_2	Velocity of car C' after time step	m/s
G	Safety gap	m
G'	Safety gap after time step	m
t	Time	s
t'	Additional time	s
α_C	Compensation deceleration from car/safety gap overlap	m/s ²
α_O	Compensation deceleration from obstacle/safety gap overlap	m/s ²
x	Position	m
v	Velocity	m/s
c_i	Size of tollbooth line i	cars
l_i	Length of tollbooth line i	m
t_{serve}	Time C enters departure area	s
t_{merge}	Time C upon passing merge point	s
v_{out}	Velocity of a car C upon passing merge point	s

Table 2.
Constants, definitions, and units.

Constant	Meaning	Units
d	toll plaza radius	m
m	Number of highway lanes	unitless
a_+	Comfortable acceleration	m/s ²
a_+	Comfortable deceleration	m/s ²
a_{brake}	Hard brake deceleration	m/s ²
L	Car length	m
v_{max}	Speed limit	m/s
s	Mean serving rate	cars/s
σ	Standard deviation of serving time	s/car
Δt	Expected reaction time	s
γ	Unexpected reaction time	s
ϵ	Line spacing distance	m

General Assumptions

Time

- Time proceeds in discrete time steps of size Δt .

Geometry of the Toll Plaza

- The highway is straight and flat and extends in an infinite direction before and after the toll plaza. The highway is obstacle-free with constant speed limit v_{\max} . The assumption of infinite highway is based on toll plazas being far enough apart that traffic delays at one toll plaza don't significantly affect traffic at an adjacent one.
- A car's position is determined uniquely by a lane number and a horizontal position. Thus, on a stretch of road with m operating lanes, the position of a car is given by the ordered pair $(x, i) \in \mathbb{R} \times \{1, \dots, m\}$.

Tollbooths and Lines

- A car comes to a complete stop at a tollbooth.
- The time required to accelerate and decelerate to move up a position in a waiting line is less than the serving time of the line. Thus, average time elapsed before exiting a line is simply a function of average serving time and line length measured in cars.
- A car cannot enter a tollbooth until the entire length of the car in front of it has left the tollbooth.
- All tollbooths have the same normally distributed serving time with mean $1/s$ and standard deviation σ .

Fork and Merge Points

- Transitions between the highway and tollbooth lanes are instantaneous.
- When transitioning at the fork point into a tollbooth lane, cars enter the lane with the shortest tollbooth lines.
- There is no additional delay associated with the division of cars into tollbooths.
- The process of transitioning at the merge points from the tollbooth lanes, called **merging**, does incur delay due to bottlenecking because we assume that there are at least as many tollbooth lanes as highway lanes.

Optimality

Measures of optimality for a toll include having minimal average delay, standard deviation of average delay, accident rate, and proportion of cars delayed [Eddie 1954]. We assume that optimality occurs when cars experience minimal average delay. Specifically, for a car C , let x_o, t_o be the position and time at which C first decelerates from the speed limit to enter the tollbooth line, and let x_f, t_f be time and position at which, having merged onto the highway once more, C reaches the speed limit. Then the delay T experienced by the car, or the time cost associated with passing through the toll plaza instead of travelling unhindered, is given by

$$T = t_f - t_o - \frac{x_f - x_o}{v_{\max}}. \quad (1)$$

We secondarily prefer toll plaza configurations with minimal construction and operating cost, i.e., toll plaza configurations with fewer tollbooths. Specifically, for a given highway, if two values of n (the number of tollbooths) give sufficiently close average delay times (say, within 1 s), we prefer the lower n .

We rephrase the problem as follows:

Given a highway configuration with m lanes and a model of traffic density, what is the least number of tollbooth lanes n that minimizes the average delay (within 1 s) experienced by cars travelling through the tollbooth?

Expectations of Our Model

- For sufficiently low traffic density, the delay time per car is relatively constant and near the theoretical minimum, because the tollbooth line does not grow and there are no merging difficulties. *We expect that for low density the optimal number of tollbooths equals or slightly exceeds the number of lanes.*
- For high traffic density, the delay time per car is very large and continues to grow, because the tollbooth queue is unable to move fast enough to handle the influx of cars; waiting time increases approximately linearly in time. *We expect that for high density, the optimal number of tollbooths significantly exceeds the number of lanes.*
- An excessive number of tollbooths leads to merging inefficiency, causing great delay in the departure region.

The Single-Car Model

Additional Definitions and Assumptions

- An **obstacle** for a car C is a point in the highway/toll plaza pair which C must slow down to avoid hitting. The only obstacle that we consider is the merge point under certain conditions.
- At a fixed time, the **closest risk** to a car C is the closest obstacle or car in front of C .
- The **unexpected reaction time** γ is the amount of time a car takes between observing an unexpected occurrence (a sudden stop) and physically reacting (braking, accelerating, swerving, etc.). The **expected reaction time** Δt is the amount of time between observing an expected occurrence (light change, car brake, tollbooth) and physically reacting.
- Cars are homogeneous; that is, all have the same L , a_+ , a_- , and a_{brake} .
- All cars move in the positive direction.
- All cars observe the speed limit v_{max} . Moreover, unless otherwise constrained, a car travels at this speed or accelerates to it. In particular, outside a sufficiently large neighborhood of the toll plaza, all cars travel at v_{max} .
- Cars accelerate and decelerate at constant rates a_+ and a_- unless otherwise constrained.
- Cars do not attempt to change lanes unless at a fork or merge point. That is to say, for a car C , $k(t)$ is piecewise constant, changing only at t such that $x(t) = -d$ or d .
- A car C prefers to keep a certain quantity of unoccupied space between its front and its closest risk, of size such that if C were to brake with maximum deceleration, a_{brake} , C would always be able to stop before reaching its closest risk [Gartner et al. 1992, §4]. We refer to this quantity as the **safety gap** G . Given the position of a car C , the position corresponding to distance G in front of C is the **safety position** with respect to C . If the safety position with respect C does not overlap the closest risk, we say C is **unconstrained**.
- A car can accurately estimate the position and velocity of itself and of the car directly in front of it and its distance from the merging point.
- If a car C comes within a sufficiently small distance ϵ of a stopped car, C stops. This minimum distance ϵ is constant.
- For each car, there is a delay, the reaction time, between when there is a need to adjust acceleration and when acceleration is actually adjusted. Green [2000] splits reaction times into three categories; the ones relevant to us are

expected reaction time Δt and unexpected reaction time γ , which are defined above. Although these times vary with the individual, we make the simplifying assumption that all cars have the same values, $\Delta t = 1$ s and $\gamma = 2$ s. Reaction times provide a motivation for discretizing time with time step Δt ; drivers simply do not react any faster.

The Safety Gap

We develop an expression for the safety gap G of car C , which depends on the speed of the closest risk C' . Let the current speeds of C and C' be v_1 and v_2 . Now suppose that C' brakes as hard as possible and thus decelerates at rate a_{brake} . In time v_2/a_{brake} , car C' stops; meanwhile it travels distance

$$v_2 \frac{v_2}{a_{\text{brake}}} - \frac{1}{2} a_{\text{brake}} \left(\frac{v_2}{a_{\text{brake}}} \right)^2 = \frac{v_2^2}{2a_{\text{brake}}}.$$

If C starts braking after a reaction time of γ , it takes total time $\gamma + v_1/a_{\text{brake}}$ to stop and travels distance

$$\gamma v_1 + \frac{v_1^2}{2a_{\text{brake}}}.$$

Thus, in the elapsed time, the distance between C and C' decreases by

$$\gamma v_1 + \frac{v_1^2 - v_2^2}{2a_{\text{brake}}}.$$

Therefore, this must be the minimum distance between the front of C and the back of C' in order to avoid collision. Accounting for the length of C' , the minimum distance between C and C' , and thus the safety gap, must be

$$G = L + \gamma v_1 + \frac{v_1^2 - v_2^2}{2a_{\text{brake}}}.$$

Now suppose that the closest risk is an obstacle, in particular the merge point. Rather than braking with deceleration a_{brake} , C will want to keep a safety gap that allows for normal deceleration of a_- . Because deceleration on approach is expected, C will opt to decelerate at a comfortable rate, a_- . Moreover, since C is reacting to an expected event, the reaction time is given by Δt . Since the length and velocity of the obstacle are both 0, the safety gap must be

$$G = \Delta t v_1 + \frac{v_1^2}{2a_-}.$$

Individual Car Behavior

An individual car C can be in one of several positions:

- No cars or obstacles are within its safety gap, that is, C is unrestricted. Consequently, C accelerates at rate a_+ unless it has velocity v_{\max} .
- The tollbooth line is within braking distance. Since this is an expected occurrence, the car brakes with deceleration a_- .
- Another car C' is within its safety gap, so C reacts by decelerating at some rate α_C so that in the next time step, C' is no longer within the safety gap. C chooses α_C based on the speeds v_1, v_2 and positions x_1, x_2 of both cars. If C assumes that C' continues with the same speed, then after one time step Δt the new positions and speeds are

$$\begin{aligned}x'_1 &= x_1 + v_1\Delta t - \frac{1}{2}\alpha_C(\Delta t)^2, x'_2 = x_2 + v_2\Delta t, \\v'_1 &= v_1 - \alpha_C\Delta t, v'_2 = v_2,\end{aligned}$$

and the new safety gap is

$$G' = \gamma v'_1 + \frac{v_1'^2 - v_2'^2}{2a_{\text{brake}}}.$$

For the new position of C_2 to not be within the new safety gap, we must have

$$x'_2 - x'_1 - L = G'.$$

Substituting into this equation, we find:

$$x_2 + v_2\Delta t - v_1\Delta t + \frac{1}{2}\alpha_C(\Delta t)^2 - L = \gamma v_1 - \gamma\alpha_C\Delta t + \frac{(v_1 - \alpha_C\Delta t)^2 - v_2^2}{2a_{\text{brake}}}.$$

Solving this equation for α_C and taking the root corresponding to the situation that C trails C' , we find that

$$\begin{aligned}c\alpha_C &= \frac{1}{\Delta t} \left(\frac{\Delta t a_{\text{brake}}}{2} + v_1 + \gamma a_{\text{brake}} \right. \\&\quad \left. - \frac{1}{2} \left([(\Delta t)^2 - 4v_1\Delta t a_{\text{brake}} + 4\Delta t a_{\text{brake}}^2 \gamma + (2\gamma a_{\text{brake}})^2 \right. \right. \\&\quad \left. \left. + 8(x_2 - x_1)a_{\text{brake}} + 8v_2\Delta t a_{\text{brake}} - 8L a_{\text{brake}} + 4v_2^2 \right]^{\frac{1}{2}} \right).\end{aligned}$$

- The merge point is within its safety gap. The safety gap equation differs from the car-following case by using a_- instead of a_{brake} and Δt instead of γ and by leaving out the L . Therefore, by the same argument as in the previous paragraph, the deceleration is

$$\begin{aligned}\alpha_o &= \frac{1}{\Delta t} \left(v_1 + \frac{3\Delta t a_-}{2} \right. \\&\quad \left. - \frac{1}{2} \sqrt{(\Delta t)^2 - 4v_1\Delta t a_- + 8(\Delta t)^2 a_-^2 + 8(x_2 - x_1) + 8v_2\Delta t a_- + 4v_2^2} \right).\end{aligned}$$

Finally, once we have determined the new acceleration α of C , we can change its position and velocity for the next time step as follows (letting x, v and x', v' be the old and new position and velocity respectively):

$$v' = v + \alpha\Delta t, \quad x' = x + v\Delta t + \frac{1}{2}\alpha\Delta t^2.$$

Calculating Delay Time

We calculate the delay time T for a car C moving through a toll plaza by breaking the process into several steps, tracing the car as soon as it starts slowing down before passing through the tollbooth, and until it merges back into a highway lane and accelerates to the speed limit.

Recalling our assumptions that cars do not change lanes, that they are evenly distributed among the lanes, and that there is no time loss associated with the distribution of cars into tollbooth lane at the fork point, we find that the period of approach to a tollbooth can be broken down as follows:

- **Deceleration from speed limit to stopping.** We assume that a car comes to a complete stop upon joining a tollbooth line as well as upon reaching the tollbooth. Therefore, the first action taken by a car approaching a toll plaza is to decelerate to zero; at constant deceleration a_- , it takes time v_{\max}/a_- to go from the speed limit to zero, over distance $v_{\max}^2/2a_-$.
- **Line Assignment.** As a car approaches the toll plaza, it is assigned to the currently shortest line. Let c_i be the number of cars in line i . The cars are spaced equidistantly throughout the line with distance ϵ between cars. Thus, as long as the length of the line is less than d , we have that the length of the line is $l_i = c_i(L + \epsilon)$, where L is the length of a car. Now, if $c_i(L + \epsilon) > d$, then the line extends to before the fork area, where there are m lanes instead of n . Assuming that the line lengths are roughly the same, increasing the minimum line length by one car increases the total number of cars by about n , and therefore each of the m lanes has an additional n/m cars. It follows that

$$l_i = \begin{cases} c_i(L + \epsilon), & \text{if } c_i(L + \epsilon) < d; \\ d + \frac{n[c_i(L + \epsilon) - d]}{m}, & \text{otherwise.} \end{cases} \quad (2)$$

- **Movement through a Tollbooth Line.** A car C joins the tollbooth line that it was assigned if such a line exists, that is, if the line length l_i is positive. In this case, C must wait for the entire line ahead to be serviced before C reaches the tollbooth. Let t_{serve} be the time when C enters the departure area, after it has been serviced. If there is an overflow of cars from the merge line such that C cannot leave the tollbooth, t_{serve} is the time when the car actually leaves, after the line in front has advanced sufficiently.
- **Movement through the Departure Region.** Different scenarios can occur in the departure region.

- Once C enters the departure area, it accelerates forward until either another car or the merge point enters its safety gap.
- If another car C' enters the safety gap of C , C slows down and follows C' until C' merges, at which time the merge point will overlap the safety gap of C .
- When the safety position of C reaches the merge point, if C does not have right of way, C will slow down so as to prevent the merge point from overlapping the safety gap, treating the merge point as an obstacle. This is in order to allow other cars who have already begun to merge, to do so until C can merge.
- Upon having the right of way, C merges and accelerates unconstrained from the departure region until reaching the speed limit. Let t_{merge} be the time at which C merges and v_{out} be its speed at that time. Then

$$t_f = t_{\text{merge}} + \frac{v_{\text{max}} - v_{\text{out}}}{a_+},$$

$$x_f = d + v_{\text{out}} \frac{v_{\text{max}} - v_{\text{out}}}{a_+} + \frac{(v_{\text{max}} - v_{\text{out}})^2}{2a_+}.$$

Thus by **(1)**, the delay experienced by C is

$$T = t_{\text{merge}} - t_{\text{line}} - \frac{l_i(t_{\text{line}}) + d}{v_{\text{max}}} + \frac{v_{\text{max}} - v_{\text{out}}}{a_+} - \frac{3v_{\text{max}}}{2a_-} - \frac{v_{\text{out}}(v_{\text{max}} - v_{\text{out}})}{a_+ v_{\text{max}}}.$$

The Multi-Car Interaction Model

We now determine the average delay time for a group of cars entering the toll plaza over a period of time. We simulate a group of cars arriving as per an arrival schedule and average their respective delay times. There are two complications: determining the arrival schedule (the distribution of individual cars over which to average) and the two variables t_{merge} and v_{out} (used in the delay-time formula above).

To determine computationally the average delay time, we must use the traffic density function $\rho(t)$ to produce a car arrival schedule. We create the arrival schedule by randomly assigning arrival times based on ρ . Using this schedule, we determine which cars begin to slow down for a given time step. Unfortunately this task is not as straightforward as determining whether a car's arrival time is less than the present time step. The arrival schedule provides the time a car reaches 0 (on the highway) if unconstrained. We wish to know when a car reaches a certain distance from the tollbooth line. Essentially given that a car would be at a set position (say 0 for the tollbooth) at time t , we seek the time t' when that car would have passed the front of the tollbooth line. This reduces to a question of Galilean relativity and we find that

$t' = t - l_i(t)/v_{\max}$. Now, up to knowing $l_i(t)$, we can exactly determine when cars join the tollbooth lines. We use (2) and the difference equation for car flow

$$\frac{\Delta c_i}{\Delta t} = \frac{m}{n} \rho \left(t - \frac{l_i}{v_{\max}} \right) - s_i$$

to keep track of the length of the tollbooth line, increasing it as cars join and decreasing it as cars are served.

As a car's arrival time (adjusted to the line length) is reached, we immediately assign it to the current shortest tollbooth line. We introduce normally distributed serving times with mean $\frac{1}{s}$ (where s is serving rate) and standard deviation σ that we assume to be $\frac{1}{6s}$.

The second consideration in simulating many cars is how to determine t_{merge} and v_{out} for each car. Our time-stepping model allows us to recursively update every car and thus to determine the actions of a single car at each time step. Following the rules in the previous section, we know exactly when and how much to accelerate (a_+) and decelerate (α_c, α_o). Furthermore, we observe that when a car that is first in its tollbooth lane approaches the merge point, it joins a merging queue (with at most n members). The only time when a car (on the merging queue) does not treat the queue as an obstacle (and consequently slow down) is when a highway lane clears and the car is taken from the queue and allowed to accelerate across the merge point and into free road. A lane is clear once the car in it accelerates $L + \epsilon$ passed the merge point.

With this model, we thus have a method, given a highway with m lanes, a certain traffic density function, and values for various constants, to calculate the optimal number of tollbooth lanes n . We can estimate a finite range of values of n in which the optimal number must lie. For each value of n we run our model, calculating the delay experienced by each car and averaging these to calculate average delay. We then compare our average delays for all n , choosing the minimal such n so that average delay is within 1 s of the minimum.

Case Study

We need reasonable specific values for our constants and density function for use in our tests. We take most of these from the Orlando–Orange Country Expressway Authority [2004] and a variety of reports on cars. We begin with a few simplifying assumptions about our traffic density function.

- To determine optimal average delay, it suffices to calculate the average delay over a suitably chosen day, as long as this day has periods of high and low density. This is reasonable because over most weekdays, traffic tends to follow similar patterns. Therefore, we limit the domain of ρ to the interval of seconds $[0, 3600 \times 24]$.
- The function $\rho(t)$ is piecewise constant, changing value on the hour. This

is reasonable: Since cars are discrete, $\rho(t)$ really is an average over a large amount of time and thus must already be piecewise constant.

- The length of the time interval between an arriving car and the next car is normally distributed.

The Orlando–Orange County Expressway Authority’s report on plaza characteristics [2004] allows us to construct a realistic traffic density function ρ for the purposes of testing. The report gives hourly traffic volume on several highways in Florida, which we use along with our assumption about normal arrival times to develop an arrival schedule for cars on the highway.

We assume several realistic values for constants defined earlier (**Table 3**).

Table 3.
Constant values used in testing.

Constant name	Symbol	Value
Comfortable acceleration	a_+	2 m/s ²
Comfortable deceleration	a_-	2 m/s ²
Hard braking deceleration	a_{brake}	8 m/s ²
Car length	L	4 m
Speed limit	v_{max}	30 m/s
Line spacing	ϵ	1 m

Our model assumes that every tollbooth operates at a mean rate of approximately s cars/s. But each type of tollbooth—human-operated, machine-operated, and beam-operated (such as an EZ-pass)—has a different service rate. We attempt to approximate the heterogenous tollbooth case by making s a composite of the respective services rates. According to Edie [1954], the average holding time (inverse of service rate) for a human operated tollbooth is 12 s/car, while according to the Orlando–Orange County Expressway Authority [n.d.], the average service rate for their beamoperated tollbooths, the E-Pass, is 2 s/car. Similarly, a report for the city of Houston [Texas Transportation Institute 2001] places the holding time for a human operated tollbooth at 10 s/car and a machine operated tollbooth at 7 s/car. Looking at these times, we find that a reasonable average holding time could be 5 s/car, giving us an average service rate $s = 0.2$ cars/s.

For verification, we consider hourly traffic volumes for six Florida highways, with from 2 to 4 lanes and varying traffic volumes [Orlando–Orange County Expressway Authority 2004]. We use the data to obtain $\rho(t)$ and test various components of our model. After model verification, we use our model to determine the optimal tollbooth allocations.

We look at two typical cases. A toll plaza radius of $d = 250$ m [Orlando–Orange County Expressway Authority 2004] is fairly standard. The hourly traffic densities of the six highways take a standard form; they differ mostly in amplitude, not in shape. Therefore, we model our density functions on two such standard highways, 4-lane Holland West (high density) and 3-lane Bee

Line (low density) (**Figure 2**). We extrapolate their traffic volume profiles to profiles for highways with 1 through 7 lanes. For m lanes, we scale the traffic volume by $m/4$ (Holland West) or $m/3$ (Bee Line). Doing so maintains the shape of the profile and the density of cars per lane while increasing the total number of cars approaching the toll plaza.

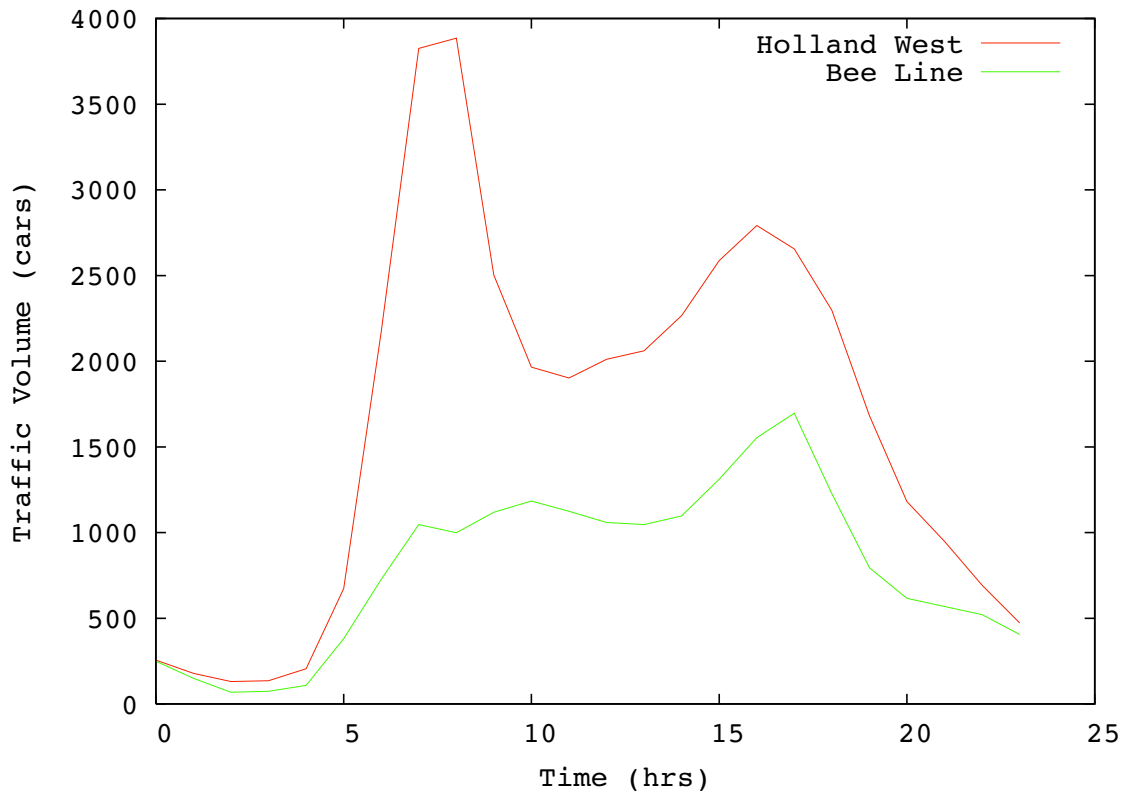


Figure 2. Traffic volume as a function of time for Holland West (top) and Bee Line (bottom).

Verification of the Traffic Simulation Model

Based on the optimality criteria, for various test scenarios we determine the minimal number of tollbooths with average delay time within 1 s of the minimal average delay. We show the results in **Table 4**.

Model results for three toll plaza match the actual numbers, and the other three differ only slightly. In the case of Dean Road, having 4 tollbooths (the actual case) instead of 5 leads to a significantly longer average delay time (70 s vs. 25 s). For Bee Line and Holland West, the difference is at most 1 s. These results suggest that our model agrees generally with the real world.

Table 4.

Comparison of model-predicted optimal number of tollbooths and real-world numbers for six specific highway/toll plaza pairs.

Highway	Tollbooths		Comparison
	Optimal	Actual	
Hiawassee	4	4	same
John Young Parkway	4	4	same
Dean Road	5	4	mismatch
Bee Line	3	5	close
Holland West	7	6	close
Holland East	7	7	same

Results and Discussion

Using real-world data from the Orlando–Orange Country Expressway Authority [2004], we create 14 test scenarios: high and low traffic density profiles for highways with 1 to 7 lanes. For each scenario, we run our model for a number n of tollbooths n ranging from the number of highway lanes m to $2m + 2$ (empirically, we found it unnecessary to search beyond this bound) and determine at which n the average delay time is least—this is the optimal number of tollbooths. We present our optimality findings in **Table 5**. For high traffic densities and more than two lanes, the optimal number of tollbooths tends to exceed the number of highway lanes by about 50%, a figure that seems to match current practice in toll plaza design; for low densities, the optimal number of tollbooths equals the number of highway lanes.

Table 5.

The optimal number of tollbooths for 1 to 7 highway lanes, by traffic density.

	High density							Low density						
	1	2	3	4	5	6	7	1	2	3	4	5	6	7
Lanes	1	2	3	4	5	6	7	1	2	3	4	5	6	7
Tollbooths	3	4	5	6	8	9	11	1	2	3	4	5	6	7

For high traffic density but only as many tollbooths as lanes, the average delay time is roughly 500 s, almost 20 times as long as the average delay of 25 s for the optimal number of tollbooths. So we strongly discourage construction of only as many tollbooths as lanes if high traffic density is expected during any portion of the day. However, when there is low traffic density, this case is optimal, with an average delay time of 22 s.

Further Study

To simulate real-world conditions more accurately, we could

- consider the effect of heterogenous cars and tollbooths;

- allow for vehicles other than cars, each with their own size and acceleration constants;
- consider the effect of changing serving rates, since research shows that average serving time decreases significantly with line length [Edie 1954]; or
- vary the toll plaza radius.

Strengths of Model

The main strength of the Multi-Car Interactive Model stems from our comprehensive and realistic development of single-car behavior. The intuitive notion of a car's safety gap and its relation to acceleration decisions, as well the effects of reaction times associated with expected and unexpected occurrence all find validation in traffic flow theory [Gartner et al. 1992]. The idea of a merge point and a car's behavior approaching that point mimics the practices of yielding right-of-way as well as cautiously approaching lane merges. Our choice of time step realistically approximates the time that normal decision-making requires, allowing us to capture the complete picture of a toll plaza both on a local, small scale, but also on the scale of overall tendencies. Finally by allowing for certain elements of normally distributed randomness in serving time and arrival time we capture some of the natural uncertainty involved in traffic flow.

A great strength of our model lies in the accuracy of its results. Our model meets all of our original expectations and furthermore predicts optimal tollbooth line numbers very close to those actually used in the real world, suggesting that our model approximates real-world practice.

Finally, the Multi-Car Interactive Model provides a versatile framework for additional refinements, such as modified single-car behavior, different types of tollbooth, and nonuniform serving rates.

Weaknesses of Model

In the real world, a car in the center lane has an easier time merging into the center lanes than a car in a peripheral lane, but this behavior is not reflected in our model. We also disallow lane-changing except at fork and merge points, though cars often switch lanes upon realizing that they are in a slow tollbooth line. Our method of determining car arrival times may be flawed, since Gartner et al. [1992, §8] suggest that car volume is not uniformly distributed over a given time block but rather increases in pulses.

Perhaps the two greatest weaknesses of our model are that all cars behave the same and all tollbooth lanes are homogeneous. While we believe that we capture much of the decision-making process of navigating a toll plaza, we recognize that knowledge is imperfect, decisions are not always rational, and all tollbooth lanes, and not all cars (or their drivers) are created equal.

References

- Adan, Idan, and Jacques Resing. 2001. *Queueing Theory*. 2001. <http://www.cs.duke.edu/~fishhai/misc/queue.pdf>.
- Chao, Xiuli. 2000. Design and evaluation of toll plaza systems. http://www.transportation.njit.edu/nctip/final_report/Toll.Plaza.Design.htm.
- Edie, A.C. 1954. Traffic delays at toll booths. *Journal of Operations Research Society of America* 2: 107–138.
- Gartner, Nathan, Carroll J. Messer, and Ajay K. Rathi. 1992. *Traffic Flow Theory: A State of the Art Report*. Revised Monograph. Special Report 165. Oak Ridge, TN: Oak Ridge National Laboratory. <http://www.tfhr.gov/its/tft/tft.htm>.
- Green, Marc. 2000. “How long does it take to stop?” Methodological analysis of driver perception-brake times. *Transportation Human Factors* 2 (3): 195–216.
- Insurance Institute for Highway Safety. 2004. Maximum Posted Speed Limits for Passenger Vehicles as of September 2004. http://www.iihs.org/safety_facts/state_laws/speed_limit_laws.htm.
- Malewicki, Douglas J. 2003. SkyTran Lesson #2: Emergency braking: How can a vehicle shorten it's [sic] stopping distance in an emergency. <http://www.skytran.net/09Safety/02sfty.htm>.
- Orlando–Orange Country Expressway Authority. n.d. E-Pass. <http://www.expresswayauthority.com/trafficstatistics/epass.html>.
- _____. 2004. Mainline plaza characteristics. <http://www.expresswayauthority.com/assets/STD&Stats%20Manual/Mainline%20Toll%20Plazas.pdf>.
- Texas Transportation Institute. 2001. Houston's travel rate improvement program. http://mobility.tamu.edu/ums/trip/toolbox/increase_system_efficiency.pdf.
- UK Department of Transportation. 2004. *The Highway Code*. <http://www.highwaycode.gov.uk/>.



Ivan Corwin, Nikita Rozenblyum, and Sheel Ganatra.

Lane Changes and Close Following: Troublesome Tollbooth Traffic

Andrew Spann

Daniel Kane

Dan Gulotta

Massachusetts Institute of Technology
Cambridge, MA

Advisor: Martin Zdenek Bazant

Summary

We develop a cellular-automaton model to address the slow speeds and emphasis on lane-changing in tollbooth plazas. We make assumptions about car-following, based on distance and relative speeds, and arrive at the criterion that cars maximize their speeds subject to

$$\text{gap} > \left\lfloor \frac{V_{\text{car}}}{2} \right\rfloor + \frac{1}{2}(V_{\text{car}} - V_{\text{frontcar}})(V_{\text{car}} + V_{\text{frontcar}} + 1).$$

We invent lane-change rules for cars to determine if they can turn safely and if changing lanes would allow higher speed. Cars modify these preferences based on whether changing lanes would bring them closer to a desired type of tollbooth. Overall, our assumptions encourage people to be a bit more aggressive than in traditional models when merging or driving at low speeds.

We simulate a 70-min period at a tollbooth plaza, with intervals of light and heavy traffic. We look at statistics from this simulation and comment on the behavior of individual cars.

In addition to determining the number of tollbooths needed, we discuss how tollbooth plazas can be improved with road barriers to direct lane expansion or by assigning the correct number of booths to electronic toll collection. We set up a generalized lane-expansion structure to test configurations.

Booths should be ordered to encourage safe behavior, such as putting faster electronic booths together. Rigid barriers affect wait time adversely.

Under typical traffic loads, there should be *at least twice as many booths as highway lanes*.

The UMAP Journal 26 (3) (2005) 317–330. ©Copyright 2005 by COMAP, Inc. All rights reserved. Permission to make digital or hard copies of part or all of this work for personal or classroom use is granted without fee provided that copies are not made or distributed for profit or commercial advantage and that copies bear this notice. Abstracting with credit is permitted, but copyrights for components of this work owned by others than COMAP must be honored. To copy otherwise, to republish, to post on servers, or to redistribute to lists requires prior permission from COMAP.

Definitions and Conventions

Car/Driver. Used interchangeably; “cars” includes trucks.

Tollbooth lane and highway lane. There are n highway lanes and m tollbooths. The tollbooth lane is the lane corresponding to a particular tollbooth after lane expansion.

Default lane. In the lane-expansion region, each highway lane is assigned a tollbooth lane such that following the highway lane without turning leads by default to the tollbooth lane, and following that in the lane-contraction region leads to the corresponding highway lane. Other tollbooth lanes begin to exist at the start of lane expansion and become dead ends at the end of lane contraction.

Delay. The time for a car to traverse the entire map of our simulated world, which stretches 250 cells before and after the tollbooth.

Gap. We represent a lane as an array; the gap is obtained by subtracting the array indices between two adjacent cars.

Assumptions and Justifications

Booths

A booth is manual, automatic, or electronic. A manual booth has a person to collect the toll, an automatic booth lets drivers deposit coins, and an electronic booth reads a prepaid radio frequency identification tag as the car drives by. A booth may allow multiple types of payment.

The cost of operating the booths is negligible. Compared to the cost of building the toll plaza or of maintaining the stretch of highway for which the toll is collected, this expense is insignificant, particularly since automated and electronic booths require less maintenance than manual booths.

Booth delays. Cars with an electronic pass can cross electronic tollbooths at a speed of 2 cells per time increment (≈ 30 mph). A car with an electronic pass can also travel through a manual or automatic booth but must wait 3–7 s for the gate to rise. A car without an electronic pass is delayed 8–12 s at an automatic booth and 13–17 s at a manual booth. We use probabilistic uniform distributions over these intervals to ensure that cars do not exit tollbooths in sync.

Cars/Drivers

Cars are generated according to a probability distribution. We start them at 1 mi from the tollbooth and generate for a fixed amount of simulated time (usually about 1 h), then keep running until all have gotten to the end of the simulated road 1 mi beyond the tollbooth. There are no entry or exit ramps in the 1 mi section leading to the tollbooth. Some vehicles are classified as trucks, which function identically but must use manual tollbooths if they do not have an electronic pass.

Drivers accurately estimate distances and differences in speed.

Car acceleration and deceleration is linear and symmetric. In reality, a car can accelerate much faster from 0 to 15 mph than from 45 to 60 mph, and the distances for braking and acceleration are different; but this is a standard assumption for cellular-automaton models.

Cars pack closely in a tollbooth line. Drivers don't want people from other lanes to cut into their line, so they follow at distances closer than suggested on state driver's license exams.

Dissatisfaction from waiting in line is a nondecreasing convex function. An especially long wait is a major annoyance. In other words, it is better to spread wait times uniformly than to have a high standard deviation.

Lanes

Toll collectors can set up new rigid barriers in the lane-expansion region.

Doing so would make certain lane changes illegal in designated locations. Since adding an extra tollbooth can be cost-prohibitive, setting up barriers to promote efficient lane-splitting and merging is important.

Signs are posted telling drivers what types of payment each lane accepts.

If drivers benefit from a certain type of booth (e.g., electronic), they will tend to gravitate toward it.

No highway lane is predisposed to higher speeds than others. Which lanes are "fast" or "slow" is dictated by the types of tollbooths that they most directly feed into.

The lane-expansion region covers about 300 ft. The lane contraction section is also assumed to be 300 ft.

Criteria for Optimal Tollbooth Configuration

Cars slowing or stopping at tollbooths make for bottlenecks. Since the speed of a car through a tollbooth must be slower than highway speed, adding tollbooths is an intuitive way to compensate.

Our goal is a configuration of lanes and tollbooths that minimizes delay for drivers. Mean wait time is the simplest criterion but not the best. Consider the case where there are no electronic passes and traffic is very heavy. In this limiting but plausible case, there are constantly lines and cars pass through each booth at full capacity. For a fixed number of tollbooths, the total wait time should be similar regardless of tollbooth-lane configuration; but if one lane is moving notably faster than the others, then the distributions of wait times will differ. Because we assume that dissatisfaction is a convex function, we give more weight to people who are stuck a long time. Klodzinski and Al-Deek [2002, 177] suggest that the 85th percentile of delays is a good criterion.

At the same time, we do not wish to ignore drivers who go through quickly. Therefore, we take the mean of the data that fall between the 50th and 85th percentiles for each type of vehicle. This will put an emphasis on cars that are stuck during times of high traffic but will not allow outliers to hijack the data. We consider separately the categories of cars, trucks, and vehicles with electronic passes, take the mean of the data that fall between the 50th and 85th percentiles, and take the weighted average of this according to the percentage of vehicles in the three categories.

We also wish to analyze effect of toll plaza layout. We therefore record the incidence of unusually aggressive lane changes, excessive braking, and cars getting “stuck” in the electronic lane that do not have an electronic pass.

Setting Up a Model

In the Nagel-Schreckenberg cellular-automaton model of traffic flow [Nagel and Schreckenberg 1992, 2222], cars travel through cells that are roughly the size of a car with speeds of up to 5 cells per time increment. This model determines speeds with the rules that cars accelerate if possible, slow down to avoid other cars if needed, and brake with some random probability. The model updates car positions in parallel. Such models produce beautiful simulations of general highway traffic, but less research has been done using the tight speed constraints and high emphasis on lane-changing that a tollbooth offers.

Creating models for multiple lanes involves defining lane-change criteria, such as change lanes if there is a car too close in the current lane, if changing lanes would improve this, if there are no cars within a certain distance back in the lane to change into, and if a randomly generated variable falls within a certain range [Rickert et al. 1996, 537]. Even with only two lanes, one gets interesting behavior and flow-density relationships that match empirical observations [Chowdhury et al. 1997, 423]. Huang and Huang even try to implement tollbooths into the Nagel-Schreckenberg model, but their treatment of lane expansion assumes that each lane branches into two (or more) tollbooths dedicated to that lane [2002, 602]. In real life, sometimes highways add tollbooth lanes without distributing the split evenly among highway lanes.

To allow for a various setups, we develop a generalized lane-expansion

structure. In the tollbooth scenario, low speeds are more common than in general stretches of highway, and there is a need to address more than two lanes. We change car-following and lane-change rules to fit a congested tollbooth area.

In the Nagel-Schreckenberg model, cars adjust their speeds based on the space in front. The tollbooth forces a universal slowdown in traffic. At these slow speeds, it is possible to follow cars more closely than at faster speeds. In the real world, we consider the speed of the car in front in addition to its distance away. Random braking is needed in the Nagel and Schreckenberg model to prevent the cars from reaching a steady state. However, in a tollbooth scenario, the desire not to let other cars cut in line predisposes drivers to follow the car in front more closely than expected. Thus, we do not use random braking but incorporate randomness into the arrival of new cars and lane-change priority orders. Instead of Nagel and Schreckenberg's rules, we propose the following rules for a cellular automaton model simulating a tollbooth scenario:

1. Cars have a speed of from 0 to 5 cells per time increment. In a single time increment, they can accelerate or decelerate by at most 1 unit.
2. Drivers go as fast as they can, subject to the constraint that the distance to the car in front is enough so that if it brakes suddenly, they can stop in time.
3. Cars change lanes if doing so would allow them to move faster. They modify the increased speed benefits of changing lanes by checking if the lane leads to a more desirable tollbooth type or if they face an impending lane merger. Before changing lanes, cars check the gap criterion of rule 2) applies to both the gap in front and the gap behind the driver after the lane change.
4. At each time step, we update positions and speeds from front to back.

We examine the rules in detail. Let us say that

- There are 250 cells in a mile (a little over 21 ft/cell).
- Each time step represents about 1 s.

Rule 1's maximum speed of 5 cells per time step corresponds to 72 mph (each unit of velocity is just under 15 mph), which is about the expected highway speed. The numbers for length and time increments do not need to be precise, since we can fix one and scale the other; what is important is that the length of a cell is a little more than the average length of a car (about 15 ft).

For any pair of following cars, we want the rear car to be able to decelerate at a rate of at most 1 unit and still avoid collision with the front car, even if the front car begins decelerating at a rate of 1 unit per time step squared. If for a given time step the rear and front cars have speeds V_{car} and V_{frontcar} and immediately begin decelerating at a rate of 1 unit squared until they stop, the total distances that they travel are

$$V_{\text{car}} + (V_{\text{car}} - 1) + \cdots + 1 = \frac{1}{2} V_{\text{car}} (V_{\text{car}} + 1),$$

$$V_{\text{frontcar}} + (V_{\text{frontcar}} - 1) + \cdots + 1 = \frac{1}{2} V_{\text{frontcar}} (V_{\text{frontcar}} + 1).$$

Our condition is equivalent to the car in back remaining behind the car in front, so the gap or difference in squares between the cars must be

$$\text{gap} > \frac{1}{2}V_{\text{car}}(V_{\text{car}}+1) - \frac{1}{2}V_{\text{frontcar}}(V_{\text{frontcar}}+1) = \frac{1}{2}(V_{\text{car}} - V_{\text{frontcar}})(V_{\text{car}} + V_{\text{frontcar}} + 1).$$

Thus, at each update, the rear car checks if it can increase its speed by 1 and still satisfy this inequality or if it must decrease its speed to maintain the inequality, and acts accordingly.

However, according to this model, if two cars are going the same speed, then they theoretically touch. Besides being a safety problem, this also contradicts the observations of Hall et al. that flow of cars as a function of percent occupancy of a location increases sharply until about 20% and then decreases thereafter [1986, 207]. With the inequality above, we could generate initial conditions with high occupancy and high flow. Before we discard our model, though, let us first check to see if these conditions would actually show up in the simulation.

We add the rule that a car tries to leave at least $\lfloor V_{\text{car}}/2 \rfloor$ empty spaces before the car in front; this would still let cars tailgate at low speeds. For high speeds, this would be a somewhat unsafe distance but consistent with aggressive merging; but we expect high speeds to be rare near the tollbooth during moderate or high congestion. Thus, our final criterion for rule 2 is that a car looks at the number of empty spaces in front of it and adjusts its speed (upward if possible) so that it still meets the inequality

$$\text{gap} > \left\lfloor \frac{V_{\text{car}}}{2} \right\rfloor + \frac{1}{2}(V_{\text{car}} - V_{\text{frontcar}})(V_{\text{car}} + V_{\text{frontcar}} + 1).$$

When changing lanes (rule 3), cars ask, "If I changed lanes, how fast could I go this time step?" Cars avoid making lane changes that could cause a collision, as determined by the gap criterion. When given an opportunity to change lanes, a car compares the values of the maximum speeds that it could attain if it were in each lane but adds modifiers. Lanes have penalties in valuation for leading to tollbooths that the driver cannot use (-2 per lane away from a usable lane before the lanes branch and -20 after) or are suboptimal (-1 per lane away from an optimal lane), where suboptimal means a car with an electronic pass in a lane that does not accept it. Leaving the tollbooth, drivers try hard to get out of dead-end lanes (-3 or -5 depending on how far it is to the end). If drivers value the lane they are in and a separate lane equally, they do not change. If drivers value both the lane on their left and the lane on their right equally more than their current lane, they pick randomly.

We update speeds in each lane from front to back, with lanes chosen in a random order. A consequence of this is that information can propagate backwards at infinite speed if for example the head of a string of cars all going at speed 1 came to a complete stop. This infinite wave-speed problem could be fixed by introducing random braking, but at slow speeds we find it more acceptable to have people inching forward continuously than to have people braking from 1 to 0 at inopportune times. This also has consequences for lane changes, in that

randomly giving lanes an update priority will have different results from processing all lane changes in parallel. Although some cellular-automaton traffic models in the literature update in parallel, we use serial updating because it makes handling the arrays easier and eliminates the problem of having people from two different lanes trying to change into the lane between them at the same time. The random update priority ordering for the lanes is changed every time increment, so that there is less systematic asymmetry in lane changing.

Generalized Lane-Expansion Structure

We develop a system to describe easily a large number of different tollbooth setups. The road both starts and ends as an n -lane highway and contains m tollbooths in the middle. The lane dividers are labeled from 1 to $n + 1$ for the highway lanes and from 1 to $m + 1$ for the tollbooth lanes. A rigid barrier consists of an (x, y) pair where the x -coordinate represents a lane divider and the y -coordinate represents a tollbooth divider. **Figure 1** shows the case $n = 4$, $m = 6$, with rigid barriers at $(1, 1)$, $(2, 3)$, $(3, 4)$, and $(5, 7)$. Cars may not make lane changes across a rigid barrier.

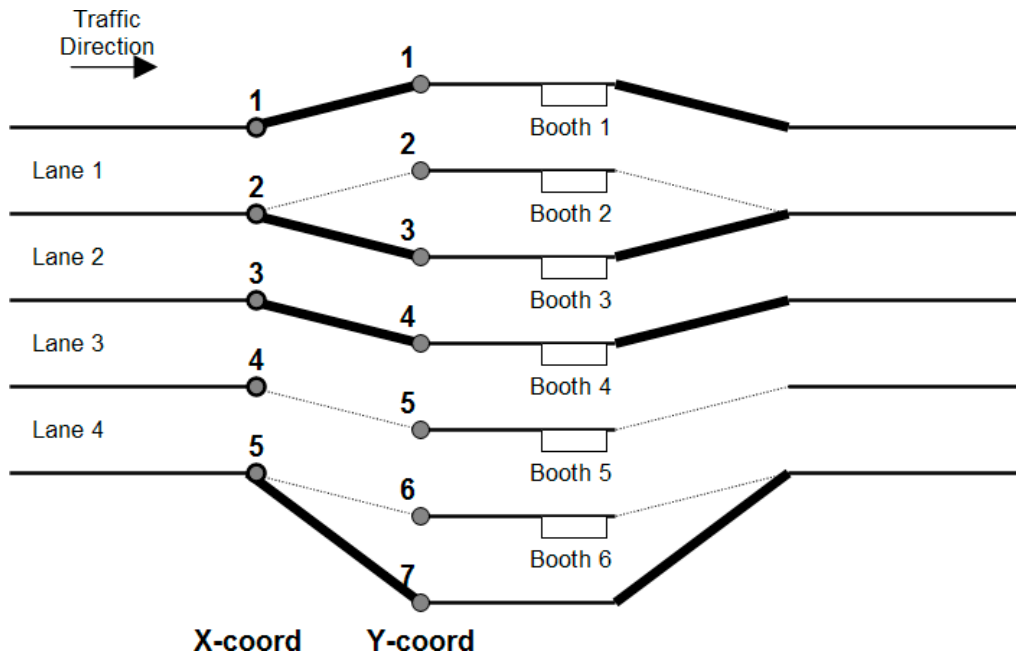


Figure 1. Generalized lane-expansion scheme.

Suppose that we have an ordered set of rigid barriers $\{(x_1, y_1), \dots, (x_k, y_k)\}$, where $x_i + 1 > x_i$ for $i = 1, \dots, k - 1$. Then the set of rigid barriers must obey the following rules:

- you cannot drive off the road: $(1, 1)$ and $(n + 1, m + 1)$ must be rigid barriers; and

- rigid barriers do not cross each other: for $i = 1, \dots, k-1$, we have $y_{i+1} > y_i$.

The dotted lines in **Figure 1** can be crossed as normal lane changes. In the lane-expansion region, each lane is assigned a “default” tollbooth lane that it most naturally feeds into. Highway lanes 1, 2, 3, and 4 feed tollbooth lanes 1, 3, 4, and 5. If there is an adjacent lane not blocked by a rigid barrier, a car can enter that lane. The default tollbooth lane then feeds back into the highway lane after the tollbooth and the other highway lanes are treated as dead-ends. Cars are given an incentive to change out of these dead-end lanes ahead of time. We assume that rigid barriers and default lanes are symmetric between lane expansion and contraction. Additionally, no lane changes are allowed on the five cells immediately preceding and following the tollbooth cell.

Results

We simulate a 70-min period when incoming traffic starts light, increases for 40 min, then decreases again. **Figure 2** shows the generation rates for light, normal, and heavy traffic. For a four-lane highway, these settings correspond to volumes of about 2200, 3000, and 3600 cars over the 70-min period.

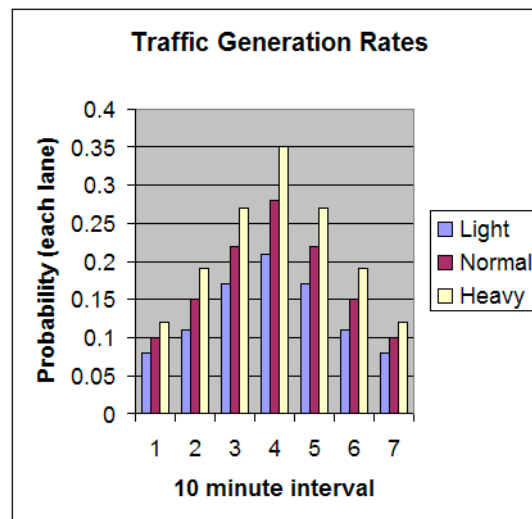


Figure 2. Traffic generation rates.

We test two cases of allocation and arrangement of tollbooths: no barriers, or else each highway lane branches into an equal number of tollbooth lanes. In both cases, we make the odd numbered lanes the default lanes. We tested both of these cases for different orderings of the tollbooths. For a 4-lane highway, we use 2 electronic booths, 4 automatic booths, and 2 manual booths. Half of the vehicles had electronic passes and 10% of the vehicles are trucks (no electronic pass). First we clustered all booths of the same type in some permutation, then we alternated types. **Figure 3** shows data averaged over 10 runs.

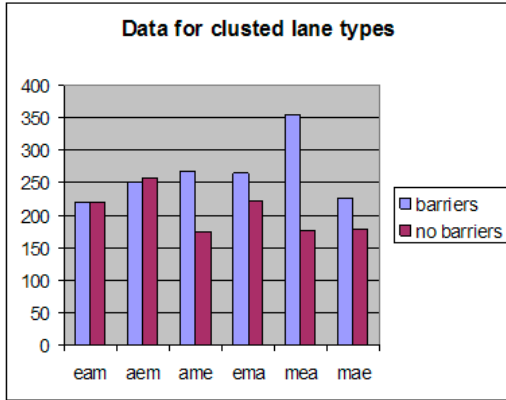


Figure 3a. Clustered lanes.

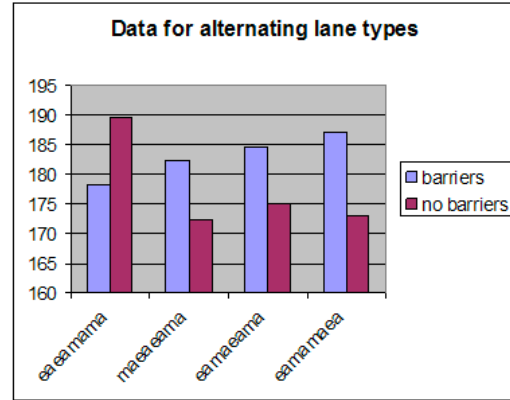


Figure 3b. Alternating lanes.

Figure 3. Average delays for two lane configurations and with vs. without barriers. All situations are for normal traffic load, 4 highway lanes, and 8 booths—2 electronic, 4 automatic, 2 manual.

The x -axis gives configurations and the y -axis is adjusted average delay time (mean of the 50th through 85th percentiles of travel time through the 250 cells before and after the tollbooth). If there were no tollbooth, then a car at full speed would have delay 100 s. Barriers are slightly worse than just allowing people to change lanes.

We note from **Figure 3a** that each of the clustered lane types is different from its mirror image, and this phenomenon is reproducible, which is puzzling. We think that it is caused by our handling of the concept of default lane, where some lanes feed directly into tollbooth lanes; with unrestricted lane expansion, this might make some lane changes easier than others.

The alternating tollbooth configurations appear to have slightly less delay, but they also generate more warning flags about dangerous turns and cars becoming stuck in tollbooth lanes that they cannot use. For each clustered configuration, either it or its mirror image gives time equivalent to the alternating tollbooth configurations. Therefore, for safety reasons, we suggest using the clustered configurations.

We next determine how many of each type of booth to use for a 4-lane highway with 8 tollbooths and a lane-expansion region with no rigid barriers. We put the electronic booths on the left and the manual booths on the right. We vary the numbers of each type of tollbooth for different distributions of cars, trucks, and vehicles with electronic passes and run the simulation under normal traffic loads. Unless the percentage of trucks is very low, allocating only 1 manual booth for the trucks generates a large number of trucks stuck in lanes that they cannot use. The number of electronic booths should be 2 or 3, depending on whether cars with electronic passes outnumber vehicles without them. Since 8 to 12 tollbooths is reasonable size for a 4-lane highway, *we recommend very roughly one-fourth electronic, one-half automatic, and one-fourth manual tollbooths.*

How many tollbooths are needed for different levels of traffic? We round down the number of manual and electronic tollbooths and round up the number of automatic tollbooths from the above proportions. Using the light, normal, and heavy traffic loads defined in **Figure 2** above, we arrive at **Figure 4**.

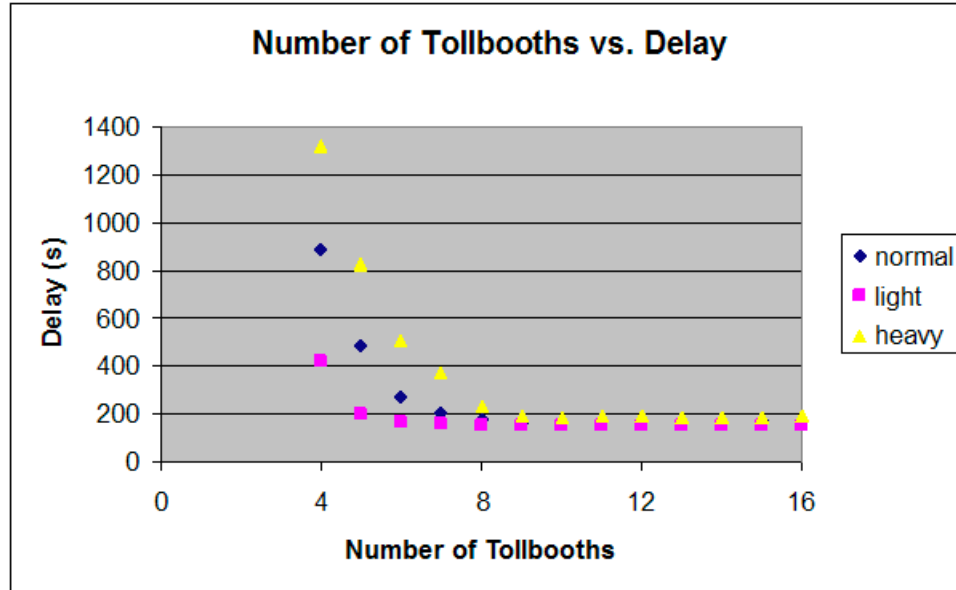


Figure 4. Delay vs. number of tollbooths.

Finally, we consider the limiting case of no trucks and no electronic passes (all tollbooths are automatic). This is the standard case directly comparable to other models in the literature. Under light, normal, and heavy traffic loads, we find that delay times are as in **Figure 5**.

Without electronic tollbooths, cars experience much longer delays, since each must stop at a tollbooth. With only one tollbooth per lane, the normal traffic load (3000 vehicles over 70 min) forces many people to wait over 45 min! It takes about 12 lanes to reach minimal delay in this situation instead of the 9 in the situation with automatic and electronic lanes.

Do the Cars Behave Reasonably?

In **Figure 6**, we graph travel time vs. arrival time for all cars, under normal traffic loads with no barriers, 4 highway lanes, 8 tollbooths (from left to right: 2 electronic, 4 automatic, 2 manual). There are two main features:

- The line represents cars with electronic passes. Even under a heavy traffic load, they are not terribly delayed, since they can pass through their booth without stopping.
- Along the top, we see the cars without electronic passes. The distribution of their wait times looks like the graph of their generation rate shifted over by

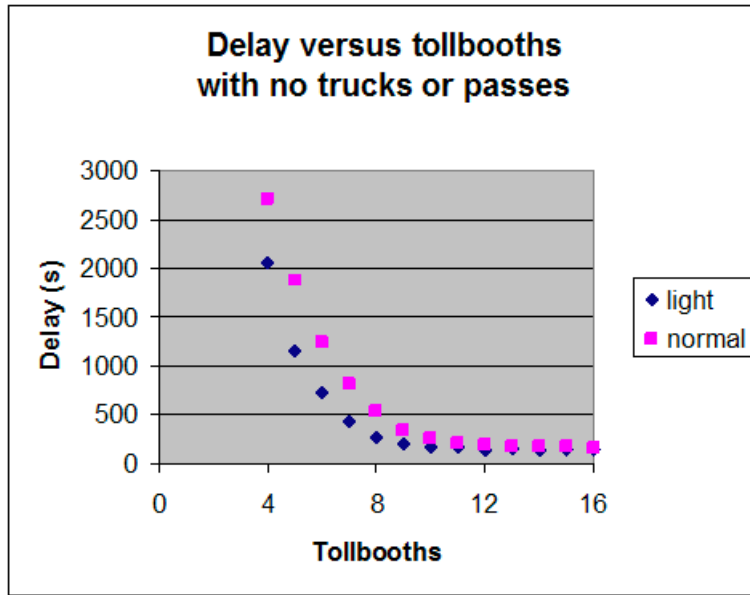


Figure 5. Delay vs. number of tollbooths—no trucks or electronic passes.

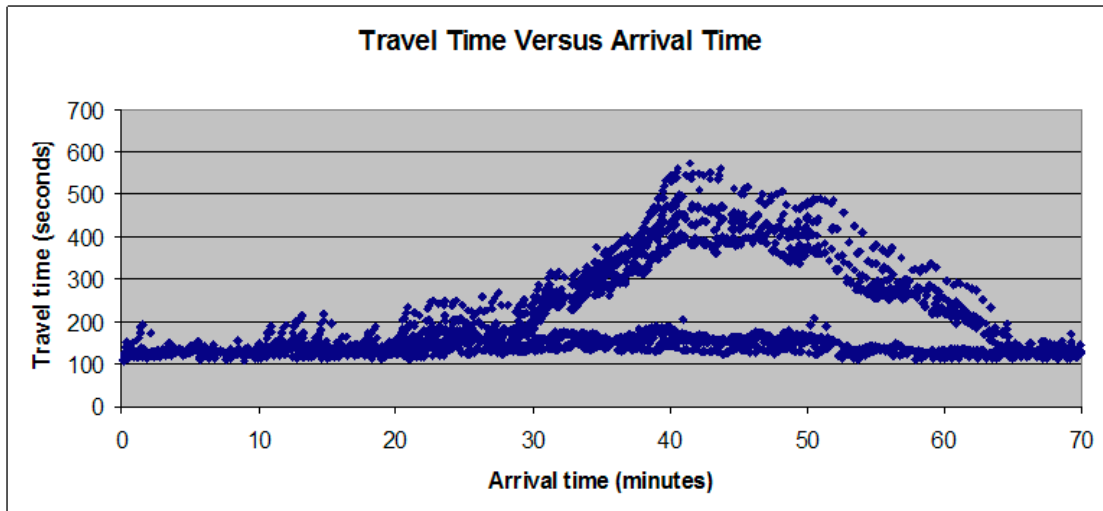


Figure 6. Travel time vs. arrival time.

about 10 min. One can even see the graph split into several “lanes,” which shows the difference between the slower truck lanes (manual tollbooths) and the normal cars (automatic tollbooths).

We are also interested in what configurations lead to potential accidents. We ran setups under the default parameters of normal traffic load, 50% electronic passes, and 10% trucks. **Figure 7** shows the number of occurrences of several types of these behaviors, out of about 3000 cars total.

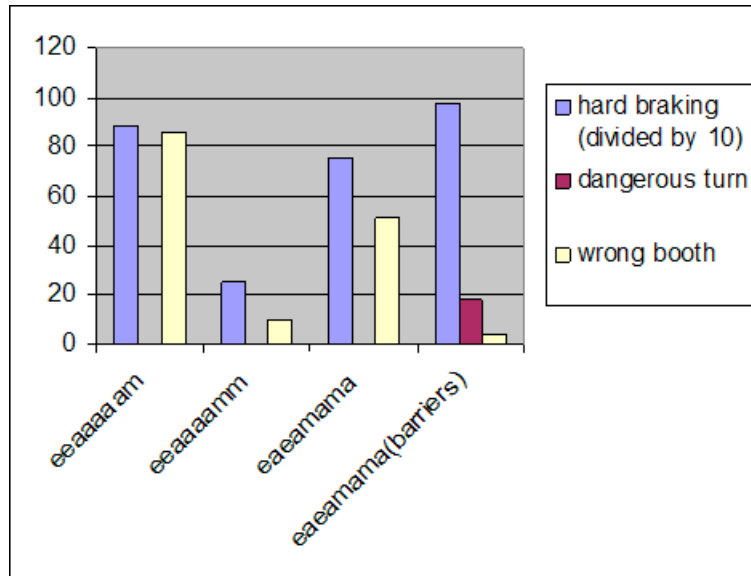


Figure 7. Incidents of dangerous behavior.

We see in the leftmost configuration that having only one manual lane leads to trucks stuck in the wrong booth. Trucks joining the wrong booth also seems to lead to an increase in hard braking; this appears to be an artifact of cars traveling at speeds of 1 or 2 not decelerating properly when nearing a tollbooth. In our experiments, this phenomenon tends to be correlated with inefficient lane-changing schemes. The second configuration from the left is our recommended configuration. The third and fourth configurations show the difference that barriers make: They cause fewer tollbooth mistakes but lead to dangerous turns and hard braking, which are probably related.

Sensitivity to Parameters

Changing the length of the lane-expansion and -contraction regions did not have a statistically significant effect on either wait times or logs of bad behaviors. The percentages of cars with electronic passes and trucks can be changed by a fair amount before they affect anything. For a general number n of highway lanes and rigid barriers, the marginal return of adding a new tollbooth after $2n$ or $2n + 1$ is small unless the traffic load is exceptionally large.

Strengths and Weaknesses

Strengths

Can handle a wide variety of possible setups. It is hard to add new tollbooths but easier to change the type of tollbooth or set up barriers.

Captures important features of the actual situation.

Behavior based on simple procedures meant to accomplish natural goals. We avoid introducing artificial effects by basing drivers' behaviors on simple methods of accomplishing natural goals, such as avoiding collisions and getting into a better lane.

Weaknesses

Need to obtain real-world parameters. If we were acting as consultants for a particular highway, we should collect data.

More complicated than simple models in literature. Our model may introduce some artificial behavior. Cellular automaton models are supposed to have complex behavior emerge from simple assumptions, not the other way around.

Infinite speed of information propagation. Due to the order in which cars are updated in our model, information about obstacles can propagate backwards at infinite speed, an effect which can lead to inaccuracies.

Conclusion

Cellular-automaton models are one effective means of studying traffic simulations. Other approaches use partial differential equations motivated by kinetics or fluid mechanics [Chowdhury et al. 1997, 213–225].

Our cellular automaton model gives us valuable insight into the tollbooth traffic problem. We can see cars flowing through the tollbooths and piling up during rush hour. We can follow the motions of individual cars and collect statistics on their behaviors. From our experiments, we make the following recommendations:

Tollbooths should be ordered based on encouraged behavior. Safety considerations should take precedence; putting faster booths on the left and slower booths on the right accomplishes this.

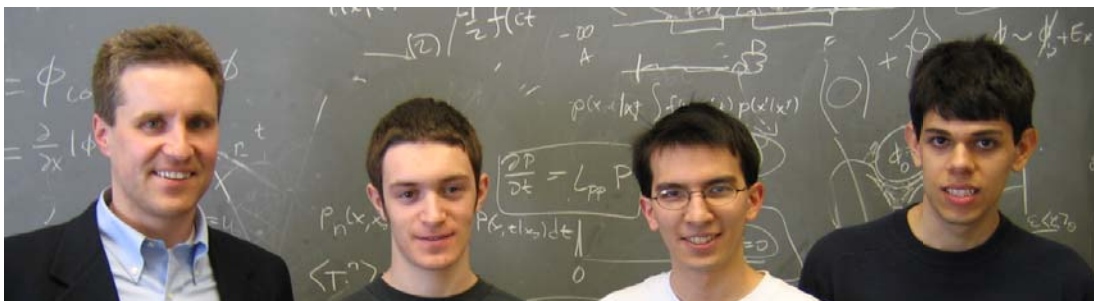
No barriers. Barriers prevent drivers getting to lanes that they need to use.

The distribution of types of cars should determine how many tollbooths. Traffic density has little effect on the number of tollbooths needed to minimize delay; the distribution of types of cars has a much larger effect.

An effective ratio of tollbooths is 1 electronic: 2 automatic : 1 manual.

References

- Chowdhury, Debashish, Ludger Santen, and Andreas Schadschneider. 2000. Statistical physics of vehicular traffic and some related systems. *Physics Reports* 329: 199–329.
- Chowdhury, Debashish, Dietrich E. Wolf, and Michael Schreckenberg. 1997. Particle hopping models for two-lane traffic with two kinds of vehicles: Effects of lane-changing rules. *Physica A* 235: 417–439.
- Haberman, Richard. 1977. *Mathematical Models: Mechanical Vibrations, Population Dynamics, and Traffic Flow*. Englewood Cliffs, NJ: Prentice Hall. 1998. Reprint. Philadelphia: SIAM.
- Hall, Fred L., Brian L. Allen, and Margot A. Gunter. 1986. Empirical analysis of freeway flow-density relationships. *Transportation Research Part A: General* 20 (3): 197–210.
- Huang, Ding-wei, and Wei-neng Huang. 2002. The influence of tollbooths on highway traffic. *Physica A* 312: 597–608.
- Klodzinski, Jack, and Haitham Al-Deek. 2002. New methodology for defining level of service at toll plazas. *Journal of Transportation Engineering* 128 (2): 173–181.
- Nagel, Kai, and Michael Schreckenberg. 1992. A cellular automaton model for freeway traffic. *Journal de Physique I* 2 (12): 2221–2229.
- Rickert, M., K. Nagel, M. Schreckenberg, and A. Latour. 1996. Two lane traffic simulations using cellular automata. *Physica A* 231: 534–550.



Martin Bazant (advisor), Daniel Kane, Andrew Spann, and Daniel Gulotta.

A Quasi-Sequential Cellular-Automaton Approach to Traffic Modeling

John Evans
Meral Reyhan
Rensselaer Polytechnic Institute
Troy, NY

Advisor: Peter Kramer

Summary

The most popular discrete models to simulate traffic flow are cellular automata, discrete dynamical systems whose behavior is completely specified in terms of its local region. Space is represented as a grid, with each cell containing some data, and these cells act in accordance to some set of rules at each temporal step. Of particular interest to this problem are sequential cellular automata (SCA), where the cells are updated in a sequential manner at each temporal step.

We develop a discrete model with a grid to represent the area around a toll plaza and cells to hold cars. The cars are modeled as 5-dimensional vectors, with each dimension representing a different characteristic (e.g., speed). By discretizing the grid into different regimes (transition from highway, tollbooth, etc.), we develop rules for cars to follow in their movement. Finally, we model incoming traffic flow using a negative exponential distribution.

We plot the average time for a car to move through the grid vs. incoming traffic flow rate for three different cases: 4 incoming lanes and tollbooths, 4 incoming lanes and 4, 5, and 6 tollbooths. In each plots, we noted at certain values for the flow rate, there is a boundary layer in our solution. As we increase the ratio of tollbooths to incoming lanes, this boundary layer shifts to the right. Hence, the optimum solution is to pick the minimum number of tollbooths for which the maximum flow rate expected is located to the left of the boundary layer.

The UMAP Journal 26 (3) (2005) 331–344. ©Copyright 2005 by COMAP, Inc. All rights reserved. Permission to make digital or hard copies of part or all of this work for personal or classroom use is granted without fee provided that copies are not made or distributed for profit or commercial advantage and that copies bear this notice. Abstracting with credit is permitted, but copyrights for components of this work owned by others than COMAP must be honored. To copy otherwise, to republish, to post on servers, or to redistribute to lists requires prior permission from COMAP.

Introduction

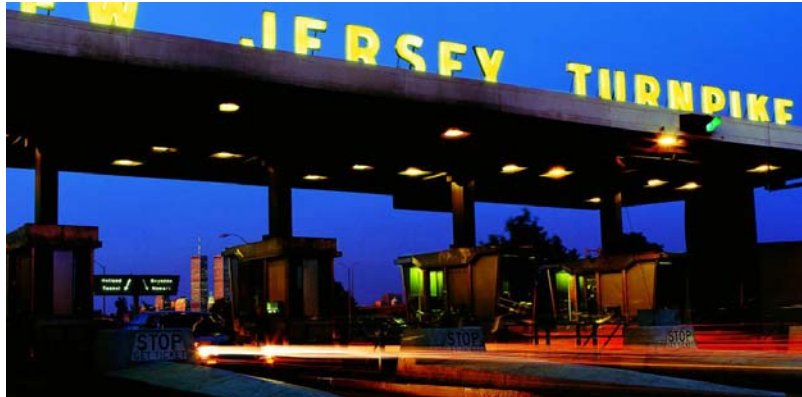


Figure 1. The New Jersey Turnpike (I-95) at night.

Models for traffic flow can be broken down into two basic types.

- The first type treats space and time as a continuum; both cars and time are continuous in nature.
- The second type, discrete models, treats space as a lattice and time discretely. A common discrete model is a cellular automaton, where space is modeled by a lattice and each lattice site represents a state of the system. The lattice sites are updated and their states change. For traffic flow, the states of the lattice sites represent whether a car is present at that spatial location or not.

Near a tollbooth, cars must stop to pay before moving on. Since each car affects the other cars in its direct neighborhood, it is not reasonable to model cars as a continuum. Discrete time also allows us to control the movement of the cars at each individual time step. Finally, discrete models in general are much easier to understand and to implement on modern computing resources.

Assumptions

- Upon nearing a toll plaza, a driver maneuvers based on local congestion to minimize travel time.
- Within 100 ft of the toll plaza, a driver remains in a lane and slows down to an average speed of about 5–10 mph. We base the speed of the cars on what is suggested in most driver's manuals: Car separation should be one car length for every 10 mph of speed.
- Once a driver pays the toll, they maneuver to a highway lane and accelerate to highway speeds.

- Drivers do not cooperate. While the drivers are not directly competing against one other, they are affecting each other and are hence fierce indirect obstacles/opponents.
- Vehicles are of constant length (17.5 ft).
- It takes about 4 s for a tollbooth employee to process a motorist [Chao n.d.].

A Quasi-SCA Model of Toll Plaza Dynamics

Case 1: Equal Numbers of Lanes and Booths

Preliminaries

Cellular automata (CA) are discrete dynamical systems whose behavior is completely specified locally. Space is represented as a uniform grid, with each cell containing data. Time advances in discrete steps, and the laws of the universe are expressed in a look-up table relating each cell to nearby cells to compute its new state. The system's laws are local and uniform.

The basic one-dimensional cellular automata model for highway traffic flow is the CA rule 184, as classified by Wolfram [Nagel et al. 1998; Jiang n.d.; Wolfram 2002]. CA 184 is a discrete time process with state space $\eta \in \{0, 1\}^{\mathcal{Z}}$ and the following evolution rule: If $\eta \in \{0, 1\}^{\mathcal{Z}}$ is the state of at time n , then the state η' at time $n + 1$ is defined by

$$\eta' := \begin{cases} 1, & \text{if } \eta(x) = \eta(x + 1) = 1; \\ 1, & \text{if } \eta(x) = 1 - \eta(x + 1) = 0; \\ 0, & \text{otherwise,} \end{cases}$$

where $\eta(x)$ denotes the value of $\eta : \mathcal{Z} \rightarrow \{0, 1\}$ at the coordinate x .

In this model, cars march to the right in a rather uniform manner, and all nodes execute their moves in parallel.

Toll plaza dynamics, while similar to traffic dynamics, are quite different.

- Toll plazas cannot be approximated as covering an infinite domain.
- Drivers must make decisions based on who moves in front of them. In this sense, we use ideas from Sequential Cellular Automata (SCA) [Tosic and Agha n.d.] instead of the classical schemes.
- Cells are updated in a slightly different manner than in classical cellular automata. To model car movement properly, "cars" are moved through cells one at a time.

Our model is like a board game. For these reasons, we dub our model a "Quasi-SCA Model of Toll Plaza Dynamics."

We divide a multilane highway into equally partitioned lanes. Each cell is approximately 25 ft long and contains information on whether it contains a car and, if it does, certain information about the car. Furthermore, there are specialized cell characteristics for different regimes, as shown in **Figure 2**. In our model, we also move forward in discrete time steps. For convenience, this time step is set to be 2 s in length.

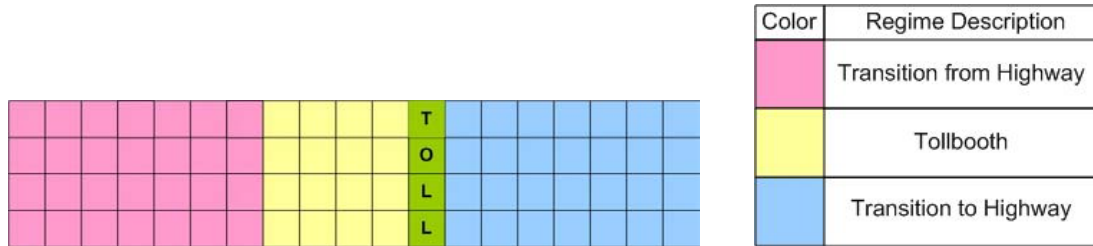


Figure 2. Possible regimes.

To implement our model, we exploit the object-oriented features of C++. We create a car class, with certain variables associated with it, as shown in **Table 1**.

Table 1.
Car class variables in C++.

Car Class Variables	
Occupied	1 = Car, 0 = Null
Congestion	Percent Measure of Local Congestion
Speed	Measure of Car Speed
TotalTimeOnGrid	Counter Measuring Time on Grid
TotalTimeInToll	Counter Measuring Time in Toll

The highway is represented as a large $50 \times n$ array of car variables, where n is the number of lanes. When initialized, this array contains empty grid spaces. As cars enter in from the left, grid spaces are activated and infused with information about the cars. Then, with this information, the state of the system at the next time step can be determined.

Vehicle Speed

The speeds of cars not in the tollbooth regime are dictated by car separation having to be one car length for every 10 mph of speed. Since our model is discrete in both space and time, this criterion must be quantized. Moving one grid space ahead in one temporal step corresponds to a speed of about 8.5 mph. If we approximate one grid space as one car length and $8.5 \text{ mph} \sim 10 \text{ mph}$, we

can generalize the speeds of the cars in the following manner:

$$s(i, j, t) := \begin{cases} 0, & \text{if } \min_{x>i}\{x \mid o(x, j, t) = 1\} = i + 1; \\ 1, & \text{if } \min_{x>i}\{x \mid o(x, j, t) = 1\} = i + 2; \\ 2, & \text{if } \min_{x>i}\{x \mid o(x, j, t) = 1\} = i + 3; \\ 3, & \text{otherwise.} \end{cases}$$

We enforce 25.6 mph as an upper limit to speed, since the vehicles must slow down as they approach the toll. At each time step, the speed for a car is updated just before it initiates movement.

Congestion

Since a driver is far more forward-focused than rearward-focused, we consider congestion to be determined only by the cars immediately in front—in particular, the nearest five cars. We write congestion for the car located in grid cell $\eta(i, j, t)$ as

$$c(i, j, t) := \frac{1}{5} \sum_{k=1}^5 o(i + k, j),$$

where

$$o(i, j, t) := \begin{cases} 1, & \text{if grid cell } (i, j) \text{ contains a car;} \\ 0, & \text{otherwise} \end{cases}$$

Sequencing

Cells are updated sequentially as opposed to simultaneously, because cars make decisions based on the cars in front. Furthermore, in a given column of our array, that is, one spatial location across four lanes, the car with the largest speed has the first initiative; the car with the second largest speed moves second, etc. In the case of a tie, the car closer to the top of the grid moves first.

Movement

Transition Regimes

Transition regimes are regions where traffic comes in from the highway or leaves to the highway. In these regimes, drivers maneuver in a manner such that they can optimize travel time but minimize effort. Thus, movement possibilities in the transition regimes can be described by **Figure 3**.

The optimal maneuver is to move forward, but a driver will enter a lane to the right or left if the move minimizes congestion.

In two locations of the transition regimes, there are special considerations.

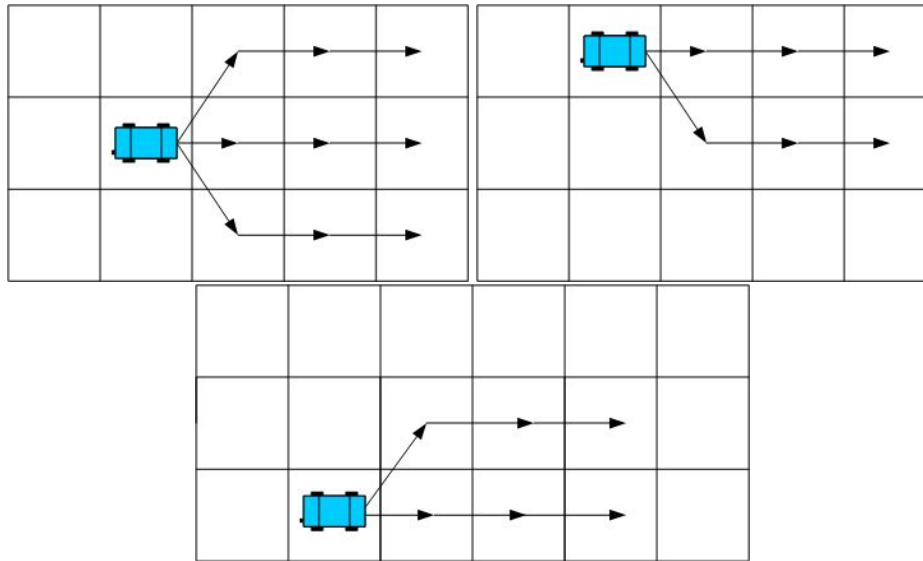


Figure 3. Movement in transition regimes: Center lane, far left lane, far right lane

- The transition from highway regime: There must be some way to depict the arrival of traffic from the highway. We discuss later how we do this.
- The tail end of the transition-to-highway regime: Provided a car has sufficient speed, we eliminate the car from the grid. We also record its TotalTimeOnGrid variable.

Tollbooth Regime

In the tollbooth regime, drivers no longer veer to the right or left. Instead, they move forward in line until they reach the tollbooth. In this region, spanning the 100 ft in front of the tollbooth, cars move at a maximum rate of one grid space per temporal element. Once in the tollbooth, they wait two entire temporal elements solely in the booth (about 4 s) until they move on to the transition regime. This is implemented by incrementing a car's TotalTimeInToll variable (initialized to zero when a vehicle enters the map) every temporal step that a car is in the booth (*for the entire step*) and checking if it is greater than 2. Often in this region, lines will form. As soon as a car emerges from the tollbooth, all of the cars behind move forward immediately. The dynamics of this regime are quite a bit different and simpler than the dynamics of the transition regime.

We illustrate this situation in **Figure 4**. The red cars in lanes one and four are stopped, waiting behind cars located in the booth. The green cars ahead of the toll are transitioning to the highway regime. The yellow car is moving into the tollbooth, and the blue car is moving further inside the region. The green car before the toll is just now moving into the tollbooth region. While its current speed is 25.6 mph, once inside the region, it decelerates to 8.5 mph.

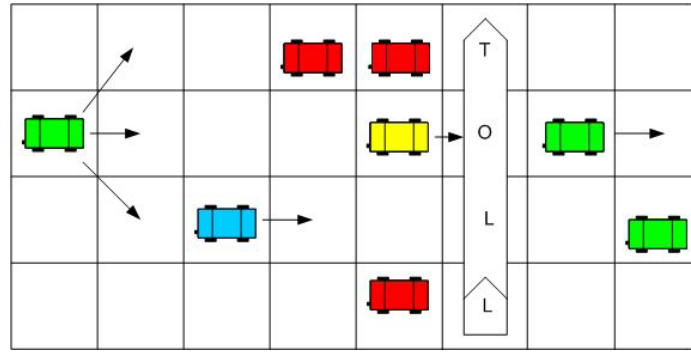


Figure 4. Movement in the tollbooth regime

Modeling the Incoming Traffic Flow

To make our model more accurate, we use a statistical distribution to predict incoming flow. Two commonly-used distributions are the Poisson and the negative exponential. However, the Poisson distribution fits well only for light traffic [Aston 1966]. The negative exponential distribution is a good fit for heavy traffic; it is used to model the variations of gap length in a traffic stream over distance and random arrivals. It has probability density function

$$f(t) = qe^{-qt},$$

where t is the time (s) between arrivals and q is the rate of arrival (cars/s), and cumulative distribution function

$$F(t) = 1 - e^{-qt}. \tag{1}$$

To implement this arrival time into our simulation, we assign it to a site of entry (a space) into the grid. A random number generator creates a random fraction F ; using (1), we solve for $t = -\ln R/q$. The value t is assigned to a “spawn site,” a place where “cars” are created. We use a counter to keep track of the time between different spawnings of cars. If this counter is greater than F and the “spawn site” is empty (contains a null car), then a car is created at the spawning site. Otherwise, the counter is incremented until one of these two conditions are met. Cars “arrive” in each lane of the simulation using this method. We use a modified q such in units of car per 2 s per lane.

Results

We simulate for varying values of q , the flow rate of cars per 2 s per lane, for a 4-lane highway with 4 tollbooths. We let q vary from 0.01 cars/s/lane (0.02 cars/s overall) to 1 car/s/lane (2 cars/s overall). Figure 6 outlines a given time evolution for a small value of q .

The time through which the cars move through the grid (or toll plaza) is an appropriate measure of congestion. Thus, we plot in Figure 7 the average time

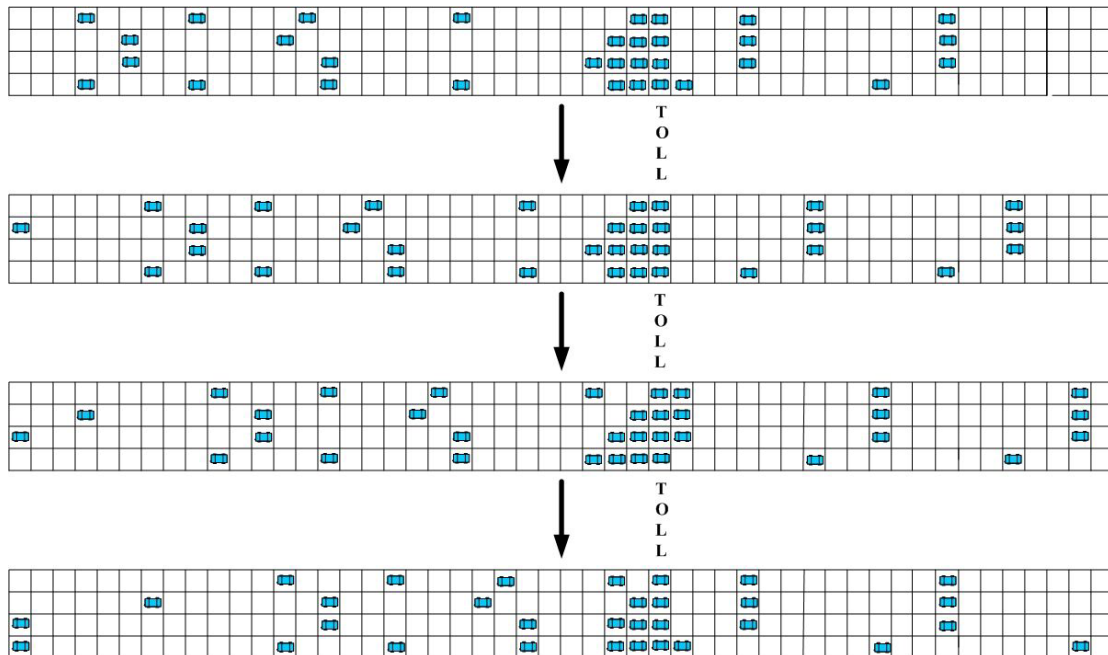


Figure 6. Time evolution of a simulation, four temporal steps.

getting through the grid versus the flow rate. The average time is obtained from a simulation accounting for one hour of traffic. We also plot for each flow value the maximum amount of time that anyone spent getting through the grid.

For q in $[0.01, 0.37]$ cars/(2 s)/lane (0.02–0.74 cars/s overall), drivers enjoy an average time through the grid below 50 s. We consider this an optimal situation. However, at around a $q = 0.36$ cars/(2 s)/lane, there appears to be a boundary layer. For $q > 0.37$, it takes drivers an average of 2 min or more to get through the quarter-mile long grid, corresponding to less than 10 mph. We demonstrate later that by adding more tollbooths, we shift the boundary layer and lower the average time for larger q . Thus, a good strategy to determine the number of tollbooths is to estimate the anticipated maximum flow rate and choose a number of lanes for which q is never beyond the boundary layer.

Congestion is at its worst during rush hour, when toll plazas serve as bottlenecks. But what do these congestion levels mean in total time through the plaza? Is the number of tollbooths optimal?

The Hiawassee M/L Toll Plaza in Florida uses a 4-tollbooth plaza. In October 2003, the Eastbound car count 7–8 A.M. was 3403 cars [Orlando–Orange County Expressway Authority 2003], so cars arrived at a rate of 0.945 cars/s/lane. With our assumption that a car is 17.5 ft long, clearly, four tollbooths are not enough to handle this heavy demand.

However, EZPass and other such programs allow one to minimize the time at a tollbooth. If even a small portion of the cars use the EZPass system, the value of q for which the boundary layer results grows vastly. If we were to accurately determine an optimal value of tollbooths for a certain value of q for a highway using such a system, we would have to approach the problem in a

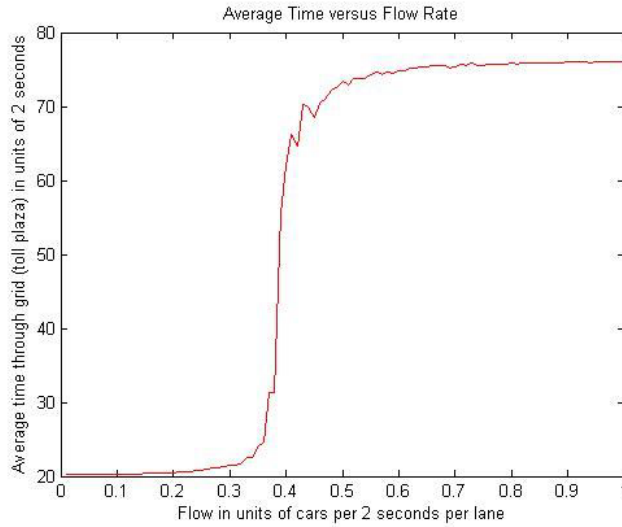


Figure 7. Average time through grid vs. flow rate.

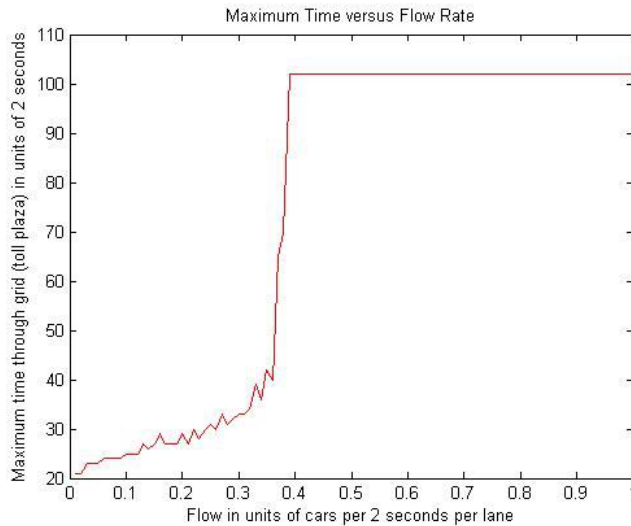


Figure 8. Maximum time through grid vs. flow rate.

slightly different fashion. In particular, we would have to vary the time drivers spend at the booth and designate certain lanes as having a quick pass system.

Case 2: More Tollbooths than Lanes

Preliminaries

The situation changes quite a bit if there are more tollbooths than incoming lanes. Drivers in the far left and right lanes start moving into the new tollbooth lanes. Hence, we introduce a new scheme, as presented in **Figure 9**.

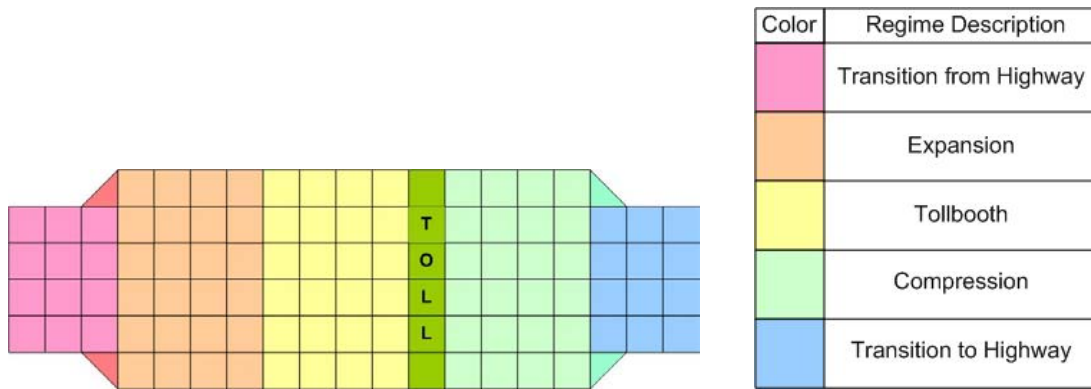


Figure 9. Possible regimes.

Movement in the Expansion Regime

The expansion regime is where the incoming traffic lanes fan out to a greater number of tollbooth lanes. For the center lanes, movement is identical to the transition regimes. On the outer lanes, however, movement is slightly different. The movement possibilities are outlined in Figure 10.

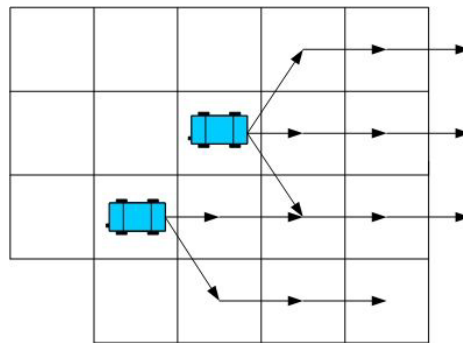


Figure 10. Movement in the expansion regime.

For a driver in the outside lane, the optimal maneuver is to move into one of the newly-created tollbooth lanes, unless the congestion is less in the current lane. Another new addition is that the driver will not try to move into one of the inner lanes—more for psychological reasons than practical reasons. According to the model, the driver assumes that the outside lanes are the least dense (and fastest), since they did not exist on the highway. Drivers on the newly created lanes are allowed to move only forward in our model. While a driver may move to an outside lane just to move back again, we consider the chance of this occurring as very slim.

Movement in the Compression Regime

The compression regime is where a greater number of tollbooth lanes collapse onto a smaller number of highway lanes. We have the movement possibilities presented in Figure 11.

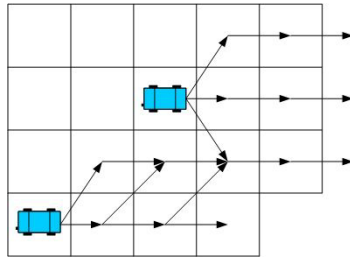


Figure 11. Movement in the compression regime.

A driver in a tollbooth lane that is a highway lane follows the same rules as in the earlier tollbooth regime. A driver not in a highway lane, however, tries to move back onto a highway lane; if this is not possible, they keep driving forward and trying again until they are forced to stop at the end of the tollbooth lane. This protocol can provide for some hectic situations.

Results

We simulate our second model for varying values of q for 4 highway lanes with 5 and 6 tollbooths. The range for q is the same as our first model. Figures 12–13 show the results for these two cases, for which we take the expansion and compression regimes to be 125 ft long.

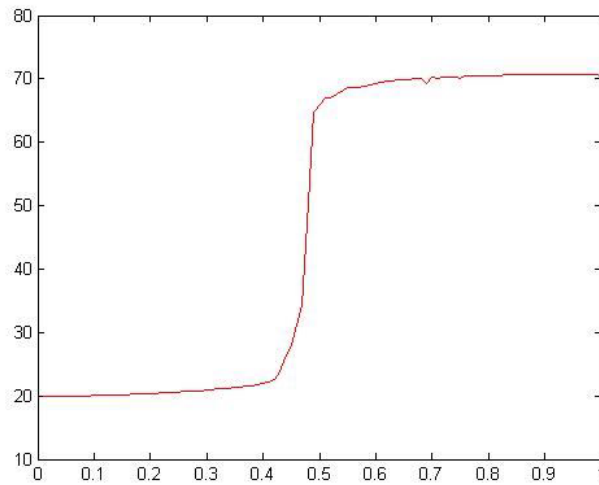


Figure 12. Average time through grid vs. flow rate, for 6 lanes.

The boundary layer is moved to the right as the number of toll lanes increases. Furthermore, the value for q on the right side of the boundary layer decreases with more toll lanes. Thus, as suggested, one should choose a sufficient number of lanes that correlates to this behavior. If the maximum flow rate one expects is a certain value, one can run a simulation for a certain number of

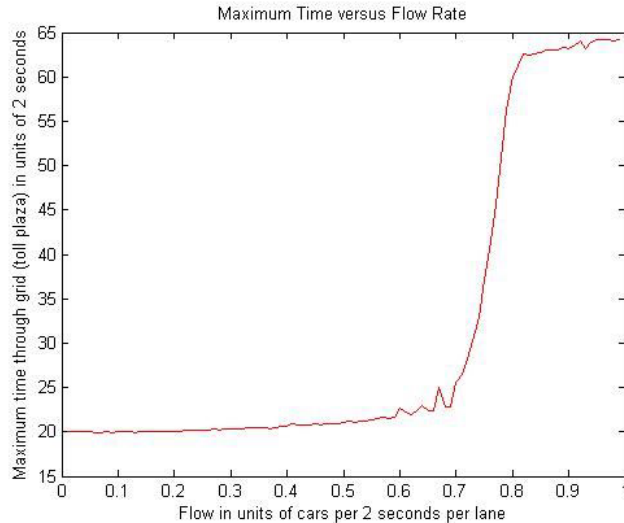


Figure 13. Average time through grid vs. flow rate, for 6 lanes.

tollbooths and choose the least number of tollbooths such that the maximum flow is to the left of the boundary layer.

However, with an increased number of lanes comes an increased maximum individual travel time: At times, people become stuck in the toll lanes and have to wait for an opportune moment to move over. In our model, this is reflected in the fact that while the four-tollbooth case results in a maximum travel time of about 3.4 min, the 5- and 6-lane cases sometimes have a maximum individual travel time near 4 min.

Model Improvements and Discussion

Drivers do not always move in a predictable manner. A probabilistic model taking into account the unpredictable nature of humans could further improve our model.

Our model also does not take into account the possibility of accidents. An accident model would surely improve our model.

While we do take into account the random nature of incoming traffic flow, we could develop an even better model to approximate the flow rate.

Lastly, our model could include a probabilistic model for the time that a car waits at a tollbooth.

Conclusion

We develop a quasi-SCA model for toll plaza dynamics that treats time and space in a discrete manner to capture the motivation and actions of drivers. We use a negative exponential distribution for the incoming flow rate of cars. We compute the average waiting time for different traffic flow rates.

At a certain flow rate, there is a boundary layer at which travel time increases sharply with flow rate. Thus, an optimal solution to the tollbooth problem is to choose the minimum number of tollbooths such that the expected rate of incoming flow corresponds to a point before the boundary layer.

References

- Aston, Winifred. *The Theory of Traffic Flow*. 1966. New York: John Wiley & Sons Inc.
- Campbell, Paul (ed.). 1999. Special Issue: The 1999 Mathematical Contest in Modeling. *The UMAP Journal* 20 (3). Lexington, MA: COMAP.
- _____. 2000. Special Issue: The 2000 Mathematical Contest in Modeling. *The UMAP Journal* 21 (3). Lexington, MA: COMAP.
- Chao, Xiuli. n.d. Design and evaluation of toll plaza systems. <http://www.transportation.njit.edu/nctip/finalreport/TollPlazaDesign.htm>.
- TranSafety Inc. 1997. Designing traffic signals to accommodate pedestrian travel. <http://www.usroads.com/journals/p/rej/9710/re971002.htm>.
- Drew, Donald. 1968. *Traffic Flow Theory and Control*. New York: McGraw-Hill.
- Edie, A.C. 1954. Traffic delays at tollbooths. *Journal of Operations Research Society of America* 2: 107–138.
- Hristova, Hristina. n.d. Lecture Notes. MIT OpenCourseWare. <http://ocw.mit.edu/0cwWeb/Mathematics/18-306Spring2004/LectureNotes/>.
- Jiang, Henry. 2003. Traffic flow with cellular automata. NKS SJSU (A New Kind of Science at San Jose State University). <http://sjsu.rudyrucker.com/~han.jiang/paper/>.
- Nagel, Kai, Dietrich Wolf, Peter Wagner, and Patrice Simon. 1998. Two-lane traffic rules for cellular automata: A systematic approach. *Physical Review E* 58-2 (August 1998). <http://www.sim.inf.ethz.ch/papers/nagel-etc-2lane/nagel-etc-2lane.pdf>.
- Orlando–Orange County Expressway Authority. 2003. Mainline plaza characteristics. <http://www.expresswayauthority.com/assets/STD&Stats%20Manual/Mainline%20Toll%20Plazas.pdf>.
- Rauch, Erik. 1996. Locality. <http://www.swiss.ai.mit.edu/~rauch/dapm/node1.html>.
- Sveshnikov, A.A. 1968. *Problems in Probability Theory, Mathematical Statistics, and Theory of Random Functions*. New York: Dover Publications.
- Tosic, Predrag and Gul Agha. n.d. Concurrency vs. sequential interleavings in 1-D threshold cellular automata. <http://osl.cs.uiuc.edu/docs/ipdps04/ipdps.pdf>.

Traffic simulations with cellular automaton model. April 30, 2000. <http://www.newmedialab.cuny.edu/traffic/gridCA1/sld001.htm>.

Wainer, Gabriel, and Norbert Giambiasi. n.d. Timed cell-DEVS: Modeling and simulation of cell spaces. <http://www.sce.carleton.ca/faculty/wainer/papers/timcd.PDF>.

Wikipedia. 2005. Toll roads. <http://en.wikipedia.org/wiki/Tollroad>. Accessed 2 February 2005.

_____. 2005. Traffic congestion. <http://www.answers.com/traffic+congestion&r=67>. Accessed 2 February 2005.

Wolfram, Steven. 2002. *A New Kind of Science*. Canada: Wolfram Media Inc.



John Evans, Peter Kramer (advisor), and Meral Reyhan.

The Multiple Single Server Queueing System

Azra Panjwani

Yang Liu

HuanHuan Qi

University of California, Berkeley
Berkeley, CA

Advisor: Jim Pitman

Summary

Our model determines the optimal number of tollbooths at a toll plaza in terms of that minimizing the time that a car spends in the plaza.

We treat the toll collection process as a network of two exponential queueing systems, the Toll Collection system and the Lane Merge System. The random, memoryless nature of successive car interarrival and service times allows us to conclude that the two are exponentially distributed.

We use properties of single server and multiple server queueing systems to develop our Multiple Single Server Queueing System. We simulate our network in Matlab, analyzing the model's performance in light, medium, and heavy traffic for tollways with 3 to 6 lanes. The optimal number of tollbooths is roughly double the number of lanes.

We also evaluate a single tollbooth vs. multiple tollbooths per lane. The optimal number of booths improves the processing time by 22% in light traffic and 61% in medium traffic. In heavy traffic, one tollbooth per lane results in infinite queues.

Our model produces consistent results for all traffic situations, and its flexibility allows us to apply it to a wide range of toll-plaza systems. However, the minimum time predicted is an average value, hence it does not reflect the maximum time that an individual may spend in the network.

General Definitions

The Network: The point at which the car enters the queue for toll collection to the point at which the car is able to drive off with current traffic speed. It consists of two systems of queues.

Toll-Collection System: The point at which cars arrive at the toll-plaza and form queues to the point at which they exit the booth after toll collection.

Lane Merge System: The point at which cars leave the tollbooth to enter the queue to merge back into the tollway lanes, to the point at which they can drive off with current speed.

Single Server Queueing System: A system with one queue and one server.

Multiple Server System: A system with one queue and multiple servers such that a customer has the freedom to choose any server available.

Arrival rate: The number of cars per minute per lane that arrive to a network or system.

Departure rate: The number of cars per minute per lane that depart from a network or system.

Service or processing: The act of toll collection.

Service rate: The number of cars per minute per booth being served.

Merge rate: The number of cars per minute per lane that merge back into the tollway lanes.

Total time: The time for a car to pass through the network.

Optimal time: The minimum feasible total time.

Idle time: The time interval during which the attendant is not serving anyone.

General Assumptions

- Car arrival times are independent, identically distributed non-negative random variables.
- Cars are served first-come-first-served.
- The service times for individual cars are independent, identically distributed nonnegative random variables with no correlation to the arrival process.
- In the long run, the rate at which cars are served is greater than the rate at which cars enter the network; otherwise, there would be infinite queues.

- There is no limit to the number of cars that can enter the network, because from the point of view of the network, the road length is arbitrarily large.
- Motorists tend to join the shortest queue in vicinity; hence, in the long run, the queue length is about the same at every tollbooth.

Table 1.
Table of variables.

Variable	Descriptions
S	The network of the Toll Collection System and the Lane Merge System
S_1	The Toll Collection System
S_2	The Lane Merge System
λ_1	Average car arrival rate per lane to the S_1 queue
λ_2	Average car arrival rate per lane to the S_2 queue
μ_1	Average service rate per lane in S_1
μ_2	Average merge rate per lane in S_2
W	Total expected time spent by a car in S
W_1	Expected time spent by a car in S_1
W_2	Expected time spent by a car in S_2
ℓ	Average length of a vehicle and the safety distance in front of it
ν	Traffic speed on the road, independent of tollbooth collection
n	The number of lanes in a tollway before the toll plaza
m	Number of tollbooths in a toll plaza
k	Number of lanes in a tollway after the toll plaza

Our Approach

We assume that the cars arrive according to a Poisson process. The arrival of a car at a time t does not affect the probability distribution of what occurred prior to t ; hence the system is memoryless [Pitman 1993]. A driver’s decision to drive on a road at a particular time is independent from that of any other driver; so the time periods between successive arrivals of vehicles are independent exponential random variables. If the tollbooth attendant is idle, the driver “goes into service”; otherwise, the car joins the queue to be served.

Similarly, the server processes cars with successive service times also being independent exponential random variables. From probability theory, we know that the sum of two exponential random variables with rates λ and μ is another exponential random variable, with rate $\lambda + \mu$.

We apply the theory of exponential queueing systems to develop a model that predicts the value of m that minimizes W .

General Model

A queueing system often consists of “customers” arriving at random times to some facility where they receive service. They depart from the facility at the same rate at which they arrive. The network S consists of two systems, the toll-collection system, S_1 , where cars arrive and join the queue and the lane-merge system, S_2 , where people join the queue to receive the “service” of merging.

Multiple Single Server Queueing System

We employ queueing theory together with continuous-time Markov chains to build our Multiple Single Server Queueing System, based on the following reasoning.

When cars get to a toll barrier, they determine which queue to join. In theory, they can join the shortest queue. In practice, however, they are unlikely to change too many lanes to join a shorter queue if there are other cars on the road. In most cases, they are limited to entering the queue directly in front of them, or a queue to their immediate left and right. Furthermore, under the assumption that the queue lengths are approximately the same for all the queues, they are most likely to join the queue directly ahead.

The process is similar to a single-server queueing system, but the fact that they have somewhat of a choice in choosing the tollbooth also gives this process properties of a multiple server queueing system. However, multiple-server queueing systems allow for only one queue and the freedom to choose any server that is not occupied. Our system does not fall exactly under either one of the two categories; hence, we coin the name “Multiple Single-Server Queueing System” for the systems in our network, which has the following properties:

- It consists of several parallel single-service queues.
- Each queue has a “super server” that has a processing rate of $\mu_1 \times m/n$.

In **Figure 1**, each colored box represents the probability that a car in a lane uses a tollbooth of that color. The bigger the box, the higher the chance of choosing that tollbooth. Most drivers use the tollbooth right ahead of them, though a few would choose the tollbooth to the left or right (with equal probability). The probability that a car uses a tollbooth that farther away is negligible. As we can see from **Figure 1**, the total areas of all the colored boxes representing the probabilities of going through the tollbooths are eventually the same from lane to lane. This implies that the service rate is the same for every tollbooth. Hence, in the long run, each lane is processed at the rate $\mu_1 \times m/n$.

Similarly, the process of waiting in a queue to merge back into the k lanes of the tollway after paying the toll can also be considered as a Multiple Single-Server Queueing System with processing rate $\mu_2 \times k/m$. To allow for more flexibility in our model, k may or may not equal n .

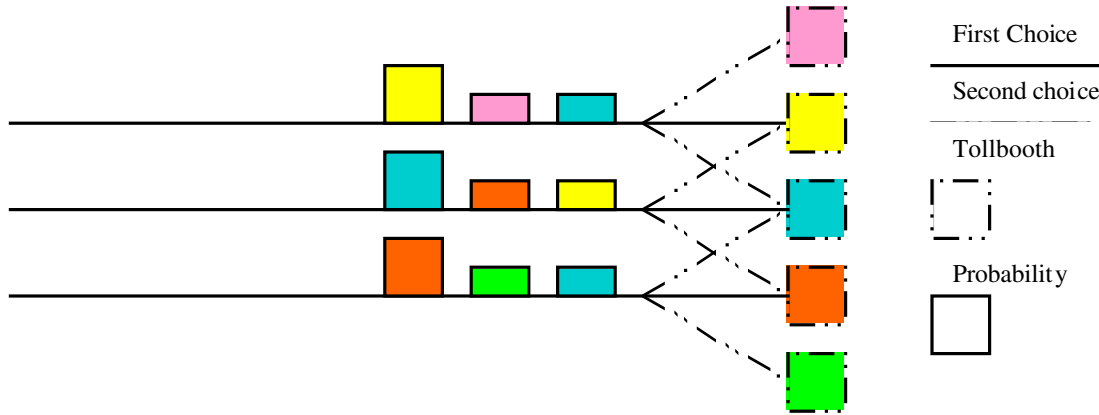


Figure 1. Each lane has equal probability over all cars.

Model Development

The total waiting W is the sum of the times to pass through the two systems, i.e., $W = W_1 + W_2$.

Based on the queueing theory equation [Ross 2003]

$$W = \frac{1}{\mu - \lambda},$$

and the discussion of service rates, we find

$$W = W_1 + W_2 = \frac{1}{\frac{m\mu_1}{n} - \lambda_1} + \frac{1}{\frac{k\mu_2}{m} - \lambda_2}.$$

Derivation of the Service Rates

We assume that on average each tollbooth attendant takes a fixed amount of time t to collect a toll, so $\mu_1 = 1/t$.

For heavy traffic situations, we also take into account driver reaction time r before stepping on the gas and moving up to the booth. We incorporate this delay into the service time to get

$$\mu_1 = \frac{1}{t + r}.$$

We estimate $t \approx 5.5$ s and $r \approx 2.5$ s.

Calculating μ_2 is a little trickier. We take into account ν , which we consider to be determined independently from the toll plaza system. This is justifiable, since whether a toll plaza interrupts a tollway or not, ν varies considerably depending on different traffic situations. Since ν is in miles per hour, and we're interested in cars per minute, we first transform the velocity into meters per minute. We also consider the fact that the car is going from 0 mph to get up to

ν , hence we use the average speed of the car during the time that it must catch up to the tollway traffic. We then divide the velocity by ℓ , which depends on ν , because the safety distance needed for cars at high speed is much greater than that for low speeds. Thus, we obtain

$$\mu_2 = \frac{\nu}{2\ell}.$$

Since cars from the m lanes of the toll plaza must merge back into the k lanes of the highway, we calculate the overall merge rate per lane, $\mu_2 \times k/m$, as described earlier, to be

$$\frac{k}{m} \frac{\nu}{2\ell}.$$

Derivation of the Second Arrival Rate

Since drivers join S_2 as soon as they depart S_1 , the rate λ_2 is the same as the departure rate from S_1 . Now, consider the departure rate from S_1 . If there are n lanes in the system and $n\lambda_1 \geq m\mu_1$, then all m servers are busy. Since each server works at rate μ_1 , the total departure rate is $m\mu_1$. On the other hand, if $n\lambda_1 < m\mu_1$, then only n servers are busy and the total departure rate is $n\lambda_1$. Since cars emerging from the tollbooth must merge into k lanes in S_2 , each of which has arrival rate λ_2 , we have

$$k\lambda_2 = n\lambda_1 \implies \lambda_2 = \frac{n\lambda_1}{k}.$$

Final Formula

Based on the discussion above, we get

$$W = W_1 + W_2 = \frac{1}{\frac{m\mu_1}{n} - \lambda_1} = \frac{1}{\frac{k\nu}{2m\ell} - \frac{n\lambda_1}{k}}.$$

Since the problem statement stipulates that under most situations $k = n$, we simplify this formula to

$$W = W_1 + W_2 = \frac{1}{\frac{m\mu_1}{n} - \lambda_1} = \frac{1}{\frac{n\nu}{2m\ell} - \lambda_1}.$$

The Range of Feasibility

Our model can calculate the optimal number of tollbooths needed only if the denominators for both W_1 and W_2 are greater than zero. Therefore,

$$\frac{m}{n} \mu_1 > \lambda_1 \quad \text{and} \quad \frac{n}{m} \frac{\nu}{2\ell} > \lambda_1.$$

Hence the feasible range for the number of tollbooths is

$$\left(\frac{\lambda_1 n}{\mu_1}, \frac{n\nu}{2\lambda_1 \ell} \right).$$

For a single tollbooth per lane, we set $m = n$; the resulting W is

$$W = W_1 + W_2 = \frac{1}{\mu_1 - \lambda_1} = \frac{1}{\frac{\nu}{2\ell} - \lambda_1}.$$

The model is still a system of two queues. Though the merge factor n/m is diminished, the cars must still catch up to traffic speed and may have to wait in a queue to do so.

Data Analysis

We implement our algorithm for W in Matlab using $n = 3, 4, 5,$ and 6 , corresponding to most tollways. We vary λ_1 from 0.5 to 5 cars/minute for light traffic, from 5 to 10 cars/minute for medium traffic, and from 10 to 15 cars/minute for heavy traffic. We establish the range of feasibility for m for each traffic situation. We then determine the number that gives minimal W .

Parameter Values

We set $\mu_1 = 11$ cars/min for the light and medium traffic; we set $\mu_1 = 7.5$ cars/min for heavy traffic, to account for the service time plus the reaction time of the cars waiting in queue.

To determine μ_2 , we set $\nu = 60$ mph for light traffic situations, since most heavily trafficked tollways have speed limits between 50 and 70 mph. We set $\nu = 46$ mph for medium traffic and $\nu = 32$ mph for heavy traffic. The average car length is between 3.5 and 5.5 m [Edwards and Hamson 1990], hence we set car length in our model to 4 m. We set the safety distance to 20 m for light traffic, 14 m for medium traffic, and 8 m for heavy traffic. The optimal number of tollbooths for the different levels of traffic and numbers of highway lanes are shown in **Table 2**.

Table 2.
Optimal numbers of tollbooths.

Traffic	Number of lanes			
	3	4	5	6
Light	5	7	9	10
Medium	5	9	9	11
Heavy	9	9	11	13

Regardless of the traffic level, the optimal number of tollbooths is always greater than the number of highway lanes. However, for light traffic, the difference between the average wait for optimal number of tollbooths vs. the average wait for $m = n$ is only about 2 s.

For medium traffic, though, the differences (≈ 15 s) are large enough to conclude that having extra tollbooths would be a wise decision.

For heavy traffic, setting single tollbooth per lane would result in infinite waiting queues for all situations examined.

Detailed Analysis of a Six-Lane Tollway

We conduct a detailed study for a six-lane tollway. The general trends observed for this dataset are typical for any number of lanes. We generate plots for the three traffic levels with number m of tollbooths as independent variable and W as dependent variable. We keep λ constant for each curve; hence we produce a set of level curves that show the optimal value for m based on the λ s.

As the traffic gets heavier, the region of feasibility for m gets smaller. This is because having too few tollbooths causes an infinite waiting time at S_1 , while having too many tollbooths causes an infinite wait at S_2 , due to the influx of cars processed in S_1 .

For light traffic, the difference in W_{ave} for $m = 5$ and $m = 18$ is merely 2 s. For medium traffic, a shift from the optimal number $m = 10$ causes a more dramatic increase in the time spent in the network. For heavy traffic, the range of feasibility reduces to a small region centered around the optimal number $m = 13$ —namely 12, 13, or 14 (**Figure 2**). The onset of heavy traffic both before and after the tollbooth excludes more extreme values of m from the feasible range. The beauty of the results is that the optimal number of tollbooths is the same for varying arrival rates.

Conclusion

It is better to have more than one tollbooth per lane. But having too many tollbooths per lane is just as bad. We recommend that for frequently traveled roads, the number of tollbooths available should be the maximum of all the optimal tollbooth numbers generated by our algorithm. The number of booths open can then vary for different traffic flows during the day.

For toll roads that usually have light traffic, having a single tollbooth per lane reduces the cost of building and running the toll plaza; reduction in waiting time does not justify more tollbooths.

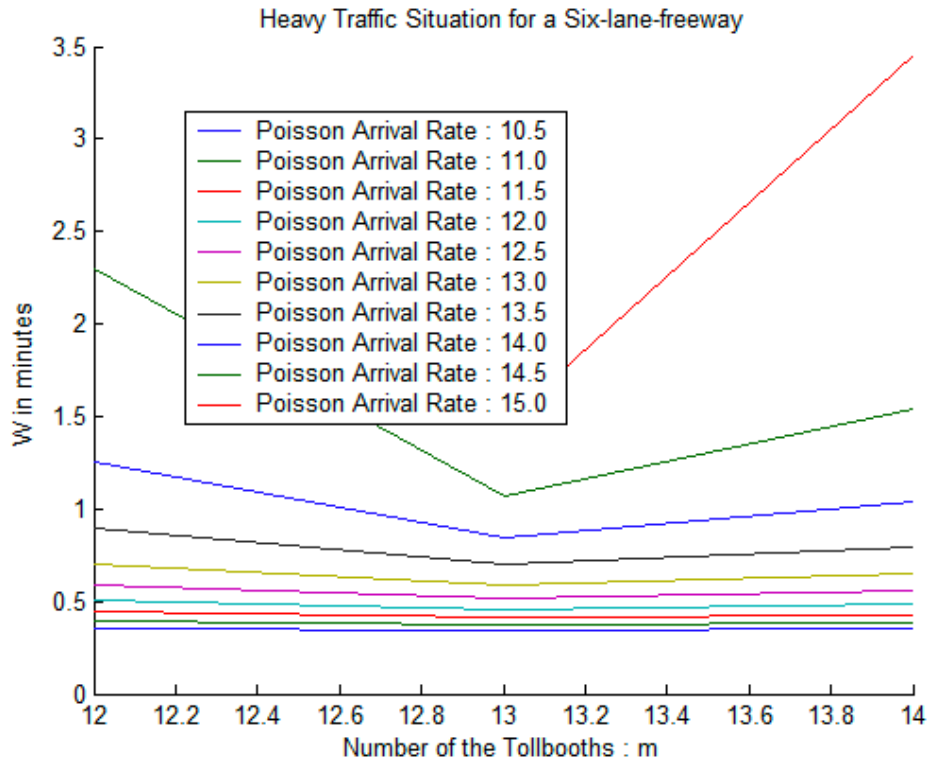


Figure 2. Wait vs. number of tollbooths for heavy traffic on a 6-lane tollway, for various arrival rates.

Strengths of Our Model

- Our model withstands many variations in parameters.
- Given reasonable values for the parameters, the algorithm generates realistic results for the optimal number of tollbooths.
- When we vary within the range of a specific traffic situation, the optimal solution is consistent for each in each situation.
- The optimal number of tollbooths differs among traffic levels, reflecting the fact that varying the number of tollbooths has a significant impact on waiting time.
- The algorithm, though rich in theory, is very easy to implement and test.

Weaknesses

- We assume that the arrival rate is less than the service rate at each system. In the long run, this assumption must hold in order to avoid infinite queues; but there can be intervals during when arrivals overwhelm the service rate.

Hence, though the average waiting time for the optimal solution may be small, the maximum waiting time for some cars may be rather large.

- Our model's range of feasibility is limited by the rates at which the cars are served at the two systems.
- Our model predicts the optimal tollbooth numbers based on the minimal time, but this may not be the most cost-effective solution.
- We don't incorporate the electronic payment passes that many toll systems use to minimize waiting time.

References

Edwards, Dilwyn, and Mike Hamson. 1990. *Guide to Mathematical Modeling*. Boca Raton, FL: CRC Press.

Pitman, Jim. 1993. *Probability*. New York: Springer-Verlag.

Ross, Sheldon M. 2003. *Introduction to Probability Models*. San Diego, CA: Academic Press.



Azra Panjwani, Jim Pitman (advisor), HuanHuan Qi, and Yang Liu.

Two Tools for Tollbooth Optimization

Ephrat Bitton

Anand Kulkarni

Mark Shlimovich

University of California, Berkeley

Berkeley, CA

Advisor: L. Craig Evans

Summary

We determine the optimal number of lanes in a toll plaza to maximize the transit rate of vehicles through the system. We use two different approaches, one macroscopic and one discrete, to model traffic through the toll plaza.

In our first approach, we derive results about flows through a sequence of bottlenecks and demonstrate that maximum flow occurs when the flow rate through all bottlenecks is equal. We apply these results to the toll-plaza system to determine the optimal number of toll lanes. At high densities, the optimal number of tollbooths exhibits a linear relationship with the number of toll lanes.

We then construct a discrete traffic simulation based on stochastic cellular automata, a microscopic approach to traffic modeling, which we use to validate the optimality of our model. Furthermore, we demonstrate that the simulation generates flow rates very close to those of toll plazas on the Garden State Parkway in New Jersey, which further confirms the accuracy of our predictions.

Having the number of toll lanes equal the number of highway lanes is optimal only when a highway has consistently low density and is suboptimal otherwise. For medium- to high-density traffic, the optimal number of toll lanes is three to four times the number of highway lanes. Both models demonstrate that if a tollway has lanes in excess of the optimal, flow will not increase or abate.

Finally, we examine how well our models can be generalized and comment on their applicability to the real world.

Statement of Problem

We are asked for a model that determines the optimal number of tollbooths in a toll plaza located on an n -lane tollway. The two criteria that we use for evaluating optimality are total throughput in number of cars and average transit time for individual cars to pass through the plaza.

Definitions

Number of highway lanes, n : The number of lanes on the highway entering and leaving the plaza.

Number of transit lanes, m : The number of tollbooths and lanes in the toll plaza.

Entry zone: The m -lane region of the toll plaza between the entry tollway and the tollbooths.

Merge zone: The m -lane region of the toll plaza between the tollbooths and the exit tollway.

Flow or throughput, q : Number of cars per second which pass through a given point x in our system.

Backlog B : Number of queued cars waiting to enter the tollbooths or exit the plaza.

Tollbooth processing time, τ_i : The number of seconds required, on average, for a car to pull into, pay, and exit a tollbooth i .

Density $\rho(x)$: number of vehicles per square meter in a given region.

m^* : the optimal number of tollbooth lanes.

Bottleneck capacity, q_b : the maximum number of cars per second that can pass through a given bottleneck b .

Assumptions

- A toll plaza consists of n highway lanes diverging into m toll lanes and converging back into n highway lanes. The toll plaza is sufficiently long to permit cars to reach all of the m tollbooths.
- Each tollbooth controls one lane and can serve at most one car at a time.
- Exit from the tollbooths is not metered.

- Drivers seek to move through the toll plaza as quickly as possible while maintaining safety.
- Within the toll plaza, all vehicles move at the safest possible maximum speed for a given density, since drivers seek to avoid accidents.

Model Development

Motivations

There are two general approaches to modeling traffic motion:

Macroscopic approaches begin with some observations about aggregate traffic behavior and attempt to approximate traffic behavior as a continuous flow over some large region or large time period.

Microscopic approaches attempt to model driver and car behavior and use this information in aggregate as the basis for modeling the large-scale behavior of traffic.

The microscopic approach often hinges on a large number of parameters that may be difficult to model accurately. For example, driver decision-making strategies, driving styles, preferred following distances, and the physical parameters of individual vehicles are highly variable.

We first pursue the macroscopic approach. Such approaches are traditionally used for modeling traffic behavior over long stretches of highway, and to model traffic jams, so it may seem that such an approach is inapplicable to a setting where highway length is not large. However, there are two advantages:

- Properties that vary significantly between drivers and vehicles are averaged out if we let the system run for a sufficiently long time and it approaches a steady-state equilibrium.
- At equilibrium, we can use the total throughput of cars through the toll plaza over a given duration as a metric for the disruption it causes.

We construct a theoretical flow model of the tollbooth plaza to determine the effect of varying numbers of tollbooth lanes for given numbers of transit lanes, and use this to predict optimal conditions.

The downside of the macroscopic approach is that traffic flow is not necessarily continuous, so approximations made in the model may not reflect reality. The best way to check them is to contrast them with real traffic data. As a result, we eventually construct a full microscopic approach to generate realistic data to test our continuous model: We design a cellular-automata simulation, constructed with an independent set of driver behaviors, to verify our macroscopic model. To represent the effect of unknown variables, we introduce a small random component to the simulation.

Flow in the Plaza

Initial Observations and Conservation of Flow

We begin by defining the flow q of traffic as the number of cars per second to pass through a perpendicular cross-section across all lanes of the highway, dx . By definition, flow follows the equation

$$q = \rho v,$$

where v is the average vehicle speed and ρ is the average vehicle density.

Two bottlenecks limit the flow in every toll plaza: the first is at the tollbooths, caused by the time required for cars to stop and pay the toll, and the second occurs when the lanes exiting the tollgates merge back into the highway.

All traffic that enters the plaza must eventually exit the plaza. Treating the motion of vehicles through the plaza as a continuous flow of traffic, we can represent this fact with the following lemma.

Lemma. *For any given cross-sectional slice dx of the system,*

$$\int_{\text{all time}} (q_{\text{out}} - q_{\text{in}}) dx = 0.$$

Using the relation $q = \rho v$, we can arrive at the following relationship, following the method of Kuhne and Michalopoulos [2002, Ch. 5, 5–8]:

$$\frac{\partial \rho}{\partial t} + \frac{\partial q}{\partial x} = 0. \quad (1)$$

This is the conservation of traffic flow equation given by Kuhne and Michalopoulos [2002, Ch. 5, 5–8], among others.

Bottlenecking Constraints on Flow

Bottlenecks along the highway restrict the maximum rate of traffic flow, as described in the following theorem:

Bottleneck Theorem. *The flow of vehicles through any system void of sources and sinks is bounded by the minimum of the bottleneck capacities along the path.*

Proof: Suppose that the flow at some point dx along the highway is in excess of the maximum of all bottleneck capacities ahead of it, i.e.

$$q(x) > \max\{q_{\text{bottleneck}_1}, \dots, q_{\text{bottleneck}_i}\},$$

where i is the number of bottlenecks ahead of dx . Since in the steady-state model all points flow at the same rate, this would mean that $\max\{q_{\text{bottleneck}}\} = q(x)$, which is a contradiction. \square

This result is used several times in the construction of our model.

A Queueing Model Based on Flow

Since the rate of flow is constrained by the bottleneck of minimum capacity, it follows that the throughput is determined by the relative rates of the bottleneck at the tollbooths and at the point where the highway retreats back to its original size (i.e., the “merge point”).

This observation reduces the problem to examining throughput solely at the endpoints of the “problem zone,” without need to consider the behavior of traffic flow between those points. Thus, we can proceed simply by modeling the behavior of traffic at these two points.

Calculating Backlogs

We find the number of cars at each of these bottlenecks at any given time, so as to determine when a backlog occurs. For an arbitrary segment of the m -lane section of the toll plaza, we integrate the conservation of flow equation (1) with respect to x over the length of the road segment (with m lanes). This gives the instantaneous number of vehicles within the segment, $B(t)$:

$$B(t) = \int_x m\rho(x, t)dx.$$

From this we obtain the rate at which the backlog or pileup in the merge zone is growing:

$$\frac{dB(t)}{dt} = \begin{cases} q_{\text{arrival}} - q_{\text{departure}}, & \text{if } q_{\text{arrival}} > q_{\text{departure}}; \\ 0, & \text{otherwise,} \end{cases} \quad (2)$$

where q_{arrival} is the rate (in cars/s) at which cars enter the segment and $q_{\text{departure}}$ is the rate at which they are exit. It then follows that:

Theorem (Flow Equilibrium). *To prevent congestion from building at a bottleneck (i.e., to keep $B(t) = 0$) while maintaining maximum system throughput, it must be that*

$$q_{\text{arrival}} \leq q_{\text{departure}_{\text{max}}},$$

where $q_{\text{departure}_{\text{max}}}$ is the bottleneck capacity and thus the maximum system throughput.

Proof : Consider the following three possible cases:

Case 1: Let $q_{\text{arrival}} > q_{\text{departure}_{\text{max}}}$. Then by (2), the number of cars building up in the system will increase at a rate of $q_{\text{arrival}} - q_{\text{departure}} > 0$.

Case 2: Let $q_{\text{arrival}} < q_{\text{departure}_{\text{max}}}$. By (2), the rate of increase in the number of cars in the system is 0, and system throughput is q_{arrival} .

Case 3: Let $q_{\text{arrival}} = q_{\text{departure}_{\text{max}}}$. Similar to Case 2, a backlog does not grow, and the system throughput is q_{arrival} . Note that, however, q_{arrival} , and thus system throughput, is at a maximum while preventing congestion at the bottleneck; therefore, this is clearly the optimal case. \square

Applications to Toll Plaza System

Adapting this general result to our model, we define

q_{in_i} to be the flow in cars/second entering the system in lane i ,

q_{tolls_i} to be the flow or turnover rate of tollbooth i , and

q_{out_i} to be the flow leaving the system (at or after the merge point) in lane i .

Our model considers the interaction between the two bottlenecks. Upon investigation, two observations become apparent:

1. The maximum flow, q_{max} through a cross-sectional slice of the highway dx is independent of the road structure before that point. In other words, the maximum flow capacity is fixed solely by the number of lanes at that point and not the number of lanes merging or diverging into it.
2. The only cross-sectional slice dx at which the maximal flow can be varied (by the model) is at the tollbooths; this is done by changing the number of tollbooths, which directly results in a change in the number of cars that can be processed per unit time.

With this in mind we apply the Flow Equilibrium Theorem. We divide the system into two segments, the first from $(-\infty, x_{\text{tolls}})$ and the second from $(x_{\text{tolls}}, x_{\text{merge}})$, where x_{tolls} is the point x along the highway where the tollbooths are and x_{merge} is the point where the m lanes of the toll plaza merge into the n lanes of the highway.

The q_{arrival} of the first segment (into the tollbooths) is simply q_{in} , and $q_{\text{departure}} = q_{\text{tolls}}$. For the second segment, $q_{\text{arrival}} = q_{\text{tolls}}$ and $q_{\text{departure}} = q_{\text{out}}$.

Since $q_{\text{tolls}} = m/\tau$, only the number of tollbooths and their individual turnover rates τ determine the flow entering the merge zone. By observation (1), we note that the bottleneck capacity of the merge point, $q_{\text{out}_{\text{max}}}$, is independent of m and q_{tolls} ; it is merely a property of an n -lane highway.

We are therefore interested in how q_{tolls} affects the flow of cars through the merge zone. By observation (2), when $q_{\text{tolls}} > q_{\text{out}}$ the backlog increases at a rate of

$$\frac{dB(t)}{dt} = q_{\text{tolls}} - q_{\text{out}}.$$

The backlog continues to grow until the entire merge zone is filled, and then it spills out into the segment before the tolls. This buildup does not fully dissipate until q_{in} reduces to below $q_{\text{out}_{\text{max}}}$, or in other words, until the incoming flow

rate is below the bottleneck capacity of the tightest bottleneck (such as at the end of rush hour).

To prevent the occurrence of this effect, let $q_{\text{tolls}} \leq q_{\text{out}}$, which allows traffic to flow through the merge zone without causing backlog. However, when $q_{\text{tolls}} < q_{\text{out}}$, the merge point is not operating at maximum flow; therefore, letting $q_{\text{tolls}} = q_{\text{out}}$ is optimal. Surprisingly, however, we show later that this is actually a *lower bound* on q_{tolls} .

From this result, we get

$$q_{\text{out}} = nq_{\text{out}_{\text{max}}} = q_{\text{tolls}} = \frac{m^*}{\tau},$$

where m^* is the optimal number of tollbooths for an n -lane highway. Solving for m^* , we get

$$m^* = n\tau q_{\text{out}_{\text{max}}}.$$

Performance When the Number of Tollbooths Exceeds m^*

We now consider toll plaza performance when the number of tollbooths m exceeds the predicted optimum m^* . This investigation is necessary. For example, if our model were to predict m^* slightly above the actual value, a backlog would build within the merge zone, but it might build so slowly that by the time its size became critical, the rush-hour mass of vehicles would already have dissipated.

As previously shown, when $m > m^*$ and $q_{\text{in}} > q_{\text{tolls}_{\text{max}}}$, a backlog builds in the merge zone at a rate of $(q_{\text{tolls}_{\text{max}}} - q_{\text{out}})$. Until the merge zone fills completely with vehicles (when vehicle density is at a maximum), the tollbooths continue to process vehicles at their maximum rate, $q_{\text{tolls}_{\text{max}}} = m/\tau$. In this case, the backlog at the tolls grows at a rate of $(q_{\text{in}} - q_{\text{tolls}_{\text{max}}})$.

As a result, the effective backlog growth is the sum of the backlog growth rates at each bottleneck:

$$\begin{aligned} \frac{d}{dt} \text{backlog}_{\text{effective}} &= \frac{d}{dt} \text{backlog}_{\text{tolls}} + \frac{d}{dt} \text{backlog}_{\text{merge}} \\ &= (q_{\text{in}} - q_{\text{tolls}_{\text{max}}}) + (q_{\text{tolls}_{\text{max}}} - q_{\text{out}}) \\ &= (q_{\text{in}} - q_{\text{out}}). \end{aligned}$$

Interestingly, this result implies that the total backlog of the system is entirely dependent on the rate at which vehicles enter and the maximum rate at which they can leave (i.e., the bottleneck capacity of the tightest bottleneck). Therefore, as long as the tollbooths do not limit the total flow capacity of the system, the exact rate at which the tollbooths process vehicles does not affect the system flow. This line of reasoning leads us to the following theorem:

Theorem (Lower bound on m^*). *The optimal number of tollbooths for an arbitrary n -lane highway is greater than or equal to $m^* = n\tau q_{\text{out}_{\text{max}}}$.*

Maximum Flow on an n -Lane Highway

Garber and Hoel [1999] observe empirically an inverse relationship between ρ and v , and several models have been proposed to describe this behavior. It is generally accepted that any such model must exhibit the following properties:

- Flow is zero when density is zero.
- As density increases to some critical value, so does flow.
- Past this critical density the flow begins to decrease.
- Flow cannot decrease beyond some minimum value.

Let v_{\max} be the maximum velocity of cars traveling freely on the highway (generally the speed limit), and let ρ_{\max} be the maximum number of cars (i.e., jam-packed) per unit area of highway (a constant).

One of the more popular models, proposed by Greenshield [Garber and Hoel 1999], establishes a linear relationship between the two:

$$v = v_{\max} \left(1 - \frac{\rho}{\rho_{\max}}\right) \quad \Rightarrow \quad q = \rho v_{\max} \left(1 - \frac{\rho}{\rho_{\max}}\right),$$

where v_{\max} is the maximum speed at which cars tend to travel when flowing undisturbed along the highway, generally taken as the speed limit.

A second popular model, introduced by Greenberg [Garber and Hoel 1999], proposes a logarithmic relationship:

$$v = v_{\max} \ln \left(\frac{\rho}{\rho_{\max}}\right) \quad \Rightarrow \quad q = \rho v_{\max} \ln \left(\frac{\rho}{\rho_{\max}}\right). \quad (3)$$

While accurate in certain cases, these models do not seem to represent effectively the motion of cars through toll plazas, because they both model the flow as zero when density has reached its maximum. Although density will tend to some maximum, flow will asymptotically approach but never reach zero, since some number of cars will still flow out of the system over a long enough time interval. This discrepancy is a direct result of the limitations inherent in treating traffic as a continuous flow. Determining the precise relationship between ρ and v is a relatively complex modeling task beyond the scope of this paper, so we accept Greenberg's model with the restriction that if $\rho = \rho_{\max}$, flow will approach some low constant value instead.

To determine a rough estimate of the maximum flow through the merge point (or any n -lane highway for that matter), we use Greenberg's model. To find the maximum flow q_{\max} , we differentiate (3):

$$\frac{d}{d\rho} q(\rho) = v_{\max} \log \left(\frac{\rho_{\max}}{\rho}\right) - v_{\max} = 0$$

Solving for ρ , we get $\rho = \rho_{\max}/2$. Therefore, flow is maximized for density $\rho_{\max}/2$, which gives

$$q_{\max} = \frac{\rho_{\max} v_{\max}}{2}.$$

Streamlined Flow Model

We made the assumption in the previous section that flow is distributed uniformly among all lanes—that is, an equal number of cars pass through each lane per second. However, in real toll plaza systems there are conditions when this does not apply. For example, on New Jersey’s Garden State Parkway users are restricted to movement between sets of individual highway lanes, before and after the tollbooths, by lane dividers. As a result, sets of lanes operate independently of each other. Moreover, one or more lanes may be reserved for low-speed vehicles (recreational vehicles or large trucks) or high-speed traffic (electronic toll collection, motorcycles, buses, or carpools).

To generalize our model, we relax this assumption to account for varying flows between lanes of traffic. We divide the total flow through the tollbooths, and the total outgoing flow through the exit, into individual lane flows, so that

$$q_{\text{tolls}} = \sum_{i=1}^m q_{\text{tolls}_i}, \quad q_{\text{out}} = \sum_{j=1}^n q_{\text{exit}_j}.$$

As observed in the **Bottleneck Theorem**, no lane can flow faster than q_{max} . However, by conservation of traffic flow (1), total traffic flow through the system remains the same, even though streams of traffic may move at different rates.

We must also consider what happens when lanes merge towards the exit of the toll plaza. Whereas in the queueing theory model we were allowed to consider only the flow at two points— q_{exit} and q_{toll} —we must now also consider the flow rate at all points where two or more lanes merge into one.

The flow rate at a merge point can never exceed q_{max} , the maximum flow for a single lane. According to the results derived earlier in the basic model, the rate of flow through each lane equals the rate of the slowest bottleneck ahead. However, it is the *combined* rate of two merging lanes that exceeds the lane bottleneck, not each individual lane, so naively setting $q_{\text{in}} = q_{\text{max}}$ would incorrectly increase the rate of the premerged lane to match the bottleneck.

As a result, each lane can contribute at most a decreased quantity such that the sum of the two lanes equals the bottleneck capacity. A simple way to represent this behavior is to allow each to contribute a proportion of flow relative to their combined size:

$$q_{1\text{reduced}} = q_{\text{max}} \frac{q_1}{q_1 + q_2}, \quad q_{2\text{reduced}} = q_{\text{max}} \frac{q_2}{q_1 + q_2}.$$

Thus, when both flows would normally overfill the lane into which they merge, each lane’s contribution to that lane’s flow, q_{out} , will be proportional to its percentage of the total amount of flow present, without ever exceeding q_{max} .

This observation lends itself to a simple recursive function in modeling toll plaza traffic as an aggregate of independent flows. Therefore, predictions of system behavior with introduction of electronic toll collection lanes and other flow-monitored lanes are significantly simplified, by applying this model at all steps of the merging process (i.e., by first merging every set of two lanes, and then merging the following two, etc.).

Simulation

Motivations for a Discrete Simulation

To validate the continuous model, we create a discrete simulation using cellular automata to generate traffic behavior. Whereas our earlier models approximate car flux as continuous, the cellular automata simulation treats individual vehicles as distinct entities that behave according to well-defined simple rules. Since the discrete model is based on an independent set of intuitions about the system and how it behaves, any agreement between the two models will suggest a high degree of accuracy in our modeling efforts.

Overview

The simulation runs on a two-dimensional grid of points, each of which corresponds to a width and length slightly greater than the average car size. The simulation takes in parameters that determine the geometry of the toll plaza as well as a probability, p , that a car enters the toll plaza in a given lane. When populating the grid, each cell can be one of four types and behaves according to its corresponding set of rules:

Free: a transient place holder when block is unoccupied.

Barrier: a boundary point of the toll plaza; this cell never changes.

Toll block: a tollbooth.

Car: a cell occupied by a vehicle.

Rules of State Evolution

The rules that create the next generation of cells (next state of the grid) from time t to $t + 1$ are:

- All cars travel at a constant speed of 1 forward cell per time step.
- A car can change lanes and move forward on the next step if there is an open adjacent cell to its side and an open cell along the appropriate diagonal.
- A car can stay in the same lane if the cell ahead is free, if the car in front of it moves forward on that step, or if it is in front of the toll and its toll delay has expired.
- As the cells in the entry of the toll plaza are freed by the evolution of the grid, at each time step new cars arrive in these with probability p , the density of incoming cars.

Stochastic State Evolution

We use random variables to make the system nondeterministic. This more closely represents real-world simulations where exact car path is unpredictable and also attempts to account for the wide range of parameters relating to driver psychology, variations in vehicles, and variations in service time in paying the toll. To generate this effect, we implement the following rules:

1. Each toll processes a car at a random rate each time, with distribution centered at $\tau = 3$:

$$p(x) = \begin{cases} 0.25, & x \in \{2, 4\}; \\ 0.5, & x \in \{3\}. \end{cases}$$

2. Cars switch lanes at random with some assigned probability, but their decision is influenced by the desirability of the target lane.
3. The arrival of cars into a lane is a Poisson process with rate λ , a parameter to the simulation.

Reporting

We run the simulation for 1,000 time steps. It returns total car throughput, total waiting time, average waiting time, total transit time, and the density of cars in each section of the system (i.e., before, within, and after the toll plaza).

Sample simulation run

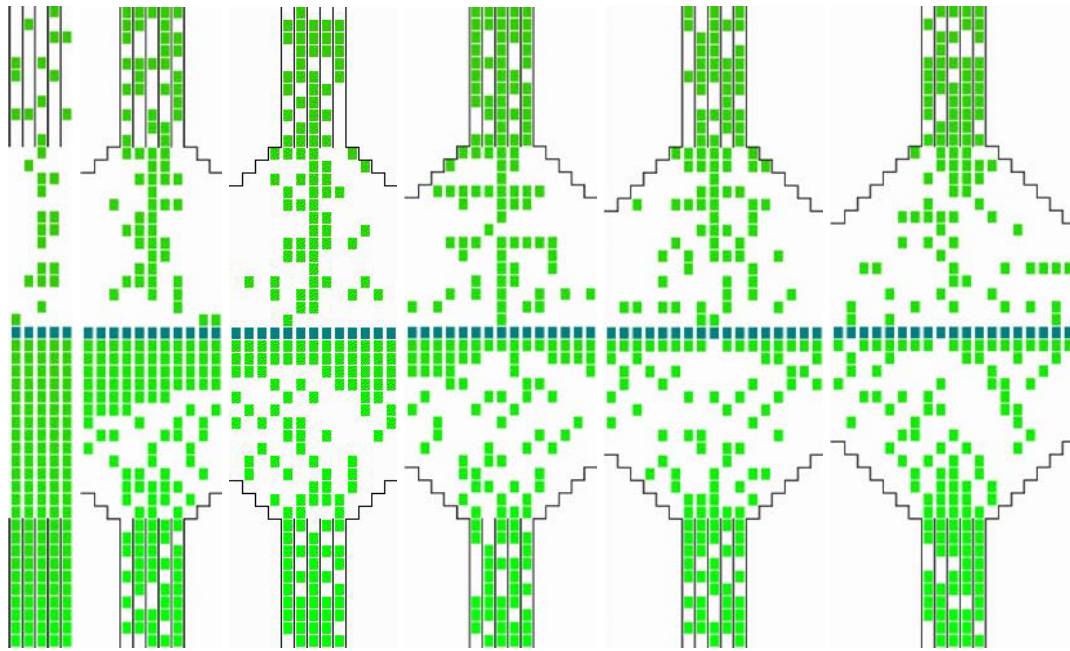
Cars are released at $t = 0$ and proceed toward the tollbooths. Upon entering the diverge zone, cars change lanes and spread out to minimize their total wait time at the tolls.

Depending on the number n of highway lanes and the number m of tollbooths, traffic eventually reaches an equilibrium flow, or else flow is reduced by the bottlenecks and backlog begins to grow. In our figures, the color of the vehicle designates the amount of time spent waiting in the system, with bright green the least, dark green moderate time, and bright red the most.

The model supports varying traffic density over time; we ran our simulations with arrival densities of 15%, 50%, and 85% percent.

Simulation Sample Images

Simulation sample activity is illustrated in **Figure 1**.



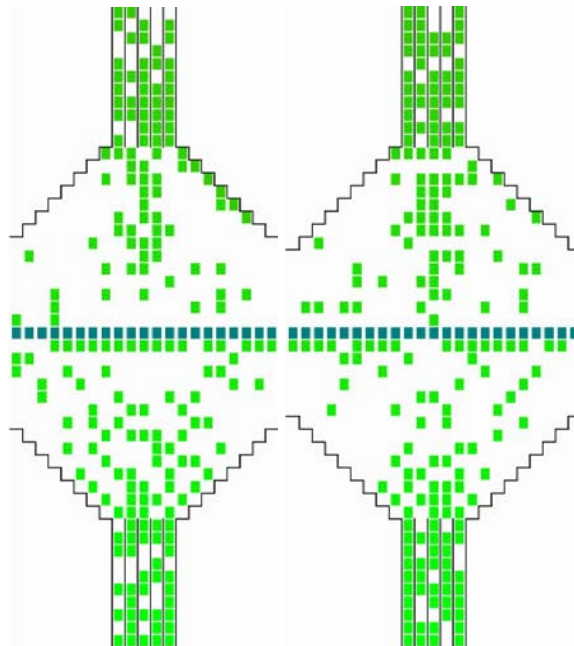
(a) m=5
(b) m=11

(c) m=13

(d) m=15

(e) m=17

(f) m=19



(g) m=21

(h) m=23

Figure 1. Simulation at step 1000 for $n=5$.

Running the Simulation

We ran the simulation for $t = 1000$ timesteps, with $\tau = 3$ steps, for all possible tollway sizes from $n = 1$ to $n = 8$, and for $m = n$ to $4n$ (for small n) or to $3n$ (for large n). For each highway size, we ran the simulation at 85%, 50%, and 15% density. We repeated this process 5 times for the sake of statistical significance. For a timestep of 1 s, a single run of the simulation corresponds to about 17 min of traffic.

Over each set of conditions, we track the total throughput of cars. We then compare the throughput achieved using m tollbooth lanes on a given n -lane tollway over the entire 1000-s period.

Results and Analysis

Model Predictions vs. Simulation Results

To compare further the accuracy of our theoretical model and our discrete simulation, we compare experimental data collected from the simulation with our model's predictions for the corresponding number of highway lanes n . To do this, we must make the following parameter assumptions.

- The average vehicle length plus its separation distance from the vehicle ahead of it is approximately 15 ft.
- At high density, vehicles travel in the merge zone on average at 15 mph.
- In correspondence with the simulation, the average processing time at the tolls is $\tau = 3$ s/car.

Computing the model's predictions based on these parameters and running the simulation for from one to seven highway lanes yields the results in **Table 1**. The values for m^* are the minimum values for which adding additional lanes does not alter performance significantly. [EDITOR'S NOTE: The experimental graphs used to derive these values are omitted here.]

Figure 3 shows that our flow model is validated as an accurate long-term predictor of traffic behavior for high density scenarios ($p = .85$). We believe that the difference between the continuous model prediction and the observed value in the simulation stems from uncertainty in the value of the parameter q_{\max} . Our prediction of $q_{\max} = 4$ was accurate only for the high-density case. For the low-density case, we almost never experience the conditions caused by q_{\max} —clogging at the merge points—and so our model does not apply. The continuous flow model does not apply when traffic flow has significant variations in speed, when density cannot be considered a regular flow.

Our flow model accurately predicts the observed optimum to within 3 lanes for high-density traffic. From this, we see a high level of agreement between

Table 1.

Experimentally observed optimal number of lanes for various traffic densities vs. predicted optimal number $[m^*]$ of lanes. There is a rough one-to-four relationship between the number of highway lanes and the optimal number of tollbooths.

Highway lanes	Simulation density ρ			$[m^*]$
	.15	.50	.85	
1	1	4	5	4
2	2	6	10	8
3	3	9	13	12
4	4	10	16	16
5	5	13	18	20
6	6	14	21	24
7	7	16	25	28

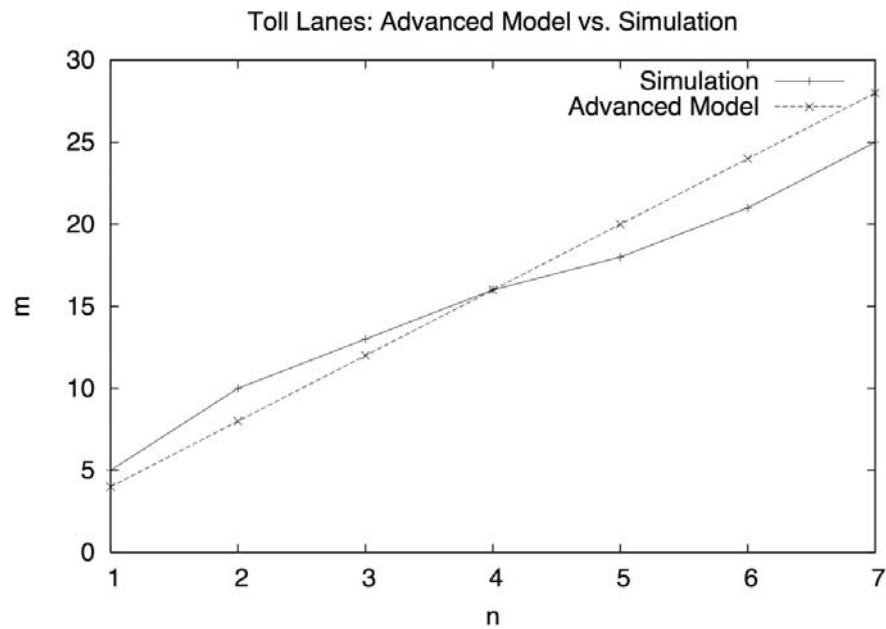


Figure 3. Observed optimal number m^* of toll lanes for given number n of highway lanes.

the two models, even though they operated on completely independent assumptions. These results suggest that our model predicts the optimal number of tollbooths for an arbitrary n -lane tollway fairly accurately.

Total Throughput vs. Average Wait Time

For every simulation that we ran, whenever throughput is higher or lower for a given pair of (m, n, ρ) , average transit time is correspondingly higher or lower. We conclude that total throughput and average wait time are highly correlated. As a result, optimizing either of them results in good performance relative to the other criterion.

Accuracy of Simulation

Sensitivity of Parameters

We examine the effect of changing parameters. Altering the processing time τ , length of the tollway, length of the merging area, and the probability distribution for random behavior all affect the absolute throughputs achieved for different numbers of tollbooths—but do not affect the optimal number of lanes.

The only parameter with a significant effect on the optimal number of lanes is length of the merging area when set to an extremely low value, so that cars couldn't switch lanes in time to utilize all of the lanes. However, this condition contradicts an initial assumptions of our model and condition is unlikely to occur in the real world.

Our simulation is therefore very robust with respect to parameter variation.

Faithfulness to Real-World Behavior

We use the cellular automata simulation to validate the effectiveness of the flow model; however, this verification is only accurate to the extent that the cellular automata is a realistic description of real-world traffic flow through tollbooths.

To validate our simulation, we examine real-world flow rates of the Union toll plaza of the Garden State Parkway at several peak flow times, where $n = 5$ and $m = 13$ [New Jersey Institute of Technology 2001, 11]. Examining the seven hours of data, we arrive at a throughput of 2393 cars/hr; our model predicts 2530 cars/hr. Our simulation matches the empirical results surprisingly well for peak density.

According to our simulation, the Garden State Parkway's performance is fairly suboptimal. The best results, according to the simulation, are obtained

for $m = 20$ tollbooth lanes, enabling an increase in average throughput by almost a factor of two.

Extensions of Base Model

Electronic Toll Collection

Under electronic fare payment systems such as Fastrack and EZ-Pass, drivers attach an electronic device to their vehicles, which is scanned automatically as they pass through a special tollbooth lane with little or no reduction in speed.

Both our model and simulation can analyze inclusion of special “fastlanes.” In the streamlined-flow model, fastlanes are simply lanes with a much higher rate of flow q_{toll_i} through the tollbooth. Since congestion still occurs later as a result of the narrow bottleneck caused by merges and q_{max} , fast progress may still be impeded by slow merging. This possibility explains the common practice of having separate fastlane toll lanes running alongside the outside of the toll plaza, so that merging happens far enough down the road.

Because merge rates are proportional to ratio of the rates of the lanes merging and the maximum possible rate, we have that

$$q_{\text{fastlane-at-mergpoint}} = q_{\text{max}} \left(\frac{q_{\text{fastlane}}}{q_{\text{fastlane}} + q_{\text{other}}} \right).$$

Since q_{fastlane} is potentially much greater than q_{other} , cars in the fastlane flow at a rate close to the maximum. As a result, users who choose a fastlane still move through the toll plaza faster than other cars, even when forced to merge with slower traffic. The more use of fastlanes, the higher overall average throughput, and the recommended number of toll lanes for regular use can drop.

Final Recommendations

- Our model predicts that the findings in **Table 1** provide the best results for high-density situations. For traffic density at or above 85% of the maximum bumper-to-bumper density, our model should be used. Lanes can be closed when density is lower.
- Our model provides a lower bound on the recommended number of tollbooth lanes. Running more tollbooth lanes than the optimal predicted value does not hinder throughput.
- The case $m = n$ suffices exactly when a road has consistently low-density traffic. For medium- and high-density traffic, this case causes suboptimal performance.

Model Assessment

Model Strengths

- The discrete and continuous models agree well at peak densities.
- We generate plausible traffic behavior through partially random behavior in our models. In particular, our models match well effects we observe in the Union toll plaza of the Garden State Parkway.
- Our model can scale successfully to represent the impact of electronic toll-taking and variable tollbooth speeds.

Model Weaknesses

- The primary shortcoming of the theoretical model is the assumption that car flux is continuous. Fractional values of car flux do not realistically represent low-density traffic.
- Our model is too sensitive to variations in the average amount of time to process a car at the tolls.
- The simulation accounts for many unknown factors with random choices. Validation of our model is accurate only insofar as this randomness accurately reflects driver behavior.
- We don't consider cost as a component of our solution.

References

- Garber, Nicholas J., and Lester A. Hoel. 1999. *Traffic and Highway Engineering*. Pacific Grove, CA: Brady/Cole Publishing Company.
- Jiang, Rui, and Qing-Song Nu. 2003. Cellular automata for synchronized traffic flow. *Journal of Physics A: Mathematical and General*.
- Kuhne, R.D., and Panos Michalopoulos. 2002. *Revised Monograph on Traffic Flow Theory: Flow Models*. Turner-Fairbank Highway Research Center.
- Mihaylova, Lyudmila, and Rene Boel. 2003. Hybrid stochastic framework for freeway traffic flow modeling. *ACM Proceedings of the 1st International Symposium on Information and Communication Technologies*.
- New Jersey Institute of Technology. 2001. *Ten Year Plan to Remove Toll Barriers on the Garden State Parkway*.
- Rastorfer, Robert L., Jr. 2004. Toll plaza concepts. ASCE Fall Conference, Houston, TX.



L. Craig Evans (advisor), Anand Kulkarni, Ephrat Bitton, and Mark Shlimovich.

For Whom the Booth Tolls

Brian Camley
Bradley Klingenberg
Pascal Getreuer
University of Colorado
Boulder, CO

Advisor: Anne Dougherty

Summary

We model traffic near a toll plaza with a combination of queueing theory and cellular automata in order to determine the optimum number of tollbooths. We assume that cars arrive at the toll plaza in a Poisson process, and that the probability of leaving the tollbooth is memoryless. This allows us to completely and analytically describe the accumulation of cars waiting for open tollbooths as an $M|M|n$ queue. We then use a modified Nagel-Schreckenberg (NS) cellular automata scheme to model both the cars waiting for tollbooths and the cars merging onto the highway. The models offer results that are strikingly consistent, which serves to validate the conclusions drawn from the simulation.

We use our NS model to measure the average wait time at the toll plaza. From this we demonstrate a general method for choosing the number of tollbooths to minimize the wait time. For a 2-lane highway, the optimal number of booths is 4; for a 3-lane highway, it is 6. For larger numbers of lanes, the result depends on the arrival rate of the traffic.

The consistency of our model with a variety of theory and experiment suggests that it is accurate and robust. There is a high degree of agreement between the queueing theory results and the corresponding NS results. Special cases of our NS results are confirmed by empirical data from the literature. In addition, changing the distribution of the tollbooth wait time and changing the probability of random braking does not significantly alter the recommendations. This presents a compelling validation of our models and general approach.

Introduction

A toll plaza creates slowdowns in two ways:

- If there are not enough tollbooths, queues form.
- If there are too many tollbooths, a traffic jam ensues when cars merge back onto the narrower highway.

We use queueing theory to predict how long vehicles will have to wait before they can be served by a tollbooth. Using cellular automata to model individual cars, we confirm this prediction of wait time. This vehicle-level model is used to predict how traffic merges after leaving the toll plaza.

Initial Assumptions

- **The optimal system minimizes average wait time.** We do not consider the cost of operating tollbooths.
- **Cars arrive at the toll plaza uniformly in time** (the interarrival distribution is exponential with rate λ). We can consider rush hour by varying the arrival rate λ .
- **Cars have a wait time at the tollbooth that is memoryless** (exponential distribution with rate μ). This assumption is confirmed by the study of tollbooths by Hare [1963].
- **Cars are indistinguishable.** All cars have the same length and the same maximum speed.
- **The toll plazas are not near on-ramps or exits.** We do not consider the possibility of additional cars merging, only those that were already on the main road.
- **Two-way highways are equivalent to two independent highways.** We consider only divided highways.

Delays Due to Too Few Tollbooths

Tollbooths As an $M|M|n$ Queue

As a vehicle approaches the toll plaza, it has a choice of n tollbooths for service. Cars tend toward the shortest queue available. We simplify this behavior by supposing that all vehicles form a single queue, and that the next car in line enters a tollbooth as soon as one of the n booths becomes available. A

real system would be less efficient, and therefore we expect longer times in a more detailed simulation.

We assume that vehicles arrive uniformly distributed in time. We additionally suppose that the length of service time is exponentially distributed as in Hare [1963]. This class of model is called a *memoryless arrivals, memoryless service times, n-server* or “M|M|n” queue (**Figure 1**).

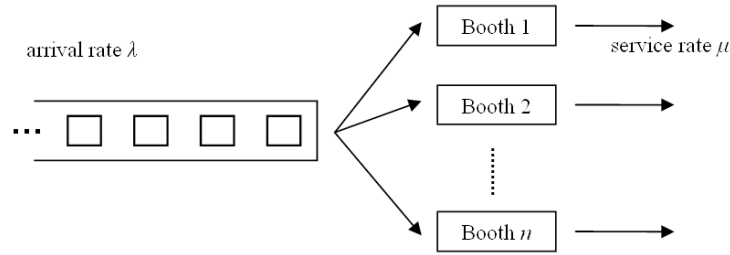


Figure 1. The M|M|n queue. Vehicles arrive at rate λ and are serviced at rate μ .

We define $X(t)$ as the number of vehicles either in the queue or at a tollbooth at time t . We also define the stationary probabilities p_k such that, in steady state, the probability that the queue has length k is p_k . From the input-output relationship of the M|M|n queue, the stationary probabilities must satisfy

$$\begin{aligned} 0 &= -\lambda p_0 + \mu p_1; \\ 0 &= \lambda p_{k-1} - (\lambda + k\mu)p_k + (k + 1)\mu p_{k+1}, & k = 1, \dots, n; \\ 0 &= \lambda p_{k-1} - (\lambda + n\mu)p_k + n\mu p_{k+1}, & k = n + 1, n + 2, \dots \end{aligned}$$

The solution to this system is [Medhi 2003]:

$$p_0 = \left[\sum_{j=0}^{n-1} \frac{\rho^j}{j!} + \frac{\rho^n}{n!(1 - \frac{\rho}{n})} \right]^{-1}, \quad p_k = \begin{cases} \frac{\rho^k}{k!} p_0, & k = 0, \dots, n; \\ \rho^{k-n} p_n, & k = n + 1, n + 2, \dots, \end{cases}$$

where $\rho = \lambda/\mu$.

Let the random variable W be the time that a vehicle spends in the system (time in the queue + time in the tollbooth). From Medhi [2003], the distribution and expected value of W are

$$\begin{aligned} P(W = w) &= \sum_{k=0}^{n-1} \frac{\left(\frac{\lambda}{\mu}\right)^k}{k!} p_0 \mu e^{-\mu w} + \frac{\left(\frac{\lambda}{\mu}\right)^n}{n!} p_0 \frac{n\mu^2}{(n-1)\mu - \lambda} \left(e^{-\mu w} - e^{-(1-\rho)n\mu w} \right), \\ E[W] &= \frac{1}{\mu} + \frac{p_n}{n\mu(1-\rho)^2}. \end{aligned}$$

This result describes the first part of the general problem: how the cars line up depending on the number n of tollbooths.

To model the traffic merging after the tollbooths, it is important to describe how vehicles leave the M|M|n queue. For an M|M|n queue, the interdeparture

times of the output of the queue are exponentially distributed with rate λ , and the output process has the same distribution as the input process. Because of the memoryless nature, interdeparture intervals are mutually independent (see Medhi [2003] or Bocharov et al. [2004] for proofs of these statements).

We define D as the number of cars departing the tollbooth during an interval Δt . Then the probability that d cars leave in that time is:

$$P(D = d) = \frac{e^{-\lambda\Delta t}(\lambda\Delta t)^d}{d!},$$

where λ is the mean number of cars that arrive at the toll plaza in a time step.

The M|M| n queue provides a simple and well-developed model of the tollbooth plaza. In particular, the average wait time and the output process are known, allowing us to verify simulation results.

Limitations of the M|M| n Queue

Though useful, the M|M| n queue is incomplete and oversimplifies the problem. Even though the M|M| n queue allows us to find the distribution of departures simply, its assumptions prevent it from being a complete solution. By using a single-queue theory, we assume that any car can go to any open server. This is overly optimistic, especially when the density is high. We would expect our predictions to be more valid for low density. Perhaps most importantly, the M|M| n queue only simulates half of the problem—the waiting times due to back-ups *in front of* the tollbooths.

Modeling Traffic with Cellular Automata

Overview

The complex system of traffic can be modeled by the simple rules of automata. We use cellular automata to model the traffic flow on a “microscopic” scale. In this scheme, we discretize space and time and introduce cars that each behave according to a small set of rules.

Cellular automata are well-suited for simulating our specific problem, since there are a large number of individual vehicles in the toll plaza, all of which are interacting. Continuous or macroscopic models could not capture this interaction and its role in causing jams that spontaneously form both before and after the toll plaza.

We first create a one-lane highway model and then add a delay for the time to pay the toll. As a one-lane simulation can allow no passing, cars accumulate behind the stopped car, creating a queue. We then extend this model into a multiple lane system, and then to a multiple lane system where the number of lanes is not constant, that is, where the road enters or leaves a toll plaza.

Single-lane Nagel-Schreckenberg Traffic

Most automata used to simulate traffic are generalizations of the Nagel-Schreckenberg cellular automata model (NS) [Chowdhury et al. 2000]. The NS model is a standard tool used to simulate traffic flow and has been shown to correspond to empirical results [Brilon et al. 1991; Chowdhury et al. 2000; Gray and Griffeth 2001; Knopse et al. 2004; Rickert et al. 1996; Schreckenberg et al. 1995].

We use this automaton to create a numerical model to confirm the queueing theory predictions.

In the NS model, a car is represented by an integer position x_n and an integer speed v_n . The vehicles are deterministically moved by their velocities, $x_n \rightarrow x_n + v_n$. The system evolves by applying the following procedure (**Figure 2**) *simultaneously* to all (x_n, v_n) .

NS Algorithm

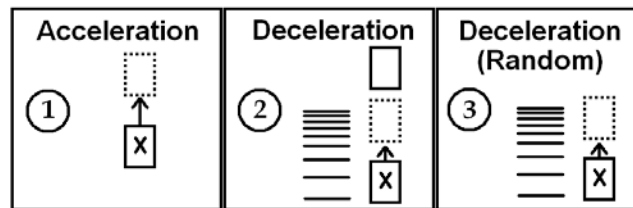


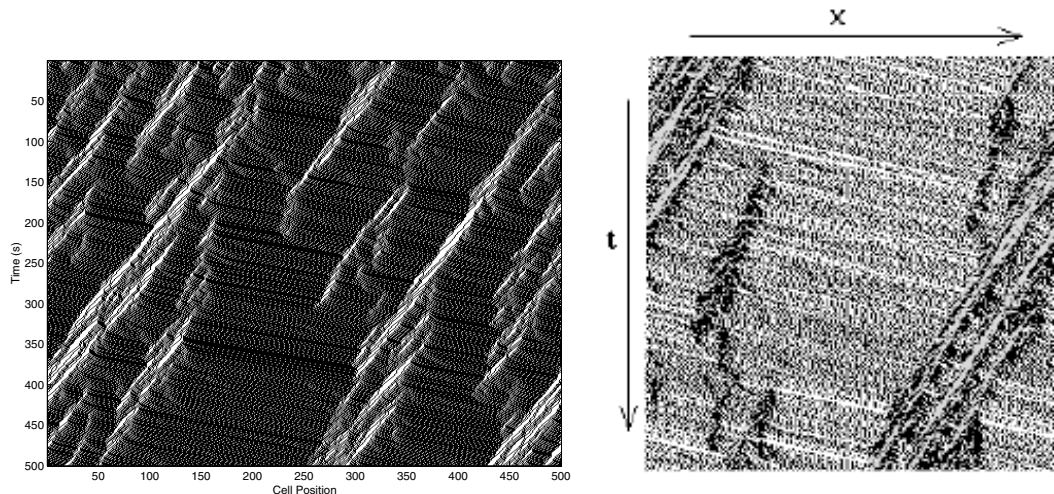
Figure 2. Rules of the NS algorithm.

1. **Acceleration.** If the vehicle can speed up without exceeding the speed limit v_{\max} , it adds one to its speed, $v_n \rightarrow v_n + 1$. Otherwise, the vehicle has constant speed, $v_n \rightarrow v_n$.
2. **Collision prevention.** If the distance between the vehicle and the car ahead of it, d_n , is less than or equal to v_n , that is, the n th vehicle will collide if it doesn't slow down, then $v_n \rightarrow d_n - 1$.
3. **Random slowing.** Vehicles often slow for nontraffic reasons (cell phones, coffee mugs, even laptops) and drivers occasionally make irrational choices. With some probability p_{brake} , we have $v_n \rightarrow v_n - 1$, presuming $v_n > 0$.

We choose the cell size to be 7.5 m to match Nagel and many others [Brilon et al. 1991; Chowdhury et al. 2000]. Since a typical maximum speed for cars is 30–35 m/s, choosing $v_{\max} = 5$ makes a single time step close to 1 s. We also use periodic boundary conditions for simplicity. (We later abandon these boundary conditions, since open boundary conditions—a Poisson generator and a sink—are consistent with the $M|M|n$ model.) In addition, research results indicate that the periodic boundary may oversimplify the distribution of vehicles [Yang et al. 2004].

We apply the above algorithm to a random initial state with a given density. This system was created by assigning each cell a probability of occupation c , which is the vehicle density parameter. This matches Gray and Griffeth's approach [2001].

The NS model produces results similar to those cited as typical by Chowdhury [2000]. In **Figure 3**, the state of the system at time step i is drawn in the i th column, with a white pixel where there is a vehicle and a black pixel for open space. Both images show generally smooth flow interrupted by congestion.



a. Results from the NS model, $c = 0.2$, $p = 0.25$. b. Results from Chowdhury et al. [2000].

Figure 3. Typical results from two models.

Properties of and Support for the NS Model

The one-lane NS model is self-consistent, flexible, and matches known empirical data.

Some of the properties of the NS model can be predicted analytically [Nagel and Herrmann 1993]. We use this information as well as experimental results to test our model. In the limiting case where the random braking probability is zero, it is possible for vehicles to “cruise,” moving at their maximum speed at all times, corresponding to a flux of $J = cv_{\max}$. This is possible only if there is sufficient space. Once the “hole density” or the remaining spaces, given by $(1 - c)$, is smaller than this flux, the lack of free space limits the speed of the vehicles. This relationship between flux and density is given by:

$$J(c) = \min\{cv_{\max}, 1 - c\}, \quad (1)$$

where J is the flux of cars, the number of cars passing a cell in unit time, and c is the density of cars. We ran our NS automaton with $p_{\text{brake}} = 0$ for 20 trials with excellent agreement between our mean and the theory, as seen in **Figure 4**.

As pretty as this graph is, it indicates only that the model is self-consistent and can be approximated; it does not show that it actually represents a real

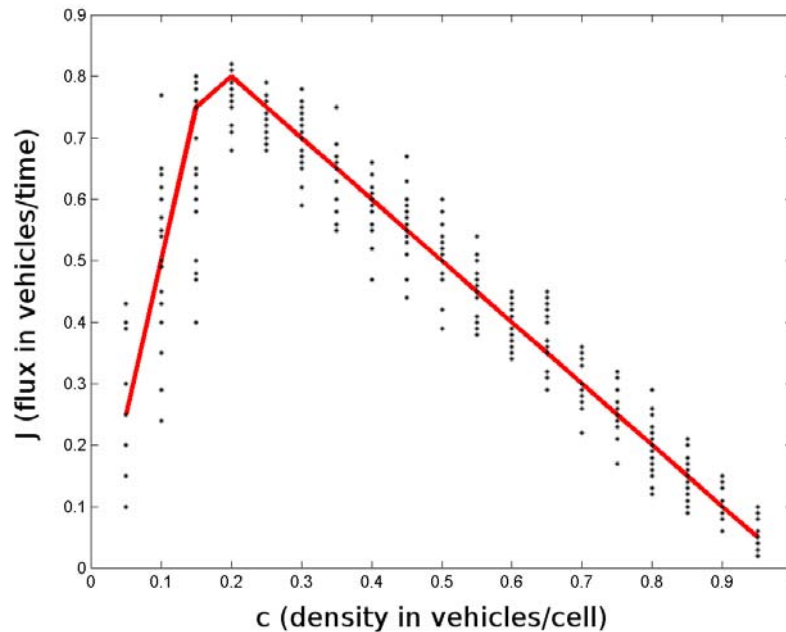


Figure 4. The flux equation (1) predicts the results of the NS model with very good accuracy.

system. We consult empirical data on vehicle flux (**Figure 5b**). Clearly, the NS model is an accurate approximation of the known data.

It is also possible to use mean field theory to describe the NS model. Even if $p_{\text{brake}} \neq 0$, the case of $v_{\text{max}} = 1$ can be solved analytically with this technique [Schadschneider and Schreckenberg 1997]. For our system, with $v_{\text{max}} = 5$, this becomes computationally difficult.

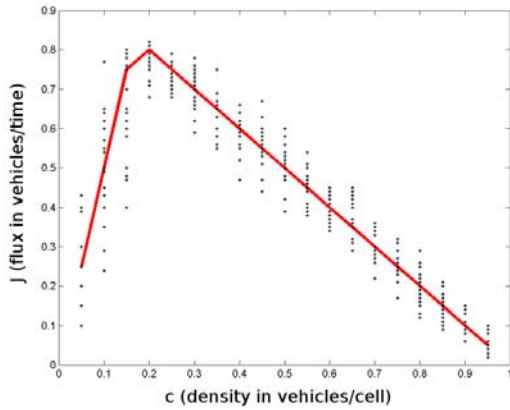
Adding Delays

Delays prevent the use of periodic boundary conditions.

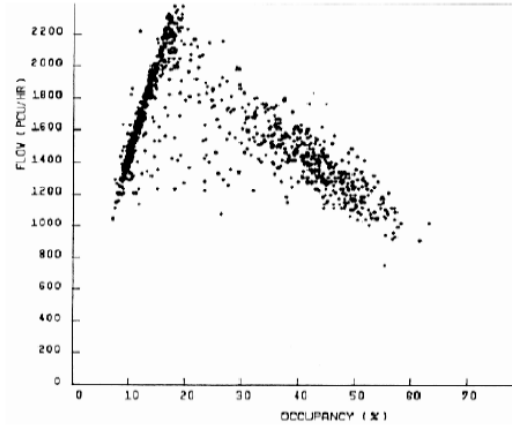
To simulate an encounter with a tollbooth, we must add a delay to the unobstructed system. Simon and Nagel model the NS automaton for a blockage but only with a fixed delay probability [1998]. We assume that the service time is exponentially distributed, with a probability of $1 - \exp(-\mu\Delta t)$ that any one tollbooth completes service in Δt , and so we use this assumption to describe the delay in our NS model as well.

Introducing this delay creates an asymmetry in the problem; particles to the right of the barrier have to loop around to reach the “tollbooth,” whereas particles on the left will impact it immediately. Because of this, we measure the flux at both the one-quarter and three-quarter points of the lane (**Figure 6**).

The fundamental diagrams in **Figure 6** confirm our intuition regarding the interaction of flux and a bottleneck (the tollbooth). The flux at the quarter point experiences a decline due to congestion at a relatively low vehicle density compared with the three-quarter point, which is beyond the bottleneck. The



a. NS model with theory.

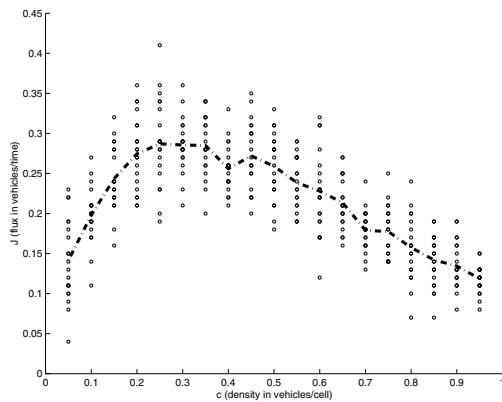


b. Empirical data from Canadian highway [Chowdhury et al. 2000].

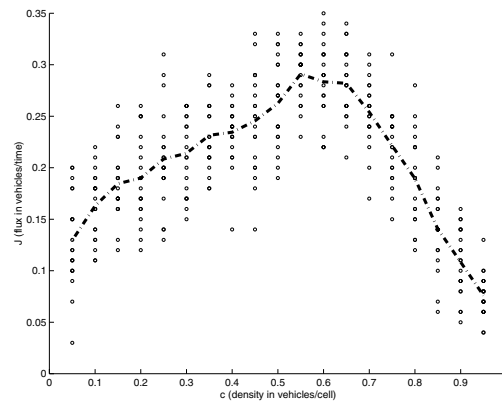
Figure 5. Comparison of model with data.

heavy incoming traffic therefore affects the accumulating queue faster than the vehicles past the tollbooth.

These fundamental diagrams show that the periodic boundary conditions are inappropriate for this calculation; with periodic boundaries, the input rate to the queue is limited by the (smaller) flux of vehicles wrapping around from the right. This is not representative of a true traffic jam; without periodic boundary conditions, jams cannot affect the flux upstream from them.



a. Fundamental diagram at one-quarter point, $p = 0$.



b. Fundamental diagram at three-quarters point, $p = 0$.

Figure 6. Fundamental diagrams.

Simulating the Complete System

Multiple Lanes

By adding a new rule to the one-lane automaton, we can model multilane highways. We use a single-lane model to ensure that our automaton is a proper representation of the real world, but the actual problem is a multiple-lane one. Two-lane system studies are less common than single-lane studies, and higher-lane models even rarer [Chowdhury et al. 2000; Nagel et al. 1998; Rickert et al. 1996]. We extend the rule set of the automaton to describe lane changes, using the one-lane NS rules with a single additional rule for lane changing (**Figure 7**).

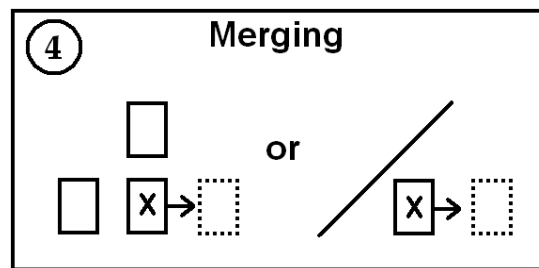


Figure 7. The multi-lane automaton rule.

4. **Merge to avoid obstacles.** The vehicle attempts to merge if its forward path is obstructed ($d_n = 0$). The vehicle randomly chooses an intended direction, right or left. If that intended direction is blocked, the car moves in the other direction unless both directions are blocked (the car is surrounded). This is consistent with the boundaries and tailgating rules proposed by Rickert et al. [1996].

Changing the Highway Shape

By using the multilane automaton, we can model a multilane highway that has realistic lane-changing behavior. This still does not, however, model a transition between highway and a number of tollbooths.

To create the toll plaza, we introduce borders that force the automata to change lanes to avoid hitting the boundary. The borders outline the edge of a ramp that moves from the highway onto a wider toll plaza and back again (**Figure 8**). This is the only aspect of this model that is not general; by imposing different boundaries, we could easily model a different problem. To simulate the wait at the tollbooth, we also add a delay at the center, as in the one-lane case.

The previous models [Gray and Griffeath 2001; Nagel et al. 1998; Rickert et al. 1996] assume a roadway of constant width—the number of lanes does not change. By restricting the geometry of our roadway to represent the toll plaza (note the “diamond” shape in **Figure 8** and introducing the behavior of

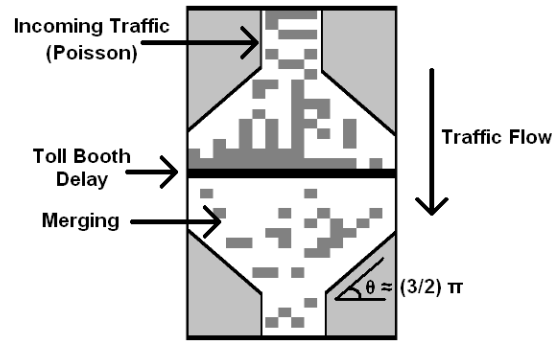


Figure 8. We introduce imaginary borders into the system to narrow and widen traffic.

merging away from obstacles, we have increased the flexibility of the model without making additional assumptions.

Consistency of $M|M|n$ Queue and NS Model

The $M|M|n$ queue is an idealized system. It predicts a shorter wait time than a real toll plaza, because it fails to account for inefficiencies in the queue (Figure 9). The $M|M|n$ queue does, however, predict the correct distribution. In addition, the stability of the queue is very different from the stability of the NS model. An $M|M|n$ queue achieves a steady state if $\lambda/\mu < n$, with λ the arrival rate, μ the service rate, and n the number of servers [Gross and Harris 1974]. We observe in the NS simulation that traffic in front of the tollbooths could create a growing backlog even when the corresponding $M|M|n$ queue would be stable.

Despite these apparent inconsistencies, there is a very strong agreement between the queueing theory predictions and the observed results. From queueing theory analysis, we know the probability distribution of the number of cars leaving the tollbooths:

$$P(D = d) = \frac{e^{-\lambda\Delta t}(\lambda\Delta t)^d}{d!}.$$

This equation provides a good deal of information about the queue, and this probability can easily be measured in the cellular automata model. We compare the simulated and theoretical probability distribution in Figure 10, and the two distributions are very similar: The difference in their means is decreasingly small and is less than 2% after 10^4 iterations of the NS model.

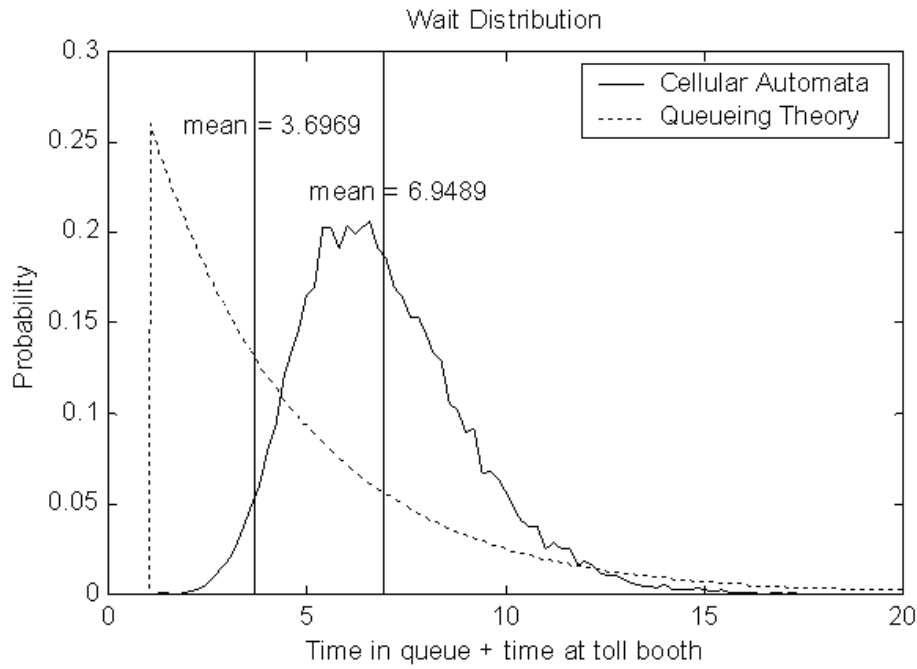


Figure 9. The $M|M|n$ distribution and NS distribution are similar, but the $M|M|n$ has a smaller mean wait time due to its optimistic assumptions.

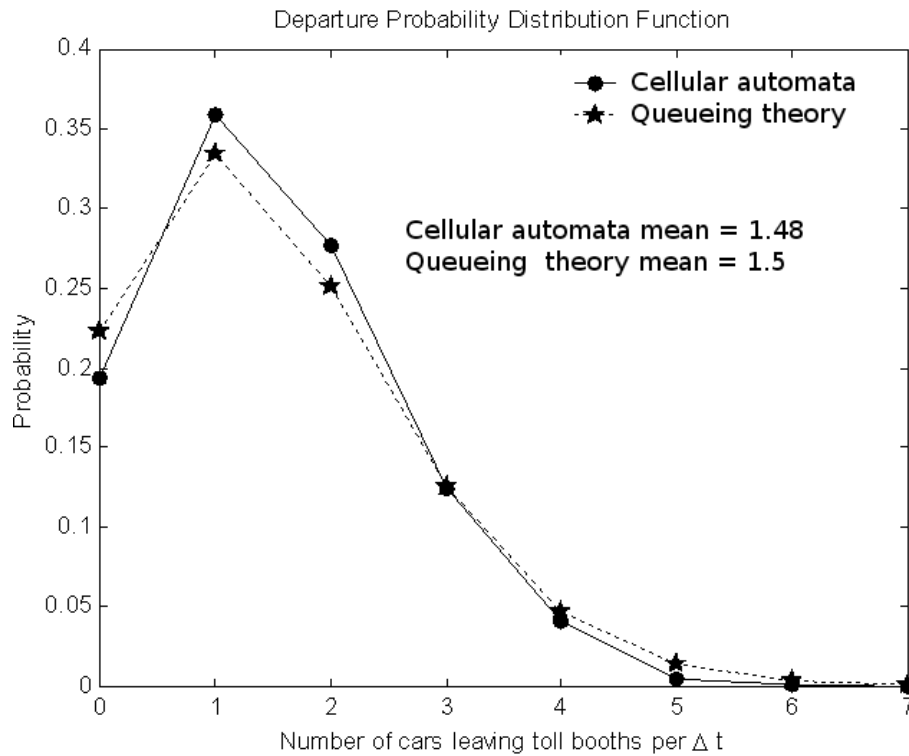


Figure 10. The simulated distribution of leaving vehicles is very close to that predicted by queueing theory.

Time Predictions of the Automata Model

The Optimal Number of Tollbooths

The optimal configuration minimizes the wait time; so to determine the correct number of tollbooths, we need to measure the average time for a vehicle to enter the toll plaza, wait in line, and then exit out onto the main road again. We do this by tracking automata and averaging the time that passes between entering and leaving the system.

Calculating Average Times

The average time required to pass through our system depends on the arrival rate (which controls congestion), the number of lanes, and the number of tollbooths. We consider the mean service rate to be fixed, at 5 s; Hare uses 9 s [1963]. However, though changing the service rate does change the average time, this change does not affect which value of n is optimal.

We fix the number l of incoming lanes and search over the number n of tollbooths and the arrival rate λ . We calculate the average wait time for a range of n and λ by using our cellular automata model and averaging over a long period of time to eliminate transient effects.

What, though, should these ranges be? We presume that n is not larger than three or four times the number of lanes. We placed this restriction after noticing that the wait time increases sharply when n is much larger than l . The range of λ is determined by commonsense restrictions. If λ is the mean number of cars arriving in a time step, then λ should be no more than the number of lanes of incoming traffic as this is the physical capacity of the road.

Optimal Results for 2 Lanes

We allow n to range from 2 to 8 and λ from 0 to 2. We plot the average time against n and λ in **Figure 11**.

The clear minimum in this graph lies along the line $n = 4$, even for different values of λ . This indicates that even for different arrival rates, the optimal number of tollbooths is 4. This is a very stable solution that does not require changes with traffic rates, at least for typical values.

Though 4 is the optimal number of booths, 2 is very near optimal and 3 is very bad. For $n = 3$, the additional lane adds more traffic jam than throughput. For small n , when there is one more booth than lanes of traffic, the wait time is a local maximum.

Optimal Results for 3 Lanes

By varying λ from 0.6 to 2.7 and n from 3 to 9, we find that the minimum occurs, once again independent of λ , at $n = 6$ (**Figure 12**).

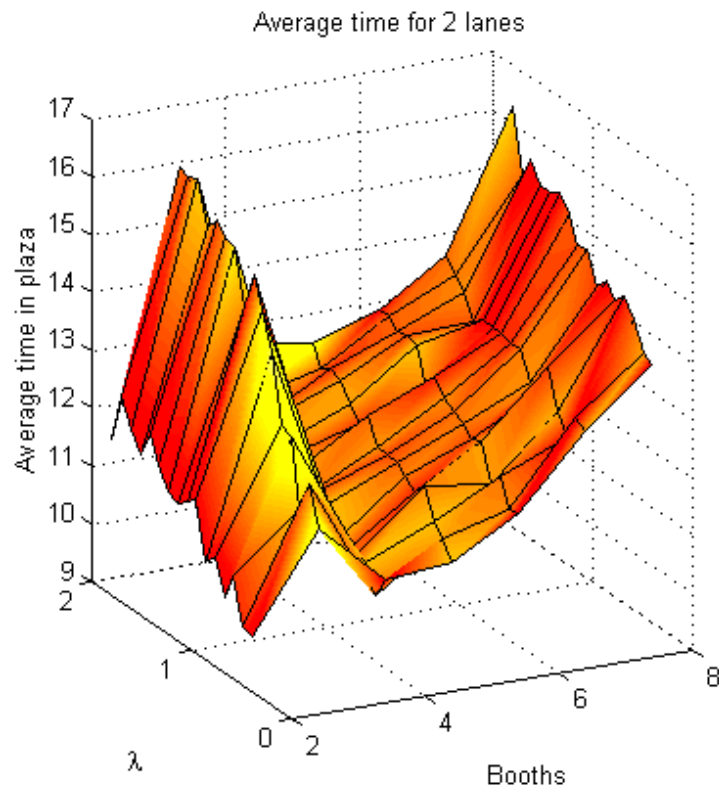


Figure 11. For a 2-lane system, the minimum time occurs for 4 tollbooths.

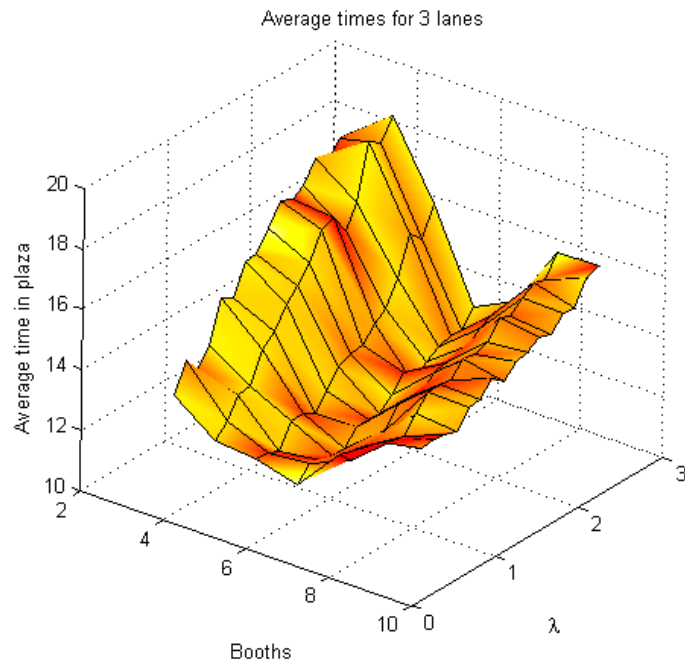


Figure 12. For a three-lane system, the minimum time occurs when there are six tollbooths.

Higher Numbers of Lanes

The results so far would suggest the naive solution of always having twice as many tollbooths as incoming lanes. Unfortunately, the 4-lane case disproves this guess. For different values of the arrival rate λ , the optimal number of tollbooths changes, from a low of 6 for small λ . The tollbooth owners could measure traffic flow, estimate λ , and open or close tollbooths as needed.

Generalizing These Results

To determine the stability of these results, we made calculations with the probability of random braking changed to 0.1 rather than 0. For each λ , even though the wait times change, the optimal numbers of tollbooths do not.

This process could be repeated for any required setup; we have illustrated a general technique for determining the optimal number of tollbooths.

One Tollbooth per Lane

If cars were not allowed to change lanes, the case with one tollbooth per lane of traffic would just reduce to l independent one-lane models, and this would be equivalent to our single-lane highway. We know that this is not the case. Cars move into the lane with the shortest queue.

In our results, the $n = l$ case is typically nonoptimal. The one exception to is the two-lane highway; here, the time for $n = 2$ is only barely longer than for $n = 4$. However, this is not because $n = l$ is always “bad,” but because there is usually a better case. As the number of lanes increases, the number of tollbooths increase significantly. If we consider cost, the $n = l$ case could be very important, since for low l ($l < 5$), the $n = l + 1$ case is a local maximum and $n = l$ is a local minimum.

Re-examining Assumptions

Though our calculations assume an exponential service probability, using a Gaussian service distribution does not change the model’s recommendations significantly.

Conclusions

We build a model of traffic flow near a toll plaza by using cellular automata modified from the one-lane Nagel-Schreckenberg automaton.

- Our model’s predictions match empirical data on vehicle distribution and are confirmed by our queueing theory analysis of the problem.

- Changing the service rate and service distribution of the tollbooths does not significantly alter the recommendations for the optimal number of booths
- We establish a general technique for determining the optimal number of tollbooths to put on a given highway.
- Though in general the optimal tollbooth results are complex and depend on the arrival rate, there are simple cases: a 2-lane highway should have 4 tollbooths and a 3-lane highway should have 6, independent of the amount of traffic.
- In general, the case of as many tollbooths as lanes is suboptimal.

Strengths and Weaknesses

Strengths

- **Consistency.** Our queueing theory model and the cellular automata model agree on the distribution of cars leaving the booths. Both models match theoretical results and past empirical results. In addition, under small changes, like adjusting the probability of braking, the recommendations of the model do not change significantly.
- **Minimal assumptions required.** By using the automata, we reduce the number of parameters and assumptions. For our queueing theory, we assume that the probability of leaving the tollbooth is exponential, but altering this distribution does not affect the recommendations.
- **Flexibility.** Our model easily adapts to problems with different geometries, such as different numbers of lanes or even different boundaries.
- **Ease of implementation.** A complex problem is simulated using very simple rules.

Weaknesses

- **No closed-form solution.** For the complete model, we must actually calculate the simulation.
- **Calculation time.** To get an accurate average time for vehicles, we need to average over a number of time steps on the order of 10,000. As the number of lanes increases, computation slows.

References

- Bocharov, P., C. D'Apice, A. Pechenkin, and S. Salerno. 2004. *Modern Probability and Statistics: Queueing Theory*. Utrecht, The Netherlands: Brill Academic Publishers.
- Brilon, W., F. Huber, M. Schreckenberg, and H. Wallentowitz (eds.). 1991. *Traffic and Mobility*. Springer-Verlag.
- Chowdhury, Debashish, Ludger Santen, and Andreas Schadschneider. 2000. Statistical physics of vehicular traffic and some related systems. *Physics Reports* 329 (199). <http://arxiv.org/pdf/cond-mat/0007053>.
- Gray, Lawrence, and David Griffeath. 2001. The ergodic theory of traffic jams. *Journal of Statistical Physics* 105 (3/4).
- Gross, D., and C. Harris. 1974. *Fundamentals of Queueing Theory*. New York: John Wiley and Sons.
- Hare, Robert R., Jr. 1963. Contribution of mathematical concepts to management. *Industrial College of the Armed Forces* <http://www.ndu.edu/library/ic4/L64-015.pdf>.
- Knopse, Wolfgang, Ludger Santen, Andreas Schadschneider, and Michael Schreckenberg. 2004. Empirical test for cellular automaton models of traffic flow. *Physical Review E* 70.
- Medhi, J.. 2003. *Stochastic Models in Queueing Theory*. 2nd ed. New York: Academic Press, Elsevier Science.
- Nagel, Kai, and Hans J. Herrmann. 1993. Deterministic models for traffic jams. *Physica A* 199 (2).
- Nagel, Kai, Dietrich Wolf, Peter Wagner, and Patrice Simon. 1998. Two-lane traffic rules for cellular automata: A systematic approach. *Physical Review E* 58 (2).
- Rickert, M., K. Nagel, M. Schreckenberg, and A. Latour. 1996. Two lane traffic simulations using cellular automats. *Physica A* 231 (4): 534–550. citeseer.ist.psu.edu/rickert95two.html.
- Schadschneider, Andreas, and Michael Schreckenberg. 1997. Car-oriented mean field theory for traffic flow models. *Journal of Physics A: Mathematical and General* 30.
- Schreckenberg, M., A. Schadschneider, K. Nagel, and N. Ito. 1995. Discrete stochastic models for traffic flow. *Physical Review E* 51 (4): 2939. citeseer.ist.psu.edu/schreckenberg94discrete.html.

Simon, P.M., and Kai Nagel. 1998. A simplified cellular automaton model for city traffic. *Physical Review E* 58 (2).

Yang, X., Y. Ma, and Y. Zhao. 2004. Boundary effects on car accidents in a cellular automaton model. *Journal of Physics A: Mathematical and General* 37.



Brian Camley, Pascal Getreuer, and Bradley Klingenberg.

Judge's Commentary: The Outstanding Tollbooths Papers

Kelly Black
Dept. of Mathematics
Union College
Schenectady, NY 12308
blackk@union.edu

Overview of the Problem

The teams were asked to examine the flow of traffic through a toll plaza. One of the difficulties in this problem is that the traffic flow through a toll plaza is not actively managed; rather, the traffic through the system is passively managed by the careful design of the roadway and the toll-collection system. On most roadways, a toll plaza consists of a long transition to an increased number of lanes, the collection system (the tollbooths), and a long transition back to the original number of lanes. Interestingly, only a very small number of entries suggested adding an active management component to the toll plaza, such as ways to restrict the way that drivers can change lanes.

In the last paragraph of the problem statement three tasks/questions were given:

- "Make a model to help determine the optimal number of tollbooths to deploy in a barrier-toll plaza."
- "Explicitly consider the scenario where there is exactly one tollbooth per incoming lane."
- "Under what conditions is this more or less effective than the current practice?"

At first glance, it would seem that the considerable power of queueing theory would be readily available for this problem. Unfortunately, this is only true to a certain extent. The nature of a toll plaza is that multiple lanes expand into even more lanes into which people can change if they feel it is advantageous. Once again, people get in the way of good mathematics.

The UMAP Journal 26 (3) (2005) 391–399. ©Copyright 2005 by COMAP, Inc. All rights reserved. Permission to make digital or hard copies of part or all of this work for personal or classroom use is granted without fee provided that copies are not made or distributed for profit or commercial advantage and that copies bear this notice. Abstracting with credit is permitted, but copyrights for components of this work owned by others than COMAP must be honored. To copy otherwise, to republish, to post on servers, or to redistribute to lists requires prior permission from COMAP.

On second thought, however, the difficulty of the problem should not be a surprise. As far as we are aware, no state's Dept. of Transportation has been able to get this problem right. Moreover, traffic designers often only have one chance to get it right. The cost of making changes to an existing toll plaza can be prohibitive.

In the following section, we provide an overview of the kinds of solutions that were submitted, including some comments on the judges' reactions. We also provide an overview of the judging process itself and the challenges that this particular problem represented to the judges. Finally, some tips and pointers are provided in reaction to some of the things that appeared in many of the team's submissions.

The Problem at Hand

Modeling a Toll Plaza

The first of the three questions required teams to create a mathematical model of a barrier-toll plaza. The most common mathematical model treated the toll plaza as a queue. Unfortunately, the complex nature of the toll plaza is not easily described as a simple queue. For example, the lanes diverge into more lanes at the entrance, and drivers are able to change lanes. Also, the lanes must combine again after the service area, and crowded traffic after the tollbooth can impact the traffic in the entrance of the toll plaza.

Of the entries that modeled a toll plaza using queueing theory, what set them apart was how they handled the various subtleties of a toll plaza. For example, teams had to make decisions on how cars move in the entrance and exit sections of a toll plaza. Teams also had to decide on how each car is handled by the tollbooth attendants. For example, some teams assumed that each car could be handled in the same amount of time. Other teams assumed that the time required for each car was a random variable with a prescribed probability distribution. To make this decision even more difficult, the teams had to decide how to handle the various payment methods available, such as cash, EZ-Pass, or other remote rapid-payment methods.

Of those teams that assumed that the service time required for each car varied, some treated the entrance section as a queue and the actual tollbooth as a separate queue. In this situation, the resulting chain of queues could be coupled and described if the two probability distributions were similar. For example, the majority of such entries assumed that the distributions of the cars entering the system and tollbooth service times were both Poisson with different parameters.

While the more advanced entries were able to bring together the entrance and the tollbooths in the plaza, the exit represented a significant difficulty. The majority of entries briefly discussed the potential problems of the traffic after the service booths but did not include the effects of the exits in their models.

In fact, the teams that did explicitly consider the exit areas usually only did so in the context of a simulation in a computational model.

In addition to the queueing theory approach, a less common approach was to model the flow of traffic as a fluid. The resulting models were much more complex than those based on queueing theory. The process of matching the physical situation to a flow and then converting the results back to what is happening within a toll plaza represented a substantial difficulty for those taking this approach.

Besides the construction of a mathematical model, the most popular approach to this problem made use of simulations based on a computational model. Such models were usually based on either a cellular automata model or a highly modified queue making use of a time-stepping scheme allowing for lane changes. The more advanced approaches also factored the exit areas into the simulation.

A computational model required a much different approach to the analysis and discussion of the results. The results are a composite of many runs and take on a statistical nature. Furthermore, the large number of variables—the number of lanes before the plaza, the number of lanes in the plaza, the waiting time, the way cars enter the system, the length of the plaza, and a wide variety of other factors—make it difficult to reach concrete conclusions about the best design for a toll plaza. This is especially true given the short time available to develop the computational model, implement it, decide which situations to use, run it, and examine the results.

The judges took this into consideration and did not expect a complete examination. This approach did require a more complete description of the computational model, though, since the number of assumptions that can be incorporated was significantly greater. There was also a heightened expectation of doing more in the way of a sensitivity analysis with respect to some of the various parameters.

While many different approaches were submitted, the entries that received the higher ratings examined at least two different models. The most common combination by far was a simple queue and a computational model. The most striking aspect of this was that few teams explicitly stated a comparison of the two results under identical circumstances. Those that did stood out, and the results of the comparison helped to establish a good benchmark of the computational model.

One Tollbooth Per Lane

The second question in the problem statement required each team to use their models for a toll plaza that has one tollbooth for each lane of travel on the road. This established a sanity check that each team had to examine. Surprisingly, a number of teams did not examine this situation, which resulted in a penalty for ignoring one of the stated requirements.

What Is “Best”

The final question required the teams to determine best practice in designing a toll plaza—to define a way to compare different configurations of a toll plaza. Each team had to balance the competing costs of each driver’s time, the cost of operating the toll plaza, and the cost of construction.

One of the most surprising aspects of this year’s competition is that few teams explicitly defined what they thought would be the cost of operating a toll plaza. The vast majority of teams simply compared the average waiting time for the drivers under various circumstances with little comment or justification. Those teams that looked at a nontrivial cost of operating the tollbooths based on the cost of lost productivity of the drivers and the cost of operating the tollbooths certainly stood apart from the others.

The few teams that did examine this part of the problem reported some of the most interesting results. In fact, in some circumstances the option of not building a tollbooth is the most satisfactory option to almost everybody except maybe the tollbooth operators themselves!

Overview of the Judging Process

We give an overview of the judging process, including some general observations about some of the entries submitted for the competition. In the subsections that follow we try to provide some insight into what the judges discussed prior to the actual judging, first impressions of a paper, and some of the small details that help to make an entry stand out.

First, we try to provide a broad overview of the judging process itself. The papers are examined in a two-step process. The first round, or triage round, is the first pass. In this round, judges are able to examine the papers for only a relatively short time. When a judge begins reading a paper in this first stage, the question is, “Should the paper be read in closer detail?” If the answer is “yes” or even “maybe,” then it is passed on to the second stage. Because we try to give each paper the benefit of the doubt, it is difficult to state what necessary essence is required to move past this round.

At the most basic level, the quality of the writing and the consistency of the summary with the rest of the paper is vital in this first stage. It is a really bad idea to make a judge work too hard on a paper. The easier it is for a judge to determine how the students interpreted the problem, the approach used, and the results, the easier it is for the judges to determine the quality of the work.

Entries that remain through the second stage are given much closer, detailed readings. For example, papers that remain on the final day of judging are read by as many as eight different judges for at least an hour per entry. During this time the judges sometimes confer with one another if they are not sure about an equation, result, or the wording in a section. For the most part, though, each judge tries to provide an independent review of the student’s work.

Discussion Before Judging Began

Before the judging began, the judges got together to discuss the problem. As usual, the problem was nontrivial, and we judges had to ensure that we understood what was being asked. The judges had to carefully parse the original question. For example, this year the problem included some very specific tasks that were given in the last paragraph of the problem, and whether or not an entry specifically addressed those questions was important.

Additionally, each judge initially read through a set of randomly chosen papers. In the second stage of the process, this set of papers was adjusted to ensure that each judge viewed papers with a wide variety of initial scores. The purpose of this protocol is to make sure that we also took into consideration how the various teams interpreted the question and how they reacted to the problem.

After these initial readings, the judges had to agree on what was important and how to provide a consistent mechanism for comparing different entries. Each year, the relative importances of the various aspects of a paper are tailored to the particular problem; but in general, the kinds of things that judges look for in a paper are relatively consistent. This year the judges decided that the following aspects were important:

Summary This is the first thing that a judge sees. A summary should provide a brief overview of the problem, a brief review of the methodologies used, and an overview of the conclusions. It is a difficult challenge to include all these things on one page and do it well, but it does provide the first impression.

Assumptions and Justifications In constructing a mathematical representation of a physical system some simplifications must be made and some subtleties must be left out. The parts of the problem deemed most important—as well as what is left out of the model—must be made explicit.

Model/Analysis One of the novel aspects of this year's problem was the close association between the mathematical model and the analysis of the problem. The stochastic nature of the problem, as well as the prevalence of entries making use of both queuing theory and simulation, made it difficult to separate these two aspects of the problem. In the end, the judges decided not to treat them separately, so that it would be easier to compare entries whose balance varied between the different approaches used.

Results/Validation It is not unusual to see many papers that make use of a variety of approaches and techniques, but this problem resulted in more entries than usual that employed at least two solution techniques. It was more important than ever for the teams to be able to compare the different results as well as interpret the results.

Sensitivity Between the stochastic nature of the problem and the wide use of simulation, the validation of the results had to include some way to test the robustness of the conclusions. One of the most important ways to do this

is to examine what happens after changing the values of certain parameters or changing the assumptions on what kind of probability distributions to use. For example, some teams that used queuing theory examined their conclusions under a variety of assumptions about the time required by an individual tollbooth attendant to complete one transaction. If a small variation in the service time resulted in a large change in the average waiting times, that is an indication that the conclusions may be circumspect.

Strength & Weakness Any mathematical model requires many assumptions and simplifications and is only good for a restricted situation. It is vital that the modeler identify the conditions under which the mathematical model is appropriate. Each team was expected to demonstrate explicitly that they had done some critical analysis of the model itself and to identify what they felt was good and bad about the model.

Clarity/Communication One of the key aspects of any problem is to be able to share the results. The methods employed, the results that are delivered, and the analysis of both the methods and the results must be clearly described. This is the filter through which all mathematics is shared.

Communicating Mathematics

As mathematicians, we are engaged in a social exercise that absolutely requires us to share our work with one another, however sharing mathematical ideas can be extremely difficult. In fact, it is difficult enough that we often try very hard to avoid putting our students through the difficult learning process associated with writing and sharing mathematical ideas. We often have our students take part in writing proofs or problem solving, but putting it all together in a formal report or a paper the first time can be an excruciating process.

There are many excellent books and other resources for students that offer a better introduction than can be expressed here. In fact, from the many excellent entries it is clear that those resources are being exploited. We focus on just a few general issues that stand out in this year's event.

- Some teams presented a *narrative of the team's activities*. An entry that lists how the team approached the problem and chronicles what the team did (or tried to do) puts the team at a severe disadvantage. In contrast, an entry in the format of a self-contained report immediately stands out. In such a report, the problem is restated, including the results; the various methodologies that are used are clearly stated; the analyses are given; and the results are clearly stated, including a critical examination of the approach and the results.
- One aspect of writing that even advanced writers struggle with is graphing. When a plot is provided, it should be clearly introduced and described in the text, including a proper reference to the figure number. It should be clear to the reader from the text of the report what to look for in the plot before

turning to look at the plot. This year's problem is an excellent example of the importance of describing plots and figures. Providing a graphical example of cars moving through a toll plaza over time is difficult and each team attempted to do this in many different ways. Furthermore, some teams provided sequences of figures to demonstrate a particular transition, and there is a huge burden on the writers to explain what the reader should be looking for and what the implications are.

In general, when a figure or plot is provided, the text should provide a detailed explanation of what is in the figure. Also, the caption and labels in the figure should succinctly describe what the figure is. Of course, the axes should be labeled and units should be provided. One thing that was different for this year, however, was that the judges gave teams more leeway in how discrete vs. continuous functions were displayed. Discrete data should be displayed as discrete and not with lines drawn between points. This year was different in that many figures represented the organization of the cars in a queue that might be discrete according to the model even though the domain (time) could be continuous.

- Some of the entries included many tables. Almost everything said above for figures also applies to tables. Tables should be clearly labeled and explained in detail in the text of the report. The easier you make it for a judge to determine what is in a table and why it is important, the more likely the judge will be happy. A happy judge is a higher-scoring judge!
- Finally, a small thing that is very likely to keep an otherwise good paper from being held back in the early rounds. Some teams have a difficult time integrating equations and citations within the text of the report. Equations and citations should be correctly integrated into each sentence using proper grammar. Some teams that do excellent work make it extremely difficult for themselves when the equations or citations are set apart from each sentence and not properly integrated into the flow of the text.

The Little Things

The vast majority of teams do great work, and it is always exciting to see what the teams are able to accomplish in such a short amount of time. It is also important to be able to share and express the ideas developed by each team in a formal report. This final product is the vehicle used to communicate the team's ideas and techniques. It is not a narrative of what the team did but is an opportunity to educate and persuade others to follow up on the team's excellent work.

There are a number of simple things that can be done to make an entry easier to read. Some of these may appear to be trivial, but they make the judges task easier which in turn makes it easier for the judges to concentrate on the ideas rather than the way the ideas are expressed:

Strengths & Weaknesses This aspect of an entry demonstrates whether or not a team has provided a critical inquiry into the methods and techniques developed. Including this aspect as a separate section of a report makes it much easier for the judges to identify easily this important aspect of the team's efforts.

Table of Contents Given the growing number of teams that use \LaTeX , it is shocking how few entries provide a table of contents. This is a trivial step that can radically improve the readability of a report.

Citations A paper that makes ample use of citations properly and consistently integrated into the text is guaranteed to stand out. For example, many papers included citations when providing the definitions of functions describing the way cars entered the toll plaza but failed to provide a citation when stating some of the results that happen to come directly from the relevant literature.

Equation Numbers Number all equations even if they are not explicitly referred to in the text. This makes it easier for judges to confer when there is a question about a particular equation.

Units Units are important. Always make sure that the definition of a variable, parameter, or function includes its units. Also, always check a result to make sure that the units are correct. This is one of the first checks judges make when confronted with a result that is not obvious. (Always keep in mind the difference between a quantity and its rate of change!)

Conclusions

Each year we are amazed at the high quality of the entries. The things that the teams can accomplish in a weekend are a testament to the quality of the team's training and hard work. The teams receiving the higher honors should be proud to stand out in such an incredible field.

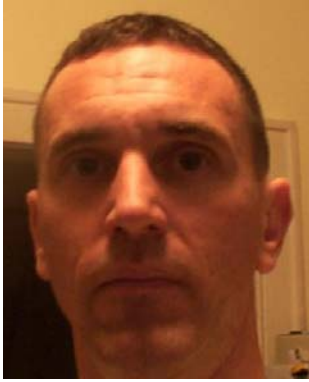
This year the teams that submitted entries for the Tollbooth Problem focused their efforts on the optimal design of a toll plaza. They had to consider the number of lanes, the lengths of lane transitions, the times required to collect the fares, and a wide variety of other factors. Most of the teams made use of either queuing theory, comparisons to fluid flow, or simulation via a computational model. The teams that received higher recognition from the judges derived more than one model and made comparisons among their models.

One aspect that set entries apart was the analysis and critical evaluation of their models and results. As usual, a sensitivity analysis of the models is important; but because of the nature of this year's problem, an even higher value was placed on this important aspect of the modeling process.

Finally, each team's entry consists of a written report designed to educate and persuade. This is a difficult task in itself, but the teams are asked to do this without the benefit of an outside editing process; they must somehow build

editing into their efforts themselves. Adding to the difficulties, good writing is most effective when it does not get in the way of the ideas that the writer is trying to convey and is not noticed until after the reader looks back and realizes what has been shared.

About the Author



Kelly Black is a faculty member in the Dept. of Mathematics at Union College. He received his undergraduate degree in Mathematics and Computer Science from Rose-Hulman Institute of Technology and his Master's and Ph.D. from the Applied Mathematics program at Brown University. His research is in scientific computing and he has interests in computational fluid dynamics, laser simulations, and mathematical biology.

Statement of Ownership, Management, and Circulation

1. Publication Title UMAP JOURNAL		2. Publication Number 0 1 9 7 - 3 6 2 2		3. Filing Date 9/15/05
4. Issue Frequency QUARTERLY		5. Number of Issues Published Annually 4		6. Annual Subscription Price \$99.00
7. Complete Mailing Address of Known Office of Publication (Not printer) (Street, city, county, state, and ZIP+4) COMAP, Inc., 57 Bedford St., Suite 210, Lexington MA 02420				Contact Person Kevin Darcy Telephone 781-862-7878 ex31

8. Complete Mailing Address of Headquarters or General Business Office of Publisher (Not printer)

SAME

9. Full Names and Complete Mailing Addresses of Publisher, Editor, and Managing Editor (Do not leave blank)

Publisher (Name and complete mailing address)
Solomon Garfunkel, 57 Bedford St., Suite 210,
Lexington MA 02420

Editor (Name and complete mailing address)
Paul Campbell, 700 College St., Beloit WI 53511

Managing Editor (Name and complete mailing address)
Pauline Wright 57 Bedford St., Suite 210, Lexington MA 02420

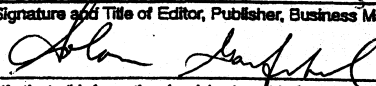
10. Owner (Do not leave blank. If the publication is owned by a corporation, give the name and address of the corporation immediately followed by the names and addresses of all stockholders owning or holding 1 percent or more of the total amount of stock. If not owned by a corporation, give the names and addresses of the individual owners. If owned by a partnership or other unincorporated firm, give its name and address as well as those of each individual owner. If the publication is published by a nonprofit organization, give its name and address.)

Full Name	Complete Mailing Address
CONSORTIUM FOR MATHEMATICS	57 Bedford St., Suite 210
AND ITS APPLICATIONS INC.	Lexington MA 02420
(COMAP, INC.)	

1. Known Bondholders, Mortgagees, and Other Security Holders Owning or Holding 1 Percent or More of Total Amount of Bonds, Mortgages, or Other Securities. If none, check box None

Full Name	Complete Mailing Address

2. Tax Status (For completion by nonprofit organizations authorized to mail at nonprofit rates) (Check one)
 The purpose, function, and nonprofit status of this organization and the exempt status for federal income tax purposes:
 Has Not Changed During Preceding 12 Months
 Has Changed During Preceding 12 Months (Publisher must submit explanation of change with this statement)

13. Publication Title <u>The HMAP Journal</u>		14. Issue Date for Circulation Data Below <u>7/1/05</u>	
15. Extent and Nature of Circulation		Average No. Copies Each Issue During Preceding 12 Months	No. Copies of Single Issue Published Nearest to Filing Date
a. Total Number of Copies (Net press run)		700	700
b. Paid and/or Requested Circulation	(1) Paid/Requested Outside-County Mail Subscriptions Stated on Form 3541. (Include advertiser's proof and exchange copies)	650	640
	(2) Paid In-County Subscriptions (Include advertiser's proof and exchange copies)	0	0
	(3) Sales Through Dealers and Carriers, Street Vendors, Counter Sales, and Other Non-USPS Paid Distribution	30	20
	(4) Other Classes Mailed Through the USPS	0	0
c. Total Paid and/or Requested Circulation (Sum of 15b. (1), (2), (3), and (4))		680	660
d. Free Distribution by Mail (Samples, complimentary, and other free)	(1) Outside-County as Stated on Form 3541	0	0
	(2) In-County as Stated on Form 3541	0	0
	(3) Other Classes Mailed Through the USPS	12	12
e. Free Distribution Outside the Mail (Carriers or other means)		0	0
f. Total Free Distribution (Sum of 15d. and 15e.)		12	12
g. Total Distribution (Sum of 15c. and 15f.)		692	672
h. Copies not Distributed		8	12
i. Total (Sum of 15g. and h.)		700	684
j. Percent Paid and/or Requested Circulation (15c. divided by 15g. times 100)		98	98
16. Publication of Statement of Ownership			
<input type="checkbox"/> Publication required. Will be printed in the <u>3rd (FALL)</u> issue of this publication.		<input type="checkbox"/> Publication not required.	
17. Signature and Title of Editor, Publisher, Business Manager, or Owner 			Date <u>9/15/05</u>
I certify that all information furnished on this form is true and complete. I understand that anyone who furnishes false or misleading information on this form or who omits material or information requested on the form may be subject to criminal sanctions (including fines and imprisonment) and/or civil sanctions (including civil penalties).			

Instructions to Publishers

- Complete and file one copy of this form with your postmaster annually on or before October 1. Keep a copy of the completed form for your records.
- In cases where the stockholder or security holder is a trustee, include in items 10 and 11 the name of the person or corporation for whom the trustee is acting. Also include the names and addresses of individuals who are stockholders who own or hold 1 percent or more of the total amount of bonds, mortgages, or other securities of the publishing corporation. In item 11, if none, check the box. Use blank sheets if more space is required.
- Be sure to furnish all circulation information called for in item 15. Free circulation must be shown in items 15d, e, and f.
- Item 15h., Copies not Distributed, must include (1) newsstand copies originally stated on Form 3541, and returned to the publisher, (2) estimated returns from news agents, and (3), copies for office use, leftovers, spoiled, and all other copies not distributed.
- If the publication had Periodicals authorization as a general or requester publication, this Statement of Ownership, Management, and Circulation must be published; it must be printed in any issue in October or, if the publication is not published during October, the first issue printed after October.
- In item 16, indicate the date of the issue in which this Statement of Ownership will be published.
- Item 17 must be signed.

Failure to file or publish a statement of ownership may lead to suspension of Periodicals authorization.